SNAP-21 PROGRAM, PHASE II

DEEP SEA RADIOISOTOPE-FUELED THERMOELECTRIC GENERATOR POWER SUPPLY SYSTEM

QUARTERLY REPORT NO. 12

Space and Defense Products
ELECTRICAL PRODUCTS GROUP
3-M CENTER, ST. PAUL, MINN. 55101, PH 633-9400
3M COMPANY

DISCLAIMER

SNAP-21 PROGRAM, PHASE II

DEEP SEA RADIOISOTOPE-FUELED THERMOELECTRIC GENERATOR POWER SUPPLY SYSTEM

QUARTERLY REPORT NO. 12

Space and Defense Products
ELECTRICAL PRODUCTS GROUP
3-M CENTER, ST. PAUL, MINN. 55101, PH 633-9400
3M COMPANY

Report No. MMM 3691-52

AEC RESEARCH AND DEVELOPMENT REPORT

This report has been prepared under Contract AT(30-1)3691
with the U. S. Atomic Energy Commission

SNAP-21 PROGRAM, PHASE II

DEEP SEA RADIOISOTOPE-FUELED THERMOELECTRIC GENERATOR POWER SUPPLY SYSTEM

QUARTERLY REPORT NO. 12

Period Covered

April 1, 1969 to June 30, 1969

Prepared by

SNAP-21
Technical Staff

Approved by

R. L. Pannemann
Manager,
SNAP-21 Program

Issued by

Space and Defense Products

MINNESOTA MINING AND MANUFACTURING COMPANY

ST. PAUL, MINNESOTA 55101

page blank

LEGAL NOTICE

page blank

DISTRIBUTION LIST

	No. of Copies
U.S. Atomic Energy Commission Division of Reactor Development and Technology Washington, D.C. 20545 Attn: S.J. Seiken	5
U.S. Atomic Energy Commission New York Operations Office 376 Hudson Street New York, New York 10014 Attn: L. Wasser	2
U.S. Atomic Energy Commission NY Patents Group Upton, New York 11973	1
Director, Nuclear Engineering Division Naval Facilities Engineering Command Washington, D.C.	1
U.S. Atomic Energy Commission RDT Site Office, 3M Company 2501 Hudson Road Space Center, Building 551 St. Paul, Minnesota 55119 Attn: John J. Stefano	1
Isotopes Development Center ORNL Post Office Box X Oak Ridge, Tennessee 37830 Attn: R.A. Robinson	2
Hittman Associates, Inc. Technical Information Department 9190 Red Branch Road Columbia, Maryland 21043	1

TID-4500
Category UC-33

page blank

TABLE OF CONTENTS

TABLE OF CONTENTS (Continued)

LIST OF ILLUSTRATIONS

LIST OF ILLUSTRATIONS (Continued)

LIST OF TABLES

page blank

1.0 SUMMARY

The most significant technical achievements on the SNAP-21 Program during this quarter include the following items:

- Disassembled system S10D3 and sent HTVIS to Linde for repair.
- Checkout and implantment of systems S10P1 and S10P2 were completed.
- Dynamic testing and the standard reference performance test of system S10P4 were completed.
- Fueled system performance predictions were completed for systems S10P1, S10P2, and S10P3.
- The biological shield which was removed from insulation system B10DL1 was incorporated into insulation system B10DL8.
- Insulation system B10D2 was leak checked and rethermally tested.
- The radiation shield, spider, spider bolt, and inner liner from insulation system B10DL3 were shipped from Linde to 3M Company.
- Thermal performance testing was conducted on insulation units B10DL7 and B10DL8.
- Insulation system B10DL6 was mated with generator A10P1 for long-term test.
- Continued testing of Phases I and II thermoelectric generators and power conditioners.
- Preliminary effort was started on the 20-watt system concept.

2.0 TASK 1 - 10-WATT SYSTEM

2.1 SYSTEMS

2.1.1 Electrically Heated Systems

2.1.1.1 System S10D2

System S10D2 completed one year of operation on June 26, 1969. The power input was reduced by 2.5% to simulate actual fuel decay over a one-year period.

Last quarter it was reported that the hot end temperature decreased at about 8°F per watt. Further analysis shows that this should be about 4°F per watt.

Table 2-1 shows the thermoelectric generator and system electrical performance. Table 2-2 shows the thermal performance for the system. Figure 2-1 shows the thermoelectric generator and system power output. Figure 2-2 shows the system instrumentation locations. Figure 2-3 shows the normalized thermoelectric performance data. From these tables and curves it can be seen that the thermoelectric generator and system thermal and electrical performance has been stable.

Indications from the generator pressure transducer show that the thermoelectric generator may be leaking. The generator pressure has decreased about 3.0 psia to its present level of 19.2 psia (as of 6/27/69). Further investigation will continue.

Table 2-1. System S10D2 Electrical Performance

Item	4/24/68	9/4/68	11/15/68	2/24/69	6/13/69
Test Hours	233	1771	3502	6798	8542
System Power Input (corrected-watts)	218	220	220	219	219
Generator Primary Load Voltage (vdc)	5.32	5.29	5.30	5.30	5.29
Generator Bias Load Voltage (vdc)	0.739	0.734	0.736	0.736	0.734
Generator Primary Load Current (amperes)	2.89	2.80	2.78	2.75	2.73
Generator Bias Load Current (amperes)	0.142	0.138	0.136	0.136	0.138
Generator Primary Power Output (watts)	15.3	14.8	14.7	14.6	14.4
Generator Bias Power Output (watts)	0.105	0.101	0.100	0.100	0.101
Generator Total Power Output (watts)	15.4	14.9	14.8	14.7	14.5
Conditioner Primary Voltage Input (vdc)	5.31	5.26	5.27	5.27	5.26
Conditioner Bias Voltage Input (vdc)	0.734	0.724	0.726	0.726	0.724
Conditioner Primary Current Input (amperes)	2.89	2.80	2.78	2.75	2.73
Conditioner Bias Current Input (amperes)	0.142	0.138	0.136	0.136	0.138
Conditioner Primary Power Input (watts)	15.2	14.7	14.6	14.5	14.4
Conditioner Bias Power Input (watts)	0.104	0.099	0.098	0.098	0.099
Conditioner Total Power Input (watts)	15.4	14.8	14.7	14.6	14.4
System Load Voltage (vdc)	24.6	24.5	24.48	24.46	24.49
System Load Current (amperes)	0.428	0.426	0.426	0.426	0.427
System Load (ohms)	57.48	57.38	57.5	57.5	57.35
System Power Output (measured) (watts)	10.5	10.5	10.4	10.4	10.4
Primary Open Circuit (volts)	9.46	9.40	9.30	9.22	9.16
Primary Load Voltage (volts)	5.32	5.29	5.30	5.30	5.29
Primary Load Current (amps)	2.87	2.80	2.78	2.75	2.73
Bias Open Circuit (volts)	1.39	1.37	1.37	1.35	1.35
Bias Load Voltage (volts)	0.739	0.734	0.736	0.736	0.734
Bias Load Current (amps)	0.142	0.138	0.136	0.136	0.138
Internal Resistance (ohms)	1.43	1.46	1.43	1.41	1.41
Total Power Output (watts)	15.4	14.9	14.8	14.7	14.5

Table 2-2. System S10D2 Temperature Profile in Water

Thermocouple Location (See Figure 2-2)	Identification	Pre-Dynamic Test 4/28/68 (°F)	Post-Hydro Test 9/4/68 (°F)	Long-Term Test		
				11/15/68	2/24/69	6/13/69
1	Segmented Ring at Pressure Vessel Wall	39	43	45	40	43
2	TEG Mounting Plate (inner)	50	54	56	50	53
3	TEG Cold Frame Center (external)	58	63	65	59	62
4	TEG Hot Frame Center (external)	1042	1040	1041	1028	1026
5	TEG Hot Frame Edge (external)	1047	1046	1046	1035	1033
6	Emitter Center	1254	1277	1278	1267	1267
7	Emitter Midway	1262	1287	1287	1276	1275
8	Emitter Edge	1305	1332	1332	1321	1319
9	Insulation System Upper	97	103	103	99	100
10	TEG Cold Frame Outer (external)	53	59	60	54	56
11	TEG Mounting Plate Male	42	47	49	42	45
12	Heater Block Bottom	1435	1470	1471	1458	1456
13	Power Conditioner Base	44	41	-	-	-
14	Pressure Vessel, Cover Upper	40	40	41	40	41
15	Pressure Vessel, Cover Center	40	41	40	40	40
16	Pressure Vessel Body Lower	40	41	40	40	41
	TEG Hot Frame (internal) – Edge	1012	1014	1009	1002	1002
	TEG Hot Frame (internal) – Center	999	998	993	985	986
	Hot Electrode – Edge	999	1001	996	990	990
	Hot Electrode – Center	976	976	971	963	965
	Cold Electrode – Edge	95	98	96	94	96
	Cold Electrode – Center	91	94	93	91	93
	Cold Frame (internal) – Edge	82	83	82	80	81
	Cold Frame (internal) – Center	74	72	72	70	71
	Follower – Edge	81	84	83	81	83
	Follower – Center	80	81	81	80	81
17	Water – Top	40	40	39	40	40
18	Water – Middle	40	40	39	40	40
19	Water – Bottom	39	40	39	40	40

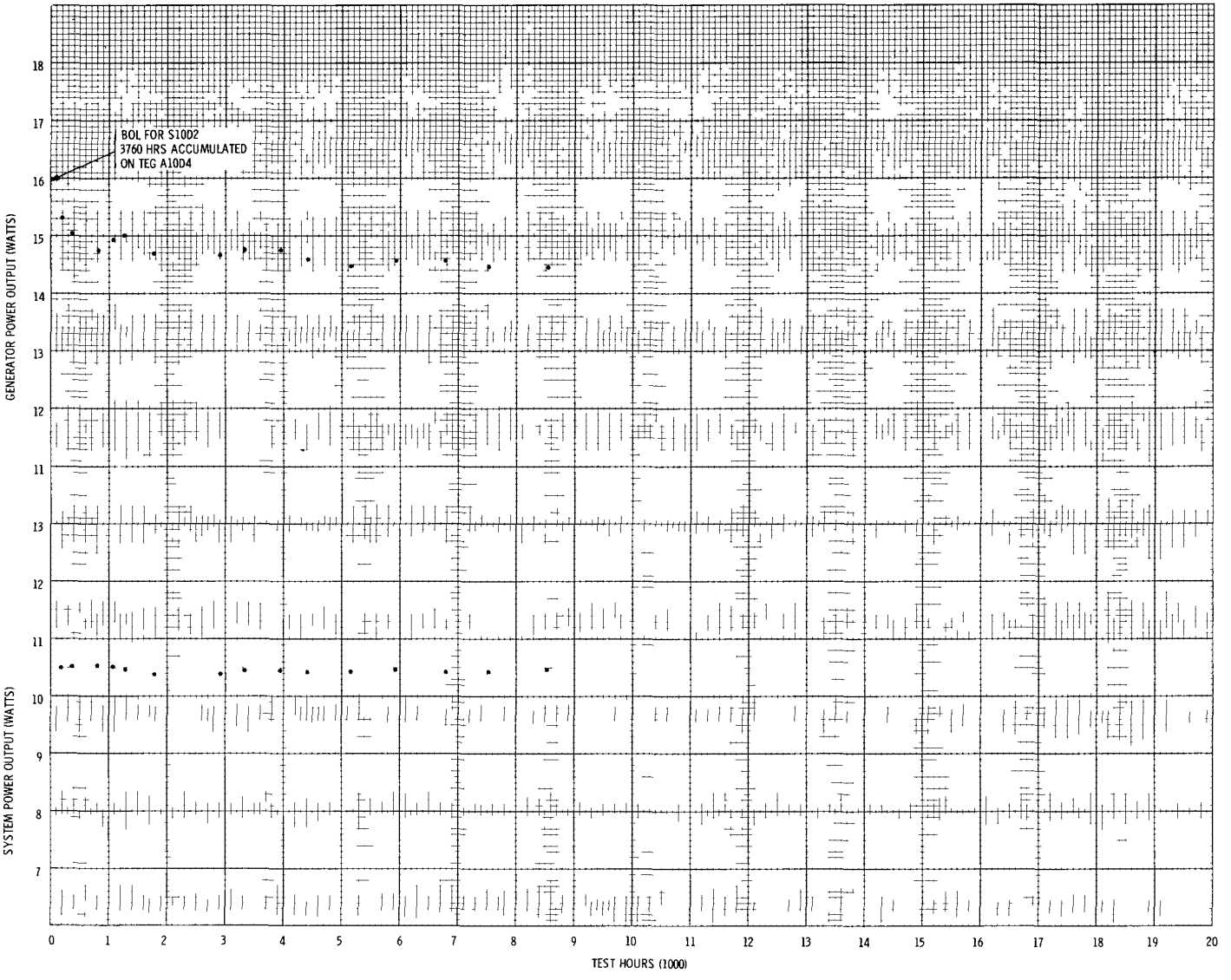

Figure 2-1. System S10D2 Performance

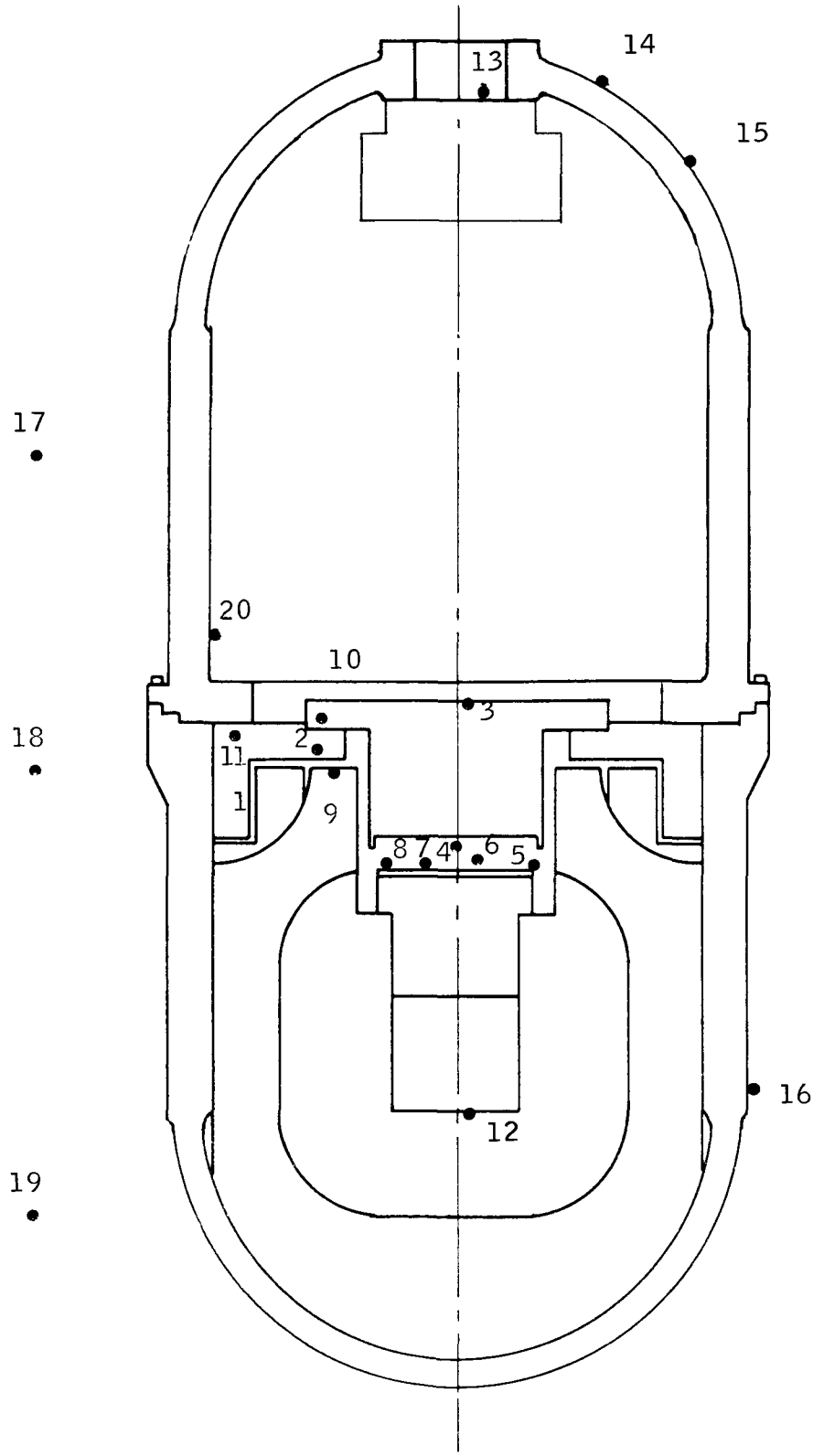

Figure 2-2. System S10D2 Instrumentation

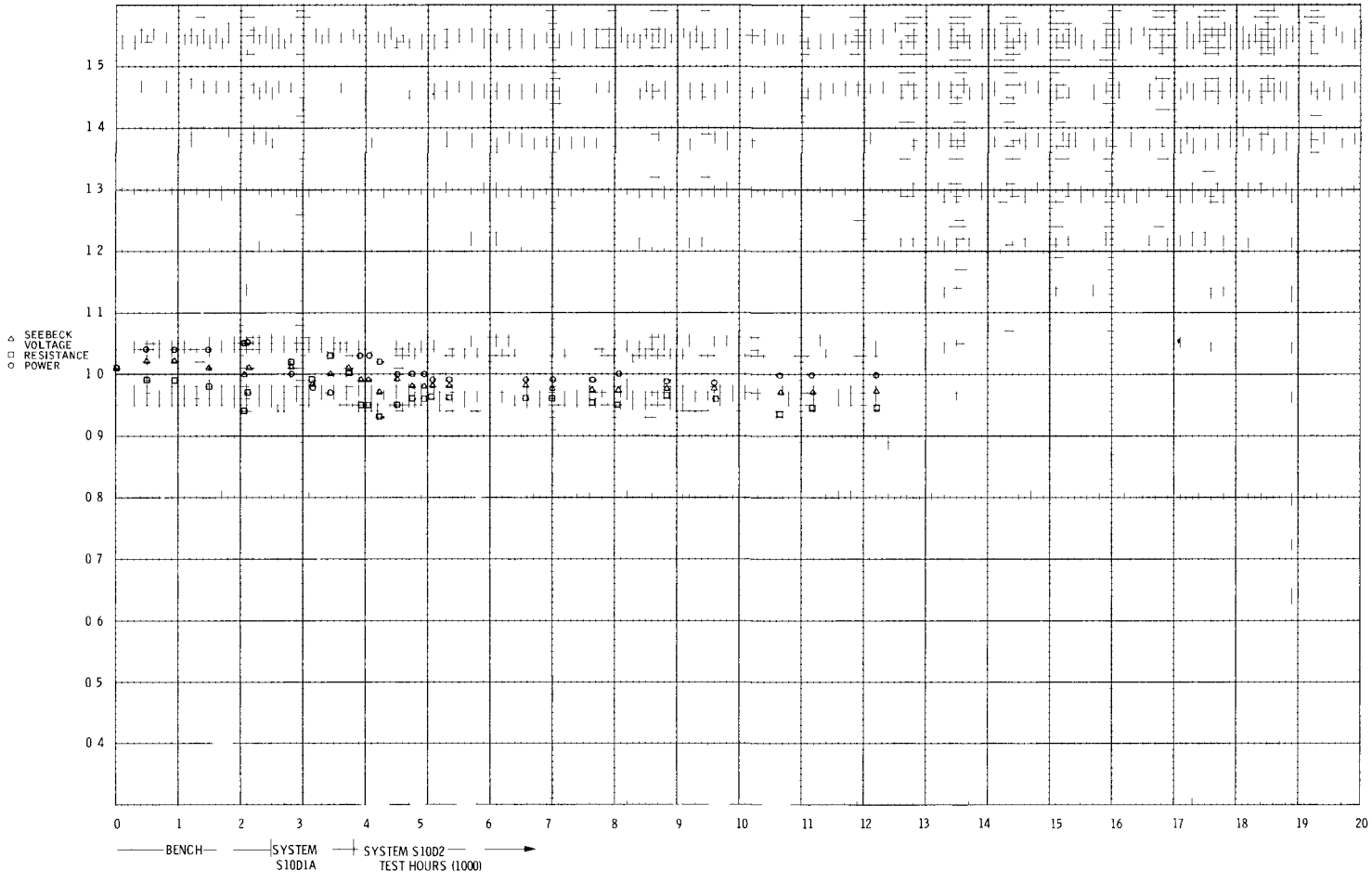

Figure 2-3. SNAP-21 Thermoelectric Generator A10D-4 Normalized Data

2.1.1.2 System S10D3

System S10D3 was used to perform the shipping container test. This test was completed on April 17, 1969. Prior to the shipping container test, this system required an additional 21 watts of power input to obtain initial BOL test conditions. In order to perform the shipping container test, the power input was increased to obtain near beginning-of-life temperature profile (refer to Quarterly Report Number 11 for more details on the condition of this system).

Table 2-3 presents the collected data for the shipping container test. Figure 2-4 shows the test setup, Figure 2-5 shows the temperature profile curves, and Figure 2-6 is a photo of the shipping container test.

Surveillance was performed by Quality Control during all phases of the shipping container elevated temperature testing.

Although S10D3 required 235 watts input (includes 4.7 watts extraneous losses) to obtain a correct thermal profile, the analysis of the shipping container test data cannot be conducted on the basis of fuel loading. The data must be studied strictly on the basis of the established temperature profile for a system. From Figure 2-5 it can be seen that the system can withstand the specification value of 130°F environmental air temperature. The limiting factor for shipment is 225°F at the cold cap. The cold cap temperature is a near linear function of the ambient air. In projecting cold cap temperature in Figure 2-5, it can be noted that the system can withstand an excess of 150°F ambient temperature. This should not be done for any extended period of time. Table 2-3 shows that a temperature of 978°F was noted at the hot junction at 130°F ambient air. The difference between the hot frame design values and the experimental data of the hot frame and button temperatures is 30°F and is due to an assumption of the design values for the radiation gap temperature drop. The radiation gap temperature difference for the design values is 180°F, while for the various systems a temperature difference between 200°F and 250°F has been experienced.

After the shipping container testing was completed, the system was placed in the water tank for testing. A check of the temperature profile as a function of the power input was performed to determine if any additional heat losses occurred

Table 2-3. Shipping Container Testing for System S10D3

Thermocouple Number*	Location	Ambient Temperature (°F)				Design** Values (°F)
		68	92	110	130	
#1	Pressure Vessel Top	90	114	137	156	--
#2	Pressure Vessel Center	92	117	140	159	--
#3	Fin Base Center	92	116	141	158	--
#4	Fin Base Bottom	86	111	134	153	--
#5	Middle Fin Outer	86	111	134	153	--
#6	Holding Fixture Cover	81	105	128	147	--
#7	Holding Fixture Bottom	70	92	114	134	--
#8	Shipping Container Top	77	102	124	144	--
#9	Shipping Container Middle	69	93	114	135	--
#10	Shipping Container Bottom (CONTROL)	68	90	110	131	--
#11	Test Chamber Top	73	98	121	141	--
#12	Test Chamber Middle	70	95	117	138	--
#13	Test Chamber Bottom	68	85	94	124	--
-	Emitter	1215	1232	1241	1253	1270
-	External Hot Frame Center	968	995	1010	1028	1090 (avg. est.)
-	External Hot Frame Edge	980	1006	1020	1039	
-	Estimated Hot Button	919	945	961	978	1020
-	External Cold Frame Center	107	131	154	171	
-	Estimated Cold Button	132	156	178	195	204
-	Pressure Vessel	85	110	134	151	143
-	Date	3/31/69	4/3/69	4/2/69	3/25/69	

*Refer to Figure 2-4
**Reference: SNAP-21 Program, Phase II, Quarterly No. 7, MMM 3691-30

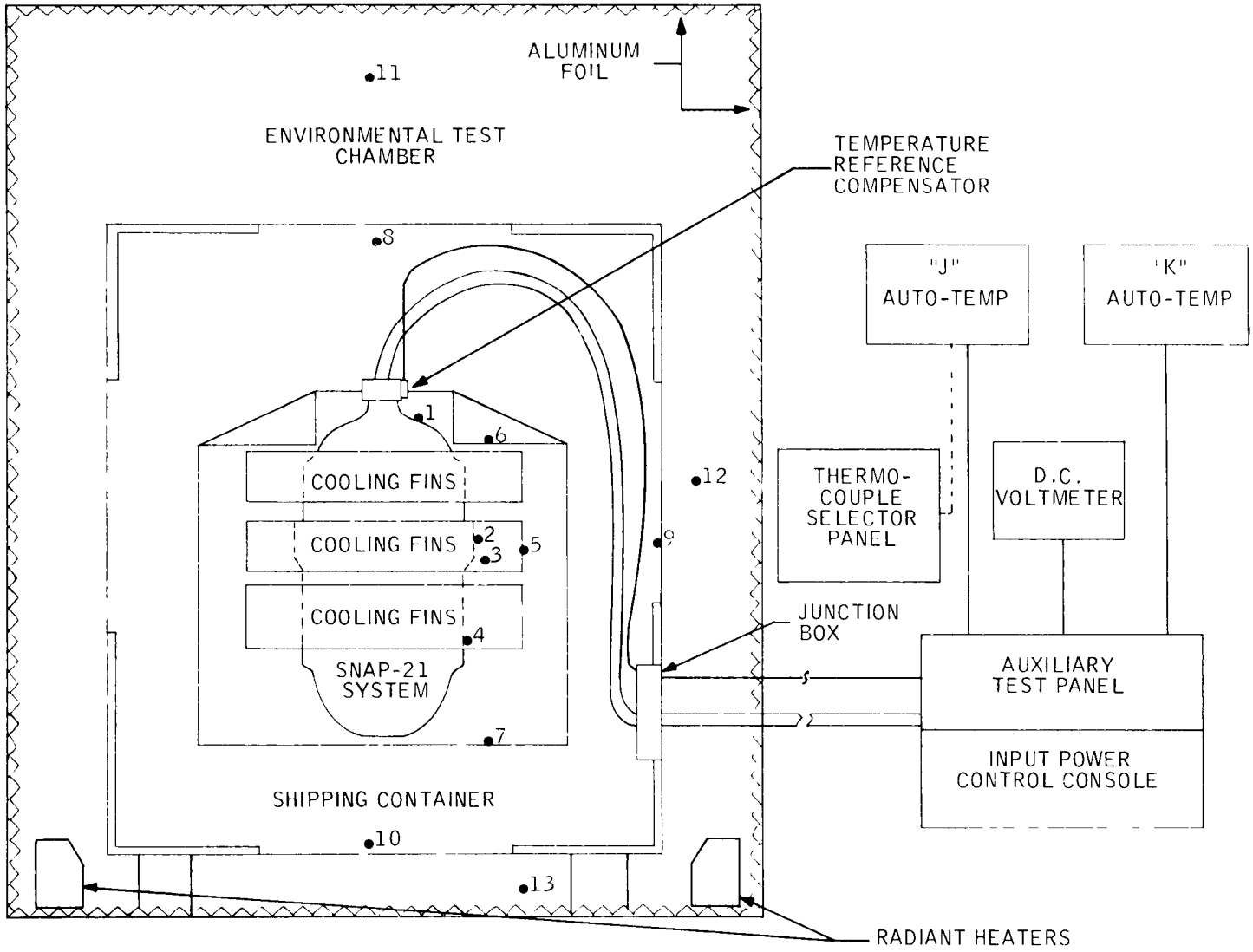

Figure 2-4. Test Set-Up and Thermocouple Location for Shipping Container Environmental Test of System S10D3

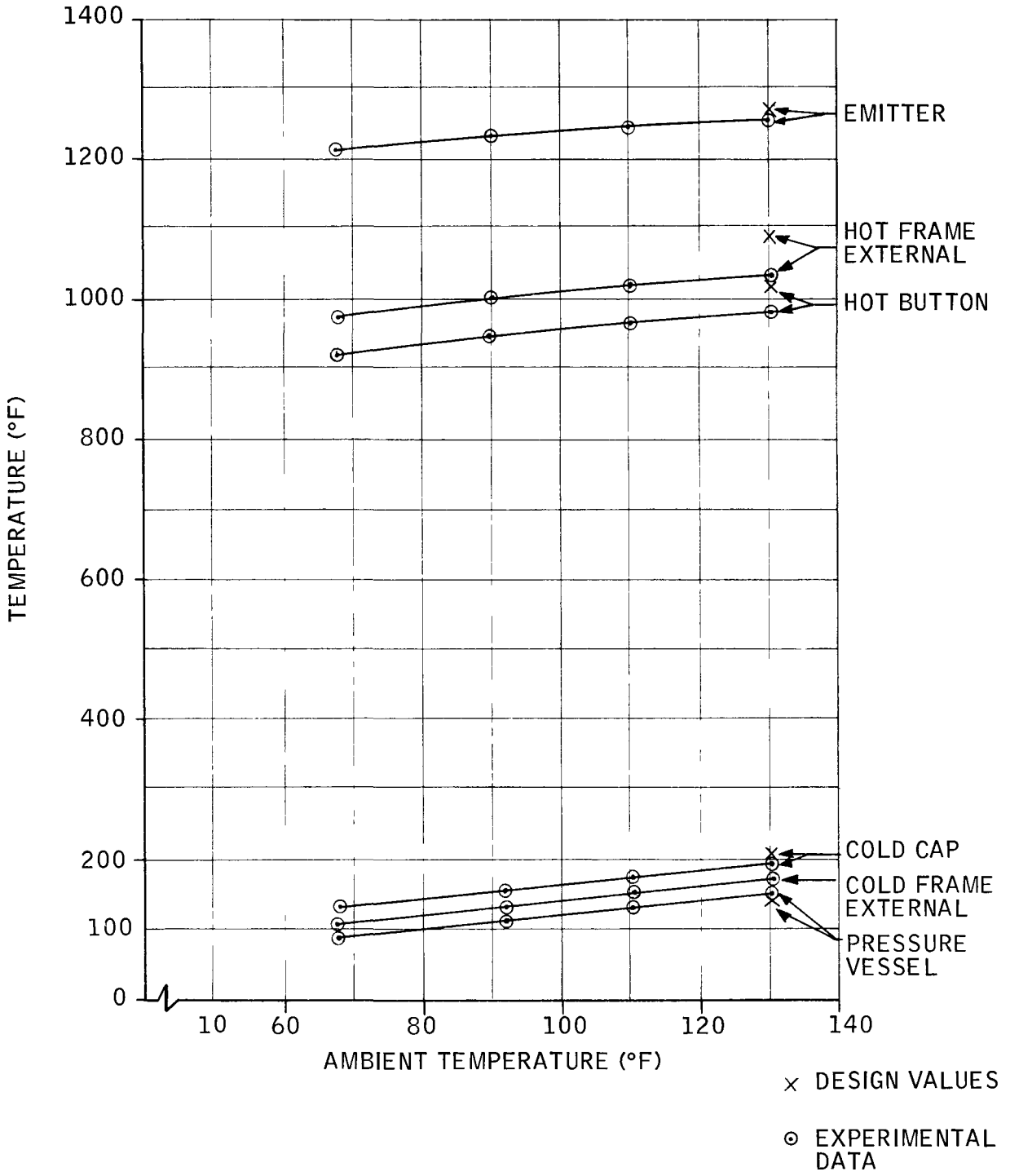

Figure 2-5. System S10D3 Temperature Profile in Shipping Container


READ INSTRUCTION MANUAL
BEFORE HANDLING
RECORD
RECEPTACLE
TIE DOWN

during the shipping container tests. The system performance did not change. The power input to S10D3 was turned off on May 7, 1969. The system was cooled to room temperature and dismantled during the week of May 12, 1969. The HTVIS was sent to Linde for a check of its efficiency to determine possible heat leaks through the insulation system. The results of this test are discussed in paragraph 2.4.1. The HTVIS will be repaired by Linde and sent back to 3M for reassembly into system S10D3.

2.1.2 Fueled Systems

2.1.2.1 System S10P1

Final tests and checkout were completed for the systems on May 29, 1969. A standard reference performance test was conducted on May 21, 1969. The system was then shipped to NRDL (San Francisco) for integration with their Data Acquisition System and checkout. Upon completion of this, it was shipped to San Clemente Island for implantment. Refer to Section 2.10 for a discussion of the system checkout and implantment.

Table 2-4 shows the performance data for S10P1. All indications are that the system performance was satisfactory. Figure 2-7 shows the location of the thermocouples on fueled systems.

2.1.2.2 System S10P2

Final tests and checkout were completed for the system on May 29, 1969. A stable referenced performance test was conducted on May 21, 1969. A system checkout, according to the Shipping and Handling Manual 10-Watt System (Report No. 3691-42), was done on May 29, 1969. The system was then shipped to NRDL (San Francisco) for integration with their Data Acquisition System and checkout. Upon completion of this, it was shipped to San Clemente Island for implantment. Refer to Section 2.10 for a discussion of the system checkout and implantment.

Table 2-5 shows the performance data for S10P2. All indications are that the system performance was satisfactory.

Table 2-4. Performance Data for Fueled System S10P1

Parameter	Pre-Environmental BOL Performance	Stable Reference Performance	Stable Reference Performance	Pre-Z Axis Shock and Vibration	Post Z Axis Shock and Vibration	Post Y Axis Shock and Vibration	Post X Axis Shock and Vibration	Stable Reference Performance	Stable Reference Performance	Hydrostatic Pressure Test	Stable Reference Performance	Stable Reference Performance	Post-Environmental BOL Performance	Short Term Performance	Stable Reference Performance (at 3Y)	Stable Reference Performance (at YRDI)	Thermocouple No. Per Figure 2.7
Date Month/Day/Year	12/10/68	12/11/68	1 14/69	1/16/69	1/17/69	1 17/6	1/17 69	1 20 69	1/2 69	1/30/69	2/24/69	3/3/69	3/5/69	3 26/69	5/21/69	6/5/69	
System Fuel Input, watts (t)	210.4	210.4	210.0	209.	209.9	20 .	20 .	20 .8	20 .7	20 7	209.3	20 .2	209.2	209.0	208.2	208.0	
Generator Primary Open Circuit (volts)	9. 8	9.81	9.95	9.84	9.79	9.78	9.78	9.93	9.89	1.58	9.79	9.84	9.42	9.40	9.73	9.68	
Generator Bias Open Circuit (volts)	1.41	1.43	1.45	1.44	1.43	1.43	1.43	1.44	1 44	1.3	1.43	1.43	1.37	1.38	1.41	1.41	
Generator Primary Load Voltage (vdc)	4.98	4.97	5.01	5.01	5.01	5.01	5.01	4.99	1.98	5.00	4.96	4.97	4.97	4.98	4.99	4.98	
Generator Bias Load Voltage (vdc)	0.695	0.686	0.691	0.697	0.696	0.695	0.686	0.688	0.687	0.692	0.686	0.687	0.698	0.699	0.693	0.691	
Generator Primary Load Currents (amps)	2.88	2.83	2.83	2.93	2.93	2. 0	2. 0	2.85	2.80	3.00	2.8	2.83	2.95	2.93	2.83	2.85	
Generator Bias Load Current (amps)	0.116	0.124	0.124	0.122	0.122	0.122	0.122	0.124	0.124	0.116	0.124	0 124	0.118	0.120	0.124	0.124	
Generator Primary Power Output, watts (e)	14.3	14.0	14.3	14.7	14.7	14.5	14.	14.2	14.1	1 .0	14.1	14.1	14.7	14.6	14.1	14.2	
Generator Bias Power Output, watts (e)	0.081	0.085	0.086	0.085	0.085	0.085	0.085	0.085	0.085	0.080	0.085	0.085	0 082	0.0838	0.086	0.085	
Generator Total Power Output, watts (e)	14.4	14.1	14.4	14.8	14.8	14.6	14.6	14.3	14.0	1 .1	14.2	14.2	14.7	14.7	14.2	14.3	
Generator Internal Resistance (ohms)	1.50	1.713	1.72	1.64	1.62	1.63	1.63	1.72	1.74	1.52	1.68	1.71	1.50	1.49	1.67	1.63	
Conditioner Total Power Input, watts (e)	14.3	14.1	14.3	14.7	14.7	14 6	14.6	14.3	14.0	15.1	14.2	14.1	14.7	14.6	14.1	14.2	
System Load Voltage (vdc)	24.6	24.4	24.6	24.7	24.6	24.6	24.6	24.6	24.5	24.5	24.4	24.5	24.4	24.5	24.5	24.5	
System Load Current (amps)	0.426	0.426	0.430	0.431	0.430	0.430	0.430	0.428	0.427	0.428	0.423	0.424	0.424	0.425	0.428	0.427	
System Power Output, watts (e)	10.5	10.4	10.6	10.6	10.6	10.6	10.6	10.5	10.	10.5	10.4	10.4	10.4	10.4	10.5	10.5	
System Load Resistance (ohms)	57.7	57.3	57.2	57.3	57.2	57.2	57 2	57.5	57.4	57 2	57.6	57.8	57.5	57.7	57.2	57.4	
Seg. Rct. Ring at Pressure Vessel Wall (°F)	44	86	87	61	61	61	61	87	94	34	87	95	43	47	90	90	1
Seg. Rct. Ring Inner (°F)	56	98	99	75	75	75	75	99	106	44	97	107	53	58	100	100	2
TEG Cold Frame Center (Ext) (°F)	64	106	107	85	84	85	84	107	113	53	106	113	62	65	108	108	3
TEG Hot Frame Center (Ext) (°F)	1050	1084	1078	1065	1061	1061	1060	1081	1079	1032	1072	1079	1033	1031	1068	1068	4
TEG Hot Frame Edge (Ext) (°F)	1066	1098	1091	1077	1073	1072	1073	1093	1093	1047	1086	1093	1047	1045	1081	1081	5
Emitter Plate Center (°F)	1249	1270	1272	1266	1265	1264	1266	1275	1270	1242	1272	1275	1249	1247	1268	1270	6
Reference (°F)	41	88	87	67	65	66	67	86	96	34	87	97	39	42	95	90	7
Water Top (°F)	40	-	--	--	--	--	--	-	-	35	--	--	39	42	--	-	8
Water Center (°F)	40	--	--	-	--	--	--	-	--	34	-	-	38	42	--	--	9
Water Bottom (°F)	40	--	-	--	--		--	--	--	32	--	--	39	42	--	--	10
Average Cold Junction (Estimated) (°F)	92	134	135	113	112	113	112	135	141	82	134	141	90	93	136	136	
Average Hot Junction (Estimated) (°F)	999	1032	1026	1012	1008	1008	1008	1028	1027	980	1020	1027	981	979	1016	1016	
Ambient (°F)	--	72	67	73	69	73	73	65	80	79	79	76	72	72	79	70	
Test Hours	135	168	975	1027	1046	1051	1052	1122	1334	1367	1960	2127	2177	2680	4032	4387	

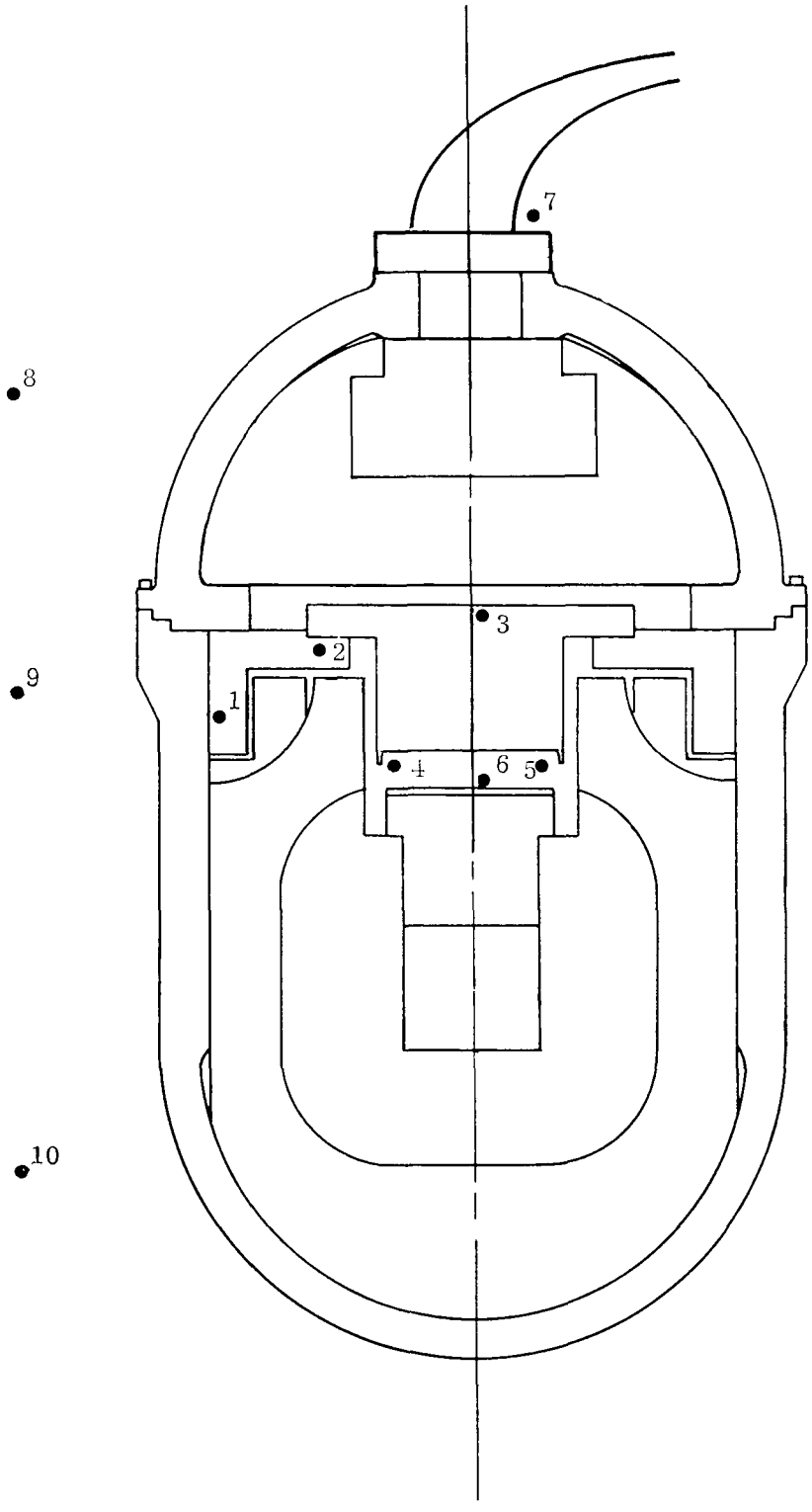

Figure 2-7. General System Instrumentation

Table 2-5. Performance Data for Fueled System S10P2

Parameter	Pre-Environmental BOL Performance	Stable Reference Performance	Stable Reference Performance	Pre-Z Axis Shock and Vibration	Post-Z Axis Shock and Vibration	Post-Y Axis Shock and Vibration	Post-X Axis Shock and Vibration	Stable Reference Performance	Stable Reference Performance	Hydrostatic Pressure Test	Stable Reference Performance	Stable Reference Performance	Post-Environmental BOL Performance	Short Term Performance	Stable Reference Performance (at 3Yr)	Stable Reference Performance (at NRDL)	Thermocouple No. Per Figure 2-7
Date Month/Day/Year	1/2/69	1/3/69	1/18/69	1/20/69	1/21/69	1/21/69	1/21/69	1/22/69	1/30/69	2/8/69	2/24/69	3/4/69	3/7/69	5/12/69	5/21/69	6/4/69	
System Fuel Input, watts (t)	207.7	207.7	207.5	207.4	207.4	207.4	207.4	207.3	207.2	207.1	206.8	206.7	206.6	205.7	205.5	205.3	
Generator Primary Open Circuit (volts)	9.33	9.37	9.72	9.58	9.50	9.46	9.48	9.69	9.71	9.32	9.64	9.66	9.25	9.20	9.63	9.55	
Generator Bias Open Circuit (volts)	1.36	1.41	1.42	1.40	1.39	1.39	1.39	1.42	1.42	1.36	1.41	1.41	1.35	1.35	1.41	1.40	
Generator Primary Load Voltage (vdc)	4.96	4.97	4.98	4.98	4.98	4.98	4.98	4.97	4.98	4.97	4.97	4.96	4.95	4.98	4.99	4.96	
Generator Bias Load Voltage (vdc)	0.686	0.681	0.681	0.687	0.686	0.686	0.686	0.681	0.683	0.682	0.680	0.679	0.688	0.693	0.684	0.679	
Generator Primary Load Current (amps)	2.80	2.73	2.73	2.78	2.78	2.78	2.78	2.78	2.79	2.85	2.79	2.79	2.83	2.80	2.73	2.73	
Generator Bias Load Current (amps)	0.118	0.122	0.122	0.120	0.120	0.120	0.120	0.122	0.122	0.114	0.120	0.122	0.118	0.118	0.122	0.122	
Generator Primary Power Output, watts (t)	13.9	13.6	13.6	13.8	13.8	13.8	13.8	13.8	13.7	14.2	13.7	13.6	14.0	13.9	13.6	13.5	
Generator Bias Power Output (watts)	0.081	0.083	0.083	0.082	0.082	0.082	0.082	0.083	0.083	0.078	0.082	0.083	0.081	0.082	0.083	0.083	
Generator Total Power Output, watts (t)	14.0	13.6	13.7	13.9	13.9	13.9	13.9	13.9	13.8	14.2	13.8	13.7	14.1	14.0	13.7	13.6	
Generator Internal Resistance (ohms)	1.59	1.67	1.72	1.62	1.62	1.61	1.61	1.69	1.72	1.52	1.69	1.70	1.51	1.48	1.69	1.67	
Conditioner Total Power Input, watts (t)	13.9	13.6	13.6	13.9	13.9	13.9	13.9	13.9	13.8	14.2	13.7	13.7	14.1	13.8	13.5	13.5	
System Load Voltage (vdc)	24.9	24.9	24.8	24.9	24.8	24.9	24.9	24.9	24.	24.4	24.9	24.4	24.4	24.5	24.5	24.4	
System Load Current (amps)	0.426	0.426	0.426	0.426	0.427	0.426	0.427	0.429	0.426	0.426	0.427	0.424	0.425	0.427	0.427	0.426	
System Power Output, watts (t)	10.4	10.4	10.5	10.4	10.5	10.4	10.5	10.4	10.4	10.4	10.5	10.4	10.4	10.5	10.5	10.4	
System Load Resistance (ohms)	57.9	57.5	57.8	57.5	57.6	57.5	57.4	57.7	57.9	57.3	57.1	57.6	57.4	57.4	57.4	57.3	
Seg. Ref. Ring at Pressure Vessel Wall (°F)	43	82	88	63	63	69	64	82	[illegible]	31	89	91	44	46	90	88	1
Seg. Ref. Ring Inner (°F)	94	94	100	74	74	79	79	98	100	43	4	101	54	56	99	98	2
TEC Cold Frame Center (Ext) (°F)	62	100	107	81	81	82	83	101	106	46	101	101	61	63	106	104	3
TEC Hot Frame Center (Ext) (°F)	1024 Est.	1035 Est.	1050 Est.	1040 Est.	1048 Est.	1043 Est.	1047 Est.	1056 Est.	1068 Est.	1004 Est.	1048 Est.	1058 Est.	1009 Est.	1006 Est.	1046 Est.	1043 Est.	4
TEC Hot Frame Edge (Ext) (°F)	1039	1069	1072	1052	1050	1050	1049	1068	1072	1019	1062	1067	1023	1020	1060	1057	5
Emitter Plate Center (F)	1241	1290	1253	1241	1241	1243	1253	1254	1255	1214	1250	1253	1225	1222	1247	1246	6
Reference (F)	40	82	87	60	61	61	62	80	0	31	88	88	40	40	86	86	7
Water Top (F)	40									32	-		39	40	--		8
Water Center (F)	40		-	-	--	-	--	-	-	33	--	-	39	40	--	--	9
Water Bottom (F)	40	--	-	-		--		--	--	30	-		39	40		--	10
Average Cold Junction (Estimated) (F)	90	128	135	10	109	110	111	129	131	77	129	136	88	90	133	131	
Average Hot Junction (Estimated) (°F)	72	1003	1007	967	85	86	964	1003	1006	93	99	1001	958	95	992		
Ambient (°F)	-	80	66	69	64	72	73	60	73	77	73	74	75	--		70	
Test Hours	139	161	522	564	591	595	597	614	813	1029	1408	1600	1673	3252	3467	3829	

2.1.2.3 System S10P3

a) Performance Testing

System S10P3 continued on test this past quarter. Table 2-6 shows performance data for the system. It appears that the performance for the system is satisfactory.

b) System Environmental and Characterization Tests

The system was characterized for various system resistive loads at 40°F - 60°F and 80°F environmental water temperatures. The following parameters will be used to define the performance; generator power voltage, current, cold junction temperature and hot junction temperature each as a function of system resistance load at each environmental water condition, system power out, current and voltage as a function of resistance load at each environmental water condition, and generator cold and hot junction temperatures as a function of time.

These data were prepared and submitted to the AEC as part of the data package accompanying each fueled system.

2.1.2.4 System S10P4

All components for system S10P4 were shipped to ORNL. The system was fueled and final-assembled during the week of May 19, 1969. As was done on system S10P3, particular attention was given to the "Blue Ribbon" connectors. In accordance with revised Process Routings, the connectors were carefully cleaned and re-examined visually to assure that no foreign material was present. This added attention was provided to prevent the occurrence of a connector problem such as was reported on system S10P2.

A Quality Assurance representative was at ORNL during the period for the assembly, fueling, BOL test, preparations for shipping, and actual shipping operations of system S10P4.

Following assembly at ORNL, the fueled system S10P4 was shipped to Sandia for dynamic testing.

Table 2-6. Performance Data for Fueled System S10P3

Parameter	Pre-Environmental BOL Performance	Stable Reference Performance	Stable Reference Performance	Pre-Y Axis Shock and Vibration	Post-Y Axis Shock and Vibration	Post-X Axis Shock and Vibration	Stable Reference Performance	Stable Reference Performance	Hydrostatic Pressure Test	Stable Reference Performance	Stable Reference Performance	Post-Environmental BOL Performance	Short Term Performance	Thermocouple No. Per Figure 2-7
Date Month Day/Year	2 [illegible] 6	2 13/6	[illegible] 6?	6?	3/1 6?	3/4 6?	3/4/69	3/ 5/69	3/19/69	3/21/69	3/23/69	4/3/69	4/8/69	6/26/69	
System Load [illegible] s(t)	2 3 >	213	213 3	213	213 3	213 3	213 3	213 3	213 1	213 0	213.0	212.8	212.8	211.7	
Generator Primary Open Circuit (volts)	9 75	10 00	10.12	9. 9	9 92	9 91	9 9[illegible]	10 08	10 04	9.84	10.05	10 04	9 65	9.51	
Generator Bus Open Circuit (volts)	1 42	1 4[illegible]	1 4[illegible]	1 41	1 41	1	1 46	1 47	1 46	1 43	1.46	1 46	1.41	1.39	
Generator Primary Load Voltage (vdc)	4	4.47	4	4.	4 9	4 98	4 98	4 97	4.99	5 00	4.99	4.98	4.98	4.96	
Generator Bus Load Voltage (vdc)	0 [illegible]0	0 69	0 700	0 702	0 701	0 703	0 702	0 69[illegible]	0 698	0 698	0.698	0 695	0.704	0.703	
Generator Primary Load Current (amps)	2 0	2.0[illegible]	2 [illegible]	2 [illegible]8	2 [illegible]8	2 [illegible]8	2 9	2 9[illegible]	2 88	5 00	2.88	2.85	2.95	2.92	
Generator Bus Load Current (amps)	0 12[illegible]	0 126	0 126	0 124	0 122	0 12[illegible]	0 124	0 124	0 124	0 118	0.124	0 124	0 120	0 120	
Generator Primary Power Output watts (c)	4 [illegible]	14 2	14 2	14 6	14 6	4 6	14 7	14 2	14 4	14 0	14.4	14 2	14.7	14.5	
Generator Bus Power Output watts (c)	0 0[illegible]	0 0	0 0[illegible]	0 087	0 0 6	0 0[illegible]	0 08[illegible]	0 086	0 086	0 082	0.086	0.086	0.084	0.084	
Generator Input Power Output, watts (c)	14	14 2	14 3	14	14 [illegible]	14	14	14 2	14 3	14 1	14. 3	14.3	14 8	14.6	
Generator Internal Resistance (ohms)	1 63	1.78	1 73	1.66	1 67	1 [illegible]	1 68	1 78	1 74	1 80	1.75	1.76	1.58	1.55	
Conditioner Input Power Input, watts (c)	14	14 [illegible]	14.3	14 6	14 [illegible]	14 6	14 [illegible]	14.[illegible]	14.4	14 0	14 4	14 1	14.6	14.3	
System Load Voltage (vdc)	24 3	24.5	24 6	24 3	24 3	24.	24 3	24 3	24 5	24 5	24.5	24.5	24.5	24.5	
System Load Current (amps)	0.42	0 426	0 42	0 428	0 42	0 42	0 42	0 427	0.428	0 428	0 428	0 428	0 426	0.425	
System Power Output watts (c)	10.	10 4	0	10	10	10 3	10 3	0 3	10 3	10 3	10.5	10.5	10 4	10.4	
System Insulation Resistance (ohms)	[illegible]	5[illegible]	5 3	5 2	57 2	57 [illegible]	57 2	57 4	57 2	57 2	57.2	57 2	57 2	57.6	
Seg Rot Ring Pressure Vessel Wall (1)	44	2		64	61	64	64	6	2	47	64	96	44	43	1
Seg Rot Ring Dome (1)	6	94	110	0	0	80	80	90	94	47	96	108	58	54	2
HG Collector Center (Ext) (1)	64	102	11[illegible]		87		97	116	102	86	104	116	66	63	3
HG Bottom Center (Ext) (1)	1090	0 3	10	100	07	1078	1077	0 3	0	1044	1083	1088	1044	1035	4
HG Hot Inner Edge (Ext) (1)	1072	1106	1010	10 6	1086	1088	1042	1110	1087	1061	1098	1104	1061	1052	5
Emitter Plate Center (1)	1236	1242	12 6	1 [illegible]	1 [illegible]6	12 6	1290	1304	1293	1261	1294	1296	1269	1262	6
Reference (1)	40	83	87	81	72	71	71	96	81	87	85	96	42	42	7
Water Top (1)	40							-	-	41			42	42	8
Water Center (1)	40		-			-	-		-		-		42	42	9
Water Bottom (1)	40	-	-			-	-		-	40	-		42	42	10
Average Condition (Estimated) (1)	92	130	145	116	11 3	1 6	115	144	130	85	132	144	84	81	
Average Heat Input (Estimated) (1)	100	1033	1044	101	1020	1022	1023	1044	1030	903	1032	1037	933	984	
Ambient (°F)	62	71	7 3	62	73	63	72	72	67	74	72	68	71	72	
Test Hours	11[illegible]	16	3 0	30	473	4 7	480	490	334	366	931	1105	1319	3113	

Table 2-7. System Environmental and Characteristics Test – S10P3

Water Temperature	System Load	Thermoelectric Generator						System		
		Hot Frame Temperature °F	Cold Frame Temperature °F	Primary Load Voltage (V)	Primary Load Current (A)	Resistance (Ω)	Primary Power Out (W)	Load Voltage (V)	Load Current (A)	Power Out (W)
40° I	37.0Ω	1047	66	4.54	3.20	1.[illegible]	14.5	21.9	0.[illegible]	12.9
	42.0Ω	1051	67	4.83	3.03	1.58	14.7	23.6	0.557	13.2
	47.0Ω	1052	66	4.97	2.9[illegible]	1.59	14.7	24.[illegible]	0.516	12.7
	51.1Ω	10[illegible]2	65	4.97	2.95	1.[illegible]8	14.7	24.[illegible]	0.47[illegible]	11.6
	57.6Ω	1052	64	4.97	2.9[illegible]	1.57	14.7	24.5	0.426	10.4
	65.0Ω	1052	66	4.97	2.9[illegible]	1.[illegible]9	14.7	24.[illegible]	0.372	9.1
	80.0Ω	1052	65	4.97	2.95	1.58	14.7	24.5	0.[illegible]06	7.[illegible]
60° I	37.0Ω	1060	81	4.[illegible]1	3.1[illegible]	1.62	14.3	21.[illegible]	0.[illegible]0[illegible]	12.[illegible]
	42.0Ω	1062	80	4.81	3.03	1.61	14.6	23.5	0.[illegible]5[illegible]	13.0
	47.0Ω	1065	80	4.97	2.93	1.62	14.6	24.[illegible]	0.51[illegible]	12.7
	51.1Ω	1064	80	4.98	2.9[illegible]	1.62	14.6	24.[illegible]	0.475	11.6
	57.6Ω	1062	82	4.97	2.90	1.62	14.4	24.[illegible]	0.426	10.4
	65.0Ω	1064	82	4.97	2.90	1.63	14.4	24.[illegible]	0.[illegible]73	9.1
	80.0Ω	1063	82	4.97	2.90	1.64	14.4	24.5	0.[illegible]06	7.5
80° I	37.0Ω	1083	101	4.45	3.15	1.70	14.0	21.6	0.[illegible]7[illegible]	12.5
	42.0Ω	1082	101	4.76	3.00	1.69	14.3	23.3	0.546	12.7
	47.0Ω	1084	100	4.97	2.90	1.69	14.4	24.[illegible]	0.[illegible]1	12.7
	51.1Ω	1084	102	4.97	2.89	1.70	14.4	24.[illegible]	0.47[illegible]	11.6
	57.6Ω	1082	101	4.97	2.83	1.70	14.3	24.5	0.426	10.4
	65.0	1082	100	4.97	2.[illegible]9	1.69	14.4	24.[illegible]	0.372	9.1
	80.0Ω	1082	100	4.97	2.89	1.69	14.4	24.[illegible]	0.30[illegible]	7.[illegible]

Shock and Vibration

A Quality Assurance representative was at Sandia during the period 10 through 13 June 1969 to witness equalization of the test equipment, preparation of fueled system S10P4 for dynamic testing, and actual testing operations. A thorough surveillance of methods and procedures with emphasis on calibration controls was made by the 3M Quality Control engineer.

The shock and vibration testing was completed on fueled system S10P4 on June 13, 1969. The required tests to specifications were successfully conducted with no change in system performance. Upon arrival at the test facility, the system and equipment were inspected for transportation damage. The temperature recorder and impactograph on the shipping container were inspected and dated.

A stable reference performance test was conducted on the system prior to removal from the shipping container.

During the stable reference performance period, a dummy load equal to system weight was placed in the shock and vibration fixture and attached to the vibration machine. The recorded shock pulses used on fueled systems S10P1, S10P2 and S10P3 were utilized on the dummy load configuration and found to be identical to previous trials and satisfactory for S10P4 shock testing.

The vibration equipment was given an operational check-out by conducting one sweep at the required input levels and duration.

Maximum acceleration (g) was measured and recorded during an emergency automatic shut-down by causing the amplifier to go into automatic shut-down at a frequency of 6 Hz.

Following equipment capability verification, system S10P4 was placed into the shock and vibration fixture, the cooling ring was attached, and the system was allowed to stabilize.

The system was subjected to the required levels and durations for vibration and shock, as indicated below:

Vibration

5 – 5-1/2 Hz at 0.8 in DA displacement

5-1/2 – 26 Hz at 1.3 g peak acceleration

26 – 40 Hz at 0.036 in DA displacement

40 – 50 Hz at 3.0 g peak acceleration

Sweep three times 5-50-5 Hz in three axes in a period of 45 minutes per axis.

Shock

Terminal peak sawtooth wave pulse with a magnitude of 6 g and a duration of 6 milliseconds.

Three shock pulses in each direction of the three major axes (total 18 shocks).

System performance readings were taken before and after each sweep of vibration and each three shock pulses. See Table 2-8.

After successfully completing the vibration and shock requirements, system S10P4 was removed from the shock and vibration fixture.

Cooling fins were attached and the system was placed into the shipping container, after which a stable reference performance test was conducted.

During the entire time that the fueled system was at the Sandia Test Laboratories, the system was monitored at least once daily for a radiation hazard by the Sandia Health/Physics Department.

No changes in radiation levels were found on the system throughout the dynamic testing.

Table 2-8. Performance Data for System S10P4

Parameter	Pre-Environmental BOL Performance	Stable Reference Performance	Stable Reference Performance	Pre-Z Axis Shock and Vibration	Post-Z Axis Shock and Vibration	Post-Y Axis Shock and Vibration	Post-X Axis Shock and Vibration	Stable Reference Performance	Thermocouple No. Per Figure
Date Month/Day/Year	5/28/69	5/29/69	6/11/69	6/12/69	6/12/69	6/12/69	6/13/69	6/16/69	
System Fuel Input, watts (t)	210.4	210.4	210.0	210.0	210.0	210.0	210.0	210.0	
Generator Primary Open Circuit (volts)	9.64	10.0	10.0	9.91	9.78	9.83	9.82	10.12	
Generator Bias Open Circuit (volts)	1.41	1.46	1.46	1.45	1.44	1.44	1.44	1.48	
Generator Primary Load Voltage (vdc)	4.98	4.99	4.99	5.00	4.99	4.98	4.99	4.99	
Generator Bias Load Voltage (vdc)	0.701	0.696	0.692	0.700	0.699	0.698	0.700	0.692	
Generator Primary Load Current (amps)	2.88	2.85	2.83	2.90	2.88	2.88	2.88	2.83	
Generator Bias Load Current (amps)	0.118	0.124	0.124	0.122	0.122	0.122	0.122	0.126	
Generator Primary Power Output (watts)	14.3	14.2	14.1	14.5	14.4	14.3	14.4	14.1	
Generator Bias Power Output (watts)	0.083	0.086	0.086	0.085	0.085	0.085	0.085	0.087	
Generator Total Power Output (watts)	14.4	14.3	14.2	14.6	14.5	14.4	14.5	14.2	
Generator Internal Resistance (ohms)	1.61	1.75	1.77	1.68	1.65	1.67	1.67	1.80	
Conditioner Total Power Input (watts)	14.3	14.2	14.1	14.5	14.4	14.4	14.4	14.2	
System Load Voltage (vdc)	24.5	24.5	24.6	24.5	24.5	24.4	24.5	24.6	
System Load Current (amps)	0.426	0.426	0.426	0.426	0.426	0.426	0.426	0.426	
System Power Output (watts)	10.4	10.4	10.5	10.4	10.4	10.4	10.4	10.5	
System Load Resistance (ohms)	57.5	57.5	57.7	57.5	57.5	57.3	57.5	57.7	
Seg. Ret. Ring at Pressure Vessel Wall (°F)	44	83	90	62	63	64	61	99	1
Seg. Ret. Ring Inner (°F)	57	96	102	78	79	80	77	111	2
TEG Cold Frame Center (Ext) (°F)	65	103	110	85	87	87	85	119	3
TEG Hot Frame Center (Ext) (°F)	1058	1094	1094	1079	1071	1072	1071	1103	4
TEG Hot Frame Edge (Ext) (°F)	1070	1106	1105	1089	1081	1083	1082	1112	5
Emitter Plate Center (°F)	1258	1283	1284	1276	1270	1270	1271	1292	6
Reference (°F)	41	84	89	68	69	69	67	98	7
Water Top (°F)	40	–	–	–	–	–	–	–	8
Water Center (°F)	40	–	–	–	–	–	–	–	9
Water Bottom (°F)	40	–	–	–	–	–	–	–	10
Average Cold Junction (Estimated) (°F)	93	131	138	113	115	115	113	147	
Average Hot Junction (Estimated) (°F)	1004	1040	1041	1024	1017	1019	1018	1049	
Ambient (°F)	70	66	72	68	74	73	74	77	
Test Hours	92	117	432	454	457	463	480	550	

Following the post-test stable reference performance test, the system was placed into a short-circuit condition and shipped to Southwest Research Institute for hydrostatic pressure testing, which is to be conducted in July 1969.

Sandia is preparing a complete test report on the shock and vibration testing.

2.1.2.5 Fueled System Performance Predictions

The electrical and thermal performance of the first three fueled SNAP-21 10-watt systems has been predicted for a range of "off-design" conditions including variable system load resistances and sea water temperatures. The results of these predictions are shown graphically in Appendix A.

The design of the SNAP-21 system was originally based on its operation in +40°F sea water at a fixed system load resistance of 57.6Ω and a BOL fuel loading of 209 watts (t). Under actual operating conditions, however, the system may operate under a wide range of sea water temperatures and load resistances, and the BOL fuel loading can vary within the manufacturing tolerances of 209-219 watts (t). The system performance characteristics are affected by these variables, as well as by normal manufacturing tolerances, and the normal thermal decay of the radioisotope fuel over the five-year life of the system. Consequently, in order to predict system performance accurately, it is necessary to evaluate each fuel loading and specific component performance.

Although the specification requirements of the SNAP-21 system are to provide a minimum of 10 watts of conditioned electrical power at the end of five years, it is desirable to compare the actual system performance with predicted performance at intermediate points in the five-year period. These comparisons are for the purpose of detecting abnormal performance that could result in a system life of less than five years.

To provide a basis for comparison, the electrical performance of each individual system was predicted at one year intervals for sea water temperatures of 40, 60 and 80°F and system load resistances varying from 30 to 85Ω. In addition, the performance of each thermoelectric generator and the temperature profile of each system was predicted for the same range of sea water temperatures at the system design load resistance of 57.6Ω.

The input data used to prepare the system performance predictions consists of: experimental test data, derived thermal properties of each individual system, the known fuel decay rate, and computer programs that characterize the performance of the thermoelectric generator and the power conditioner. A simplified flow diagram showing the data inputs and the analytical procedure used for these predictions is shown in Figure 2-8. Further details of the analytical procedure are presented in Appendix B.

As mentioned previously, the SNAP-21 system is designed to operate at a fixed load resistance of 57.6Ω. When operated in this condition, the power output of the system will be a constant 10 – 10.5 watts because the power conditioner contains a voltage regulator circuit that maintains the output voltage at 24 ± 1 vdc. The excess power produced by the TEG prior to the end-of-life is dissipated within the voltage regulator circuit of the power conditioner. When system load resistance is increased, the power output will be reduced since the voltage is limited. However, when system load resistance is decreased, the reduced resistance with constant voltage results in an increased current flow and thus increased power. The power output will continue to increase until all available power from the TEG is being delivered to the load, and the only losses are those due to the efficiency of the power conditioner. If the system load resistance is reduced far enough, the voltage will fall below the minimum specification limit of 23 vdc and will continue to fall until the power conditioner becomes unstable.

At extreme "off-design" values of system load resistance which result in system load voltages below 23 vdc, the analytical model of the power conditioner does not precisely predict system performance due to the non-linear characteristics of the power conditioner circuit. Therefore, some deviation between predicted and actual data can be observed in the low resistance regime.

It should also be noted that the test data used to predict system performance was measured on systems operating in clean fresh water with a clean pressure vessel. Operation in a sea environment where sediment and fouling may be present could affect cold end heat rejection and therefore system performance. Another factor that may cause a difference between laboratory and sea environment data is the slight cooling water agitation that is present in the laboratory test set-up. This agitation is created by the introduction of a small amount of air at the bottom edge

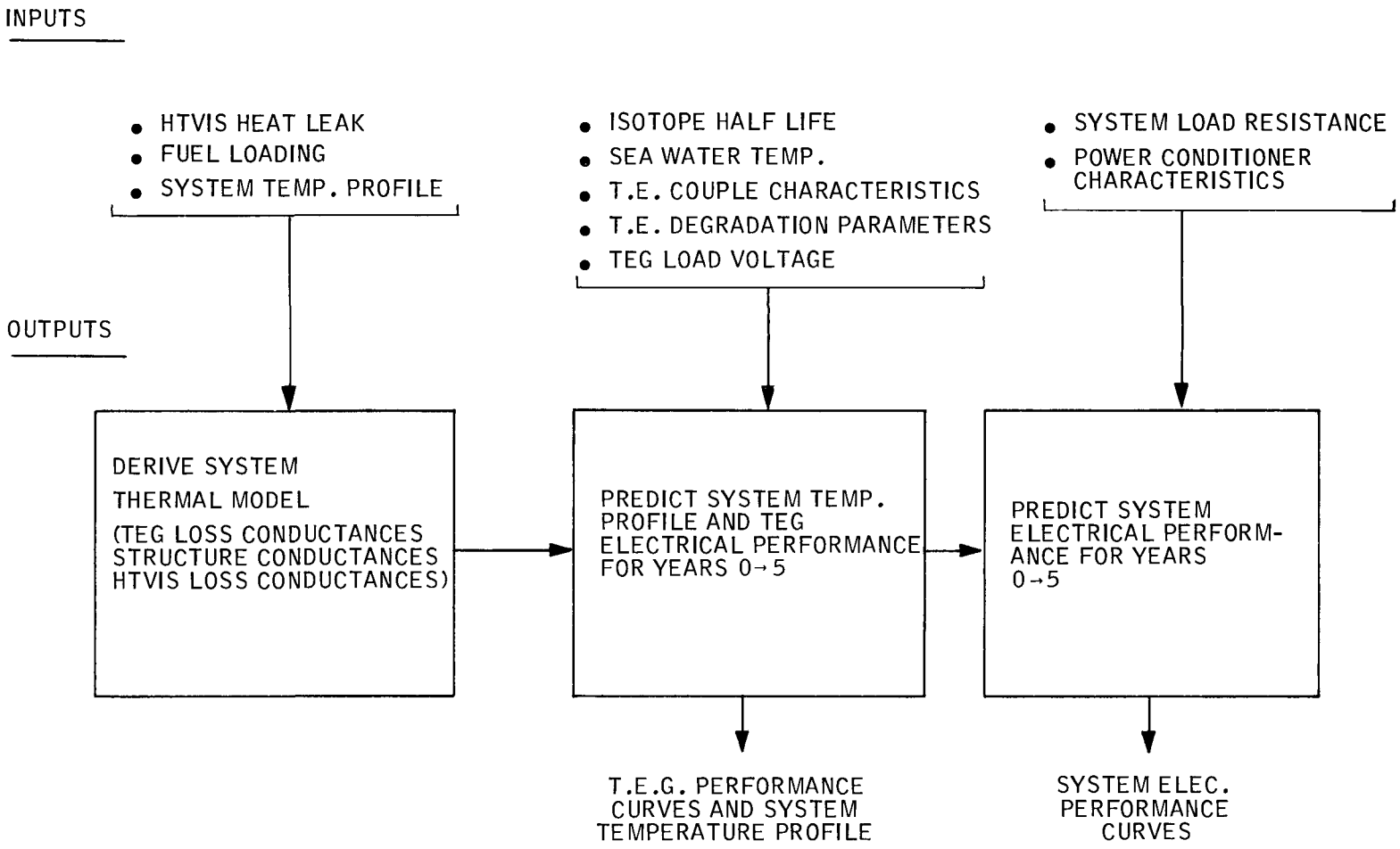

Figure 2-8. Flow Diagram for Performance Prediction of 10-Watt SNAP-21 Fueled Systems

of the water tank to improve heat transfer from the cooling coils to the water and thus prevent cooling coil freeze-up. This agitation also increases the film conductance between the pressure vessel and the cooling water which lowers the cold end temperature profile over that of quiescent water. The effect of this improved heat transfer is expected to be less than 10°F on the cold end temperatures.

2.2 FUEL CAPSULE

No effort was expended on this component during this report period.

2.3 BIOLOGICAL SHIELD

The biological shield which was removed from insulation system B10DL1 was received by 3M Company, cleaned, gamma stabilized, and replated with copper. Quality Control personnel provided both surveillance of the refurbishing process and surveillance of the plating vendor. The vendor was conditionally approved for the special plating process. The shield was crated and shipped to Linde, where it was incorporated into insulation system B10DL8.

2.4 INSULATION SYSTEMS

2.4.1 Rethermal Test and Leak Check of Unit B10D2

Development Unit B10D2 was rethermal tested and leak checked during this reporting period. This unit was sealed-off on December 26, 1967 and delivered to 3M Company. Recently while the unit was on long-term test at 3M, it was noted that the power requirement to maintain a constant emitter plate temperature was increasing, indicating that the system heat loss was increasing. To aid in determining what was causing the higher heat loss of the system, Linde was asked to rethermal test the unit and compare the performance to the original as delivered performance.

Upon receipt at Linde, the unit was prepared for a thermal test by installing the unit in a unit manipulating fixture and insulating the neck tube area above the heater block with Min-K 2000 insulation in the same manner as was originally performed in order that the thermal performance determinations would be directly

comparable. The unit was electrically heated to the 1285°F operating temperature, it was determined that it required 98.6 watts to maintain this temperature. The two-dimensional subtractibles to account for the heater wires and Min-K insulation were previously calculated to be 24.2 watts, which yields an insulation system heat loss of 74.4 watts. The previously measured unit heat loss in December 1967 was 47.7 watts. The difference between the unit performance now and originally is, therefore, an increase of 26.7 watts. It was expected that this deterioration in performance was caused by a leak in the unit causing a partial loss of vacuum. Following the thermal performance test, the unit was fast cooled using the 3M company-supplied water-cooled copper chill block.

In light of the deteriorated thermal performance, it was decided that Linde recommend that the insulation space pressure and gas composition be determined and, that if a leak was apparent, the leak should be located and the absolute leak rate should be determined.

The unit pressure was determined by drilling into the unit through the seal-off device plug using a vacuum sealed drill apparatus. While drilling into the unit, it was determined that the vacuum space pressure was 6.03 torr. Two 0.50 liter glass sample bulbs were filled with the gas in the insulation space and were analyzed with a mass spectrometer to determine the gas composition. The results of the analysis of this gas was as follows:

	Analysis 13431-81-22 Percent	Analysis 13431-81-30 Percent	Average Percent
Hydrogen	0.08	0.10	0.09
Argon	15.8	16.95	16.38
Nitrogen	84.2	82.90	83.55

This analysis clearly shows that the pressure in the vacuum space is the result of a leak in the vacuum system in that nitrogen and argon do not result in any appreciable quantity from off-gassing. The presence of hydrogen and nitrogen further shows that the getter has been totally used. The lack of any oxygen in the analysis results from the fact that there is a considerable surface area in the unit which is oxidizing, thus causing the removal of the free oxygen. Following

the pressure determination, the unit was evacuated and subjected to a helium leak check. The absolute leak rate was 3.1×10^{-4} atm. cc air/sec. This leak was found to be in the solder joint where the vacuum gauge adaptor is threaded into the upper enclosure head on the side nearest the inner liner.

Pending instructions as to the disposition of this unit, the unit has been placed in a HTVIS shipping container for storage.

2.4.2 Salvage of Components from Damaged Unit B10DL3

Upon return of Unit B10DL3 by common carrier truck from Ogden Technological Laboratories in Deer Park, Long Island, New York, disassembly was performed to salvage reusable components.

The initial step prior to actual disassembly was to determine if the vacuum had been lost when the neck tube was buckled due to a test machine malfunction. A small hole was put in the neck tube with a center punch. Air could be heard entering, and the bottom head became hot to the touch in the getter area, indicating that the getter was still active and that a vacuum had been maintained. It is, therefore, concluded that the buckling of the neck tube did not cause a vacuum leak. Next, the unit was mounted on a shaft and put in a horizontal position in a unit handling fixture. Each receptacle seal-off plug was drilled out and the tension rod anti-rotation pins were removed. The female tension rods were easily unthreaded but were not removed. The bottom enclosure head was cut off with a seam grinder. The female tension rods were removed and it was noted that all three rods were slightly bent near the spherical ball.

The lower head was removed and the insulation cut circumferentially, approximately two inches below the head cut-off point. The insulation was removed from the bottom of the unit; it was noted that black radioactive powder covered the bare shield, but there was no evidence of flaking as was noted on Unit B10DL1. When the spider bolt safety wire was cut, the bolt, as well as the spider, was found to be only finger tight. In removing the male rods from the spider, two of the retainer pins broke. The rods were free in the spherical sockets. All three rods were bent slightly to different degrees, generally in the same plane as the retainer pin hole.

Following cleaning of the lower end of the radiation shield, the unit was placed on the floor in a vertical position. The upper head was removed by chiseling through the neck tube slightly above the bolt flange. The upper head and insulation were then removed and it was noted that the upper end of the radiation shield had the same appearance as the lower end. After starting to remove the liner bolts safety wire, it was observed that the bolts were loose. This was not due to unthreading, but to an increase in thread clearance. All bolts were only finger tight, and when removed allowed the liner to move freely in the radiation shield and to be removed easily.

All components were cleaned under supervision of the Linde Radiation Safety Officer. The radiation shield, spider, spider bolt and washer, liner washers and bolts, and the inner liner were packaged and shipped to 3M Company.

2.4.3 Insulation System B10DL6

This insulation system continued on test this past quarter. Table 2-9 shows performance data for this unit. Refer to Figure 2-9 for location of thermocouples.

2.4.4 Insulation System B10DL7

The Linde and 3M-supplied components were inspected by Quality Control personnel. The spider sockets were lapped with the support rod's male end. The spider and inner liner were attached to the biological shield.

A Quality engineer was at Linde during the period of April 1 and 2, 1969, to survey Linde operations. The dimensional inspection and initial assembly of this system were witnessed. Application of the insulation material to the biological shield was then completed. The top enclosure head was aligned and semi-automatically welded to the inner liner. The bottom enclosure head was automatically welded to the top enclosure head. The tension rods were installed at an angle of 27 degrees and 30 minutes. The tension rod spherical washers were pinned to the receptacles, the anti-rotation pins were installed, and the receptacle seal-off plugs were welded into place. The unit was evacuated and subjected to a helium leak test with the result being that the leak rate was acceptable.

Table 2-9. HTVIS B10DL6 Thermal Performance Data

Thermocouple Number Refer to Figure 2-9	Location	Performance Data		
		4/30/69	5/20/69	6/24/69
# 1	Cold Frame	83	88	81
# 2	Cold Frame	83	88	81
# 3	Hot Frame External Edge	1050	1043	1032
# 4	Hot Frame External Middle	1068	1065	1053
# 5	Hot Frame External Center	1046	1042	1028
# 6	Emitter Top Edge	1249	1244	1233
# 7	Emitter Top Middle	1266	1260	1250
# 8	Emitter Top Center	1253	1248	1237
# 9	Emitter Bottom Center	1273	1268	1257
#10	Heater Block Side	1392	1387	1377
#11	Heater Block Bottom	1406	1401	1391
	Power Input	208	206	208*
	Test Hours	1344.5	1824	2664.5

*Watt transducer was calibrated on 6/16/69 and was found to be reading 1.5 watts high.

The unit was then instrumented for conditioning. The unit was evacuated, heated to 1400°F and held at this temperature for 48 hours to provide the required processing. Following the conditioning, the unit was cooled to operating temperature, and the pressure rise rate was determined to be acceptable.

Following the pressure rise rate determination, 15 grams of regular getter were installed in the unit, and the unit was sealed off.

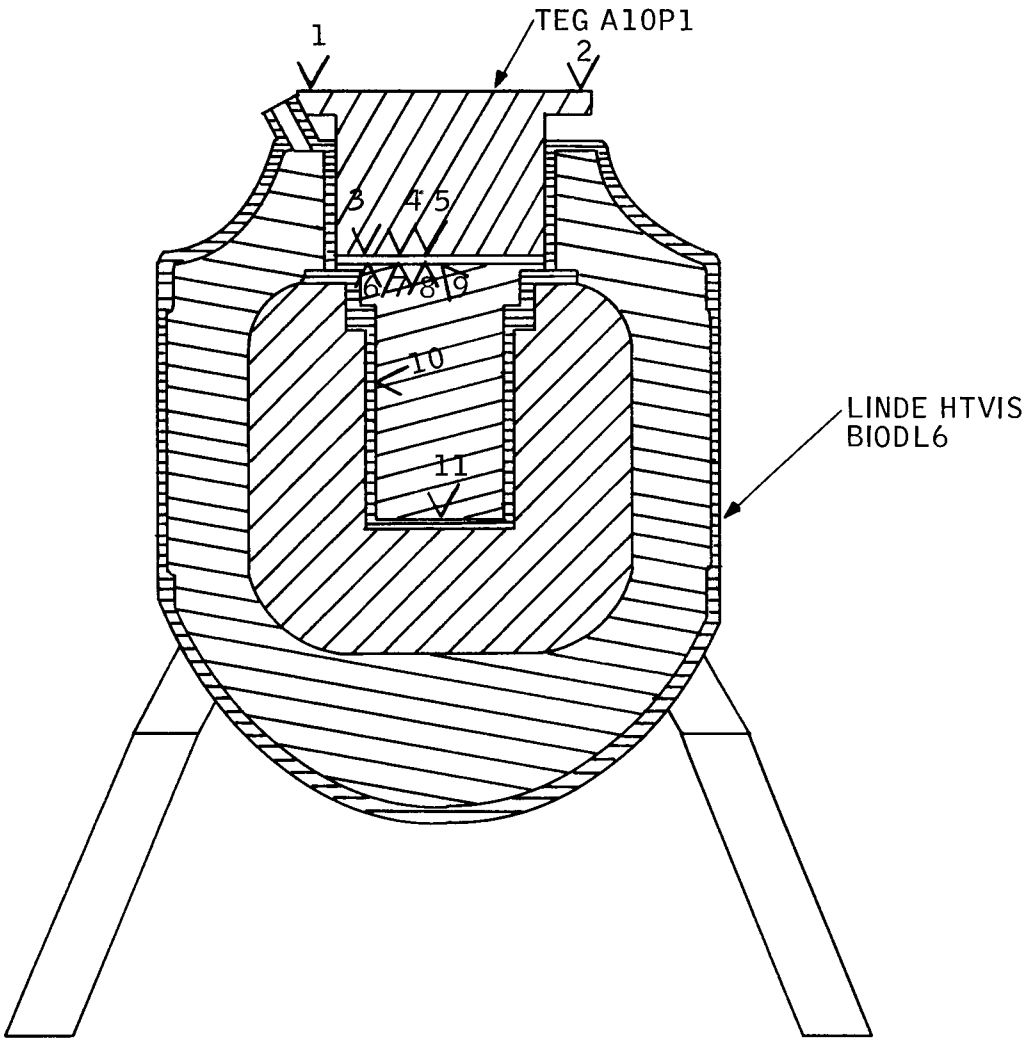

Figure 2-9. Instrumentation for HTVIS B10DL6 and TEG A10P1

The thermal performance test was then conducted. It was found that a corrected power input of 67.2 watts was required to maintain the unit at a nominal 1285°F operating temperature. The subtractable heat loss due to the Min-K insulation, heater and thermocouple wires, and power lead loss is 14.1 watts. This yields a total heat loss of the unit of 53.1 watts. The required heat loss at test conditions to be equivalent to the specification heat loss of 45 watts is 42.6 watts. This unit, therefore, has a heat loss in excess of specifications of 10.5 watts.

Following the thermal performance test, the unit was fast cooled using a chill block. After cooldown, the unit was installed in a HTVIS shipping container and shipped to Oak Ridge National Laboratory. An impactograph was mounted to record the shocks transmitted to the unit during transit. This unit was incorporated into system S10P4.

2.4.5 Insulation System B10DL8

The inner liner and spider for this system were plated and then ground to match the biological shield. All components were inspected by Linde, and the assembly of the biological shield, inner liner, and spider was completed. The insulation material was then applied to the biological shield. The top enclosure head was aligned and semi-automatically welded to the inner liner. The bottom enclosure head was automatic-welded to the top enclosure head. This welding was recorded on 16 mm movies by 3M photographers.

Continuing with the fabrication of this unit, the tension rods were installed at an angle of 27 degrees and 30 minutes. The tension rod spherical washers were pinned to the receptacles, the anti-rotation pins were installed, and the receptacle seal-off plugs were welded into place. The unit was evacuated and subjected to a helium leak test with the result being that the leak rate was acceptable.

The unit was then instrumented for conditioning. The unit was evacuated and heated to 1400°F and held at this temperature for 48 hours to provide the required processing. Following the conditioning, the unit was cooled to operating temperature and the pressure rise rate was determined to be acceptable. To determine if further conditioning would reduce the unit heat loss, a thermal performance test was conducted while still evacuating the unit. This thermal test showed the unit

to have a heat loss of 53.0 watts. Following the thermal test, the unit was again heated to 1400°F and maintained at this temperature for an additional 106 hours to condition the unit further. The unit was cooled to operating temperature and the pressure rise rate was determined to be acceptable. Fifteen grams of regular getter were installed in the unit.

After the unit was sealed off, the thermal performance test was conducted as presented in the Acceptance Test Plan. It was found that it required a corrected power input of 64.1 watts to maintain the unit at a nominal 1285°F operating temperature. The subtractable heat loss due to the Min-K insulation, heater and thermocouple wires, and power lead loss is 14.1 watts. This yields a total heat loss of the unit of 50.0 watts. The required heat loss at test conditions to be equivalent to the specification heat loss of 45 watts is 42.6 watts. This unit, therefore, has a heat loss in excess of specifications of 7.4 watts.

Following the thermal performance test, the unit was fast cooled. After cooldown, the unit was installed in a HTVIS shipping container and shipped to 3M Company. An impactograph was mounted to record the shocks transmitted to the unit during transit.

The additional 106 hours of conditioning at 1400°F caused the insulation system heat loss to be reduced by 3.0 watts. Table 2-10 presents a summary of the thermal performance of all the Task I HTVIS units. It appears that the delivery units (DL series) would exhibit a lower heat loss than measured if more complete conditioning could be performed, as was accomplished on Unit B10D4. Presently, conditioning cannot be performed at 1550°F because creep in the tension rods would cause the loss of preload.

2.5 THERMOELECTRIC GENERATOR

2.5.1 Phase I

Data collection and analysis of the Phase I 6-couple modules and prototype generators continued during this quarter. Performance data for 6-couple modules A1, A3, and A4 is given in Table 2-11 and Figures 2-10 through 2-12. Data from prototypes P5, P6, and P7 are given in Tables 2-12 through 2-14 and Figures 2-13 through 2-15.

Table 2-10. Summary of HTVIS Unit Thermal Performance

Unit Number	Unit Heat Loss at 1285°F Watts	Insulation Composition	Conditioning Time and Temperature While Evacuating
B10D1	50.2	45 layers nickel 60 layers copper 60 layers aluminum	Temperature rise from 1300°F to 1470°F in 88 hours
B10D2	47.7	45 layers nickel 60 layers copper 60 layers aluminum	46 hours at 1550°F
B10D3	47.0	45 layers nickel 60 layers copper 60 layers aluminum	21 hours at 1550°F
B10D4	42.9	105 layers copper 60 layers aluminum	33 hours at 1550°F
B10DL1	48.1	105 layers copper 60 layers aluminum	48 hours at 1400°F
B10DL2	49.1	105 layers copper 60 layers aluminum	48 hours at 1400°F
B10DL3	50.6	105 layers copper 60 layers aluminum	48 hours at 1400°F

Table 2-10. Summary of HTVIS Unit Thermal Performance (Continued)

Unit Number	Unit Heat Loss at 1285°F Watts	Insulation Composition	Conditioning Time and Temperature While Evacuating
B10DL4	53.9	105 layers copper 60 layers aluminum	48 hours at 1400°F
B10DL5	50.8	105 layers copper 60 layers aluminum	48 hours at 1400°F
B10DL6	47.7	105 layers copper 60 layers aluminum	Overhaul of B10Q1 used for thermal force cycles
B10DL7	53.1	105 layers copper 60 layers aluminum	48 hours at 1400°F
B10DL8	53.0	105 layers copper 60 layers aluminum	48 hours at 1400°F
	50.0	105 layers copper 60 layers aluminum	Additional 106 hours at 1400°F

Table 2-11. Performance Data of SNAP-21 6-Couple Modules

Module	Date	T_h (°F, est)	T_c (°F)	E_o (volts)	E_L (volts)	I_L (amps)	P_o (watts)	R (milliohms)	P_I (watts)	Hours
A1	8-4-64	1100	115	1.31	0.66	1.96	1.29	342	38.0	192
	2-25-65	1100	114	1.35	0.68	2.09	1.41	323	39.0	5,112
	7-23-65	1100	114	1.35	0.67	2.00	1.34	341	37.0	8,664
	10-7-65	1100	113	1.35	0.68	1.97	1.33	342	38.0	10,488
	10-9-65			Power Input Reduced						
	10-9-65	1080	114	1.33	0.67	1.94	1.29	340	36.0	10,536
	4-14-66	1080	113	1.33	0.65	1.91	1.25	352	36.0	15,021
	10-13-66	1080	113	1.33	0.65	1.88	1.21	364	36.0	19,389
	10-13-66			Power Input Reduced						
	10-17-66	1060	113	1.29	0.64	1.84	1.17	355	36.0	19,485
	6-23-67	1060	115	1.29	0.63	1.83	1.15	361	36.0	25,581
	10-16-67	1060	115	1.30	0.64	1.86	1.18	356	36.0	28,341
	10-19-67			Power Input Reduced						
	10-25-67	1040	115	1.27	0.63	1.82	1.15	351	35.0	28,557
	3-20-68	1040	113	1.26	0.62	1.76	1.09	365	35.0	32,085
	8-27-68	1040	114	1.28	0.63	1.73	1.10	373	32.0	35,879
	9-16-68	1040	116	1.27	0.63	1.73	1.09	369	32.0	36,359
	10-21-68	1040	114	1.27	0.63	1.73	1.09	369	32.0	37,199
	11-25-68	1040	115	1.27	0.63	1.72	1.09	370	32.0	38,039
	12-9-68	1040	115	1.27	0.63	1.71	1.08	374	32.0	38,375
	12-9-68			Power Input Reduced						
	12-11-68	1020	116	1.24	0.62	1.67	1.03	374	35.0	38,423
	12-16-68	1020	115	1.24	0.61	1.67	1.03	375	35.0	38,543
	1-7-69	1020	115	1.24	0.62	1.71	1.06	362	35.0	39,071
	1-17-69	1020	115	1.24	0.62	1.71	1.06	363	35.0	39,311
	2-10-69	1020	116	1.24	0.63	1.69	1.06	364	35.0	39,887
	2-26-69	1020	117	1.25	0.62	1.67	1.03	380	35.0	40,271
	3-11-69	1020	115	1.24	0.62	1.69	1.05	367	35.0	40,583
	3-18-69	1020	116	1.24	0.62	1.69	1.05	367	35.0	40,751
	4-24-69	1020	115	1.24	0.62	1.69	1.05	367	35.0	41,639
	4-30-69	1020	114	1.24	0.62	1.67	1.03	372	35.0	41,783
	5-9-69	1020	115	1.24	0.61	1.67	1.03	375	35.0	41,999
	5-20-69	1020	115	1.24	0.61	1.67	1.02	375	35.0	42,263
	6-13-69	1020	115	1.24	0.61	1.67	1.02	375	35.0	42,839
	6-18-69	1020	115	1.24	0.62	1.67	1.03	373	35.0	42,959

Table 2-11. Performance Data of SNAP-21 6-Couple Modules (Continued)

Module	Date	T_h (°F, est)	T_c (°F)	E_o (volts)	E_L (volts)	I_L (amps)	P_o (watts)	R (milliohms)	P_I (watts)	Hours
A3	9-17-64	1106	114	1.35	0.65	1.93	1.26	360	–	72
	1-21-65	1100	111	1.35	0.69	2.10	1.44	316	45.0	3,096
	10-7-65	1100	119	1.35	0.67	1.91	1.27	359	47.0	9,312
	10-9-65			Power Input Reduced						
	10-9-65	1080	118	1.33	0.66	1.90	1.25	351	46.0	9,360
	5-27-66	1080	120	1.32	0.66	1.86	1.23	356	46.0	14,877
	10-13-66	1080	118	1.33	0.66	1.86	1.22	361	47.0	18,213
	10-13-66			Power Input Reduced						
	10-17-66	1060	118	1.30	0.65	1.84	1.20	353	46.5	18,309
	5-13-67	1060	119	1.30	0.65	1.84	1.20	356	47.0	23,241
	10-18-67	1060	119	1.31	0.65	1.82	1.18	364	47.0	27,081
	10-19-67			Power Input Reduced						
	10-25-67	1040	120	1.27	0.63	1.77	1.12	360	45.5	27,225
	5-10-68	1040	119	1.28	0.65	1.78	1.15	355	46.5	31,931
	8-13-68	1040	117	1.30	0.65	1.76	1.14	372	46.5	34,211
	9-16-68	1040	119	1.29	0.64	1.76	1.13	367	46.5	35,027
	10-21-68	1040	119	1.31	0.64	1.77	1.14	376	46.5	35,867
	11-7-68	1040	118	1.31	0.65	1.77	1.14	375	47.0	36,275
	11-25-68	1040	119	1.31	0.65	1.76	1.14	378	47.0	36,707
	12-9-68	1040	120	1.30	0.65	1.77	1.14	370	47.0	37,043
	12-9-68			Power Input Reduced						
	12-11-68	1020	117	1.28	0.63	1.74	1.10	371	45.5	37,091
	12-16-68	1020	117	1.28	0.63	1.74	1.10	372	45.5	37,211
	1-7-69	1020	117	1.28	0.63	1.74	1.10	372	45.5	37,739
	1-17-69	1020	117	1.28	0.63	1.74	1.10	372	45.5	37,979
	2-10-69	1020	117	1.28	0.64	1.71	1.09	374	45.5	38,555
	2-26-69	1020	116	1.28	0.64	1.71	1.09	374	45.5	38,939
	3-11-69	1020	116	1.28	0.64	1.72	1.10	371	45.5	39,251
	3-18-69	1020	116	1.28	0.64	1.71	1.09	375	45.5	39,419
	4-23-69	1020	116	1.29	0.64	1.71	1.10	379	46.0	40,283
	4-30-69	1020	115	1.29	0.64	1.71	1.10	380	46.0	40,427
	5-9-69	1020	115	1.29	0.64	1.71	1.10	378	46.5	40,643
	5-20-69	1020	116	1.30	0.65	1.71	1.10	382	46.5	40,907
	6-13-69	1020	115	1.30	0.64	1.72	1.11	382	46.5	41,483
	6-18-69	1020	116	1.29	0.64	1.70	1.09	382	46.5	41,603

Table 2-11. Performance Data of SNAP-21 6-Couple Modules (Continued)

Module	Date	T_h (°F, est)	T_c (°F)	E_o (volts)	E_L (volts)	I_L (amps)	P_o (watts)	R (milliohms)	P_I (watts)	Hours
A4	10-29-64	1099	115	1.39	0.70	2.22	1.54	312	45.0	240
	1-5-65	1100	114	1.39	0.72	2.30	1.66	291	48.0	1,872
	4-2-65	1100	115	1.39	0.70	2.36	1.64	294	47.0	3,960
	7-7-65	1100	116	1.39	0.69	2.16	1.50	322	46.0	6,264
	8-25-65	1100	114	1.39	0.69	2.15	1.48	327	45.0	7,440
	10-7-65	1100	117	1.39	0.68	2.14	1.46	330	44.0	8,472
	10-9-65			Power Input Reduced						
	10-9-65	1080	116	1.36	0.68	2.10	1.42	326	43.0	8,520
	11-16-65	1080	115	1.36	0.68	2.11	1.43	324	42.0	9,432
	1-27-66	1080	115	1.36	0.67	2.09	1.40	330	41.0	11,160
	5-26-66	1080	116	1.36	0.66	2.03	1.35	343	40.0	14,013
	10-13-66	1080	116	1.36	0.63	1.89	1.18	387	40.0	17,373
	10-13-66			Power Input Reduced						
	10-17-66	1060	117	1.31	0.62	1.87	1.15	373	39.0	17,469
	6-23-67	1060	117	1.29	0.66	2.30	1.52	274	39.0	23,385
	10-16-67	1060	117	1.30	0.68	2.38	1.63	259	40.0	26,169
	10-19-67			Power Input Reduced						26,241
	10-25-67	1040	116	1.27	0.64	2.44	1.55	259	39.0	26,385
	3-14-68	1040	118	1.25	0.60	2.26	1.36	287	39.0	29,769
	8-13-68	1040	117	1.24	0.62	2.28	1.42	271	39.5	33,571
	10-21-68	1040	119	1.24	0.61	2.20	1.33	288	39.5	35,027
	12-9-68	1040	117	1.24	0.56	2.04	1.15	332	39.5	36,203
	12-9-68			Power Input Reduced						
	12-11-68	1020	112	1.22	0.56	2.03	1.13	327	38.8	36,251
	1-17-69	1020	115	1.22	0.61	1.44	0.871	427	37.5	37,139
	2-26-69	1020	115	1.23	0.45	0.993	0.450	782	37.0	38,099
	3-11-69	1020	115	1.22	0.04	0.081	0.003	14,590	37.0	38,411
	3-18-69	1020	115	1.22	0.03	0.061	0.002	18,880	37.0	38,579
	4-9-69	1020	115	1.05	0.51	0.743	0.378	730	37.0	39,107
	4-23-69	Shorted Out Couple No. 1 Because of High Resistance								
	4-24-69	1020	114	1.03	0.087	0.413	0.036	2,280	37.0	39,467
	4-30-69	1020	115	1.01	0.015	0.073	0.001	13,630	37.0	39,611
	5-9-69	1020	114	1.00	0.006	0.029	0.0002	34,280	37.0	39,827
	5-20-69	1020	116	1.02	0.0075	0.036	0.0003	28,130	37.0	40,091
	6-13-69	1020	115	0.977	0.0026	0.013	0.00003	74,950	37.0	40,667
	6-18-69	1020	115	0.978	0.0025	0.012	0.00003	81,290	37.0	40,787

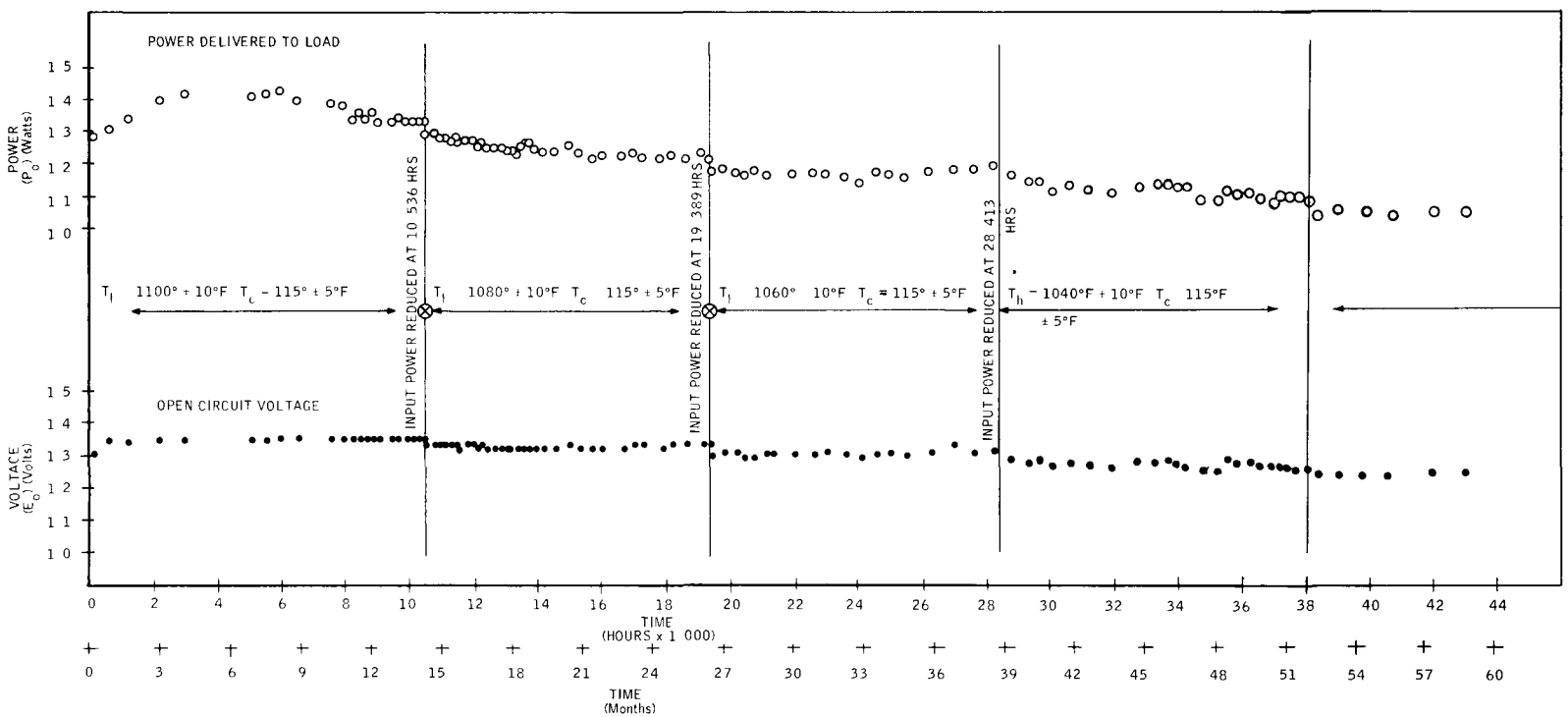

Figure 2-10. SNAP-21B 6-Couple Module A1

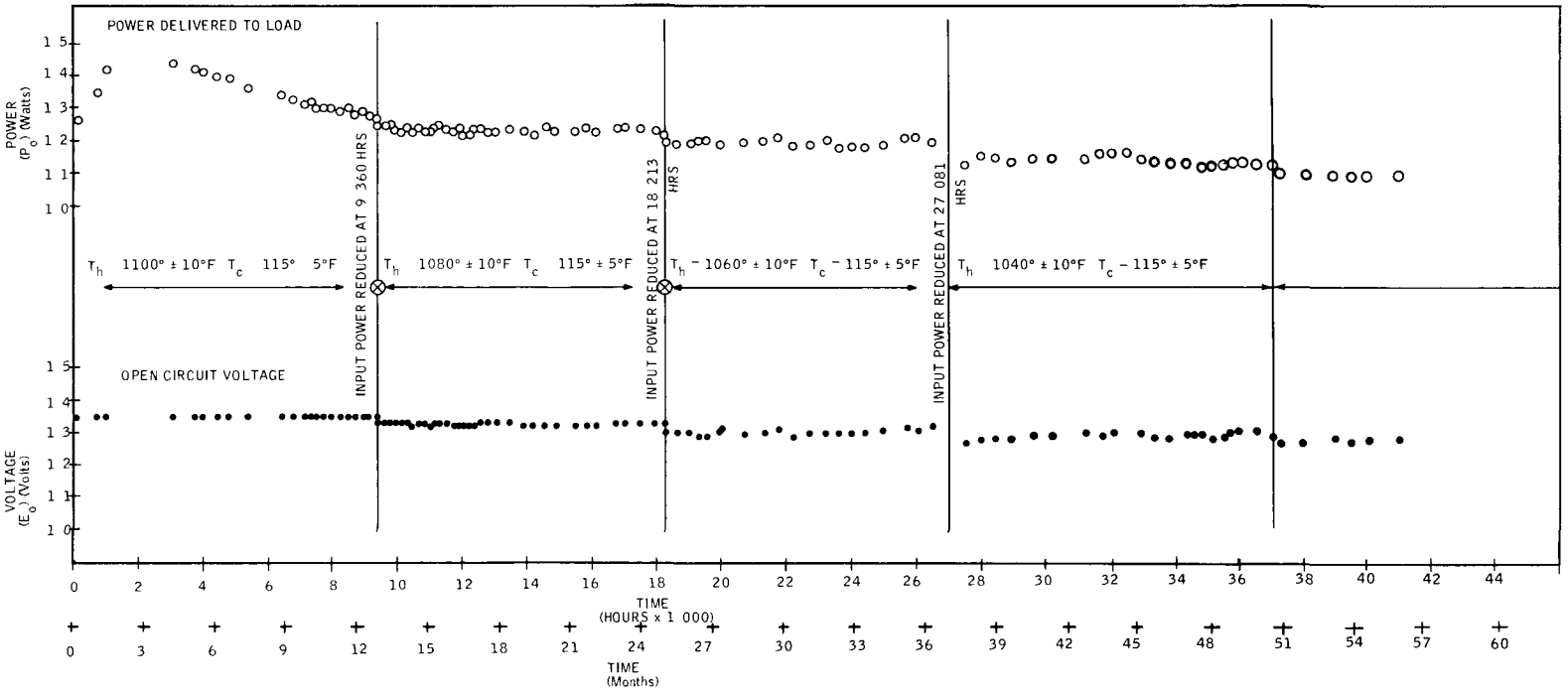

Figure 2-11. SNAP-21B 6-Couple Module A3

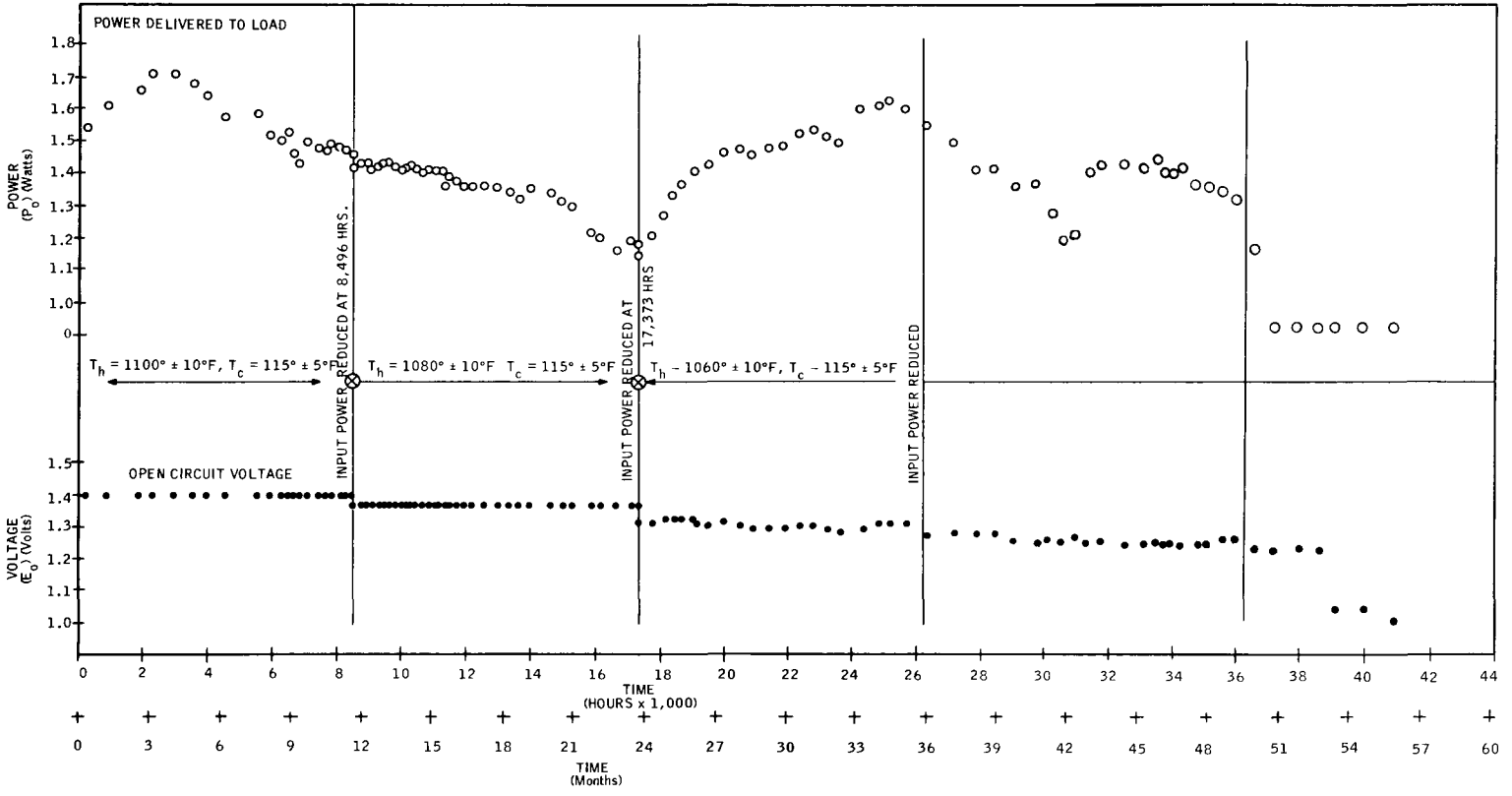

Figure 2-12. SNAP-21B 6-Couple Module A4

Table 2-12. Typical Performance Data SNAP-21B Prototype P5*

Date	T_h[1] (°F)	T_c[2] (°F)	E_o (volts)	E_L (volts)	I_L (amp)	P_o (watts)	R (ohms)	P_I (watts)	E_x/E_c	R_x/R_c	P_x/P_c	Hours on Test
4-19-65	1112	117	11.20	5.60	2.04	11.42	2.74	-	0.99	1.26	0.78	24
5-12-65	1115	127	10.92	5.46	2.00	10.92	2.73	--	0.97	1.24	0.77	576
6-30-65	1097	135	10.65	5.32	2.02	10.74	2.64	176	0.97	1.20	0.78	1,320
7-26-65	1097	142	10.68	5.34	2.01	10.72	2.66	176	0.98	1.21	0.79	1,944
9-10-65	1095	144	10.60	5.30	2.06	10.92	2.57	-	0.97	1.17	0.81	3,048
10-26-65	1097	147	10.56	5.28	2.05	10.81	2.58	180	0.97	1.16	0.82	4,152
12- 1-65	1102	151	10.58	5.29	2.10	11.11	2.52	--	0.98	1.13	0.84	5,016
1-28-66	1094	149	10.56	5.28	2.14	11.30	2.47	180	0.98	1.11	0.86	6,408
3-28-66	1094	152	10.54	5.27	2.16	11.38	2.44	180	0.98	1.10	0.87	7,821
4-28-66	1074	151	10.20	5.10	2.19	11.17	2.33	176	0.97	1.07	0.87	8,565
6-21-66	1073	151	10.24	5.00	2.18	10.90	2.40	174	0.97	1.10	0.86	9,834
8-12-66	1078	161	10.15	5.07	2.20	11.15	2.30	178	0.97	1.04	0.89	11,081
9-14-66	1075	161	10.16	5.07	2.19	11.10	2.32	175	0.97	1.06	0.89	11,873
12-27-66	1077	153	10.22	5.11	2.19	11.19	2.33	184	0.97	1.07	0.87	14,369
1-31-67	1073	159	10.12	5.06	2.20	11.13	2.30	179	0.96	1.05	0.90	15,209
4- 1-67	1074	148	10.20	5.10	2.24	11.42	2.28	175	0.97	1.05	0.89	16,649
5-24-67	1076	150	10.28	5.14	2.20	11.31	2.34	179	0.97	1.08	0.88	17,921
6-30-67	Power Failure, Emergency Power Came On at 8:28 PM to 10:30 PM											
7- 1-67	1067	159	10.00	5.00	2.19	10.95	2.28	173	0.95	1.00	0.88	18,833
8- 5-67	1061	164	10.01	5.00	2.22	11.10	2.26	170	0.95	1.01	0.90	19,673
9-26-67	1068	160	10.04	5.02	2.17	10.89	2.31	172	0.96	1.05	0.88	20,921
11- 6-67	1067	158	10.08	5.04	2.19	11.04	2.30	174	0.96	1.00	0.89	21,953
12-29-67	1066	150	10.20	5.10	2.22	11.32	2.30	173	0.97	1.06	0.90	23,225
1-15-68	Power Failure, Emergency Power Came On for One Hour											
1-30-68	1070	151	9.90	4.95	2.21	10.94	2.26	173	0.94	1.01	0.87	23,993
2-17-68	Power Failure, Emergency Power Came On for Five Hours											
2-19-68	1068	149	10.10	5.05	2.17	10.96	2.33	177	0.96	1.00	0.87	24,473
3-14-68	1052	156	9.96	4.98	2.19	10.91	2.27	177	0.98	1.03	0.90	25,049
5-22-68	1077	154	10.02	5.02	2.22	11.14	2.25	176	0.95	1.04	0.87	26,705
6-17-68	1042	157	9.92	4.96	2.14	10.61	2.32	171	0.98	1.06	0.90	27,329
6-17-68	Reduced Input Power											
8-13-68	1044	166	9.80	4.90	2.09	10.24	2.34	169	0.98	1.14	0.87	28,697
9-16-68	1050	164	9.82	4.90	2.01	10.24	2.33	169	0.97	1.14	0.86	29,513
11-6-68	1052	162	9.76	4.88	2.10	10.25	2.32	170	0.97	1.13	0.87	30,737
12-16-68	1052	152	9.86	4.93	2.13	10.60	2.29	170	0.97	1.13	0.86	31,637
1-16-69	1052	151	9.88	4.94	2.12	10.47	2.33	170	0.97	1.13	0.87	32,441
1-27-69	Regulator Failure Power Increased for 12 Hours											
2-10-69	1052	149	9.88	4.94	2.21	10.92	2.24	171	0.97	1.10	0.88	33,041
3-10-69	1050	154	9.85	4.89	2.21	10.83	2.24	172	0.96	1.09	0.89	33,713
3-18-69	1052	152	9.78	4.89	2.19	10.71	2.23	172	0.96	1.09	0.87	33,905
4-24-69	1050	152	9.78	4.89	2.18	10.66	2.24	172	0.96	1.09	0.86	34,649
4-30-69	1052	155	9.85	4.89	2.19	10.71	2.26	172	0.96	1.10	0.88	34,793
5- 9-69	1052	155	9.83	4.89	2.19	10.71	2.26	172	0.96	1.10	0.88	35,009
5-19-69	1052	156	9.84	4.92	2.18	10.73	2.26	172	0.96	1.10	0.88	35,249
6-12-69	1052	160	9.80	4.89	2.16	10.56	2.27	172	0.97	1.10	0.88	35,825
6-17-69	1052	161	9.80	4.85	2.16	10.48	2.29	172	0.97	1.11	0.87	35,945
6-17-69	Reduced Input Power											
6-18-69	1032	159	9.57	4.77	2.14	10.21	2.24	168	0.97	1.11	0.88	35,969

Begin test on 4-19-65
Turned off from 5-20-65 to 6-7-65

1 Based on average of two N leg Seebeck voltages
2. Based on average of four cold electrode thermocouples.

Table 2-13. Typical Performance Data SNAP-21B Prototype P6*

Date	I_h[1] (°F)	T_c[3] (°F)	E_o (volts)	E_L (volts)	I_L (amp)	P_o (watts)	R (ohms)	P_I (watts)	$\frac{\Gamma_x}{\Gamma_c}$	$\frac{R_x}{R}$	$\frac{P_x}{P_c}$	Hours on Test
6- 2-65	1095[1]	132	10.88	5.44	2.38	14.03	2.10	204	1.03	1.02	1.02	24
6-30-65	1095[2]	14	10.88	5.44	2.34	12.73	2.32	206	1.04	1.11	0.96	720
7-29-65	1095[2]	157	10.88	5.44	2.28	12.40	2.38	--	1.04	1.13	0.96	1,416
9- 1-65	1095[2]	162	10.80	5.40	2.20	11.88	2.45	201	1.04	1.16	0.93	2,184
9-30-65	1095[2]	166	10.72	5.36	2.13	11.74	2.45	198	1.04	1.15	0.93	2,880
11-17-65	1095[2]	169	10.80	5.40	2.16	11.66	2.50	201	1.05	1.16	0.94	4,032
12-28-65	1095[2]	171	10.78	5.39	2.18	11.75	2.47	200	1.05	1.15	0.95	5,016
2- 9-66	1095[2]	171	10.74	5.37	2.14	11.48	2.51	197	1.04	1.17	0.93	5,952
3-28-66	1095[2]	171	10.74	5.39	2.13	11.44	2.52	197	1.04	1.17	0.92	7,173
4-28-66	1095[2]	172	10.76	5.38	2.11	11.35	2.55	201	1.04	1.17	0.92	7,941
8-12-66	1075[2]	181	10.52	5.23	2.05	10.72	2.58	191	1.05	1.20	0.92	10,152
9-14-66	1075[2]	182	10.53	5.24	2.06	10.78	2.57	190	1.05	1.20	0.93	11,244
12-27-66	1075[2]	176	10.82	5.41	2.03	11.28	2.59	192	1.07	1.22	0.95	13,740
1-27-67	1075[2]	176	10.84	5.42	2.10	11.38	2.58	191	1.08	1.22	0.96	14,484
3-13-67	1075[2]	173	10.86	5.43	2.09	11.35	2.60	198	1.08	1.23	0.95	15,764
4-27-67	1075[4]	168	10.38	5.19	2.07	10.72	2.51	194	1.03	1.20	0.89	16,524
6-16-67	1075[4]	176	10.58	5.29	2.03	10.84	2.58	194	1.05	1.23	0.90	17,844
6-22-67	Power Input Reduced							186				17,988
6-30-67	1055[4]	Bilg Power Failure, Emergency Power for Approx. 2 Hours										
7- 1-67	1055[4]	172	10.10	5.05	2.04	10.28	2.48	184	1.03	1.20	0.88	18,204
8- 4-67	1055[4]	178	9.95	4.98	2.03	10.11	2.45	185	1.02	1.18	0.90	19,020
9-26-67	1055[4]	175	10.08	5.04	2.02	10.18	2.50	186	1.03	1.21	0.88	20,292
11- 6-67	1055[4]	172	10.08	5.04	2.02	10.18	2.50	189	1.03	1.21	0.87	21,324
11-30-67	1055[4]	166	10.00	5.00	2.04	10.20	2.45	190	1.02	1.20	0.86	21,900
1-15-68	Bilg. Power Was Off—Emergency Power Came On for One Hour											
1-17-68	1055[4]	166	10.04	5.02	2.03	10.19	2.47	192	1.02	1.20	0.86	23,052
2-17-68	Bilg. Power Was Off—Emergency Power Came On for 5 Hours											
3-14-68	1055[4]	171	10.02	5.01	2.04	10.22	2.46	192	1.02	1.19	0.88	24,420
5- 9-68	1055[4]	169	10.00	5.00	2.04	10.20	2.45	192	1.01	1.19	0.87	25,764
7-10-68	1035[4]	173	9.76	4.88	1.97	9.61	2.48	188	1.03	1.23	0.87	27,252
8-13-68	1035[4]	182	9.76	4.88	1.99	9.71	2.45	188	1.04	1.21	0.89	28,068
9-16-68	1035[4]	175	9.76	4.88	1.98	9.66	2.46	188	1.03	1.22	0.87	28,884
5-9-68	1055	169	10.00	5.00	2.04	10.20	2.45	192	1.01	1.19	0.87	25,764
6-17-68	Reduced Input Power											
7-10-68	1035[4]	173	9.76	4.88	1.97	9.61	2.48	188	1.03	1.23	0.87	27,252
8-13-68	1035[4]	182	9.76	4.88	1.99	9.71	2.45	188	1.04	1.21	0.89	28,068
9-16-68	1035[4]	175	9.76	4.88	1.98	9.66	2.46	188	1.03	1.22	0.87	28,884
11-6-68	1035[4]	174	9.80	4.89	1.99	9.73	2.47	188	1.04	1.22	0.88	30,108
12-16-68	1035[4]	180	9.80	4.89	2.00	9.78	2.46	188	1.03	1.23	0.87	31,068
1-16-69	1035[4]	180	9.83	4.90	2.00	9.80	2.47	188	1.03	1.24	0.87	31,812
1-27-69	Regulator Failure Power Increased for 12 Hours											
2-10-69	1035[4]	184	9.83	4.91	2.03	10.07	2.40	188	1.03	1.20	0.89	32,412
3-10-69	1035[4]	186	9.86	4.92	2.06	10.14	2.40	190	1.04	1.20	0.90	33,084
3-18-69	1035[4]	188	9.81	4.90	2.05	10.05	2.40	190	1.03	1.19	0.90	33,276
4-24-69	1035[4]	188	9.80	4.90	2.04	10.00	2.40	190	1.03	1.19	0.89	34,020
4-30-69	1035[4]	170	9.82	4.90	2.04	10.00	2.41	190	1.03	1.20	0.89	34,164
5- 9-69	1035[4]	171	9.81	4.90	2.04	10.00	2.41	190	1.03	1.20	0.89	34,380
5-19-69	1035[4]	173	9.81	4.90	2.03	9.95	2.42	190	1.04	1.20	0.89	34,620
6-12-69	1035[4]	176	9.80	4.91	2.00	9.82	2.45	190	1.04	1.21	0.88	35,196
6-17-69	1035[4]	178	9.82	4.92	2.01	9.89	2.44	190	1.04	1.20	0.87	35,316
6-17-69	Reduced Input Power											
6-18-69	1015[4]	175	9.55	4.77	1.99	9.49	2.40	185	1.04	1.20	0.88	35,340

Begin test 6-1-65

1 Based on average of two hot electrode thermocouples
2 Based on hot frame thermocouple referenced to 6-2-65
3 Based on average of two cold electrode thermocouples
4 Based on average input power from 6-5-66 to 12-27-66

Table 2-14. Typical Performance Data SNAP-21B Prototype P7*

Date	T_h[1] (°F)	T_c[2] (°F)	E_o (volts)	E_l (volts)	I_l (amp)	P_o (watts)	R (ohms)	P_l (watts)	$\frac{I}{I_c}$	$\frac{R_x}{R_c}$	$\frac{R_x}{P_c}$	Hours on Test
6- 8-65	1099[1]	127	10.80	5.40	2.44	13.17	2.21	200	1.01	1.08	0.33	168
7-14-68	1098[1]	142	10.80	5.40	2.21	11.95	2.44	194	1.01	1.18	0.88	1,032
8-24-65	1100[3]	152	10.82	5.41	2.13	11.52	2.54	192	1.03	1.21	0.68	1,968
10-12-65	1100[3]	156	10.86	5.43	2.11	11.47	2.57	191	1.01	1.22	0.62	3,144
11-17-68	1095[3]	158	10.80	5.40	2.08	11.23	2.60	188	1.04	1.23	0.87	4,008
12-28-65	1095[3]	159	10.78	5.39	2.07	11.16	2.60	191	1.04	1.23	0.88	4,992
2-10-66	1095[3]	158	10.82	5.41	2.06	11.14	2.63	191	1.04	1.24	0.88	6,048
3-28-66	1095[3]	160	10.80	5.40	2.05	11.07	2.63	191	1.04	1.24	0.87	7,149
5-16-66	1095[3]	163	10.82	5.41	202	10.93	2.68	189	1.04	1.26	0.86	8,324
6- 4-66	Reduced Input Power											
6-21-66	1075[3]	158	10.72	5.40	1.99	10.75	2.67	186	1.06	1.28	0.87	9,181
6-28-66	Moved Test from I.C.A. to Space Center											
8-12-66	1075[3]	173	10.56	5.26	1.96	10.31	2.65	188	1.03	1.26	0.86	10,428
10- 3-66	1075[3]	178	10.62	5.31	1.95	10.35	2.72	186	1.05	1.27	0.89	11,676
12-28-66	1075[4]	165	10.70	5.35	1.94	10.37	2.76	186	1.05	1.31	0.84	13,760
1-31-67	1075[4]	171	10.70	5.35	1.96	10.48	2.73	188	1.06	1.30	0.86	14,376
3-13-67	1075[4]	174	10.60	5.30	1.94	10.26	2.74	186	1.06	1.29	0.86	15,960
5-13-67	1075[4]	175	10.61	5.30	1.91	10.11	2.78	186	1.06	1.31	0.85	17,024
6-22-67	Input Power was Reduced							180				
6-23-67	1055[4]	171	10.30	5.15	1.91	9.84	2.70	180	1.03	1.31	0.84	18,003
6 30-67	Bldg. Power Failure, Emergency Power was on for Approx. 2 Hours											
7- 1 67	1055[4]	165	10.30	5.15	1.86	9.58	2.77	180	1.05	1.33	0.81	18,192
8- 8-67	1055[4]	182	10.19	5.10	1.92	9.79	2.65	178	1.03	1.27	0.86	19,110
9-26-67	1055[4]	166	10.26	5.13	1.92	9.85	2.67	179	1.04	1.30	0.83	20,280
10-20-67	1055[4]	171	10.14	5.07	1.91	9.68	2.65	176	1.03	1.29	0.83	21,091
1-15-68	Bldg. Power was off - Emergency Power came on for One Hour											
1-17-68	1055[4]	169	10.40	5.20	1.92	9.98	2.71	177	1.06	1.32	0.83	23,204
2-17-68	Bldg. Power was off - Emergency Power came on for about 5 Hours											
2-19-68	1055[4]	164	10.20	5.10	1.92	9.79	2.68	180	1.04	1.30	0.83	23,975
3-20 68	1055[4]	169	10.28	5.14	1.92	9.87	2.68	181	1.0	1.30	0.85	24,717
4-18-68	1055[4]	177	10.20	5.10	1.93	9.84	2.64	189	1.04	1.28	0.85	25,884
5- 9-68	1055[4]	179	10.28	5.14	1.93	9.92	2.66	180	1.04	1.28	0.87	25,917
6-17-68	1055[4]	182	9.94	4.97	1.90	9.44	2.62	176	1.02	1.26	0.83	26,808
8-13-68	1035[4]	177	9.78	4.89	1.91	9.34	2.56	174	1.04	1.27	0.83	28,221
9-16-68	1035[4]	173	9.75	4.88	1.90	9.27	2.56	174	1.03	1.27	0.84	29,047
6-17-68	1035[4]	182	9 94	4 97	1 90	9 44	2 62	176	1 02	1 26	0 83	26, 08
6-17-68	Reduced Power Input											
8-13-68	1035[4]	177	9 78	4 89	1 91	9 34	2 56	174	1 04	1 27	0	28,221
9-16-68	1035[4]	173	9 75	4 88	1 90	9 27	2 56	174	1 03	1 27	0 4	29,047
11-6-68	1035[4]	170	9 82	4 91	1 87	9 18	2 63	174	1 03	1 30	0 2	30,261
12-16-68	1035[4]	159	9 83	4 93	1.88	9 27	2 61	174	1 03	1 30	0 12	31 271
1-16-69	1035[4]	153	9 88	4 94	1.92	9 48	2 57	174	1 04	1 30	0 4	31 6
1-27-69	Regulator Failure, Power Increased for 12 Hours											
2-10-69	1035[4]	158	9.90	4 94	1.96	9 68	2 53	175	1 04	1.28	0 95	32 964
3-10-69	1035[4]	162	9.91	4 94	1.97	9.73	2 52	175	1.04	1 27	0 86	33 237
3-18-69	1035[4]	159	9.91	4.94	1 97	9 73	2.52	175	1.04	1 27	0.85	33,429
4-24-69	1035[4]	162	9.92	4.94	1.95	9.63	2.55	175	1 04	1 28	0.84	34 173
4-30-69	1035[4]	163	9.89	4.93	1.95	9.61	2 54	175	1 04	1 27	0.85	34 317
5- 9-69	1035[4]	164	9.84	4.92	1.94	9.54	2.54	175	1.03	1 27	0.84	34 533
5-19-69	1035[4]	164	9.83	4.92	1.93	9.54	2.54	175	1 03	1.27	0.84	34,773
6-12-69	1035[4]	169	9.83	4.92	1.91	9.40	2.57	175	1 03	1 28	0.84	35,314
6-17-69	1035[4]	171	9.84	4 92	1 91	9 40	2.58	175	1.04	1 28	0.84	35 469
6-17-69	Reduced Power Input											
6-18-69	1015[4]	168	9 62	4.81	1.91	9 19	2 52	172	1 04	1 28	0.84	35 493

*Begin test 6-2-65

1. Based on average of two hot electrode thermocouples
2. Based on average of two cold electrode thermocouples.
3. Based on hot frame thermocouple referenced to 6-30-65
4. Based on average input power from 7-13-66 to 11-12-66

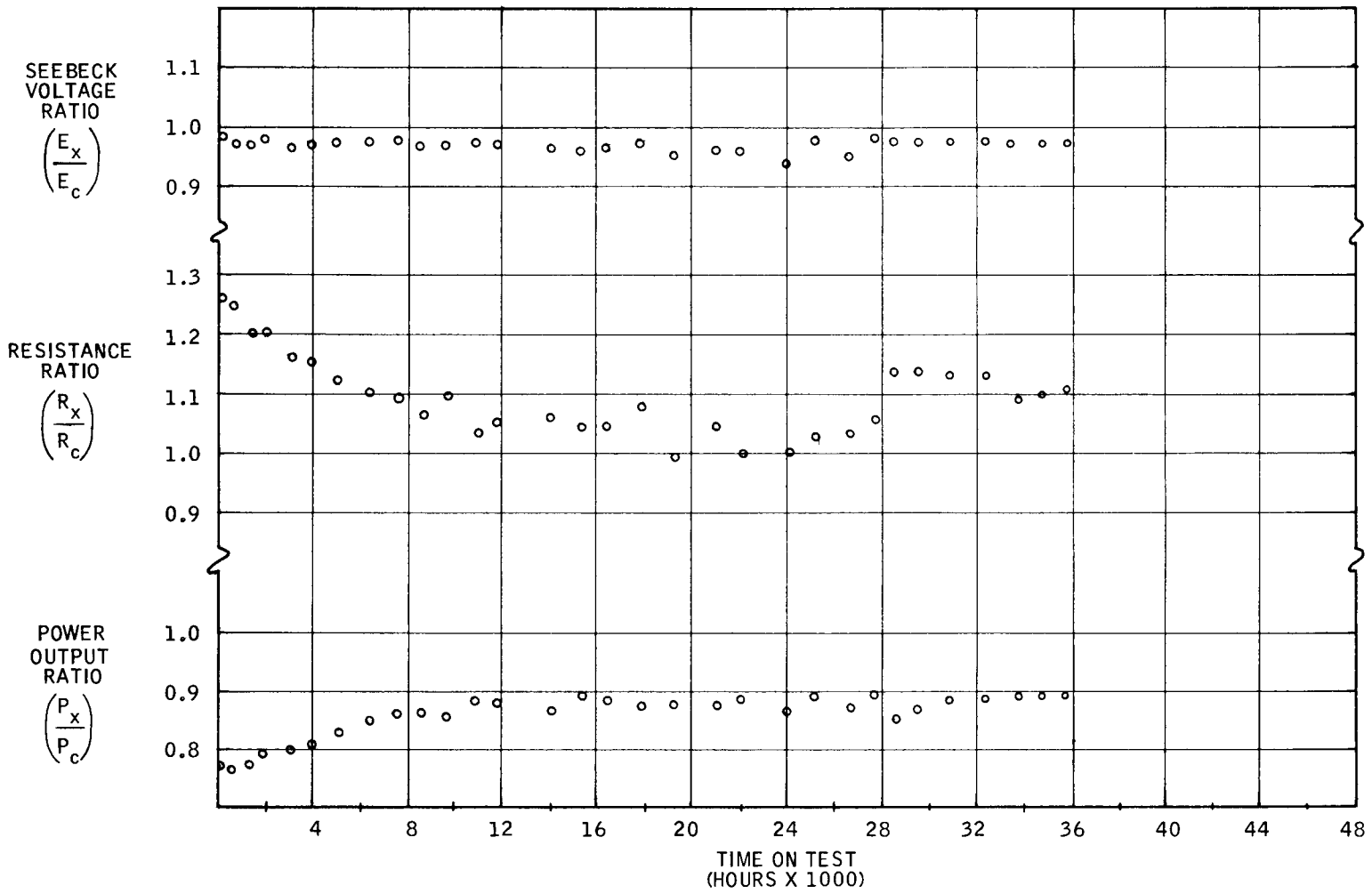

Figure 2-13. SNAP-21B 48-Couple Prototype Generator P5 Performance Ratios (Experimental/Calculated)

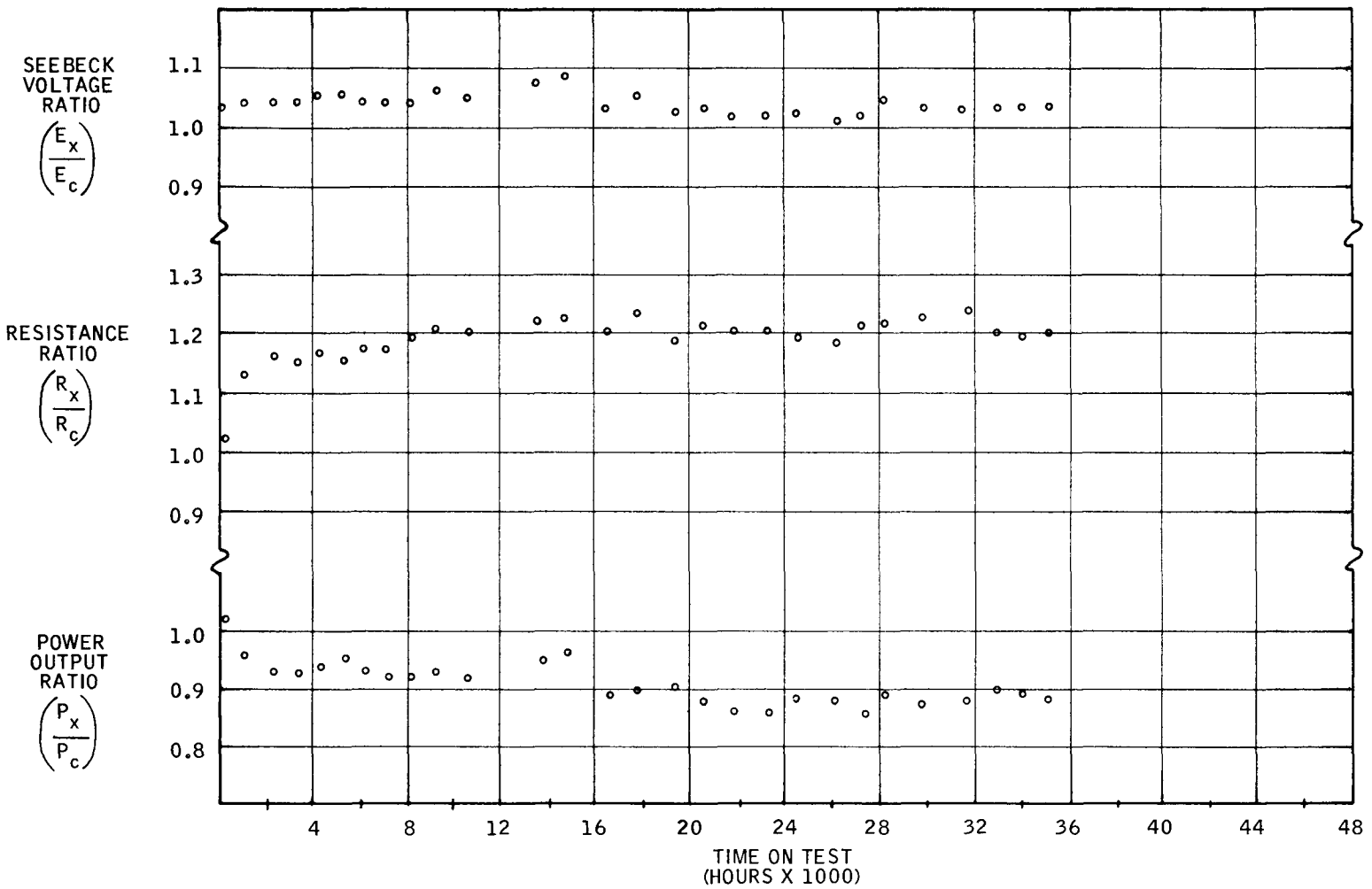

Figure 2-14. SNAP-21B 48-Couple Prototype Generator P6 Performance Ratios (Experimental/Calculated)

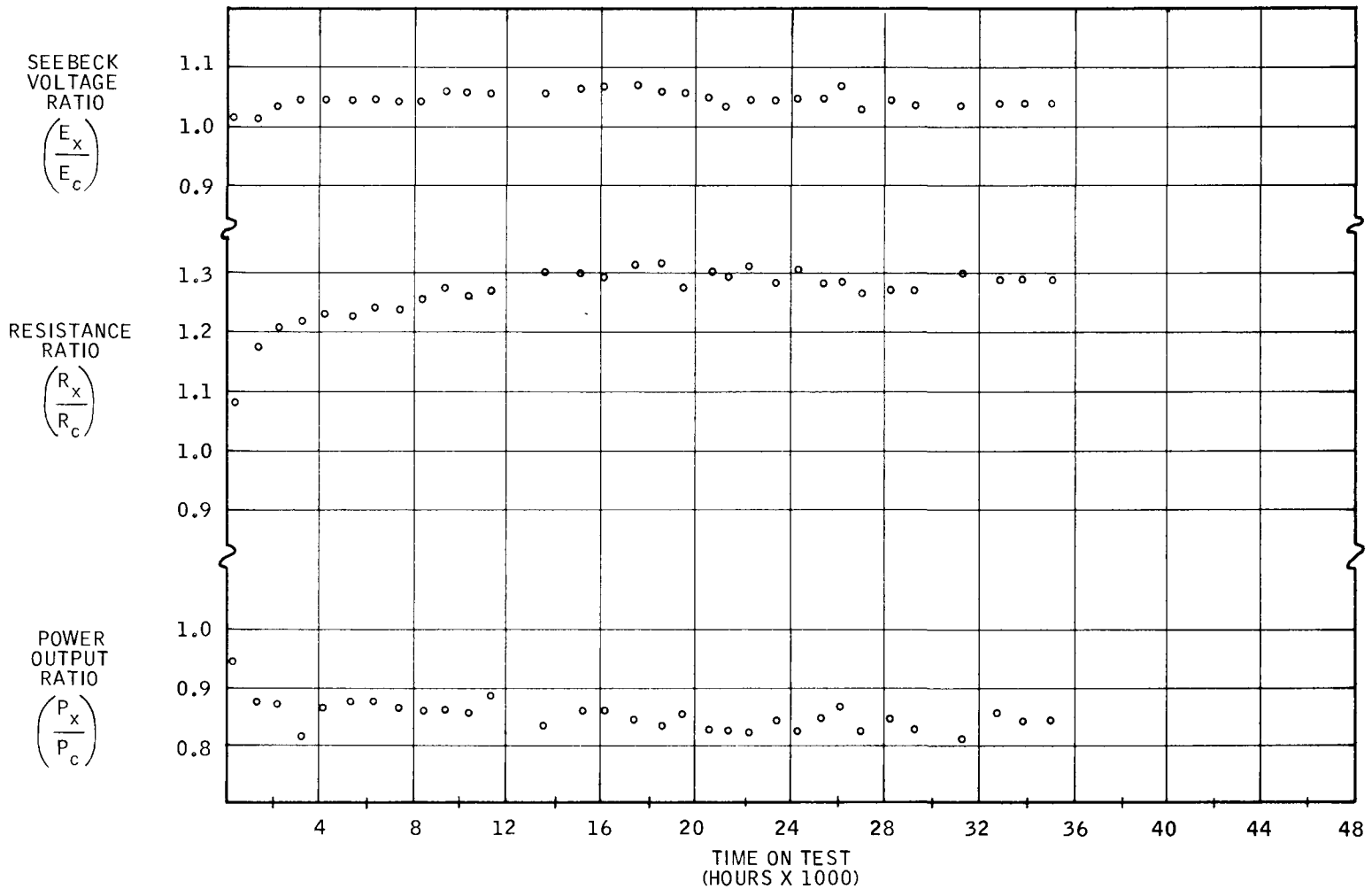

Figure 2-15. SNAP-21B 48-Couple Prototype Generator P7 Performance Ratios (Experimental/Calculated)

Performance for 6-couple modules A1 and A3 remained stable this past quarter.

Module A4 continued to decrease in power. The major cause for this is an increase in internal resistance.

During this past quarter, this module (A4) had been operating with couple #1 shorted. This was due to a high impedance in this section. It also appears that a high impedance has developed in the other section of the circuit. Disposition of this module will be made next quarter.

Prototype generators P5 through P7 continued to operate satisfactorily this past quarter. The input power was reduced to obtain a 20°F drop in hot button temperature. This is the fourth annual simulated isotope fuel decay.

It should also be pointed out that the prototype generators appear to have returned to their operating point prior to the regulator failure (refer to Quarterly #11).

2.5.2 Phase II

2.5.2.1 Performance Testing

A10D1

The power-out for this generator decreased about 5% over this past quarter (refer to Figures 2-16a through 2-16c). The major cause for this is the increase in internal resistance. The Seebeck voltage for this past quarter was fairly constant. Generally, sublimation at the hot end of the legs is a cause of this performance degradation.

A10D2

Generator A10D2 decreased slightly in power this past quarter. Figures 2-17a through 2-17c show performance curves for this thermoelectric generator. This power decrease has been due to a slight increase in resistance. The Seebeck voltage was fairly stable this past quarter.

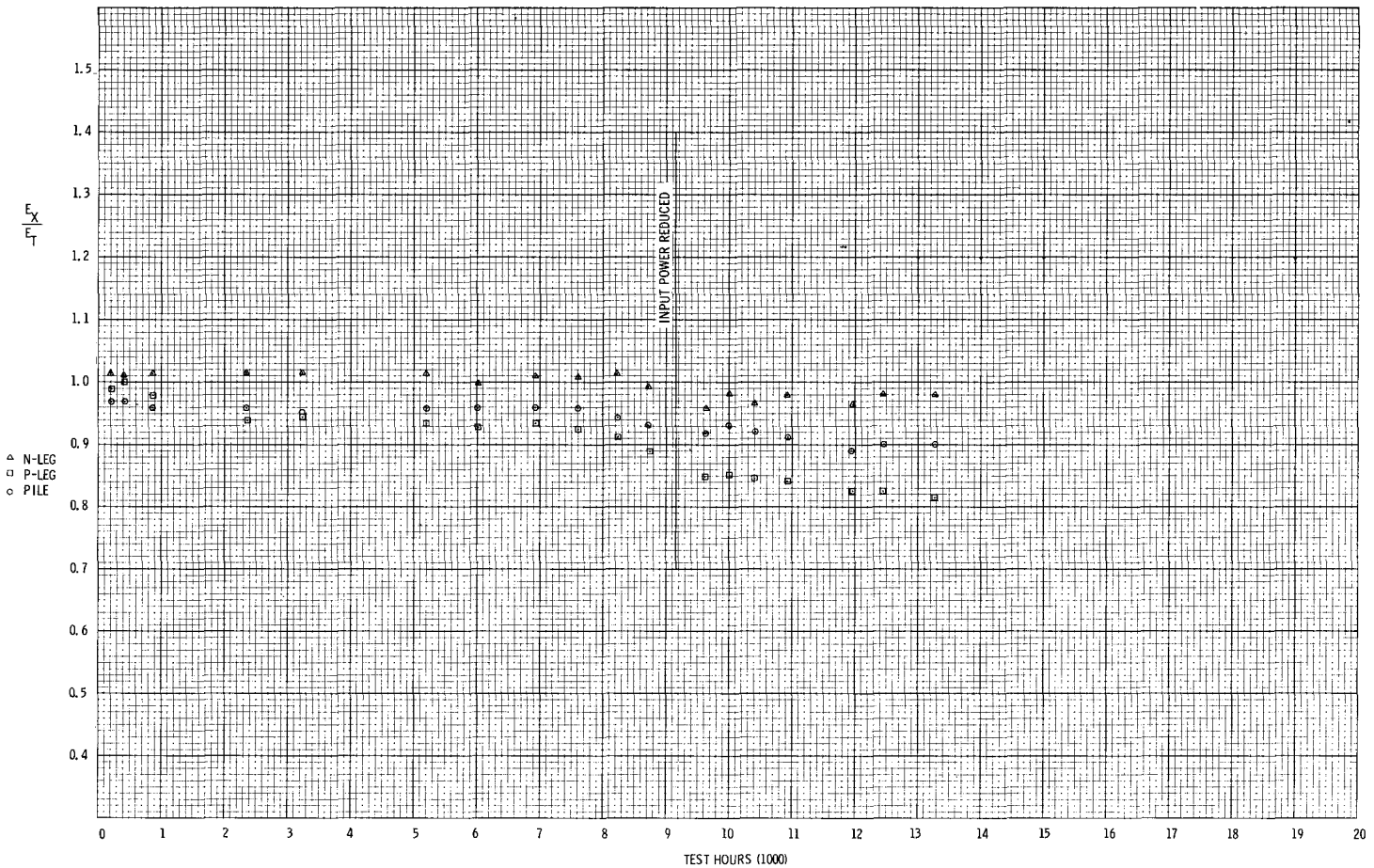

Figure 2-16a. SNAP-21 Thermoelectric Generator A10D1 Normalized SEEBECK VOLTAGE RATIO

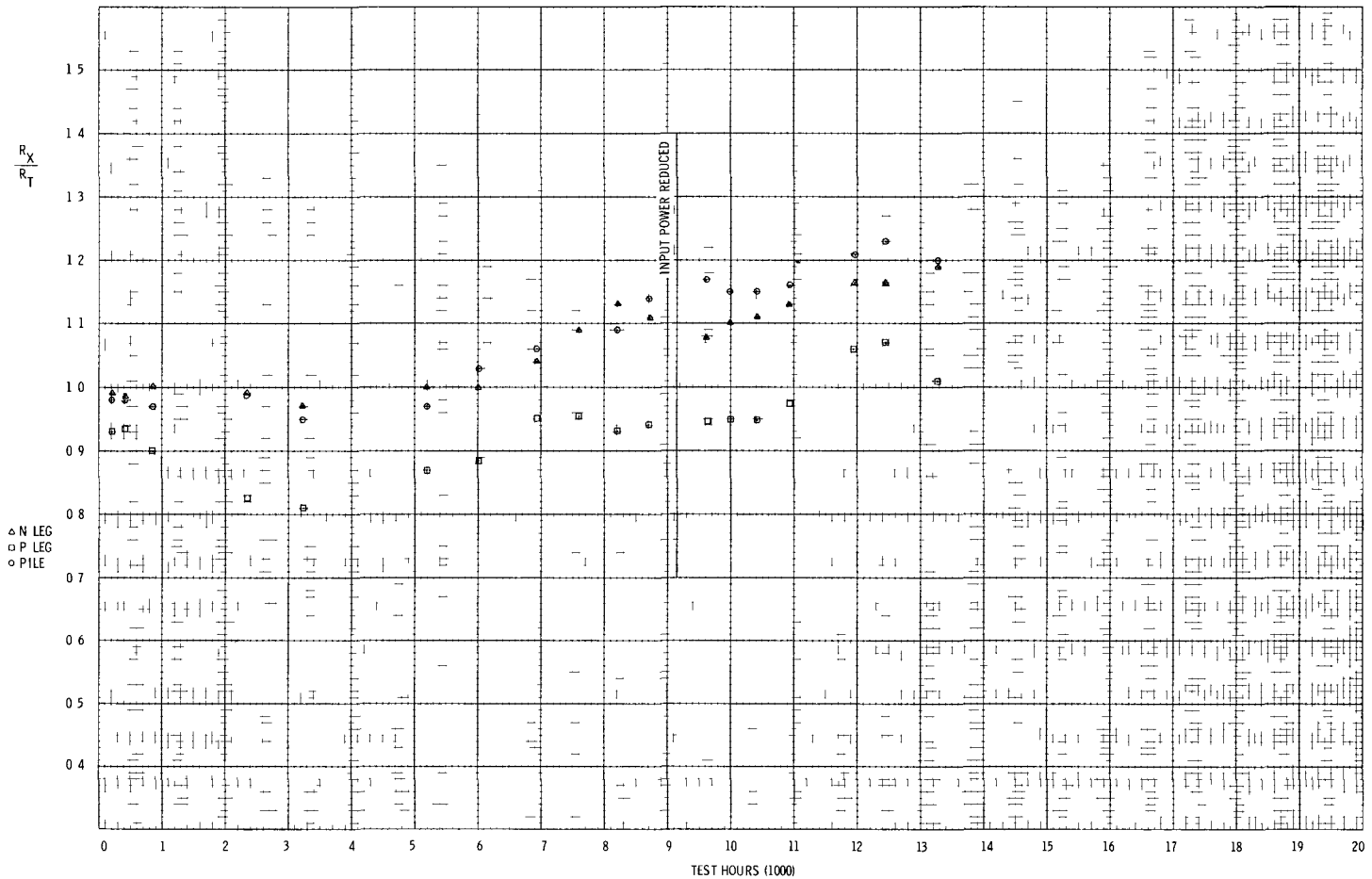

Figure 2-16b. SNAP-21 Thermoelectric Generator A10D1 Normalized RESISTANCE RATIO

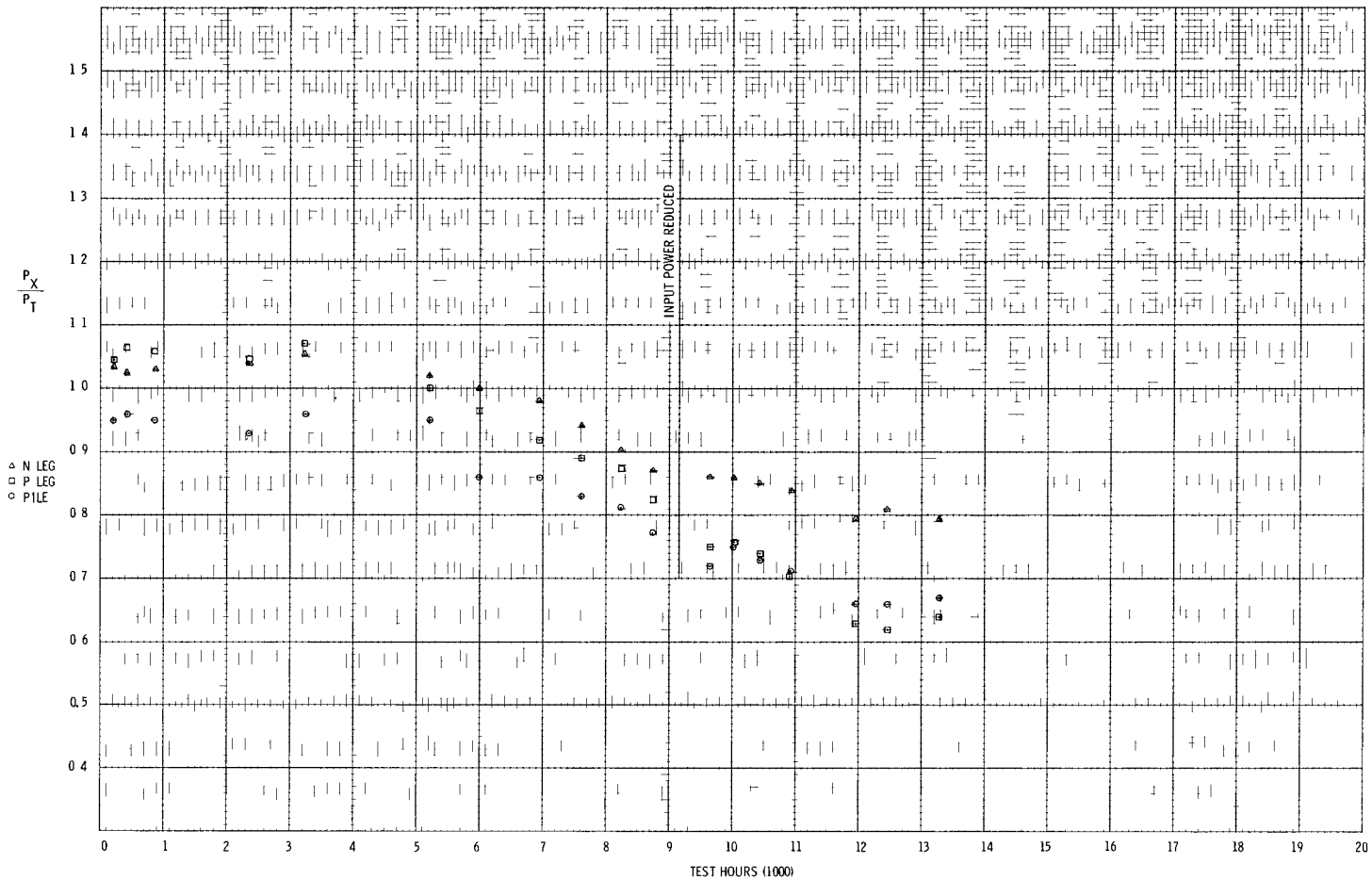

Figure 2-16c. SNAP-21 Thermoelectric Generator A10D1 Normalized POWER RATIO

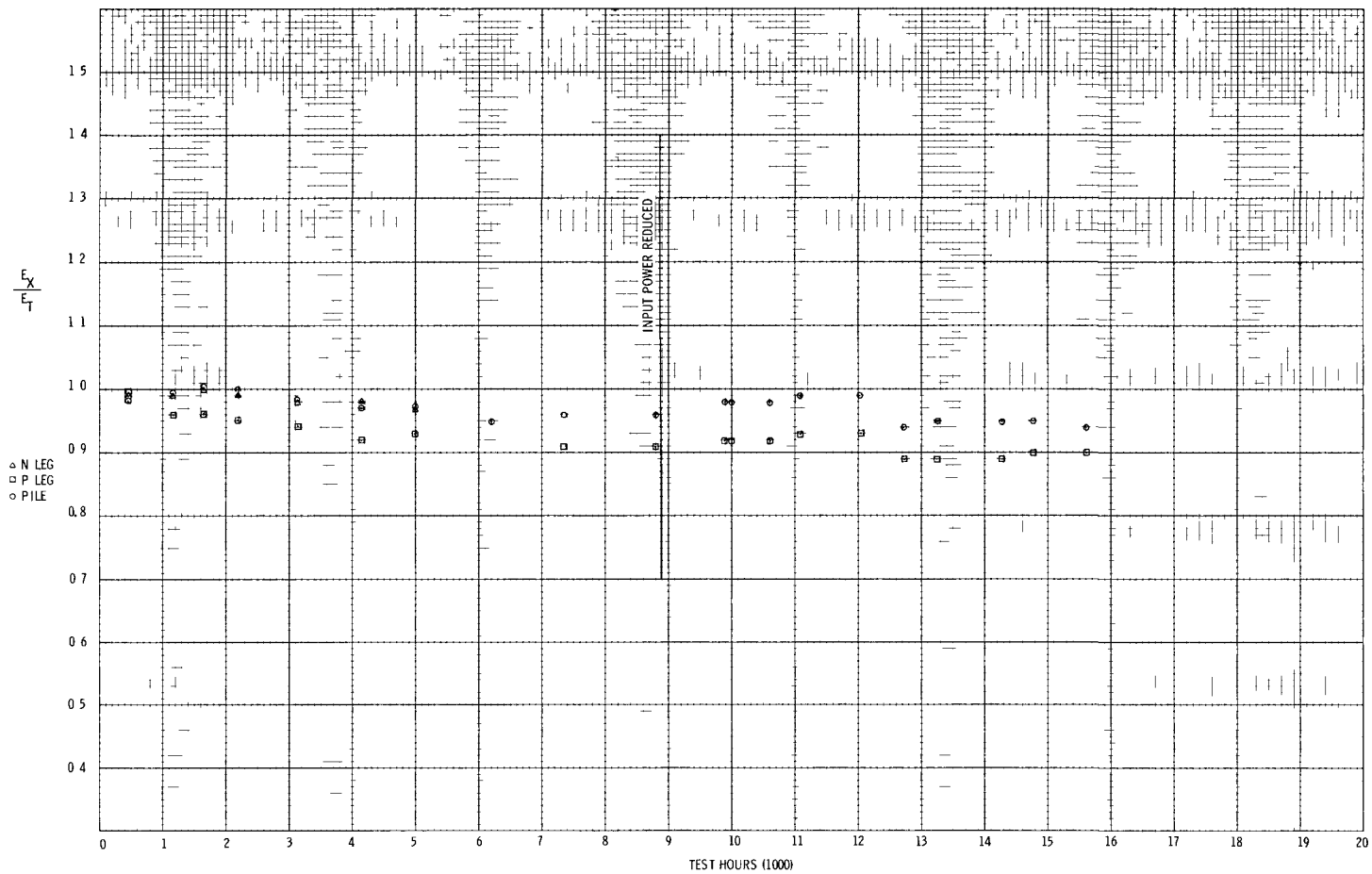

Figure 2-17a. SNAP-21 Thermoelectric Generator A10D2 Normalized SEEBECK VOLTAGE RATIO

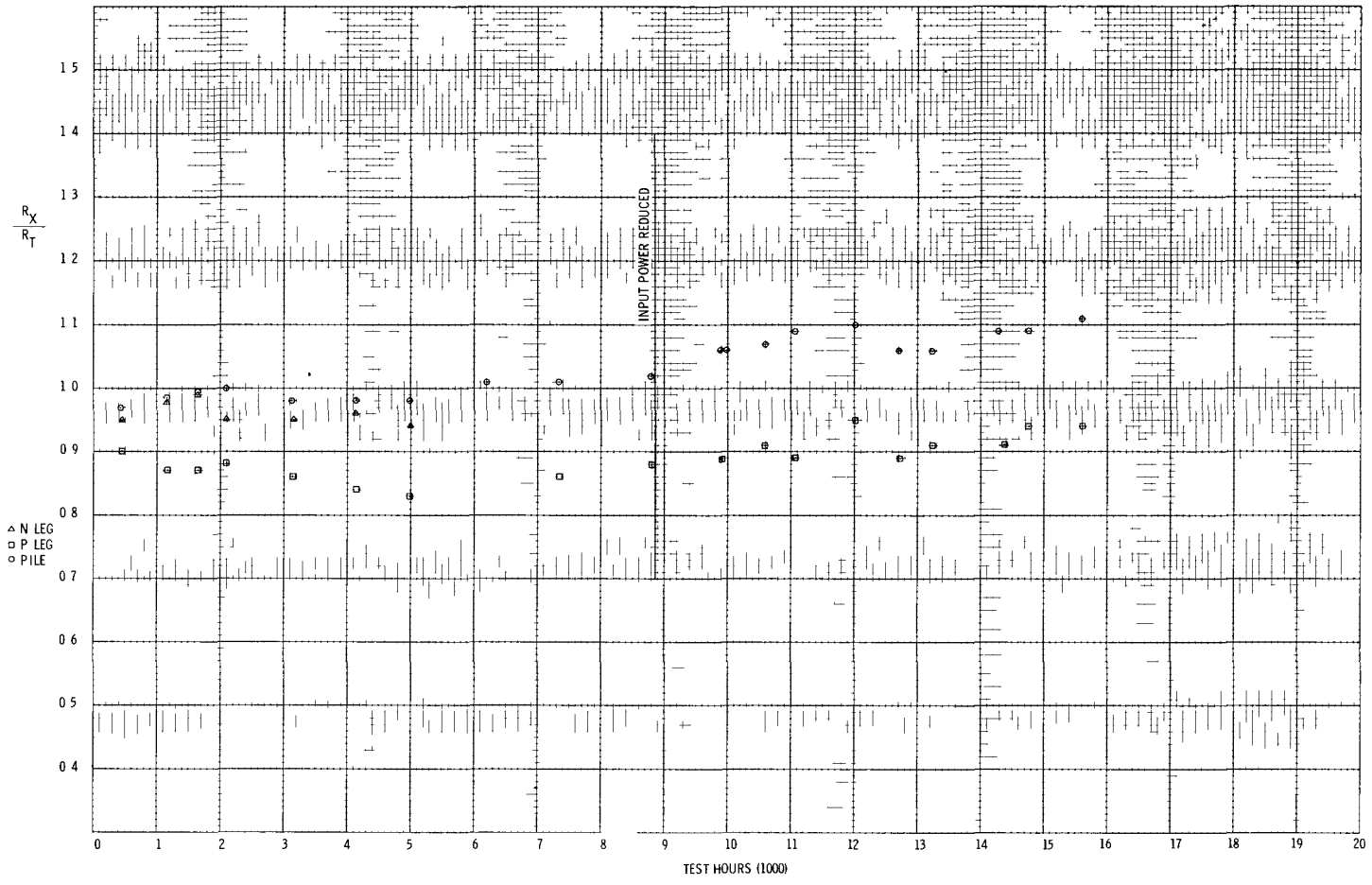

Figure 2-17b. SNAP-21 Thermoelectric Generator A10D2 Normalized RESISTANCE RATIO

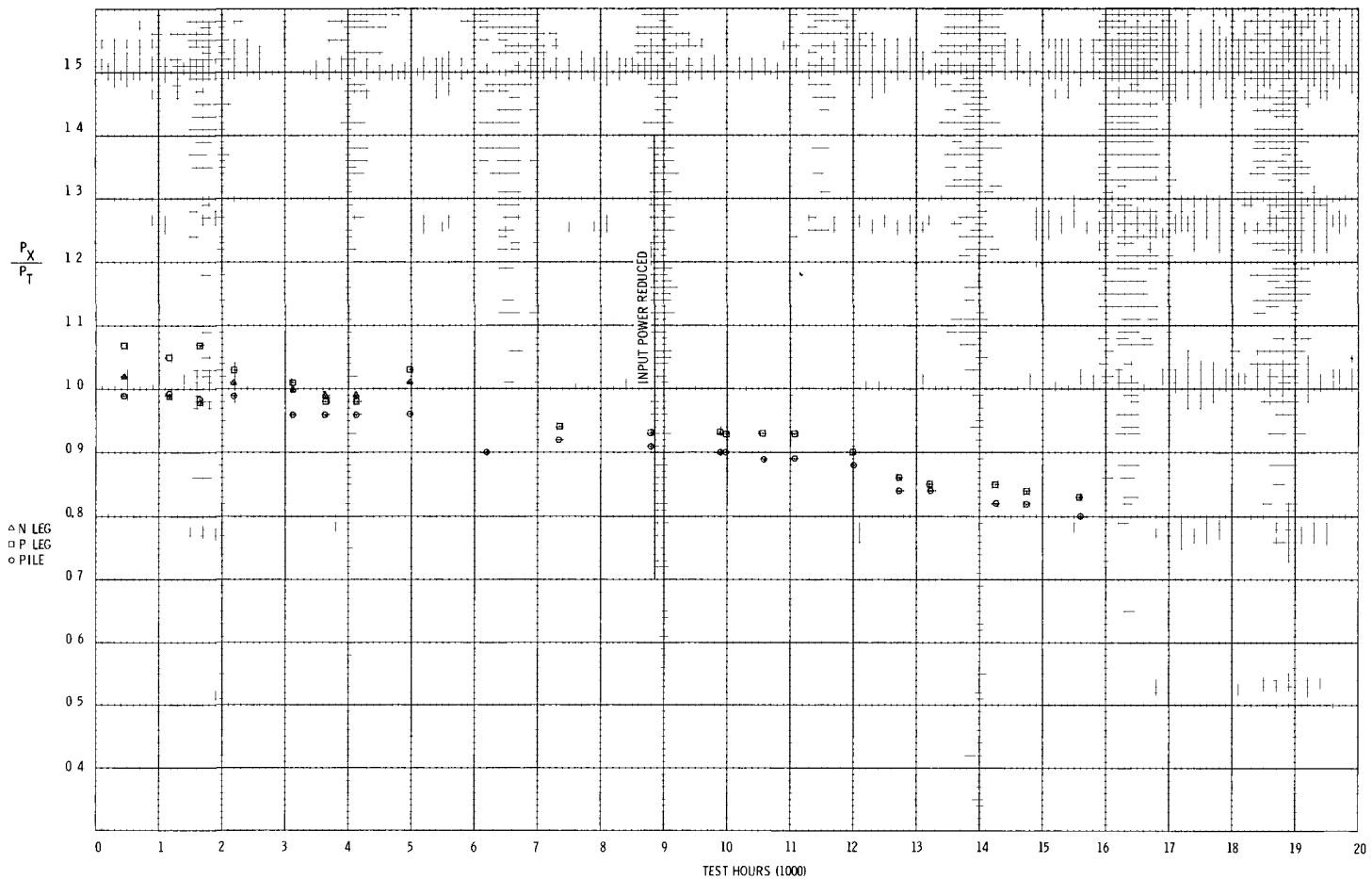

Figure 2-17c. SNAP-21 Thermoelectric Generator A10D2 Normalized POWER RATIO

A10D4

Refer to paragraph 2.1.1.1 for evaluation of generator A10D4 performance.

A10D6

Figures 2-18a through 2-18c are performance curves for this generator. From the curves, it can be seen that the performance for this generator has been stable this past quarter.

A10D7

Figures 2-19a through 2-19c show the performance curves for this generator. The resistance for this generator appears to have stabilized. As a result of the resistance, the power output from the generator has also stabilized. The Seebeck voltage for the generator was fairly stable.

A10P1

Figure 2-20 shows performance data for this generator. It can be seen that the performance for the generator has been stable this report period.

Further investigation into the performance data ratios has shown that the data before 5,140 hours should be about 0.3 of a unit higher than is shown on Figure 2-20. The error was introduced because an erroneous ΔT for external hot frame to the hot button was used in the data reduction computer program.

A ΔT of 60°F was used while a ΔT of 80°F should have been used. The dashed lines indicate the corrected performance for the generator during this period.

2.6 POWER CONDITIONERS

2.6.1 Phase I Power Conditioners

Phase I electronic component testing continued this past quarter with the automatic selector switch, power conditioner MP-C, and regulators operating satisfactorily.

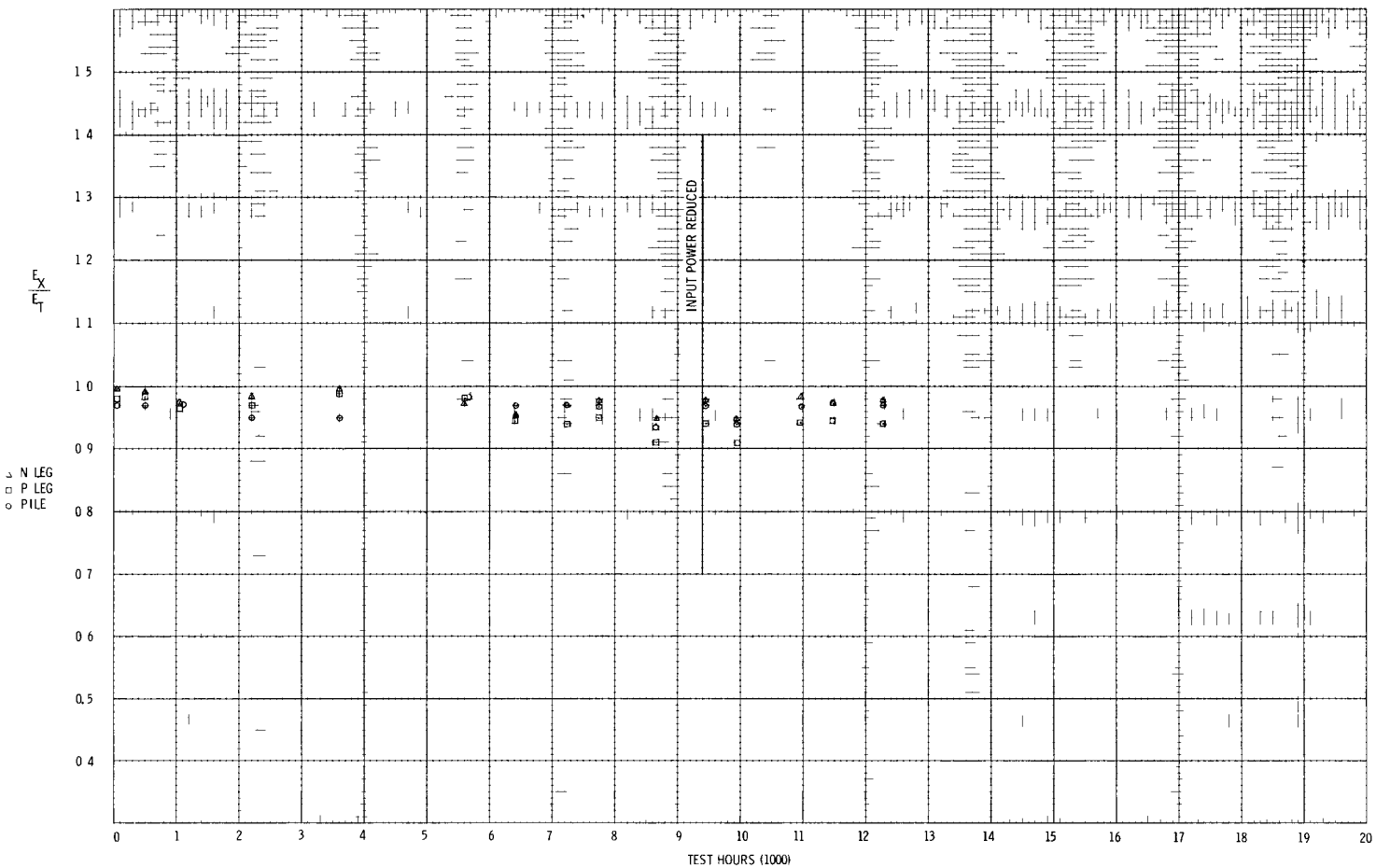

Figure 2-18a. SNAP-21 Thermoelectric Generator A10D6 Normalized SEEBECK VOLTAGE RATIO

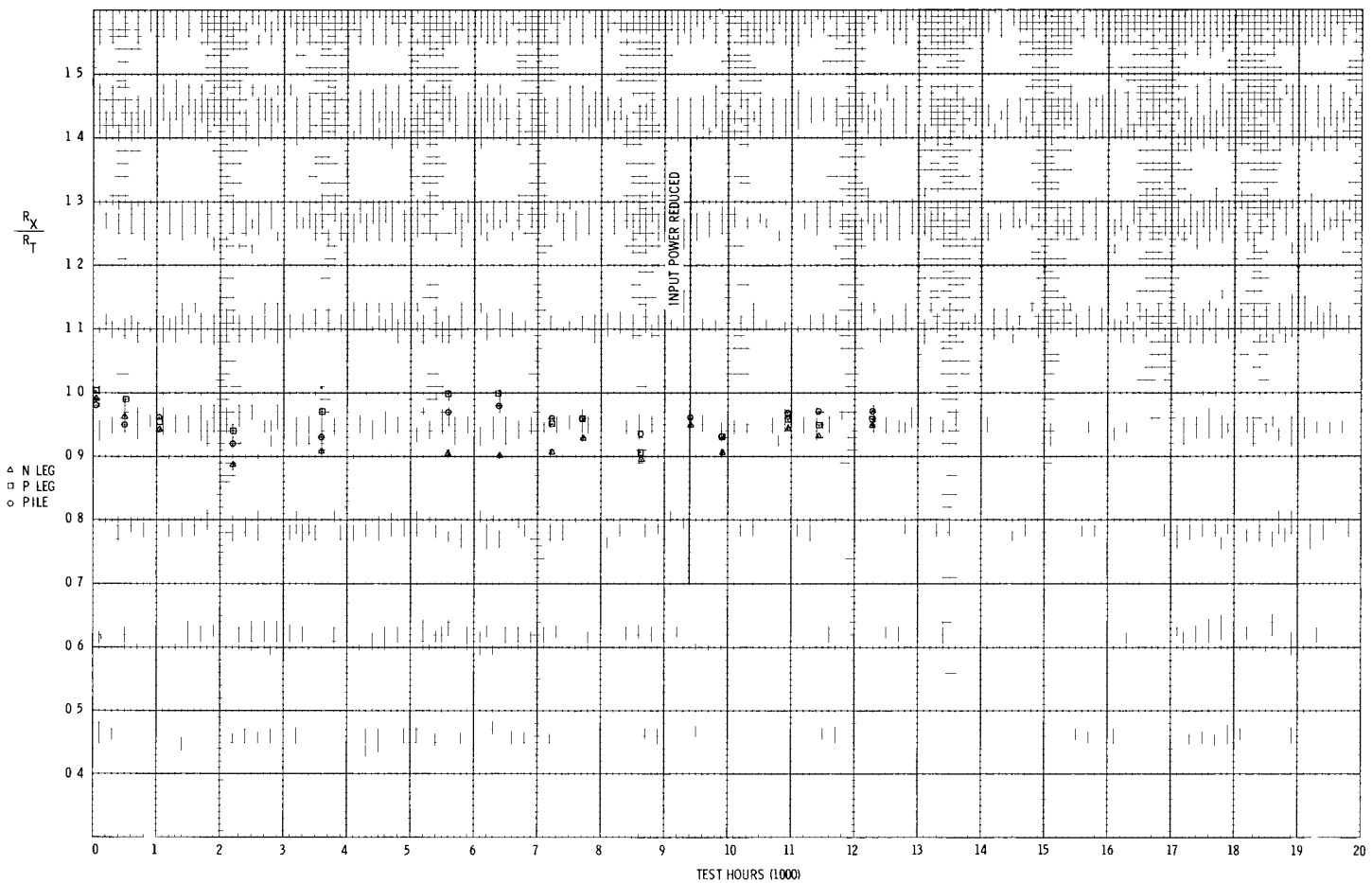

Figure 2-18b. SNAP-21 Thermoelectric Generator A10D6 Normalized RESISTANCE RATIO

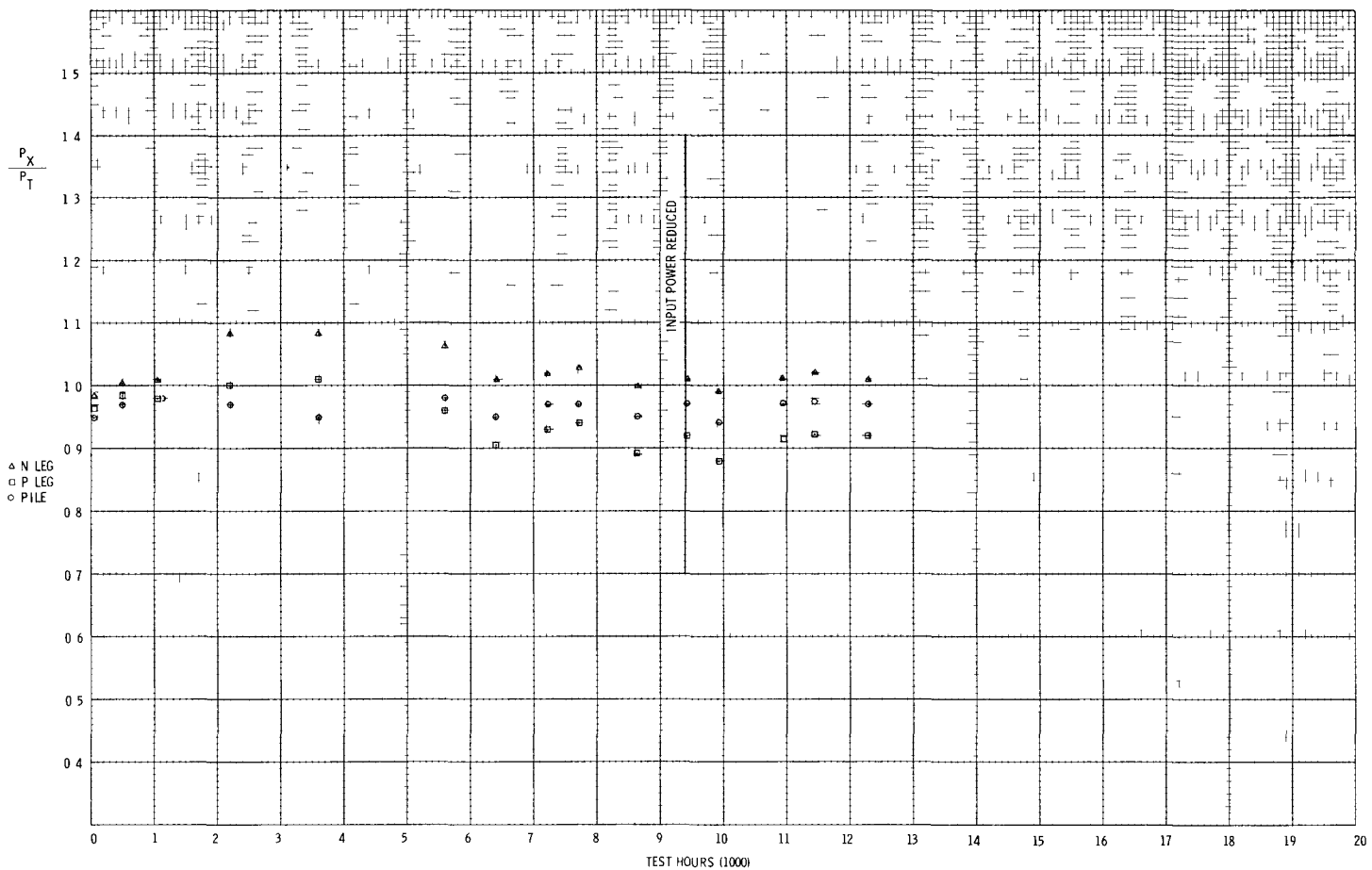

Figure 2-18c. SNAP-21 Thermoelectric Generator A10D6 Normalized POWER RATIO

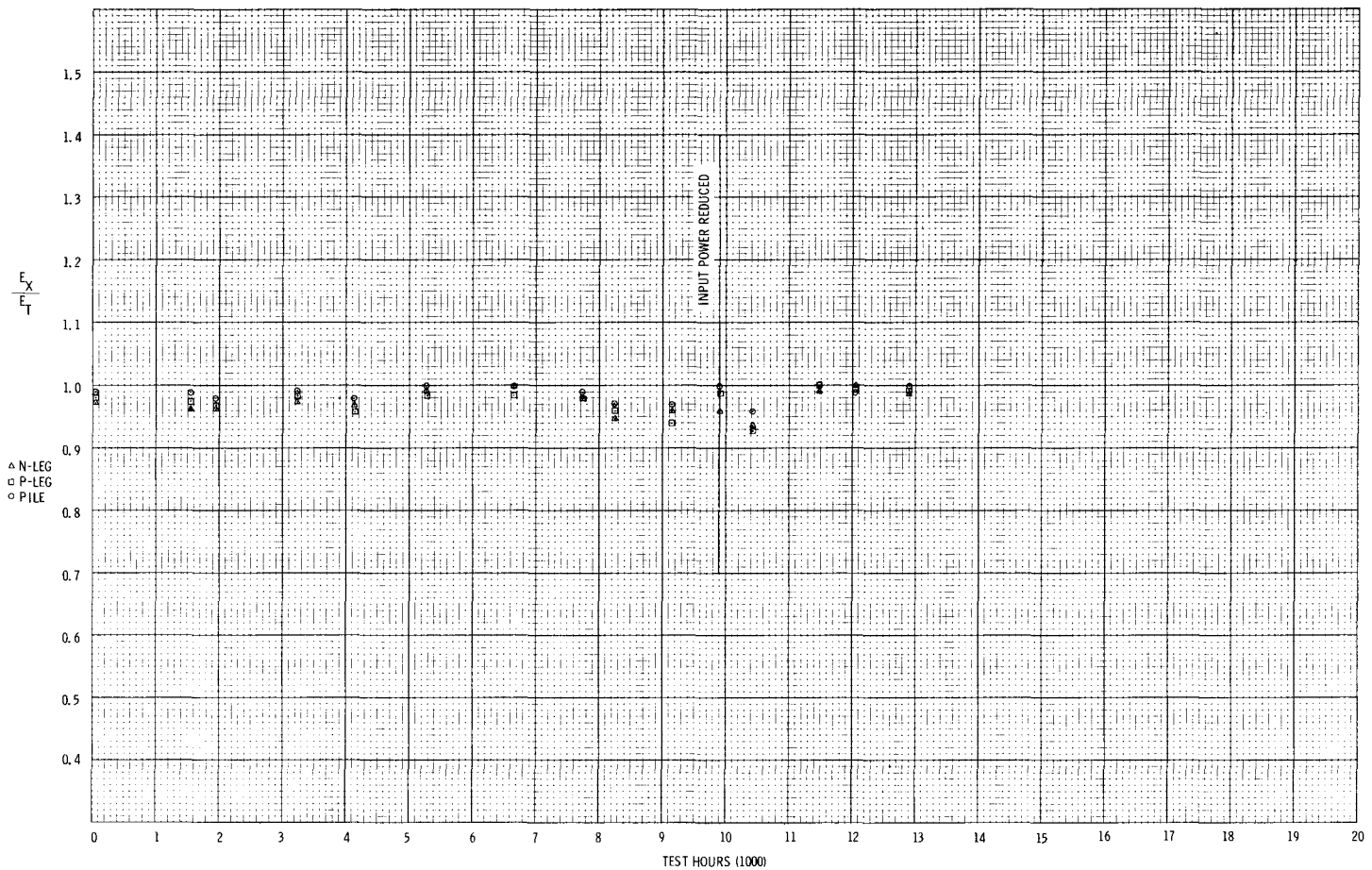

Figure 2-19a. SNAP-21 Thermoelectric Generator A10D7 Normalized SEEBECK VOLTAGE RATIO

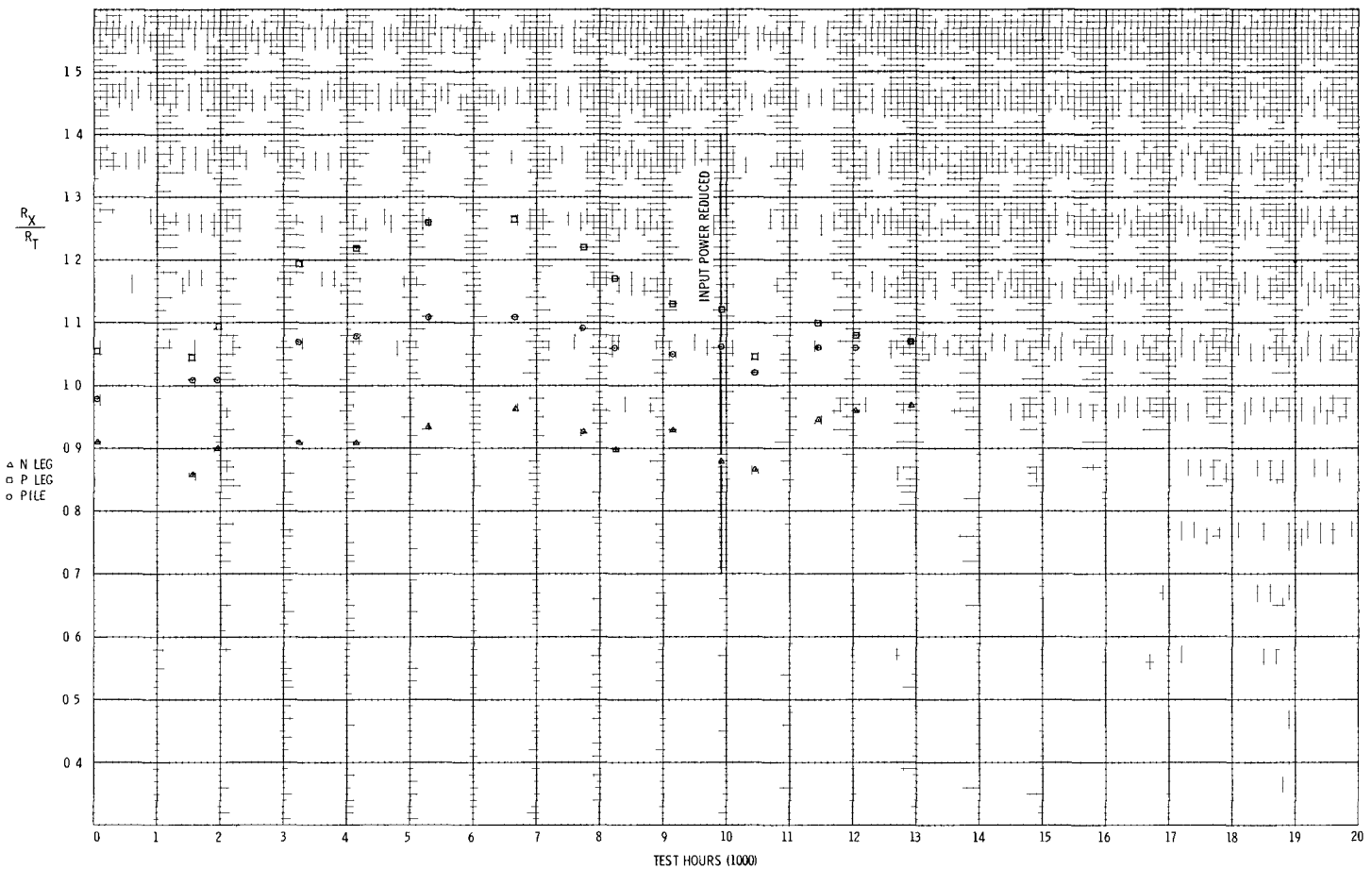

Figure 2-19b. SNAP-21 Thermoelectric Generator A10D7 Normalized RESISTANCE RATIO

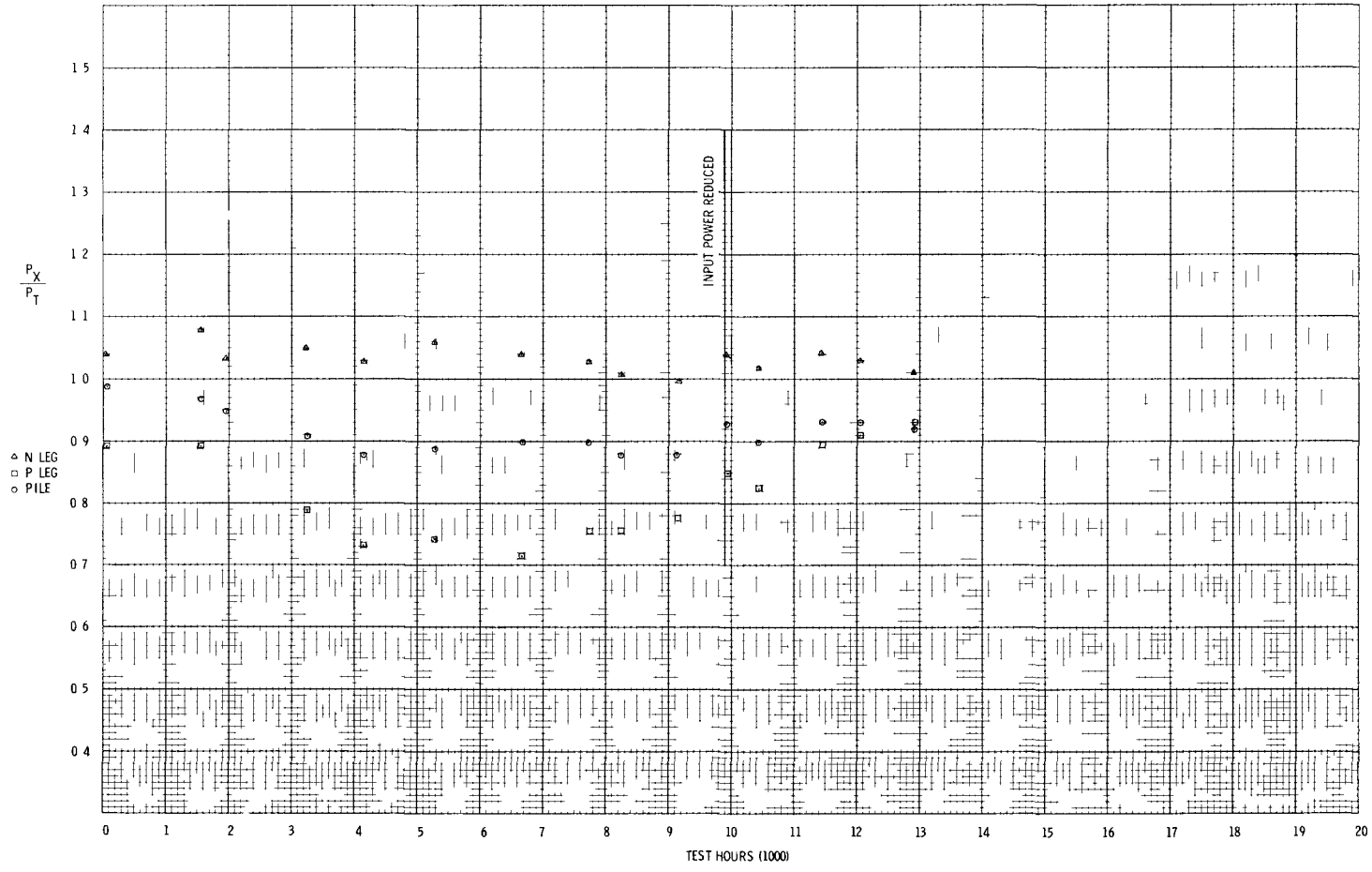

Figure 2-19c. SNAP-21 Thermoelectric Generator A10D7 Normalized POWER RATIO

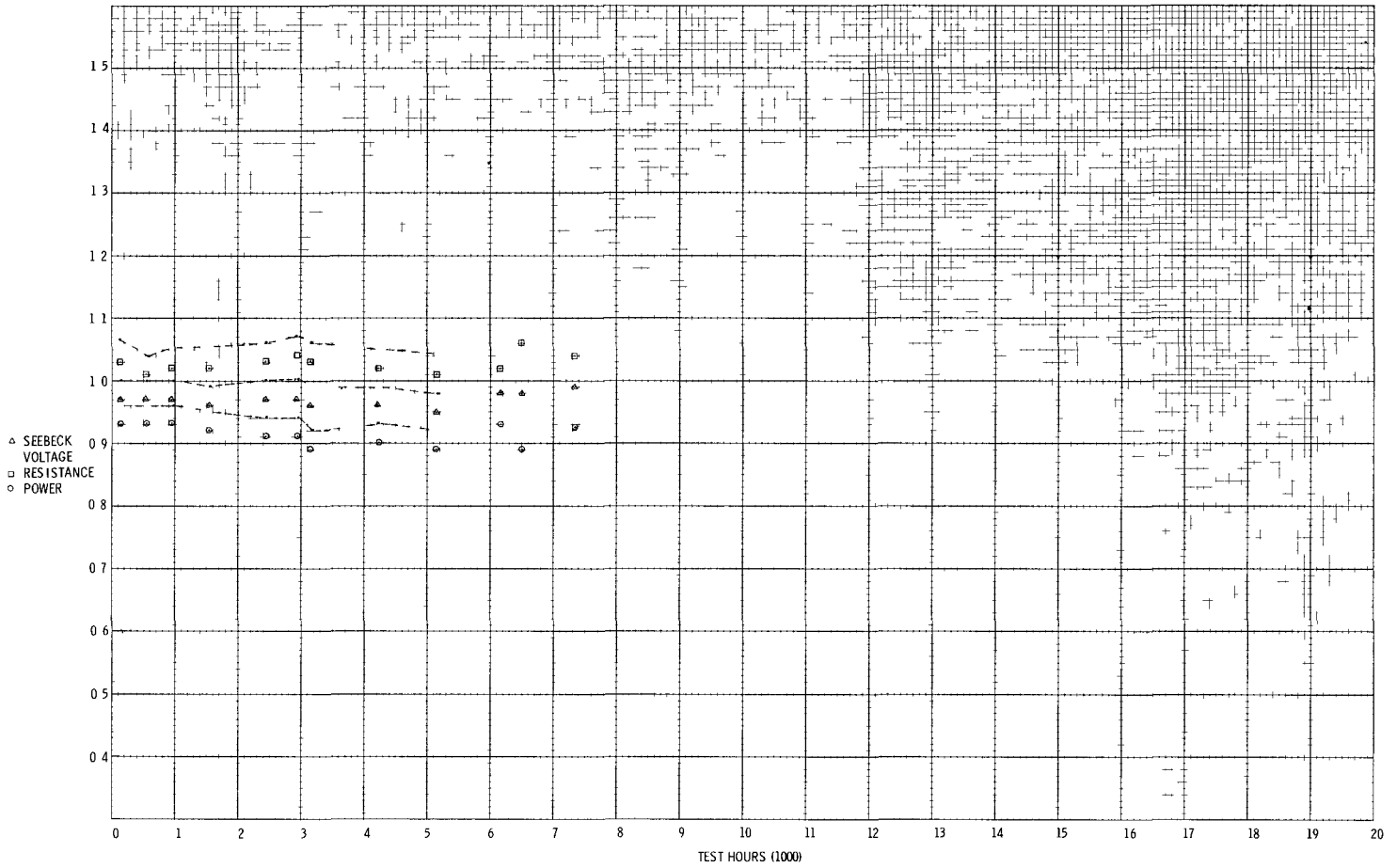

Figure 2-20. SNAP-21 Thermoelectric Generator A10P1 Normalized Data

Tables 2-15 through 2-18 are the life data for these electronic units. As can be seen, the performance for these units has been stable.

2.6.2 Phase II Power Conditioners

Tables 2-19 and 2-20 are the performance data for power conditioners H10D3 and H10D6. As can be seen, the performance for these units has been stable this past report period.

Table 2-15. Phase I Regulator Test Fixture Performance Data

Operating Hours	A Output (vdc)	TRIO-LAB Regulators			High Power Regulator-A HPR-A	
		C Output (vdc)	D Output (vdc)	F Output (vdc)	Output (vdc)	Operating Hours
0	21.7	21.92	22.58	21.36	26.78	0
552	21.82	21.96	22.56	22.04	26.67	451
1,029	21.83	21.98	22.56	22.08	26.76	1,267
1,965	21.82	21.93	22.55	21.98	26.78	2,010
3,045	21.80	21.89	22.54	22.00	26.76	2,929
4,011	21.82	21.92	22.56	22.02	26.78	3,961
5,043	21.81	21.90	22.55	22.00	26.81	4,945
6,147	21.78	21.87	22.52	21.95	26.78	6,121
7,015	21.79	21.88	22.53	21.98	26.77	6,792
8,023	21.80	21.88	22.53	21.98	26.80	8,017
9,125	21.78	21.86	22.52	21.99	26.81	9,504
10,133	21.75	21.82	22.50	21.94	26.82	10,590
11,143	21.79	21.87	22.52	21.98	26.82	11,314
12,031	21.79	21.85	22.52	21.97	26.75	14,288
18,369	21.75	21.86	22.49	21.93	26.78	17,552
18,729	21.72	21.79	22.47	21.90	26.77	17,912
19,257	21.72	21.78	22.46	21.89	26.80	18,440
19,401	21.72	21.78	22.46	21.88	26.81	18,584
19,881	21.54	21.63	22.41	21.88	26.46	19,064
20,265	21.53	21.55	22.42	21.90	26.47	19,448
20,673	21.53	21.46	22.42	21.88	26.51	19,856
21,117	21.49	21.39	22.40	21.84	26.51	20,360
21,161	21.52	21.37	22.39	21.85	26.51	21,344
22,617	21.60	20.79	22.40	21.88	26.48	21,800
23,145	21.46	21.45	22.35	21.82	26.45	22,328
23,769	21.46	21.13	22.31	21.82	26.36	22,952
24,297	21.35	21.52	22.41	21.82	26.31	23,480
24,777	21.43	20.93	22.33	21.76	26.34	23,960
25,137	21.49	21.00	22.36	21.83	26.47	24,320

Table 2-15. Phase I Regulator Test Fixture Performance Data (Continued)

Operating Hours	TRIO-LAB Regulators				High Power Regulator-A HPR-A	
	A Output (vdc)	C Output (vdc)	D Output (vdc)	F Output (vdc)	Output (vdc)	Operating Hours
25,449	21.49	21.00	22.39	21.84	26.53	24,632
25,929	21.50	20.97	22.39	21.83	26.56	25,112
26,381	21.51	20.95	22.40	21.84	26.60	25,564
26,693	21.74	21.81	22.46	21.92	26.93	25,876
28,061	21.52	21.30	22.41	21.83	26.52	27,244
28,541	21.51	21.27	22.38	21.81	26.56	27,724
29,525	21.48	21.00	22.33	21.75	26.52	28,708
30,773	21.46	21.01	22.31	21.75	26.52	29,956
31,733	21.48	20.82	22.32	21.76	26.53	30,916
32,189	21.49	20.28	22.33	21.80	26.51	31,372
33,029	21.51	20.25	22.36	21.78	26.55	32,212
33,941	21.61	21.07	22.39	21.81	26.73	33,124
34,541	21.70	21.73	22.39	21.83	26.78	33,724
35,405	21.70	21.74	22.40	21.85	26.85	34,588
36,317	21.71	21.74	22.41	21.86	26.87	35,500
37,325	21.70	21.74	22.40	21.84	26.86	36,508
37,709	21.63	21.35	22.37	21.78	26.85	36,892
38,405	21.63	21.35	22.37	21.78	26.84	37,588
38,765	21.69	21.73	22.40	21.85	26.85	37,948
39,101	21.70	21.72	22.40	21.82	26.83	38,284
39,413	21.70	21.74	22.41	21.90	26.88	38,596

Table 2-16. Performance of Phase I Power Conditioner MP-C

Converter Performance Power Conditioner	E_I (volts)	I_I (amps)	P_I (watts)	E_o (volts)	I_o (amps)	P_o (watts)	Efficiency %	Hours on Test	Notes
	4.909	2.386	11.814	24.00	0.434	10.42	88.10	23	
	4.912	2.380	11.792	24.00	0.433	10.39	88.08	577	
	4.911	2.388	11.830	24.00	0.434	10.43	88.16	1,072	
	4.909	2.388	11.824	24.00	0.435	10.43	88.22	2,064	
	4.908	2.383	11.798	24.00	0.434	10.42	88.30	3,069	
	4.913	2.382	11.804	24.00	0.433	10.39	88.03	4,058	
	4.910	2.379	11.782	24.00	0.433	10.39	88.20	5,054	
	4.910	2.363	11.602	24.00	0.429	10.30	87.89	6,017	
	4.910	2.372	11.749	24.00	0.431	10.34	88.04	7,165	
	4.910	2.373	11.754	24.00	0.431	10.34	88.00	8,154	
	4.909	2.366	11.718	24.00	0.430	10.32	88.07	9,136	
MP-C	4.913	2.395	11.809	24.00	0.436	10.464	88.61	15,783	
	4.908	2.360	11.606	24.00	0.429	10.296	88.71	16,143	
	4.909	2.374	11.757	24.00	0.432	10.368	88.19	16,671	
	4.910	2.378	11.779	24.00	0.433	10.392	88.22	16,815	
	4.906	2.372	11.740	24.00	0.432	10.368	88.31	17,295	
	4.905	2.374	11.747	24.00	0.432	10.368	88.26	17,679	
	4.904	2.353	11.642	24.00	0.428	10.272	88.23	17,087	
	4.909	2.389	11.831	24.00	0.439	10.416	88.04	18,591	
	4.912	2.395	11.867	24.00	0.436	10.464	88.18	19,575	
	4.913	2.396	11.878	24.00	0.436	10.464	88.10	20,031	
	4.910	2.375	11.764	24.00	0.432	10.368	88.13	20,559	
	4.908	2.371	11.740	24.00	0.431	10.344	88.11	21,183	
	4.909	2.375	11.762	24.00	0.432	10.368	88.15	21,811	
	4.909	2.376	11.767	24.00	0.432	10.368	88.11	22,098	
	4.910	2.375	11.764	24.00	0.432	10.368	88.13	22,485	
	4.912	2.403	11.907	24.00	0.438	10.512	88.28	22,770	
	4.911	2.377	11.776	24.00	0.433	10.380	88.92	23,250	
	4.909	2.357	11.674	24.00	0.428	10.270	87.99	24,066	Note Unit accidentally shut down. Discovered on 12/22/67. Power restored 12/22/67
	4.908	2.368	11.725	24.00	0.431	10.344	88.22	25,434	
	4.908	2.368	11.725	24.00	0.430	10.320	88.02	25,914	
	4.908	2.374	11.755	24.00	0.432	10.368	88.21	26,898	
	4.908	2.376	11 764	24.00	0.432	10 368	88.13	28,146	
	4.910	2.378	11.779	24.00	0.433	10.384	88.16	29,106	
	4.910	2.395	11.862	24.00	0.435	10.440	88.01	29,562	
	4.909	2.395	11.860	24.00	0.435	10.440	88.03	30,402	
	4.907	2.375	11.757	24.00	0.432	10.368	88.18	31,314	
	4.905	2.373	11.743	24.00	0.434	10.416	88.70	31,914	
	4.904	2.371	11.730	24.00	0.431	10.344	88.18	32,778	
	4.907	2.381	11.780	24.00	0.433	10.392	88.21	34,698	
	4.907	2.381	11.780	24.00	0.433	10.392	88.21	36,618	
	4.910	2.375	11.760	24.00	0.433	10.392	88.37	37,002	
	4.909	2.375	11.760	24.00	0.433	10.392	88.37	37,698	
	4.911	2.384	11.810	24.00	0.434	10.416	88.20	38,058	
	4.910	2.378	11.780	24.00	0.433	10.392	88.22	38,394	
	4.910	2.391	11.840	24.00	0.433	10.392	87.77	38,706	

Table 2-17. Phase I Automatic Selector Switch Performance Data

Notes	Hours	Output Voltage	
		Conditioner MP-A (vdc)	Conditioner MP-D (vdc)
	360	24.60	24.45
	646	24.47	24.58
	1,056	24.47	24.59
	1,968	24.46	24.49
	2,975	24.48	24.59
	4,103	24.45	24.57
	5,087	24.46	24.58
	6,071	24.47	24.58
	7,415	24.44	24.56
	13,583	24.54	24.59
	14,471	24.56	24.60
Note: System turned off from 4/24/67 to 6/6/67.	15,095	24.62	24.58
	15,887	24.50	24.59
	16,799	24.45	24.57
	17,951	24.50	24.55
	18,959	24.47	24.57
	19,631	24.48	24.58
	20,687	24.45	24.56
	20,999	24.48	24.56
	22,367	24.49	24.60
Note: At 22,367 hours system shut down to install into cabinet type mount (2/28/67).	22,895	24.49	24.56
	24,119	24.49	24.57
	24,719	24.50	24.57
Note: 8/27/68 unit put back on test.	25,583	24.51	24.58
	26,495	24.48	24.55
	27,503	24.48	24.56
	27,887	24.46	24.56
	28,583	24.46	24.55
	28,943	24.50	24.56
	29,279	24.46	24.55
	29,591	24.50	24.58

Table 2-18. Phase I Regulator Performance Data
Conditioner: MP-C
Regulator: I

Operating Hours	No-Load Voltage (vdc)
23	24.55
577	24.55
1,072	24.53
2,064	24.53
3,069	24.53
4,059	24.53
5,054	24.53
6,017	24.53
7,165	24.53
8,154	24.54
9,136	24.54
10,088	24.54
15,783	24.54
16,815	24.53
18,087	24.53
20,031	24.52
22,098	24.51
22,770	24.50
23,250	24.51
24,066	24.51
25,434	24.49
26,898	24.52
28,146	24.52
29,106	24.52
30,402	24.51
31,314	24.52
32,778	24.52
34,698	24.52
36,618	24.52
37,002	24.51
37,698	24.51
38,058	24.53
38,394	24.51
38,706	24.51

Table 2-19. Power Conditioner H10D3 Performance Data

E_I Primary (volts)	I_I Primary (amps)	P_I Primary (watts)	E_I Bias (volts)	I_I Bias (amps)	P_I Bias (watts)	E_o (volts)	I_o (amps)	P_o (watts)	Efficiency (%)	Temp (°F)	Test* Hours
5 06	2 17	11 02	0 646	0 132	0 085	23 77	0 424	10 08	90 77	82	1296
5 06	2 17	11 00	0 657	0 132	0 085	23 76	0 423	10 05	90 66	82	1413
5 08	2 18	11 07	0 658	0 134	0 087	23 80	0 422	10 04	89 99	82	1576
5 08	2 18	11 07	0 647	0 132	0 085	23 81	0 422	10 05	90 09	80	1894
5 08	2 18	11 07	0 648	0 132	0 086	23 83	0 422	10 06	90 18	81	2106
5 08	2 18	11 07	0 648	0 134	0 087	23 82	0 422	10 05	90 10	86	2904
5 08	2 18	11 07	0 647	0 134	0 087	23 81	0 422	10 05	90 07	86	3575
5 08	2 18	11.07	0 648	0 134	0 087	23 82	0 422	10 05	90 07	86	4244
5.08	2.18	11.07	0.648	0.134	0.087	23.83	0.422	10.06	90.17	86	5058
5.08	2.18	11.07	0.648	0.134	0.087	23.82	0.422	10.05	90.08	87	5928
5.08	2.18	11.07	0.648	0.134	0.087	23.83	0.422	10.06	90.17	87	6476
5.08	2.18	11.07	0.648	0.134	0.087	23.85	0.422	10.06	90.17	92	7468
5.08	2.18	11.07	0.648	0.134	0.087	23.84	0.422	10.06	90.17	90	7684
5.07	2.18	11.05	0.646	0.134	0.087	23.79	0.422	10.04	90.15	93	8081
5.07	2.18	11.05	0.646	0.134	0.087	23.79	0.422	10.04	90.15	92	8327
5.07	2.18	11.05	0.647	0.134	0.087	23.80	0.422	10.04	90.15	92	8640

Includes 1241 hours of short-term tests.

Table 2-20. Power Conditioner H10D6 Performance Data

E_I Primary (volts)	I_I Primary (amps)	P_I Primary (watts)	E_I Bias (volts)	I_I Bias (amps)	P_I Bias (watts)	E_o (volts)	I_o (amps)	P_o (watts)	Efficiency (%)	Temp (°F)	Test* Hours
4 81	2 35	11 30	0 646	0 122	0 079	24 00	0 430	10 32	90 69	82	1296
4 81	2 35	11 30	0 646	0 122	0 079	24 00	0 430	10 32	90 69	82	1437
4 82	2 35	11 33	0 648	0 122	0 079	24 08	0 425	10 23	89 67	82	1600
4 83	2 35	11 35	0 648	0 122	0 079	24 20	0 430	10 41	91 08	80	1968
4 83	2 35	11 35	0 648	0 122	0 079	24 09	0 425	10 24	89 60	81	2278
4 82	2 35	11 33	0 648	0 122	0 079	24 07	0 425	10 23	89 67	87	2904
4 82	2 35	11 33	0 647	0 122	0 079	24 07	0 425	10 23	89 67	86	3575
4 82	2 35	11 33	0 648	0 122	0 079	24 07	0 425	10 24	89 75	87	4244
4.82	2.35	11.33	0.648	0.122	0.079	24.08	0.425	10.23	89.67	87	5058
4.82	2.35	11.33	0.647	0.122	0.079	24.07	0.430	10.35	90.72	88	5928
4.82	2.35	11.33	0.648	0.122	0.079	24.10	0.425	10.24	89.75	87	6476
4.82	2.35	11.33	0.648	0.122	0.079	24.10	0.430	10.36	90.80	93	7468
4.82	2.35	11.33	0.648	0.122	0.079	24.09	0.425	10.24	89.75	89	7684
4.82	2.35	11.33	0.648	0.122	0.079	24.06	0.425	10.23	89.67	94	8081
4.82	2.35	11.33	0.647	0.122	0.079	24.04	0.425	10.22	89.81	93	8327
4.81	2.35	11.30	0.647	0.122	0.079	24.04	0.425	10.22	89.81	89	8640

Includes 1271 hours of short-term tests.

2.7 ELECTRICAL RECEPTACLE AND STRAIN RELIEF PLUG

No effort was expended in this area during the report period.

2.8 PRESSURE VESSEL

No effort was expended in this area during this report period.

2.9 NSRDC 10-COUPLE MODULES

A 3M Company engineer and technician were at NSRDC to instruct and assist in the assembly of 10-couple module number 5. The module was assembled and processed. All instrumentation was intact at the end of processing.

The following comments are made on the operation at NSRDC.

- The relative humidity in the assembly area was approximately 50 percent. A relative humidity of 35 percent is desired.
- The welding and machine shops are not familiar with the type of work done on these modules. The reject rate of the closely machined parts from the machine shop was near 100 percent. The welding shop experience is largely in the area of heavy structural and high pressure joint welding. The welder who observed the 3M Company welding techniques had become sick and was not present. The welding of the outer case to the top cover and pedestal showed this loss of experience. The welding was done too slowly and with such heat penetration that the soft solder header joints opened up. These joints were sealed by potting.
- There are no formalized inspection or sign off procedures during assembly or processing. A quality job is dependent on the skill of the technician. Although the technicians assigned to this task are capable, without the documentation to prove proper assembly and processing, analysis of any future problems associated with the testing of these modules would be difficult.

2.10 NRDL SYSTEM TESTING

Systems S10P1 and S10P2 were shipped from 3M and arrived at NRDL (San Francisco) on June 2, 1969. System checkout on both systems indicated that the systems were operating satisfactorily.

Table 2-21 shows a comparison of the data received from 3M's SRP test set-up on S10P2 and from the NRDL Data Acquisition System (DAS).

Table 2-21. Data Comparison (System S10P2)

	NRDL Data Acquisition System 6/12/69	3M Test Console 6/12/69	Percent Difference
$T_{press\ vessel}$	89	90	1.1
$T_{seg\ ring}$	100	100	0
$T_{cold\ frame}$	107	106	0.94
$T_{hot\ frame\ center}$	---	---	---
$T_{hot\ frame\ edge}$	1061	1060	0.094
$T_{emitter}$	1251	1250	0.08
V_{gbr} (TEG bias shunt voltage)	0.0062	0.0060	3.3
V_{gpr} (TEG primary shunt voltage)	0.0109	0.0109	0
V_{gbl} (TEG bias load voltage)	0.690	0.678	1.76
V_{gpl} (TEG primary load voltage)	4.97	4.95	0.4
E_{gbo} (TEG bias open circuit voltage)	1.42	1.39	2.15
E_{gpo} (TEG primary open circuit voltage)	9.61	9.56	0.52
V_{sr} (system shunt voltage)	0.0416	0.0426	2.3
V_{sl} (system load voltage)	24.5	24.4	0.4
E_{so} (system open circuit voltage)	9.61	9.56	0.52

From Table 2-21 it can be seen that the thermal data agrees closely but there appears to be some differences in the electrical data. The following comments can be made with regard to these major differences:

V_{gbr} - The cause for the 3.3% difference is that NRDL has a slightly different shunt resistance than is in 3M's test console. It was desired to use a resistor with the same value, 0.05Ω, but an error was introduced with the actual placement of the monitoring leads. The bias shunt resistors of all the cables were measured prior to potting and these new values will be used for calculating the bias current.

V_{gbl} - The 1.76% difference is due to the different amount of lead resistance introduced into the bias circuit for the two test set-ups. With the 3M test console about 24 feet of 16-gauge wire is introduced while with NRDL's test cable only about one foot is introduced.

E_{gbo} - The difference in this reading is probably due to a difference in timing and sequence when the open circuit voltage is read.

V_{sr} - The cause for the 2.3% difference is the same as for V_{gbr} (that is, that some extraneous rèsistance was introduced with the actual placement of the monitoring leads). All the system shunt resistors were measured prior to potting. These values will be used in the calculation of the system load current.

After checkout was completed at San Francisco, both systems and related equipment were sent to San Clemente Island for implantment.

On June 25, 1969, system S10P1 was removed from the shipping container on San Clemente Island, positioned in the implantment structure, hoisted aboard the implantment barge and transported to the pier near the implantment site. No problems were encountered with this phase of the operation except that the thermoelectric generator shorting plug, prepared by NRDL, was found to be incorrectly wired. This was quickly remedied using the island's electronics shop equipment.

Implantment procedures involved laying the instrumentation cable (by barge) from the pier to the site, connecting the cable to the system, and implantment. Prior to these operations, the cable was connected to the system at the pier to verify system and instrumentation integrity. At this point it was discovered that the NRDL data system was not functioning properly.

After several hours of trouble shooting, the problem was traced to the data processor (digital computer) and could not be immediately resolved. Verification of system and data transmission integrity was accomplished using auxiliary equipment inserted prior to the data processor in the data transmission chain. At this point the decision was made to proceed with the implantment and debug the data acquisition system at a later date.

System S10P1 was successfully implanted in approximately 50 feet of water.

On June 26, 1969, nearly the same course of events transpired for system S10P2, with the exception that during the pier side checkout, the thermocouple data signal appeared to be in error, even when measured prior to the data processor. Simple Seebeck calculations conducted by 3M personnel and correlated to known system performance characteristics indicated that the thermocouple signals had to be in error. System integrity was confirmed by 3M personnel by removing the instrumentation cable and probing the system via the receptacle pins with portable temperature measuring equipment. Analysis of the situation again indicated that the trouble was in the data acquisition system. And again the decision was made to proceed with the implantment.

After minor difficulties in laying the cable and positioning the barge, system S10P2 was successfully implanted in approximately 120 feet of water.

Data taken manually after implantment indicated that both systems are operating as expected.

Complete photographic documentation of the implantment was obtained.

3.0 TASK II – 20-WATT SYSTEM

3.1 CONCEPTUAL DESIGN

Conceptual design effort on the 20-watt system was authorized to commence during this report period. This effort was initiated twice before, once in the third quarter of 1966 and once in the second quarter of 1968. Both of these previous starts were terminated after approximately one quarter of low level effort.

Significant accomplishments of these previous efforts are summarized below:

- System design criteria were formulated (Reference Quarterly Report No. 8, MMM 3691-35).
- Two basic design concepts were established for further analysis. Concept I which utilizes two 10-watt thermoelectric generators positioned at each end of the biological shield, and Concept II which utilizes a single 20-watt thermoelectric generator and is basically a scaled-up 10-watt system (reference Quarterly Report No. 8, MMM 3691-35).
- Several methods of supporting the biological shield within the HTVIS for each concept were investigated by Linde, and the heat leak for each method was calculated.
- Preliminary performance data for a single 20-watt thermoelectric generator for use in system Concept II was prepared (reference Quarterly Report No. 9, MMM 3691-39).
- Several methods of improving the heat rejection efficiency of the single TEG system (Concept II) were investigated. One method appeared to be technically feasible (reference Quarterly Report No. 9, MMM 3691-39).

- Based on the limited conceptual design analysis that was performed, a comparison of the key characteristics of both system concepts was made (Table 3-1).

- Based on the results of the concept comparison, Concept II was identified as the best concept. A summary of the physical characteristics and performance predictions for the selected concept is shown in Table 3-2. Included in the summary is the effect of two fuel forms (SrO_2 and $SrTiO_3$) on system characteristics.

The conceptual design effort, which was initiated during this report period, is planned to be more comprehensive in nature than the previous efforts. It will culminate in the preparation of a Conceptual Design Description that selects and justifies the 20-watt system concept to be designed and developed during Task II.

The design criteria applied to the current conceptual design effort is the same as used for the initial efforts (reference Quarterly Report No. 8, MMM 3691-35) with one exception. This exception is the fuel form. The current conceptual design will consider $SrTiO_3$ as the fuel form rather than SrO_2, however the advantage of utilizing SrO_2 will be investigated.

The effort during this report period has consisted of investigating various design concepts for supporting the biological shield in the High Temperature Vacuum Insulation System (HTVIS) and revisions to the Generator Mounting Plate and HTVIS retention system. These components are being studied for both Concept I (Dual TEG) and Concept II (Single TEG). In addition to the conceptual design effort being conducted by 3M, Linde is also investigating variations in the HTVIS design for both concepts. Further details of the effort on each concept are presented in the following paragraphs.

3.2 CONCEPT I (DUAL TEG)

The system configuration designated as Concept I consists of two 10-watt TEG's positioned axially at each end of a directly shielded fuel capsule. The major problems associated with this concept are:

Table 3-1. Concept Comparison Based on Preliminary Conceptual Analysis

Item	Concept I (Dual TEG's)	Concept II (Single TEG)
High Temperature Vacuum Insulation System	New Concept – Development and Fabrication Problems Anticipated	Scale up of 10-watt HTVIS allowing use of existing methods.
Thermoelectric Generator	Uses (2) 10-watt TEG's	New TEG using proven technology and many existing components.
Power Conditioners	Uses (2) 10-watt PC's	New PC using proven technology.
Pressure Vessel	Covers – Use 10-watt forgings, requires new final dimensions. Body – New forging and size.	Cover and body – new forging and size.
Electrical Receptacle	Uses (2) 10-watt receptacles for external power lead combination or (1) 10-watt receptacle with internal power lead combination.	Uses (1) 10-watt receptacle.
Handling Equipment	Requires many new tools and methods.	Uses existing methods and minimum new tooling.
Number of Pressure Vessel Penetrations	4	2
Weight – Short Cover (lbs) Long Cover	900 1130	770 880
Diameter (Inches)	16.4	18.0
Length – Short Cover (in.) Long Cover	33.4 50.0	28.0 38.0
Fuel Loading (BOL) (Watts)	403	386

Note: This table is valid for comparison of concepts only. Actual system performance prediction was based on an additional design iteration.

Table 3-2. Conceptual Design Performance Prediction (1)

Concept II (Single TEG)

Fuel Form	Weight (Lbs) (3)		Maximum Diameter (Inches)	Length (In.)		Biological Shield Weight (Lbs)	Fuel Capsule Redesign	Fuel Loading BOL (Watts)	System Efficiency % - EOL
	Long Cover	Short Cover		Long Cover	Short Cover				
$SrTiO_3$	950	840	18.0	38.0	28.0	375	Yes	386	5.89
SrO_2 (2)	880	770	18.0	38.0	28.0	310	No (2)	378	6.00
Specification Requirement (3)	890	775	18.0	44.0	32.0	None	---	372	6.11

Note: (1) This prediction is based on a second design iteration so that shield weight is based on a more accurate prediction of fuel loading.

(2) The predicted fuel loading of 378 watts of SrO can be contained in the existing 10-watt system fuel capsule.

(3) Predicted weights are based on a beryllium-copper pressure vessel. Specification limits are based on a titanium vessel.

(a) Design of the biological shield support system within the HTVIS,

(b) Support of the HTVIS within the pressure vessel,

(c) Potential fabrication and assembly problems, and

(d) Designing the system to be thermally symmetrical to avoid unequal heat flow through the thermoelectric generators.

During the most recent conceptual design effort, the first three problem areas listed were investigated; however, the problem of thermal symmetry was not explored. A re-evaluation of all aspects of this system concept will be conducted during this conceptual design effort.

The first two major components to be investigated were the HTVIS and the generator mounting plate and HTVIS retention system. Details of the effort to date on these components follows.

3.2.1 HTVIS

Biological Shield Support System

During the initial conceptual design effort, a number of biological shield support systems were considered by both 3M Company and Linde. As a result of this investigation, a support system consisting of a neck tube at one end with a bellows and three tie rods at the other end was selected as the best choice based on heat leak, development risk and manufacturing considerations. This configuration was essentially the same as the existing 10-watt system with the addition of a bellows-sealed opening at the opposite end of the shield from the neck tube.

In the course of reviewing the HTVIS from the standpoint of thermal symmetry, it became obvious that the optimum system from a thermal symmetry standpoint is one that has an equal heat leak from each end of the HTVIS. A support method that would provide this symmetry is one that has a bellows and three tie rods at each end of the shield. A sketch of this concept is shown in Figure 3-1. This method of shield support (six tie rods) was considered early in Task I but was not considered feasible at that time because the thermal expansion of the shield and tie rods could not be matched. The use of an adjustable tie rod (a new concept) however, now makes

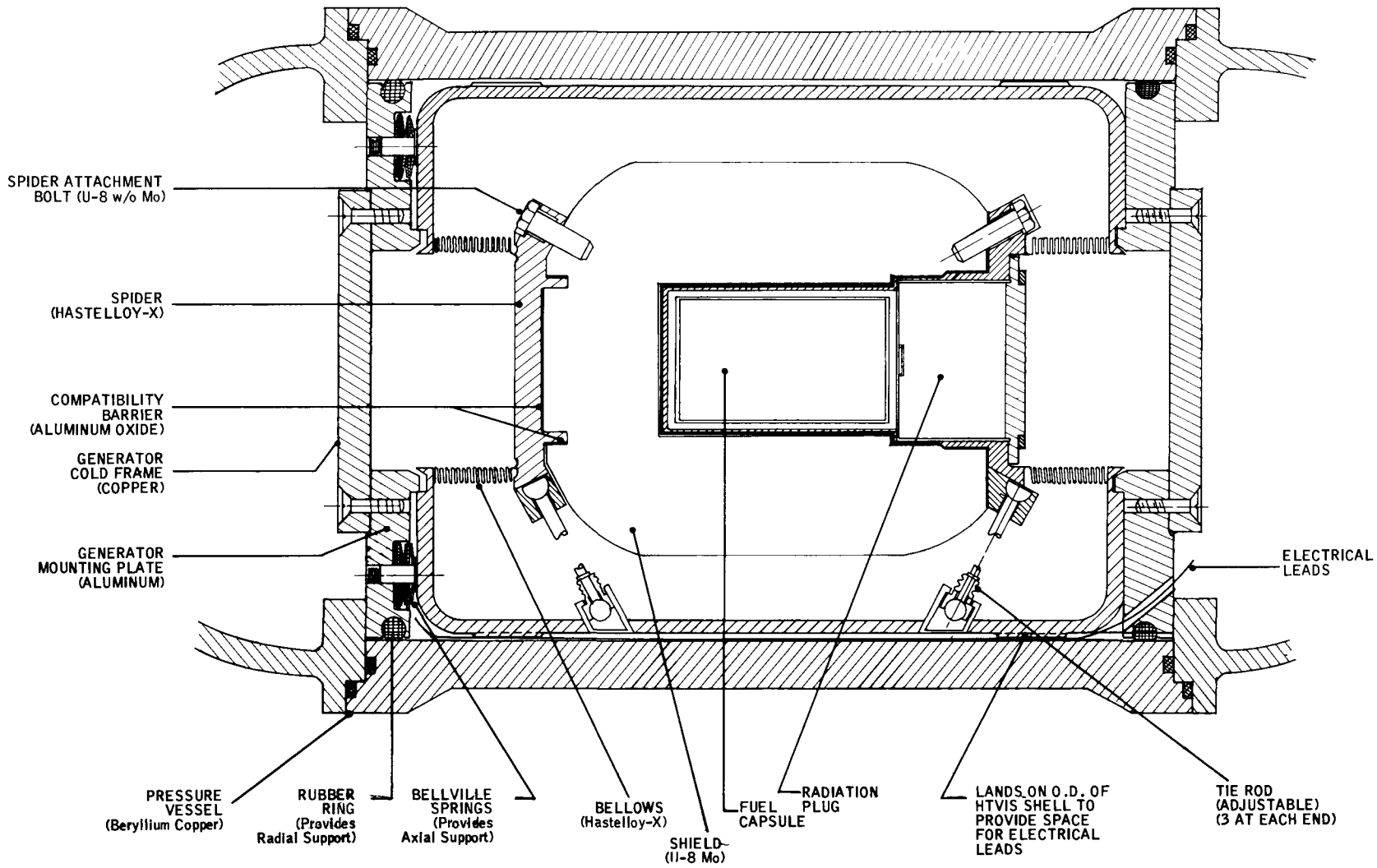

Figure 3-1. SNAP-21 Concept I (Dual TEG) (Illustration of Six Tie Rod Shield Support Concept and Revised Generator Mounting Plate Design)

this method technically feasible. This concept is currently being analyzed by 3M and Linde from the standpoint of thermal efficiency (heat leak), fabrication ease, development risk and cost.

Bellows Design

The double-ended HTVIS will require a bellows to seal the TEG opening. A preliminary design of a bellows that can be used in this application was prepared. The characteristics of the bellows are as follows:

Material	– Hastelloy-X or Inconel 625
Thickness	– 0.006 inch
Convolutions	– 15
Convolution Pitch	– 0.12 inch
Inside Diameter	– 4.9 inch
Outside Diameter	– 5.62 inch

Analysis of the bellows is continuing to determine its heat leak. Contact is being made with bellows manufacturers to determine fabrication feasibility and potential problems.

Shield-to-HTVIS Shell Attachment

A problem common to all of the HTVIS configurations for Concept I is that of securing the shield to the HTVIS shell at the bellows end of the system. Previous experience has shown that utilization of a flat disc ("spider") with large biological shield contact area and three tension tie rods is optimum from the standpoints of minimum heat leak with maximum structural stiffness.

Two basic alternatives in mounting the tie rod spider to the biological shield are being considered. One is a tapered groove contact surface and the other is the cylindrical groove interface that is used on the 10-watt system. With the last approach, physical contact between the spider and the shield can be maintained. This is important when a double generator design is considered since heat transfer between the biological shield and TEG hot frame will occur with the spider as an emitting surface. Contact with the shield over large areas is important in minimizing the temperature drop across the shield-to-spider interface. The latter

method of shield-spider interface is shown in Figure 3-1. Further analysis of this interface will be conducted to determine the temperature differential.

3.2.2 Generator Mounting Plate and HTVIS Retention System

The generator mounting plate and HTVIS retention system serves a dual purpose:

(a) It must align the HTVIS within the pressure vessel and prevent movement of the HTVIS during shock and vibration of the system, and

(b) It must serve as a mounting plate for the TEG and provide an efficient heat rejection path from the TEG cold frame to the pressure vessel wall. In the 10-watt system these functions are performed by the segmented retaining ring.

Although this component is functionally adequate, it is a complex component with a number of close tolerance parts.

It appears feasible to replace the segmented retaining ring by a thick plate using stacked "Belleville" washers for spring loading in the vertical direction, plus utilization of a large rubber "o-ring" between the plate periphery and the inner surface of the pressure vessel cylinder. The rubber ring will allow small changes in radial dimensions due to thermal and pressure effects, while at the same time providing transverse support. The preliminary configuration embodying the above concepts is the one shown in Figure 3-1. Thermal analysis is being conducted in order to establish heat-rejection capabilities for this design.

This concept also offers the advantage of using thermally similar components for the heat rejection path of each TEG thereby maintaining thermal symmetry.

3.3 CONCEPT II (SINGLE TEG)

The system configuration designated as Concept II is basically a scaled-up 10-watt system (see Figure 3-2).

The basic problems associated with this concept are the design of a 20-watt TEG and the problem of rejecting heat from the TEG to the sea water with an acceptable temperature drop.

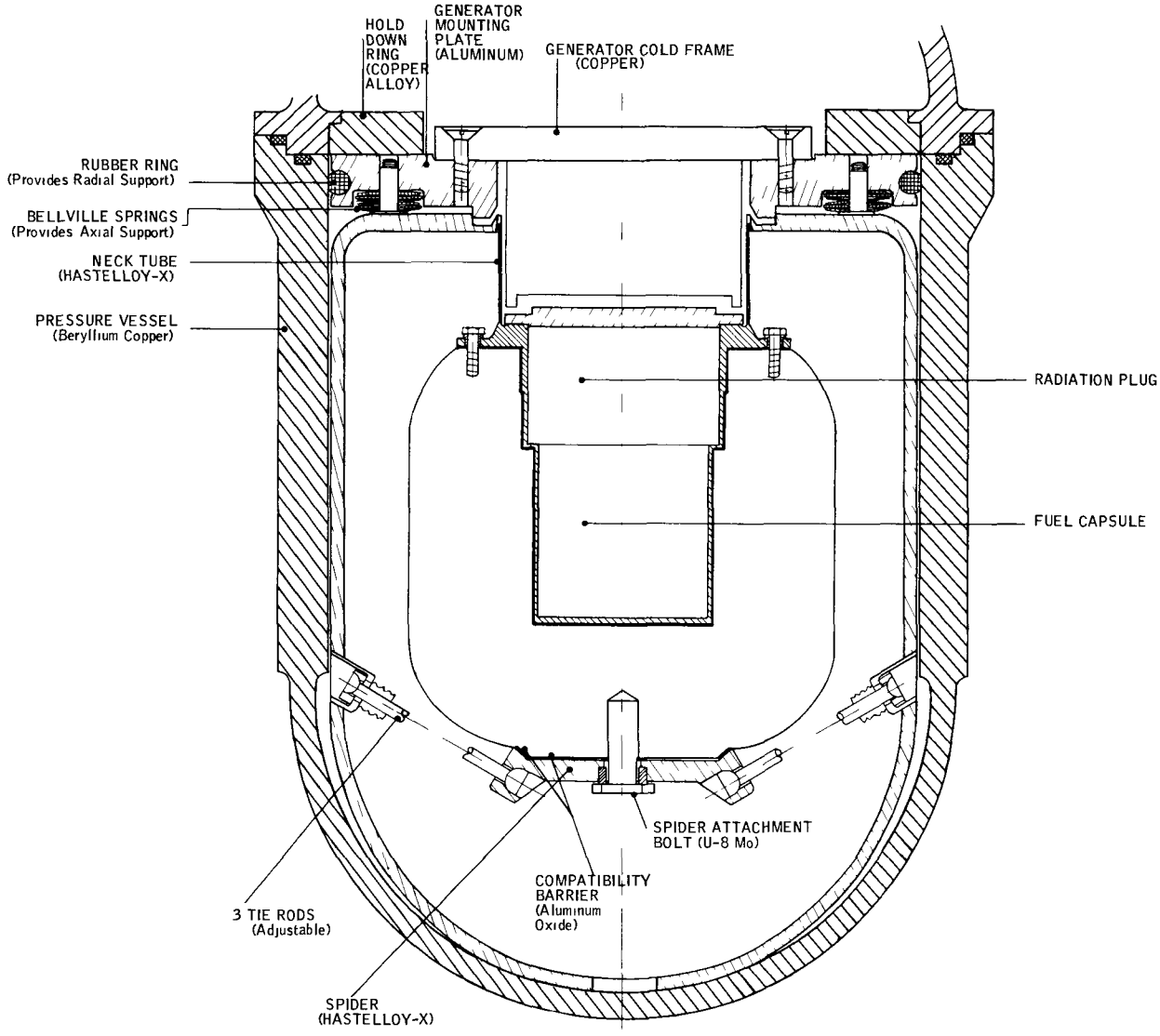

Figure 3-2. SNAP-21 Concept II (Single TEG) (Illustration of Spider-Shield Interface and Revised Generator Mounting Plate) (Note: All Materials are the Same as Concept I)

Conceptual design effort on this concept during this report period has consisted of preliminary evaluation of spider-to-shield attachment methods and cold end heat rejection systems.

3.3.1 HTVIS

Shield-to-Spider Interface

In the 10-watt system the shield-to-spider interface is controlled by a close fitting diameter to provide radial positioning and an axial bearing surface to control the axial position and an axial bearing surface to control the axial position of the tie rod socket on the spider. Both the axial and radial position of the spider have to be closely controlled to maintain the tie rods in a tight condition when the system temperature varies from room temperature to operating temperature.

For the 20-watt system an adjustable tie rod concept is being considered. This concept will allow adjustment of the tie rods to compensate for slight variations in the axial length of the shield assembly.

The ability to make tie rod adjustments after system assembly makes it possible to consider a different type of shield-to-spider interface. This new interface consists of a tapered seat as shown in Figure 3-2. This concept offers the advantage of simpler machining and looser tolerances.

3.3.2 Generator Mounting Plate and HTVIS Retention System

The feasibility of using the same type of simplified mounting plate for Concept II as shown for Concept I is being considered. The system concept shown in Figure 3-2 includes this type of plate.

An analysis of the heat transfer efficiency of this concept must be performed to determine its feasibility. This effort is now in progress. A potential method of improving the heat transfer effectiveness of this concept is shown in Figure 3-3.

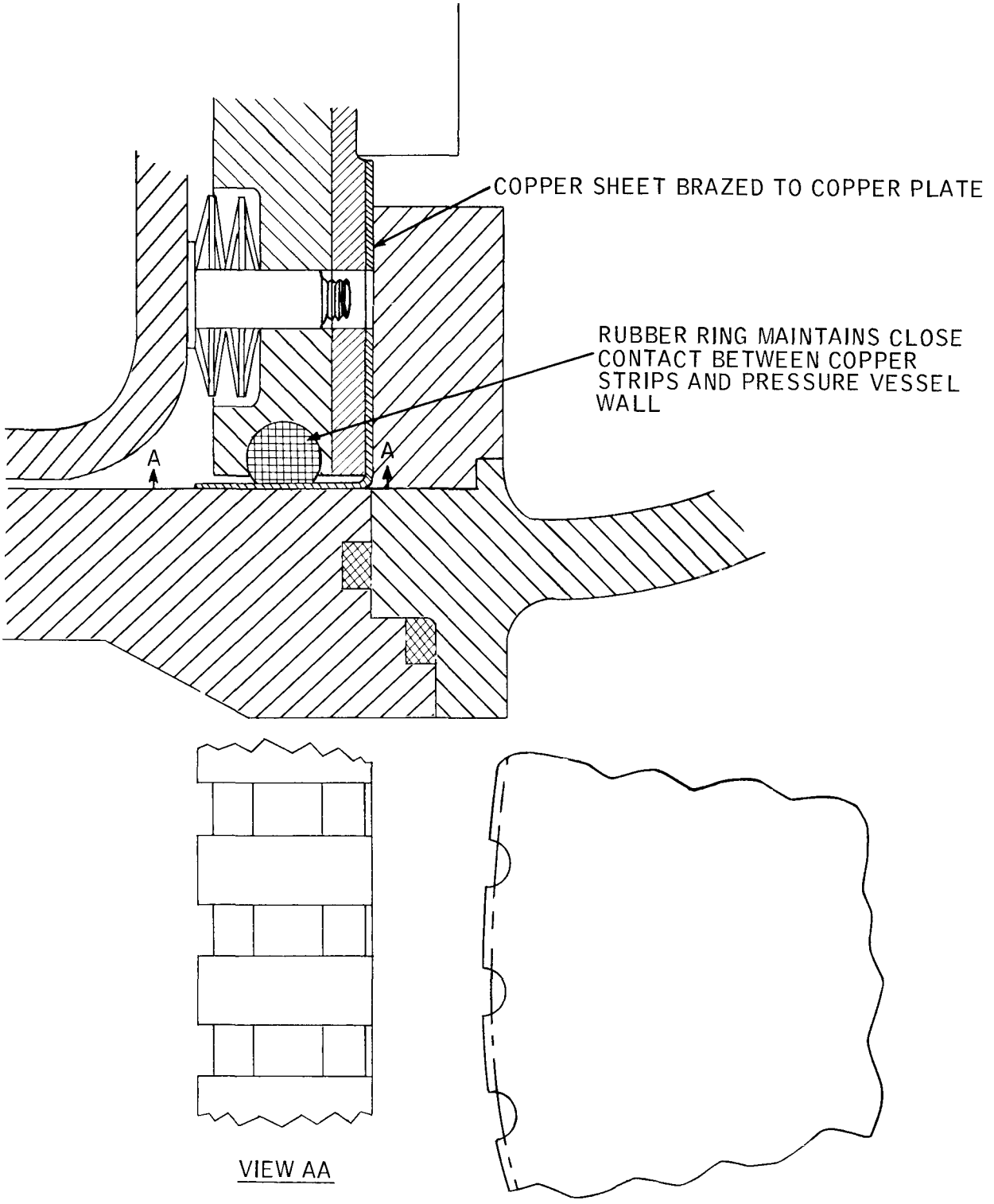

Figure 3-3. Optional Concept for Increasing Heat Transfer from Mounting Plate to Pressure Vessel Wall

4.0 PLANNED EFFORT FOR NEXT QUARTER

- Complete Final System Design Description
- Complete Final Safety Analysis Report
- Complete Revision 5 of Program Plan
- Complete Updating TASK I System Drawings
- Complete TASK II Preliminary Design Description
- Hydrostatic Test System S10P4
- Complete Thermal and Electrical Characterization of System S10P4
- Implant System S10P3 Off San Clemente Island
- Repair Insulation System B10D2 and replace it in System S10D3
- Complete 16mm SNAP-21 Documentary Film
- Complete Evaluation of Machine Wrapping of Insulation Systems
- Start investigation into Alternate Thermoelectric Material for SNAP-21 Generators
- Begin Long-Term Test of System S10P4
- Continue Testing Phase I and Phase II Thermoelectric Generators
- Continue Long-Term Test of Phase II Power Conditioners

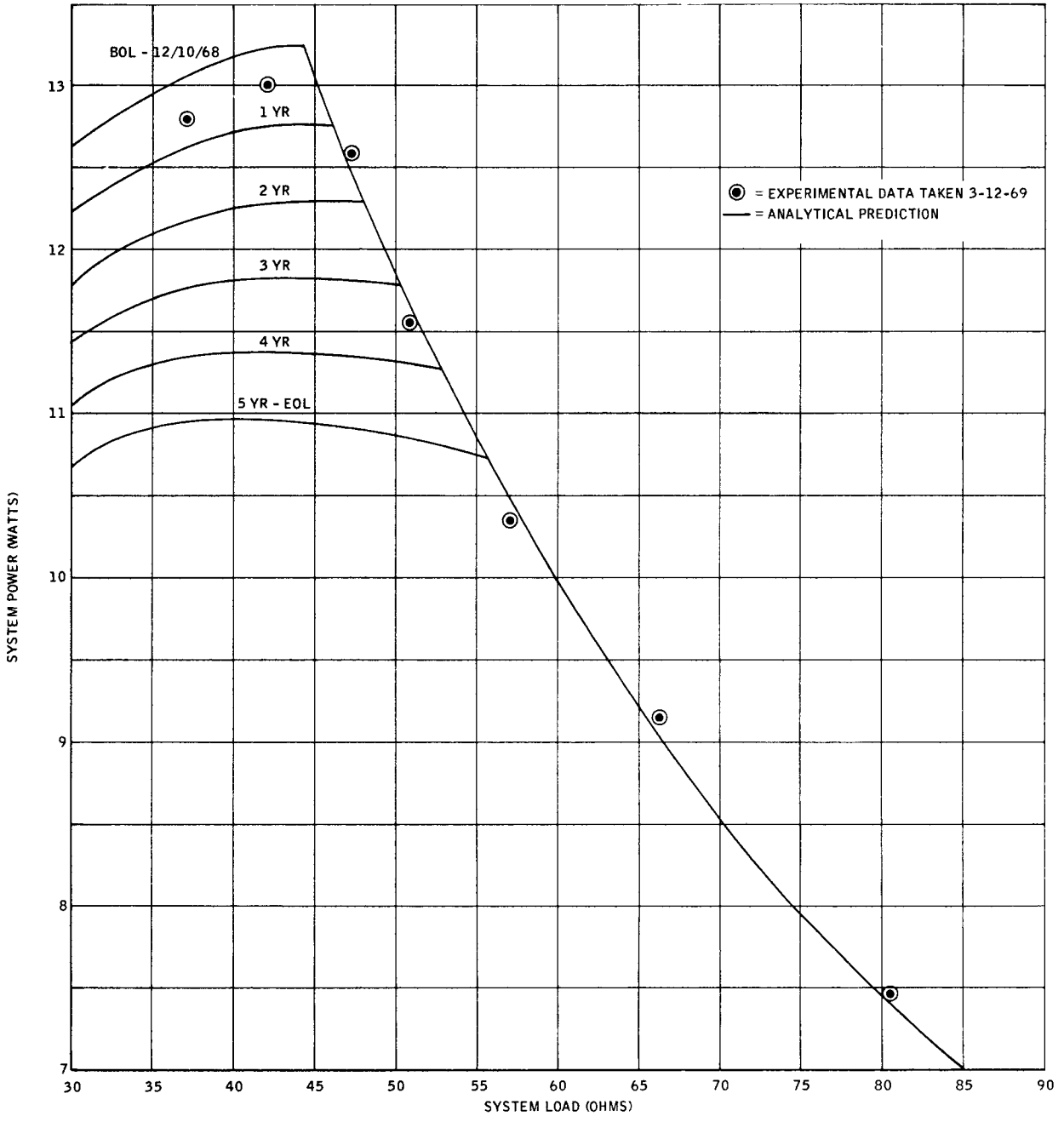

Figure 1. System S10P1 Performance
Power vs. Load Resistance in 40°F Water

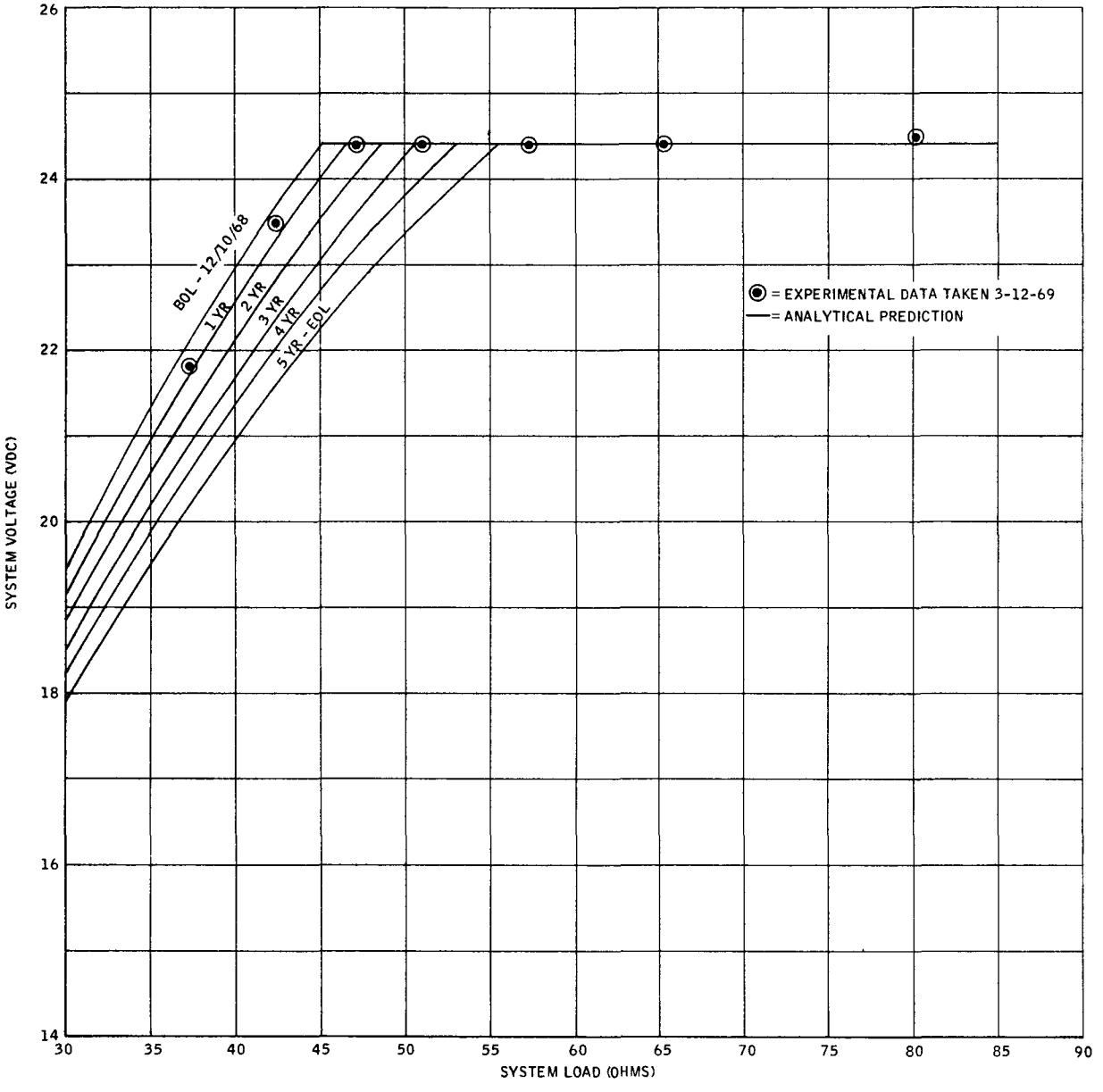

Figure 2. System S10P1 Performance
Voltage vs. Load Resistance in 40°F Water

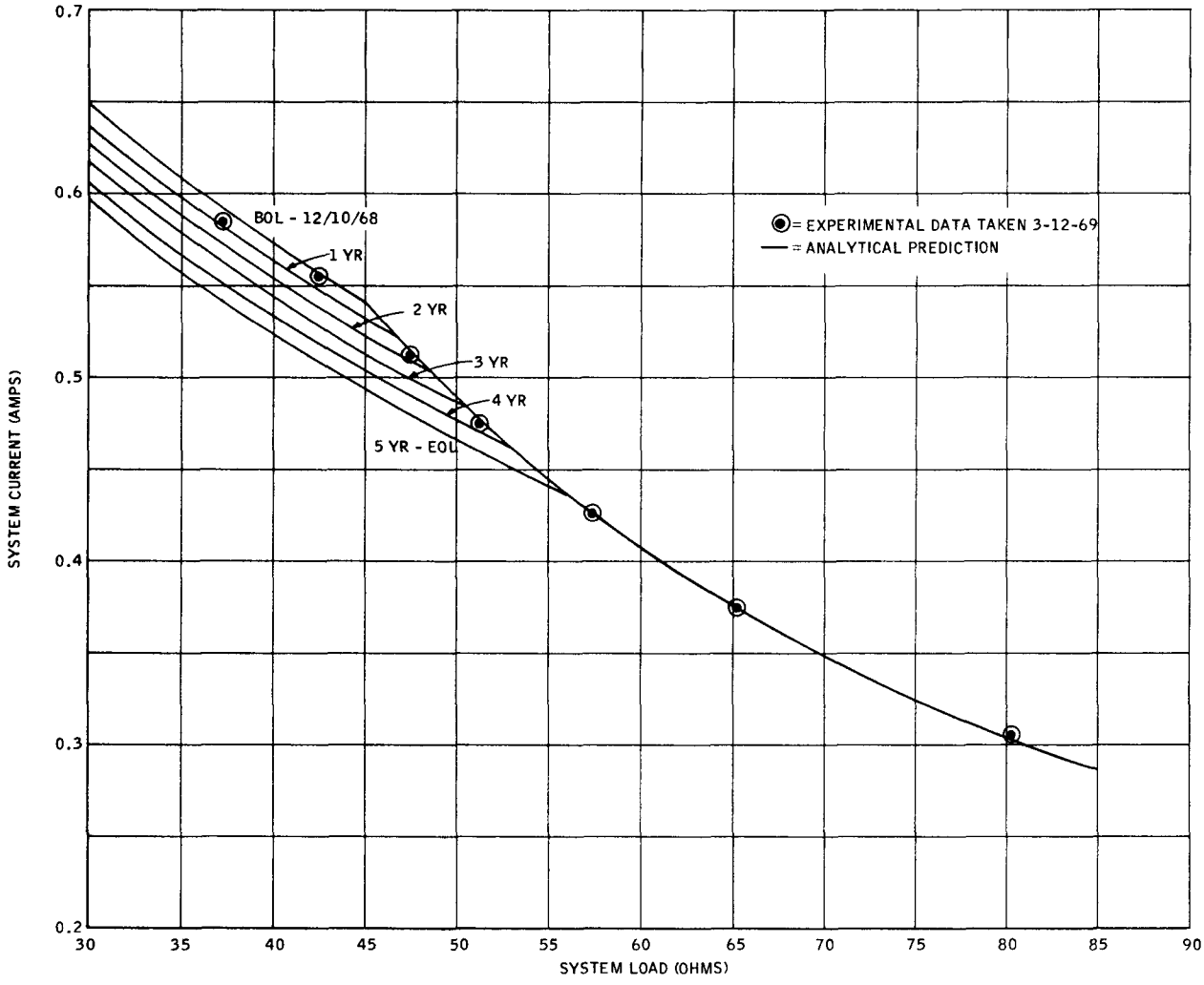

Figure 3. System S10P1 Performance
Current vs. Load Resistance in 40°F Water

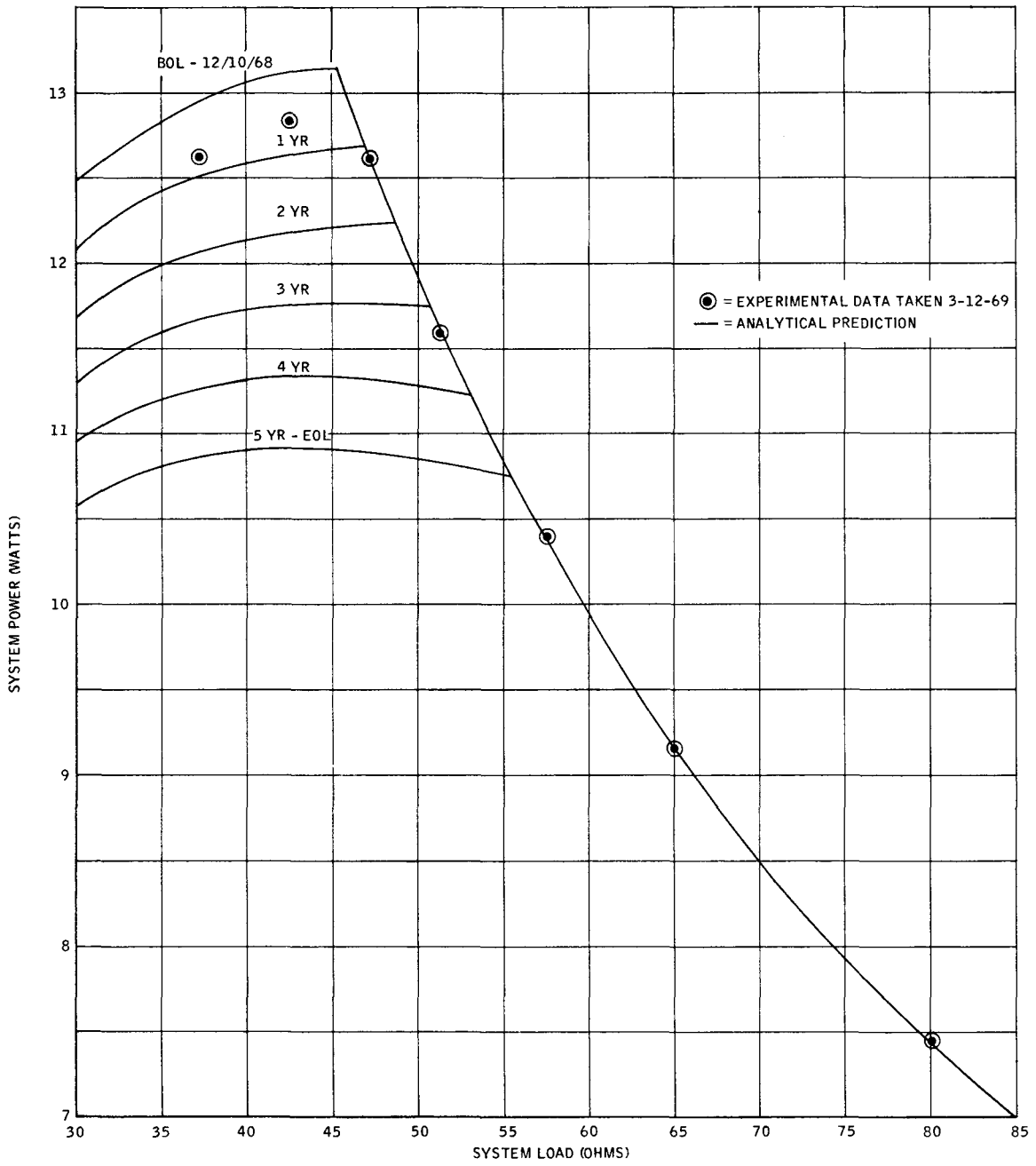

Figure 4. System S10P1 Performance
Power vs. Load Resistance in 60°F Water

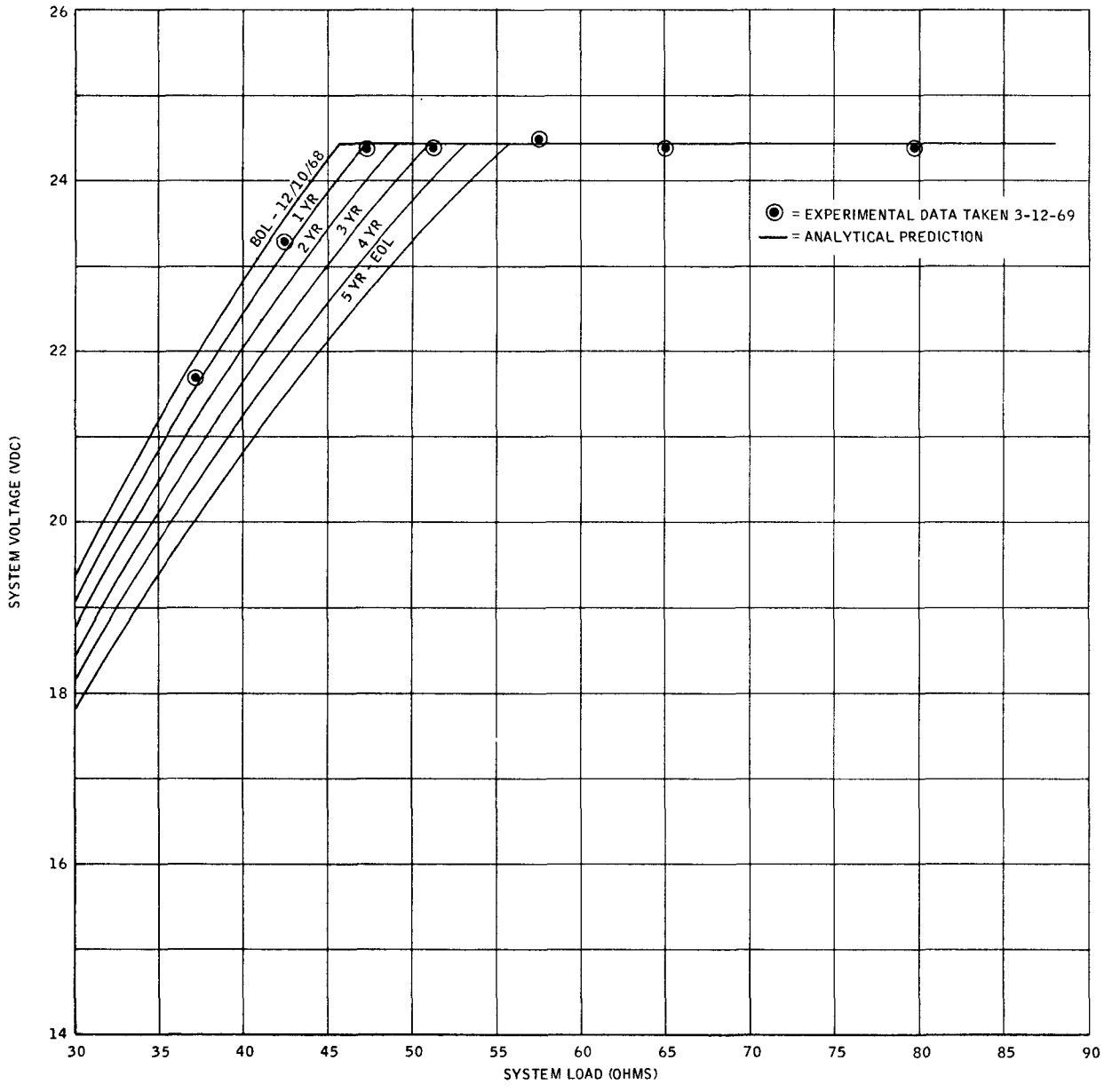

Figure 5. System S10P1 Performance
Voltage vs. Load Resistance in 60°F Water

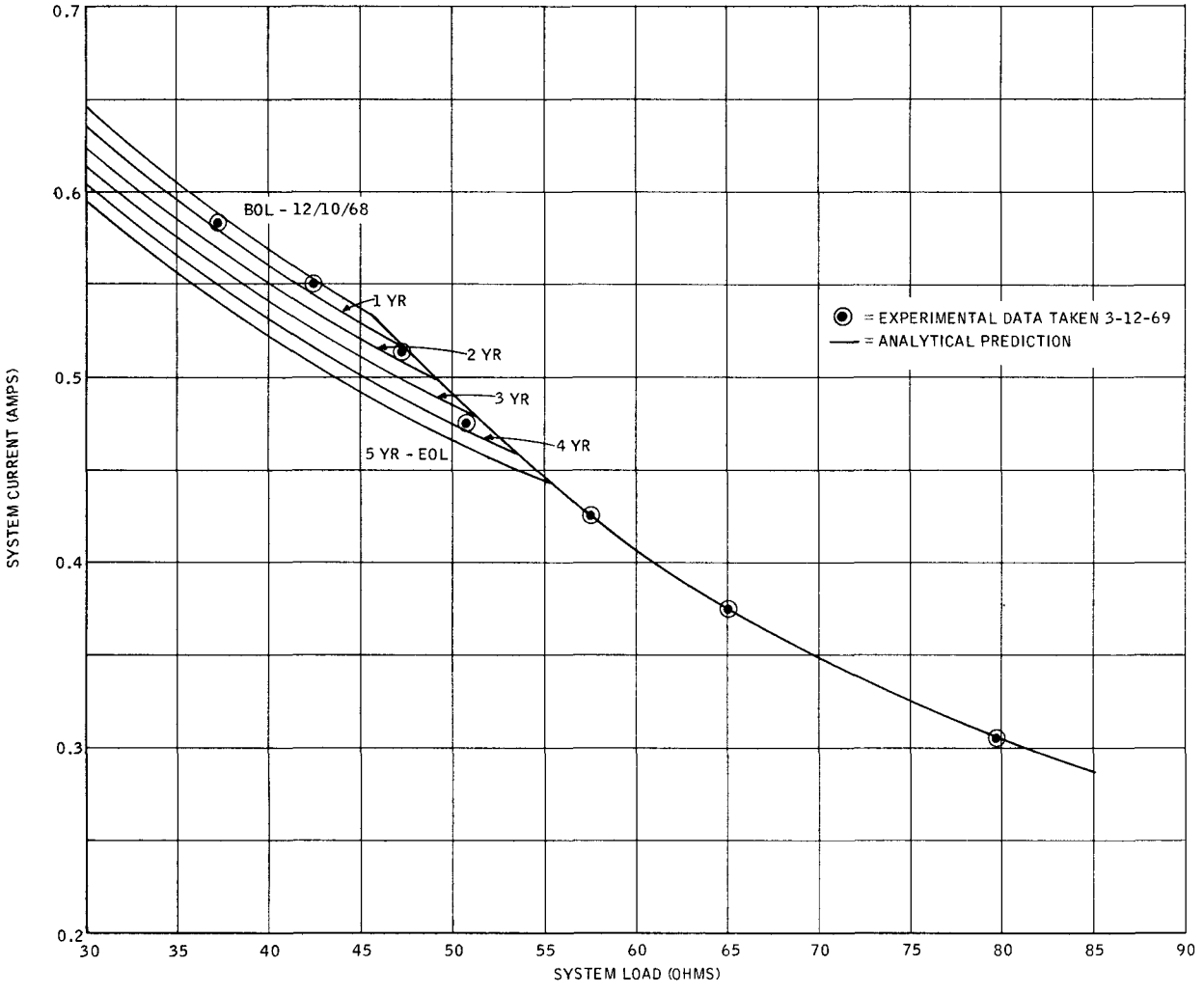

Figure 6. System S10P1 Performance
Current vs. Load Resistance in 60°F Water

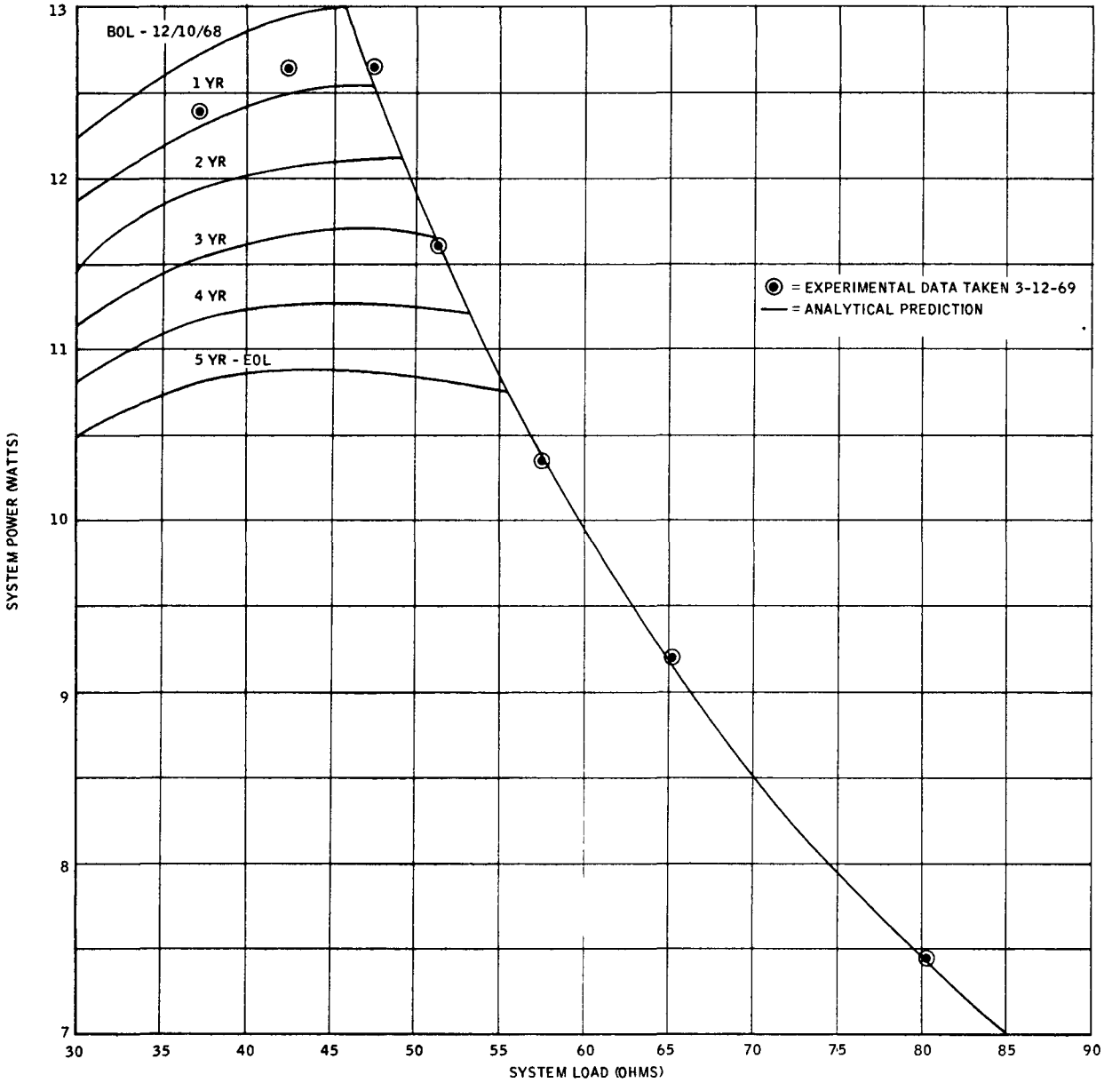

Figure 7. System S10P1 Performance
Power vs. Load Resistance in 80°F Water

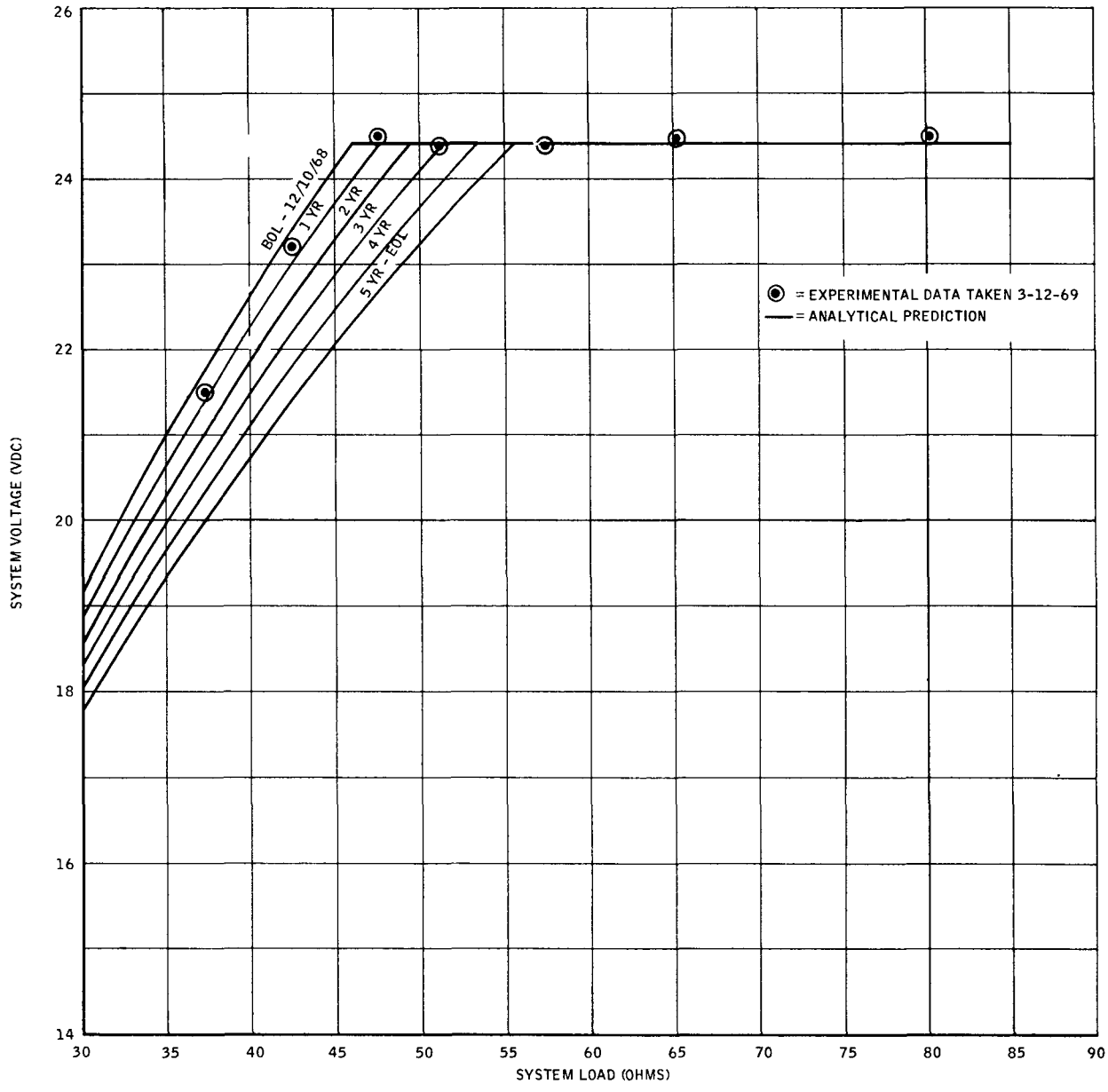

Figure 8. System S10P1 Performance
Voltage vs. Load Resistance in 80°F Water

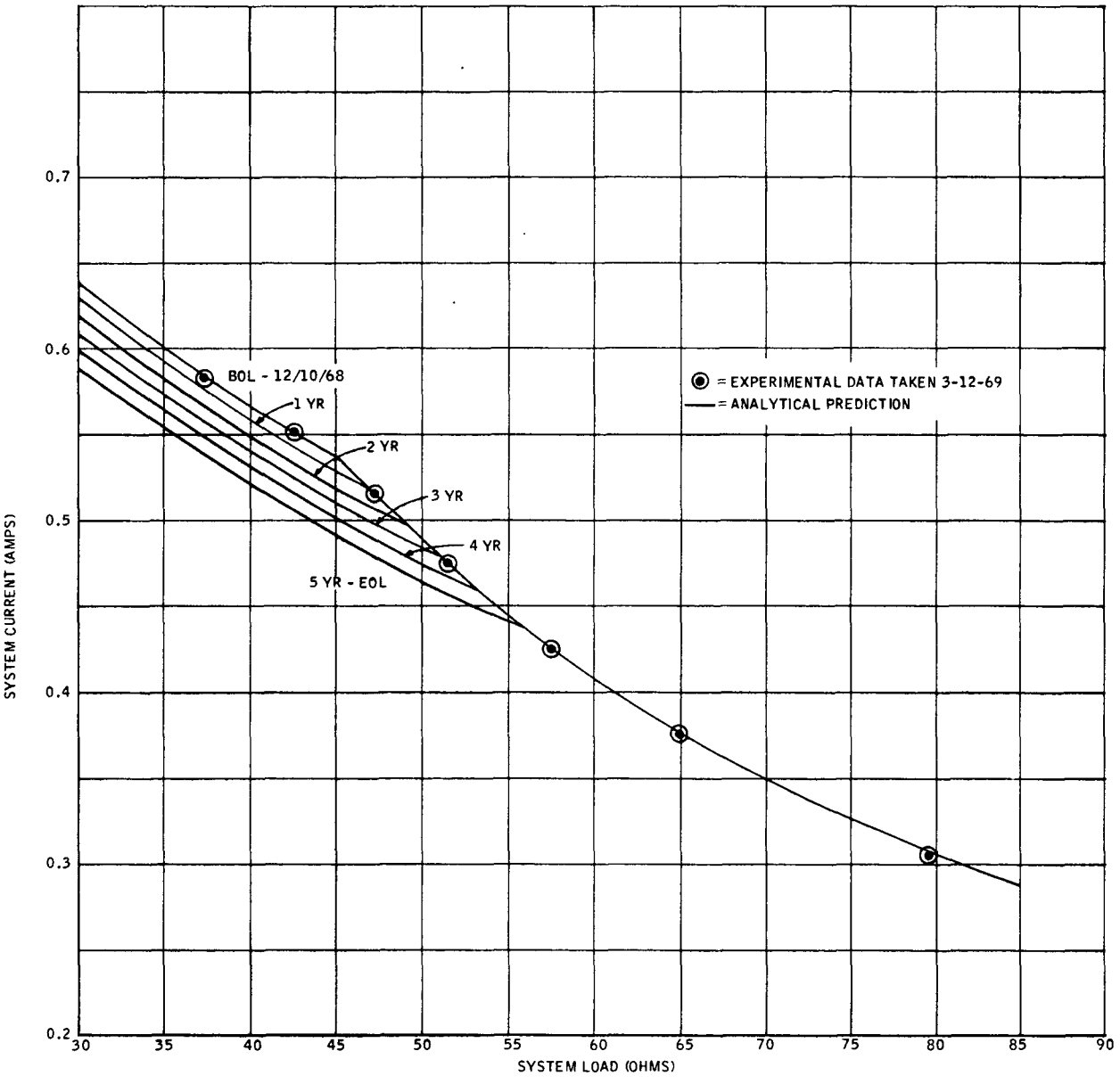

Figure 9. System S10P1 Performance
Current vs. Load Resistance in 80°F Water

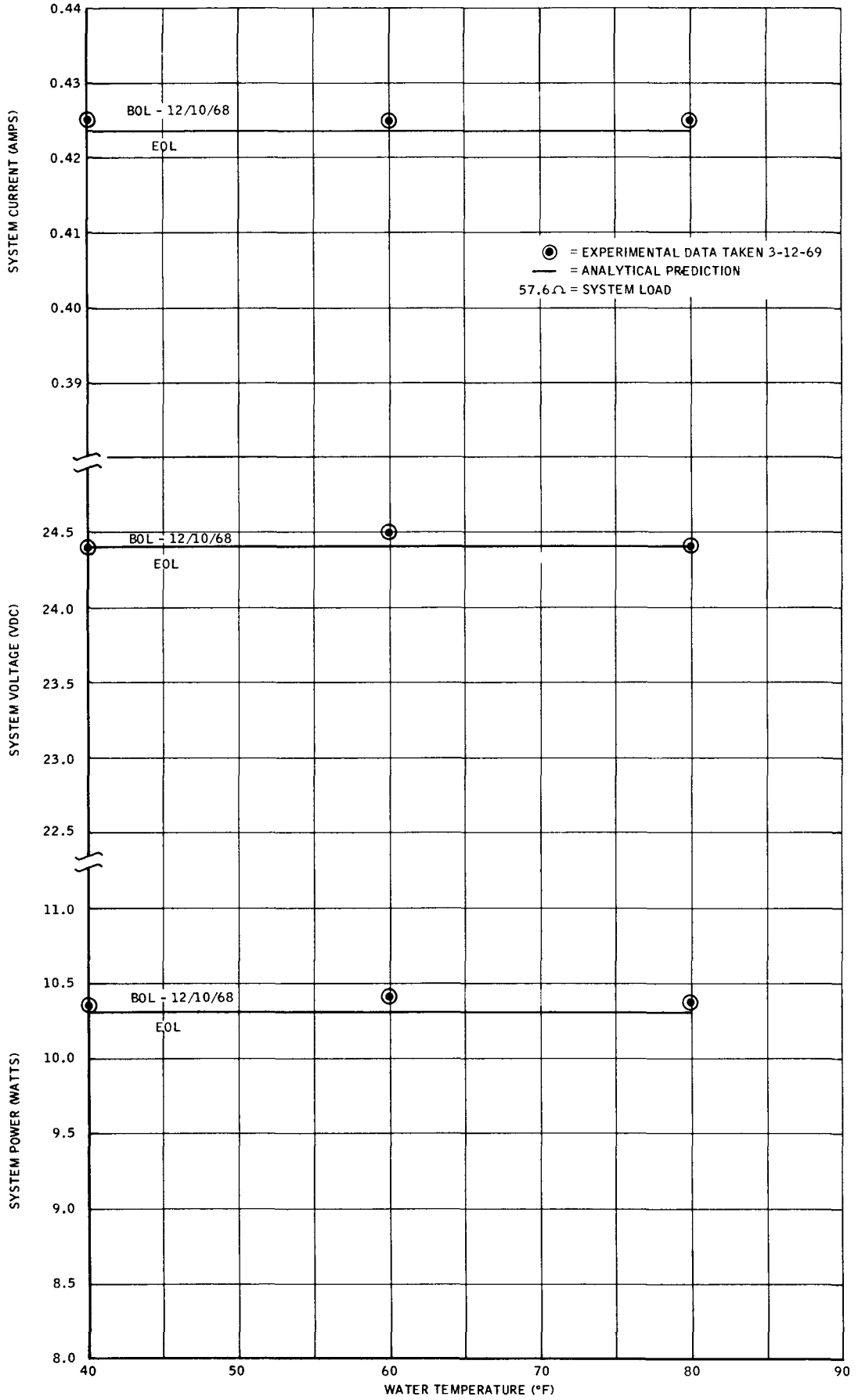

Figure 10. System S10P1 Performance
System Power, Voltage and Current vs. Water Temperature

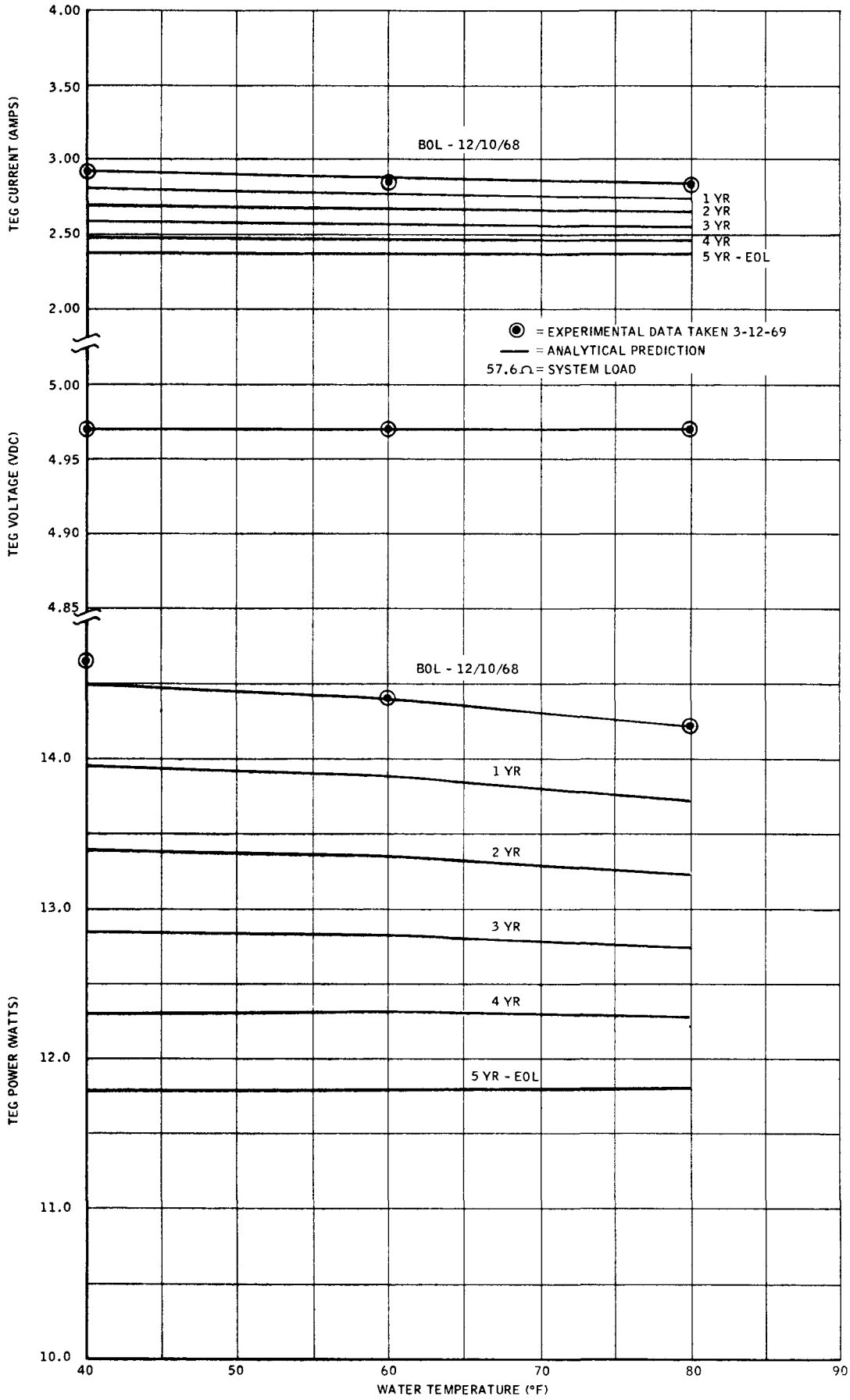

Figure 11. System S10P1 Performance
TEG Power, Voltage and Current vs. Water Temperature

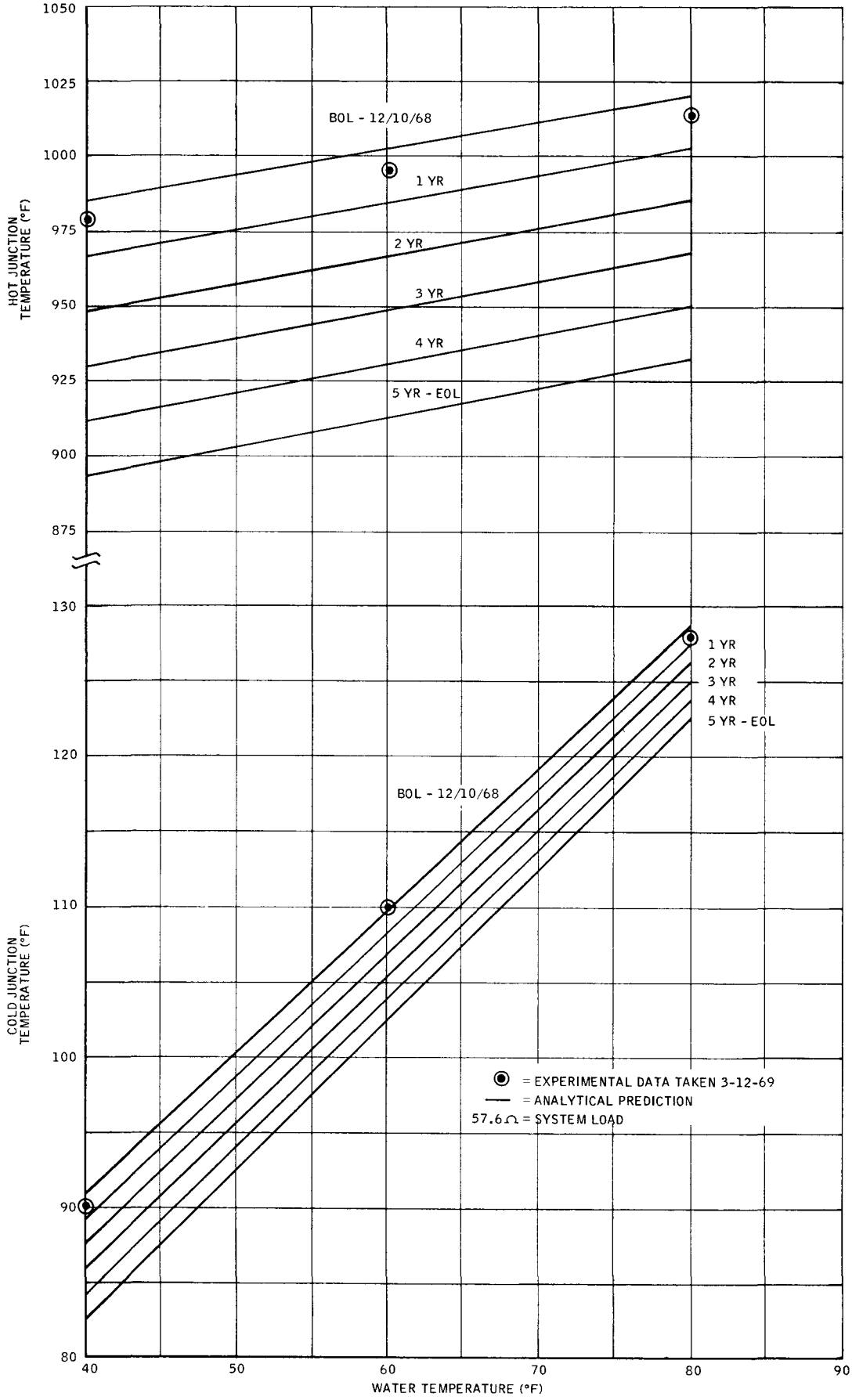

Figure 12. System S10P1 Performance
System Temperatures vs. Water Temperatures

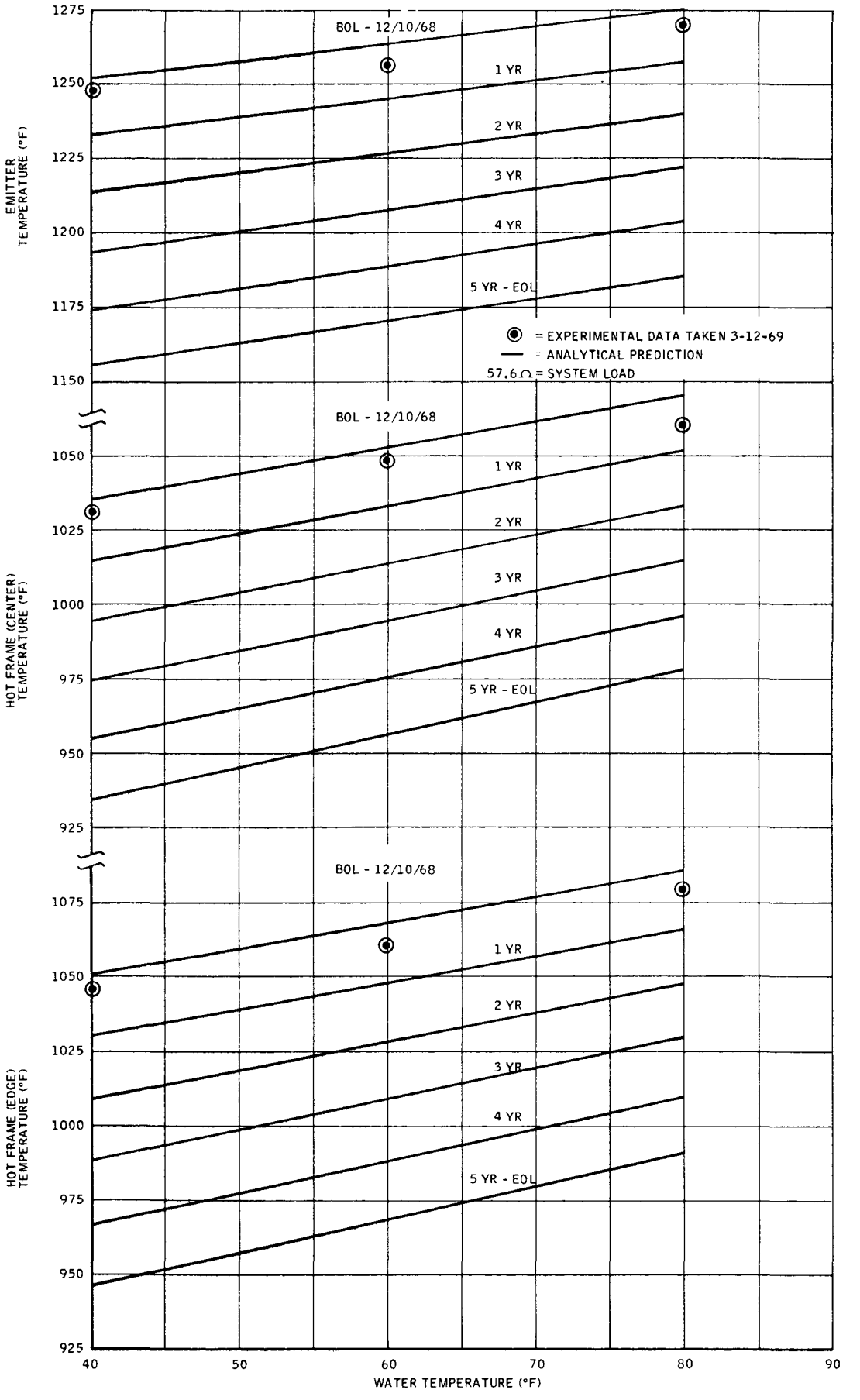

Figure 13. System S10P1 Performance
System Temperatures vs. Water Temperatures

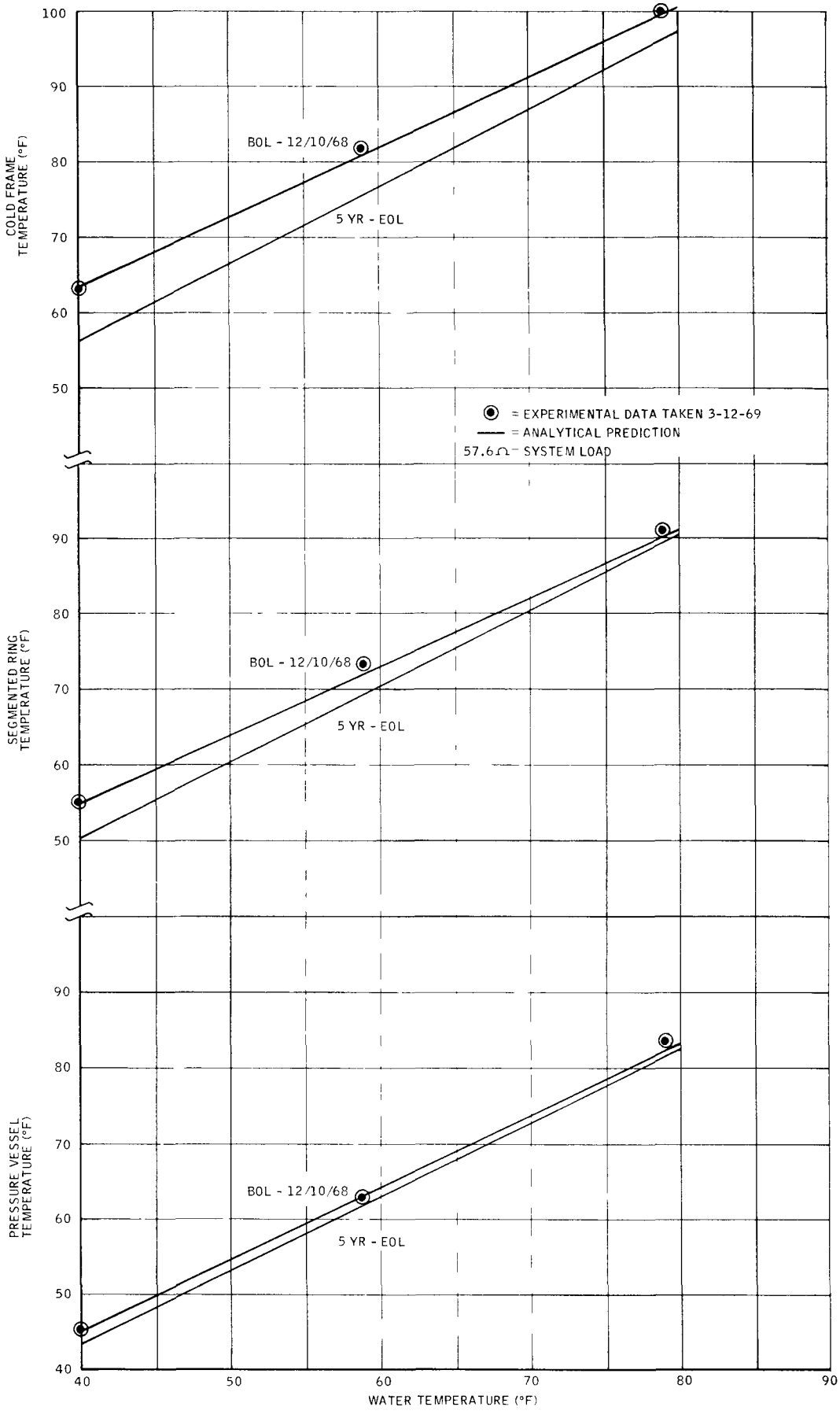

Figure 14. System S10P1 Performance
System Temperatures vs. Water Temperatures

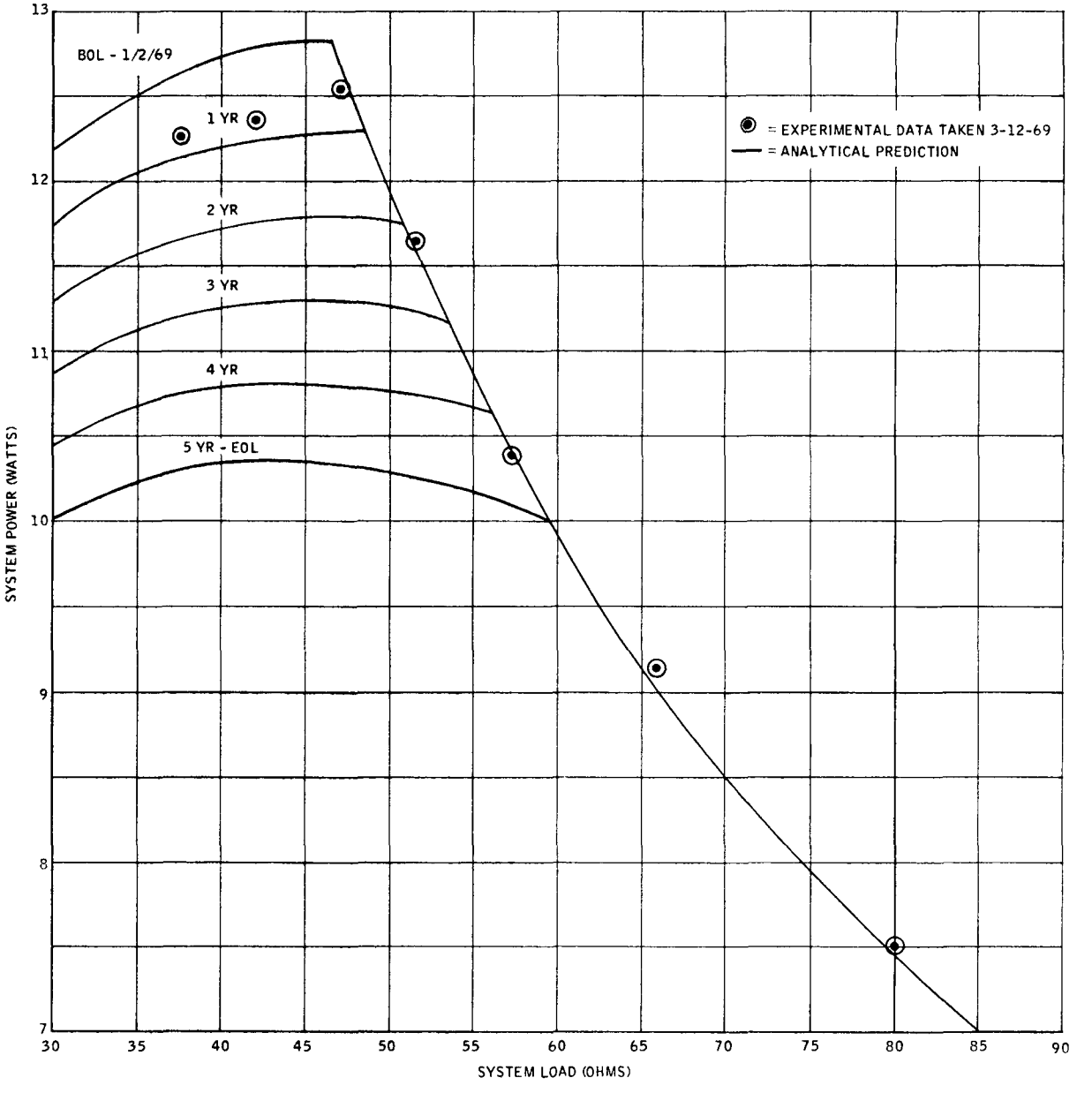

Figure 1. System S10P2 Performance
Power vs. Load Resistance in 40°F Water

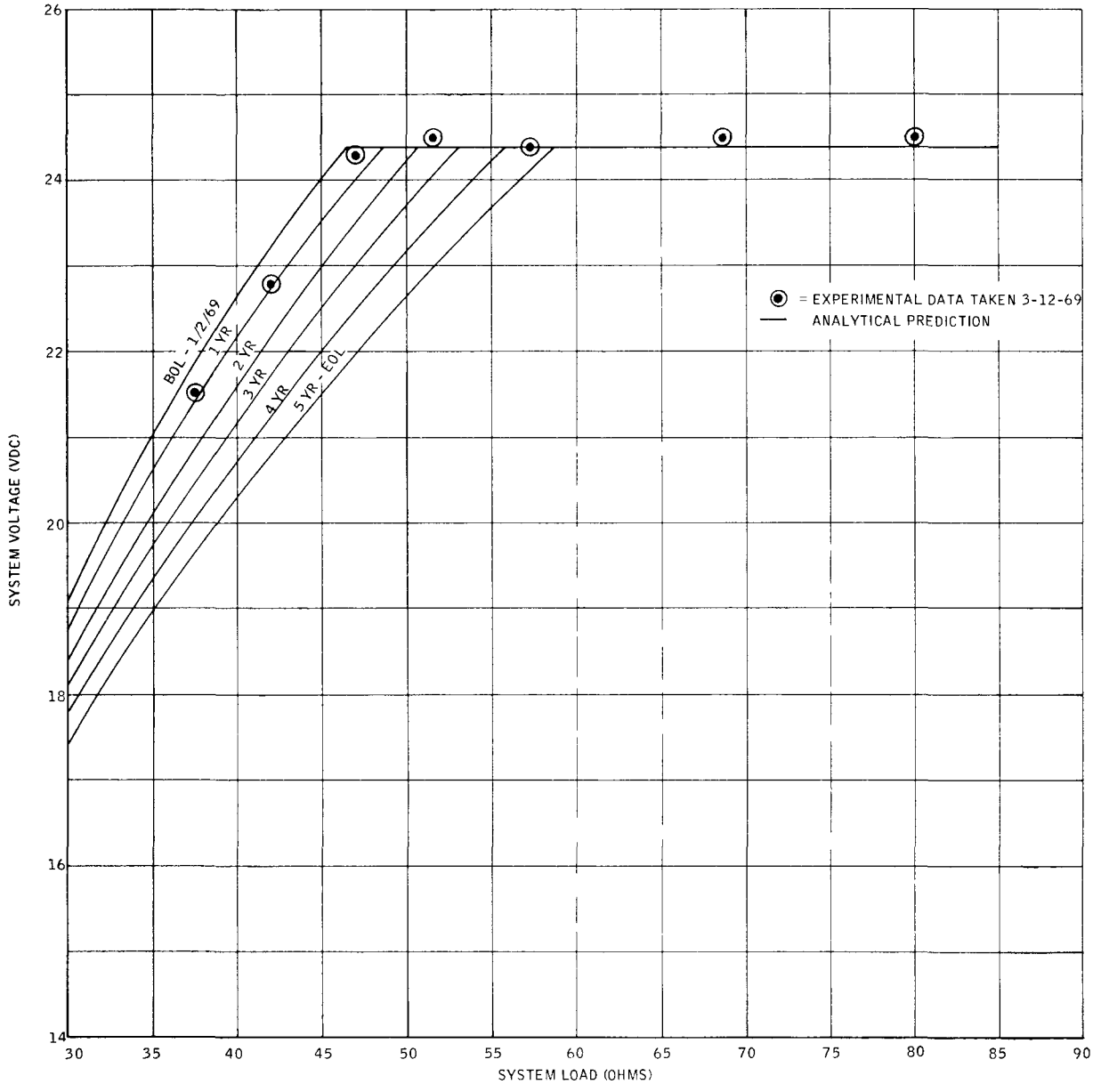

Figure 2. System S10P2 Performance
Voltage vs. Load Resistance in 40°F Water

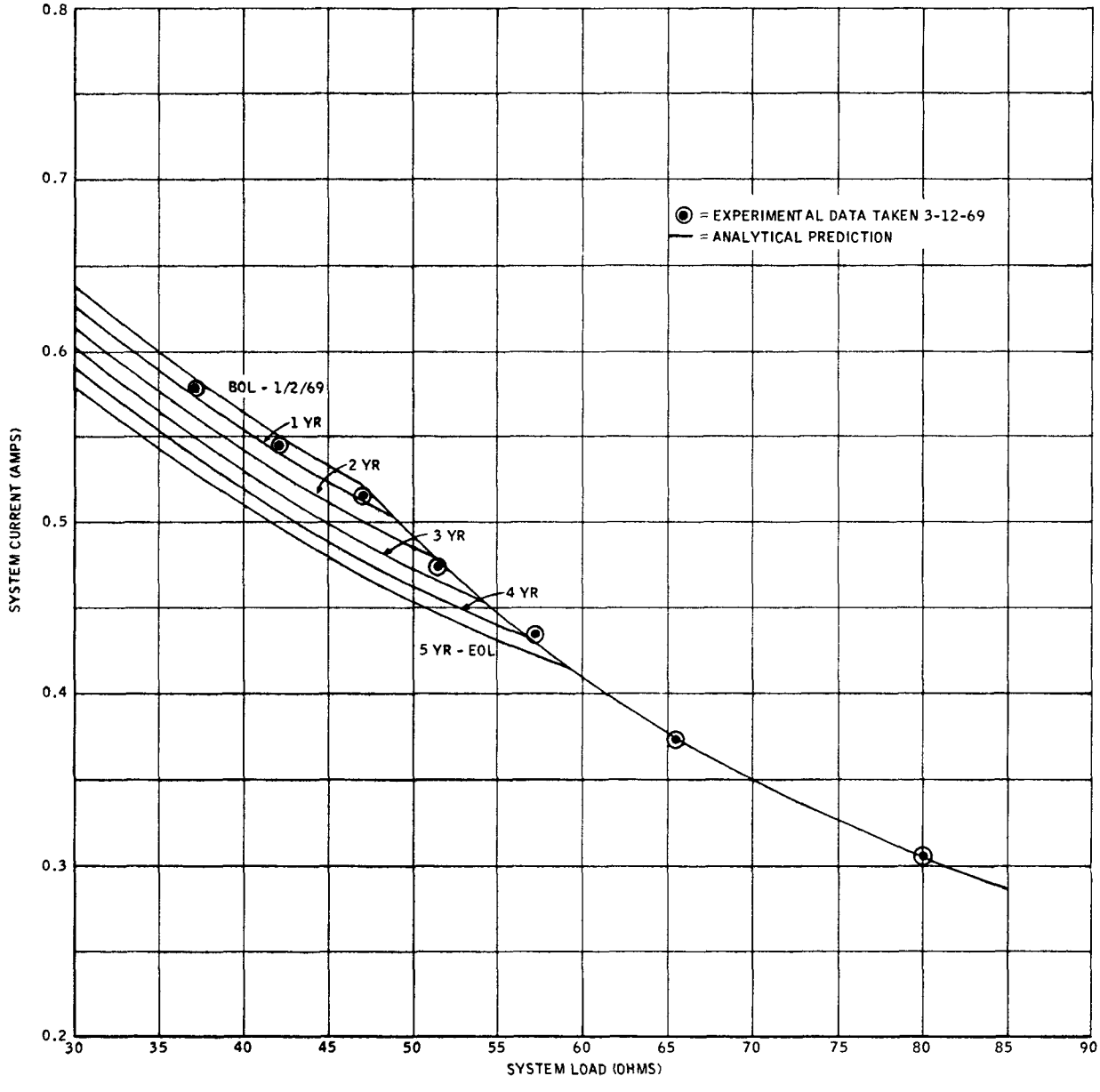

Figure 3. System S10P2 Performance
Current vs. Load Resistance in 40°F Water

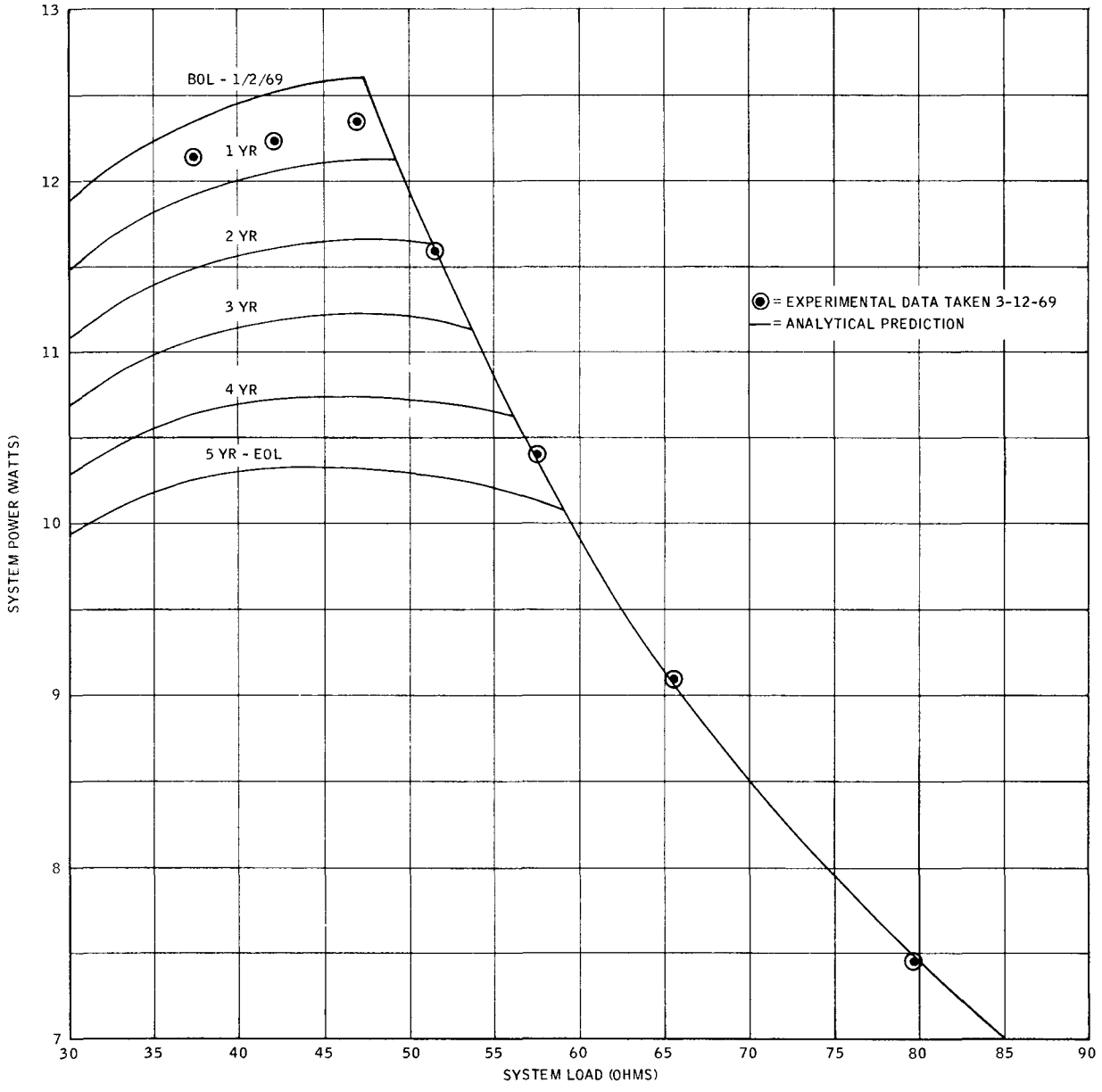

Figure 4. System S10P2 Performance
Power vs. Load Resistance in 60°F Water

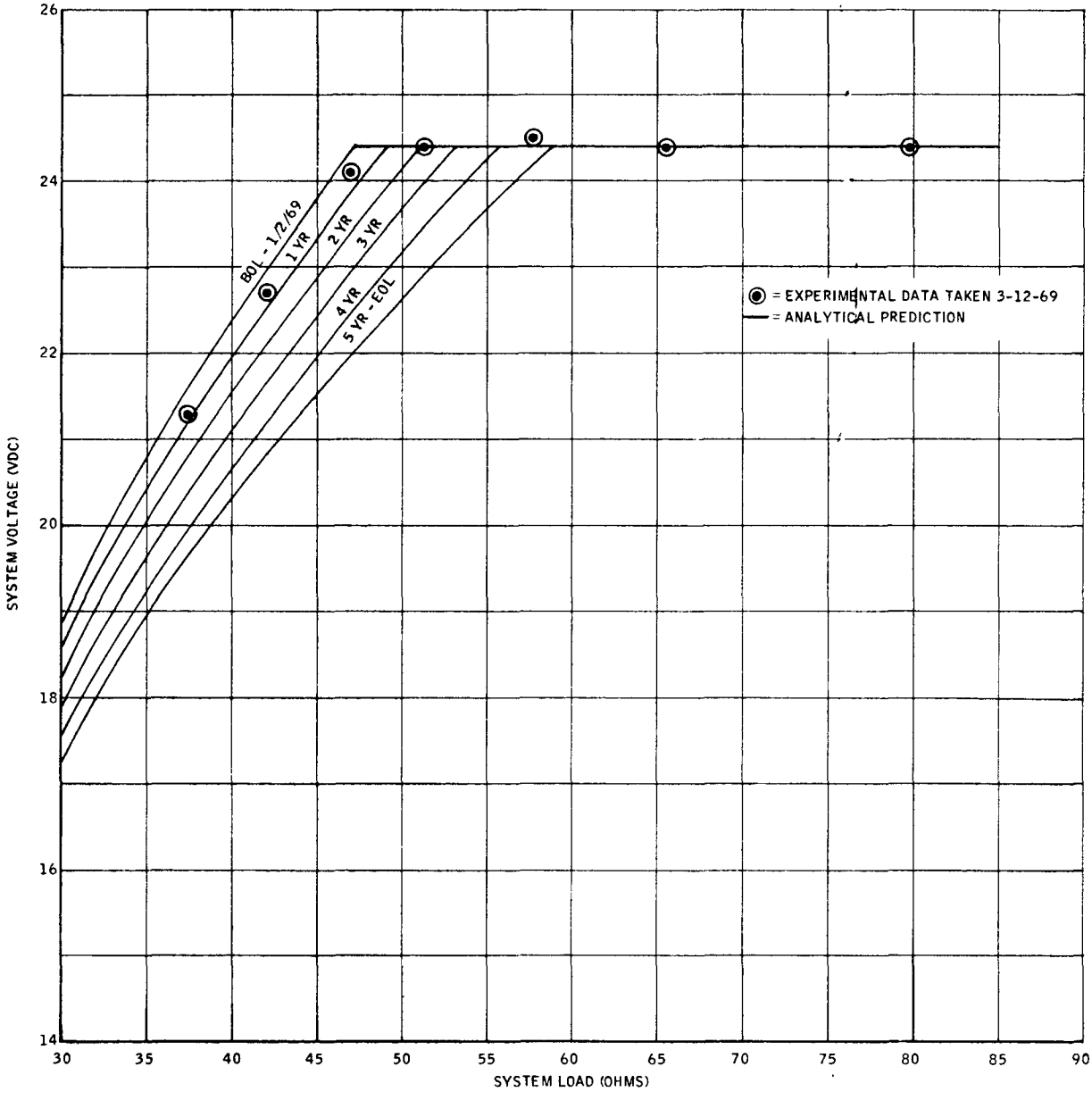

Figure 5. System S10P2 Performance
Voltage vs. Load Resistance in 60°F Water

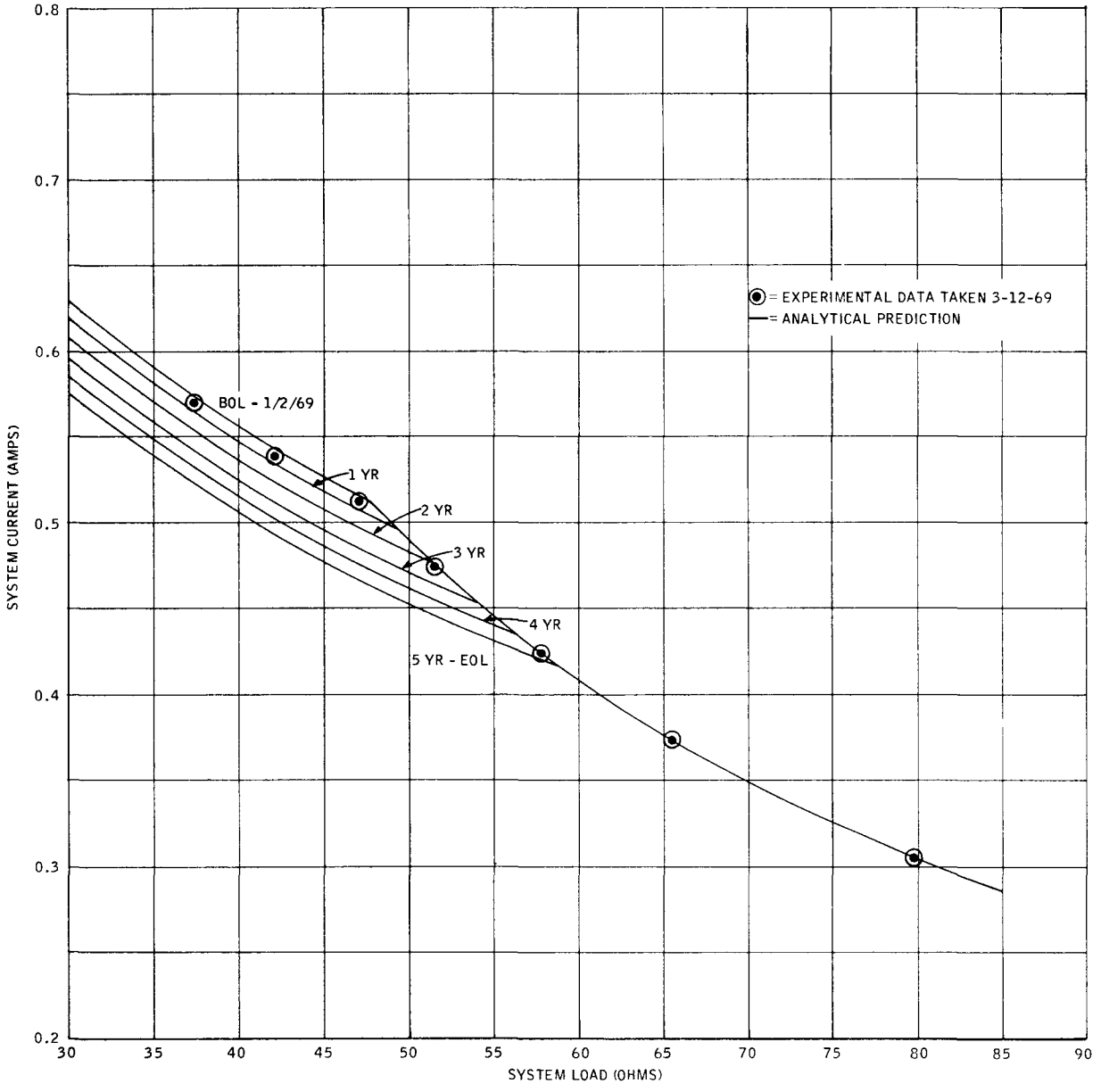

Figure 6. System S10P2 Performance
Current vs. Load Resistance in 60°F Water

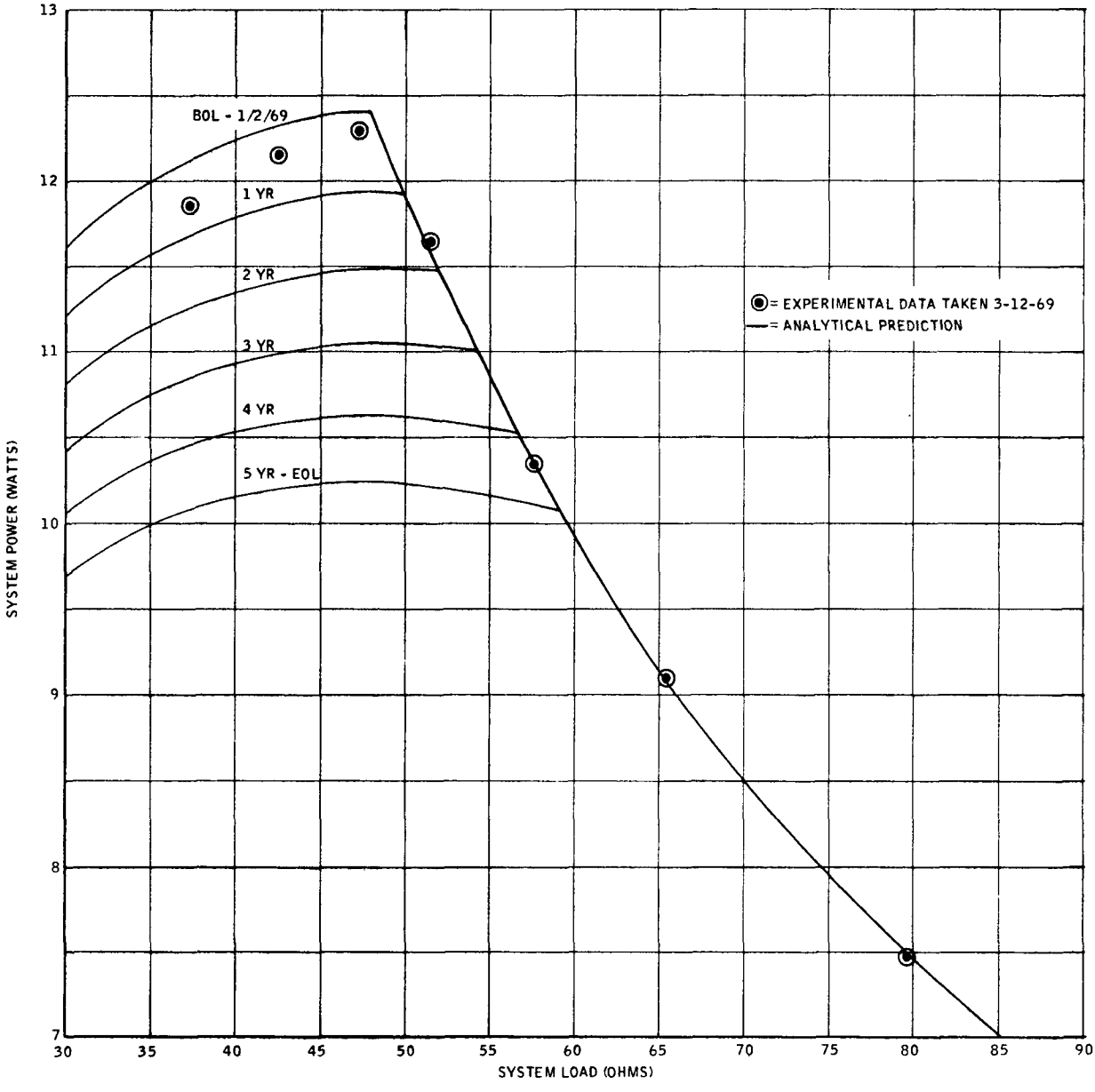

Figure 7. System S10P2 Performance
Power vs. Load Resistance in 80°F Water

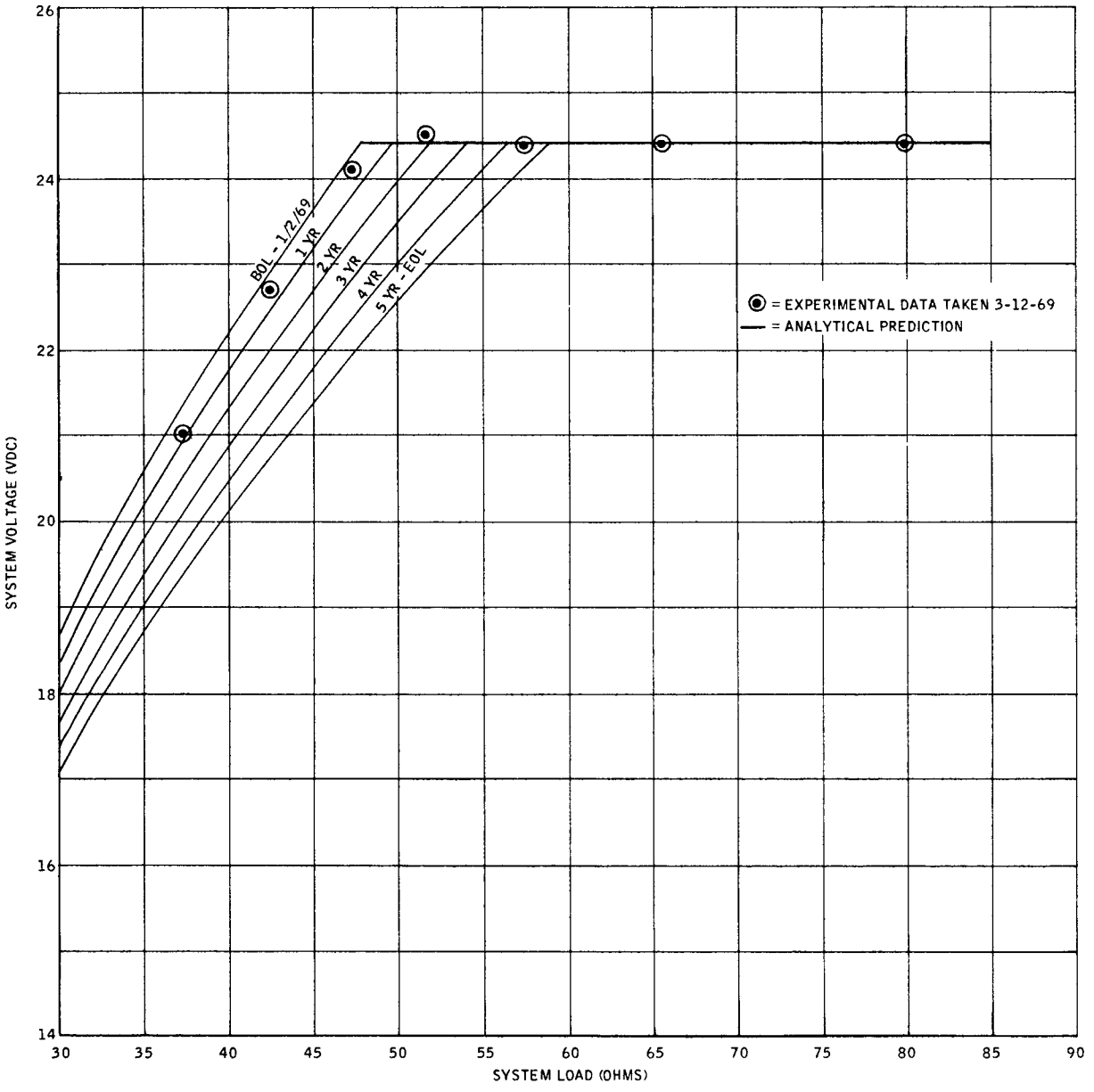

Figure 8. System S10P2 Performance
Voltage vs. Load Resistance in 80°F Water

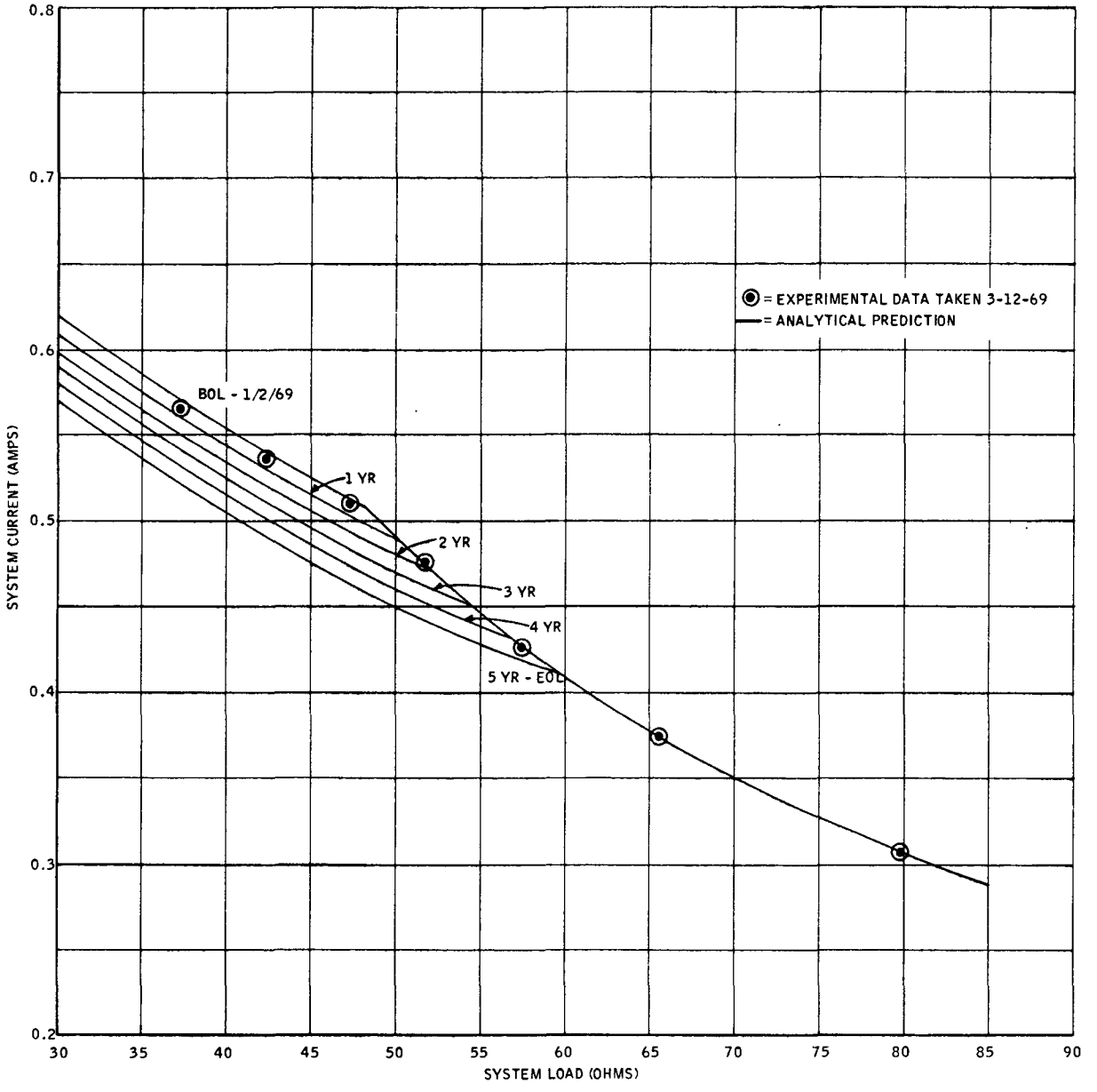

Figure 9. System S10P2 Performance
Current vs. Load Resistance in 80°F Water

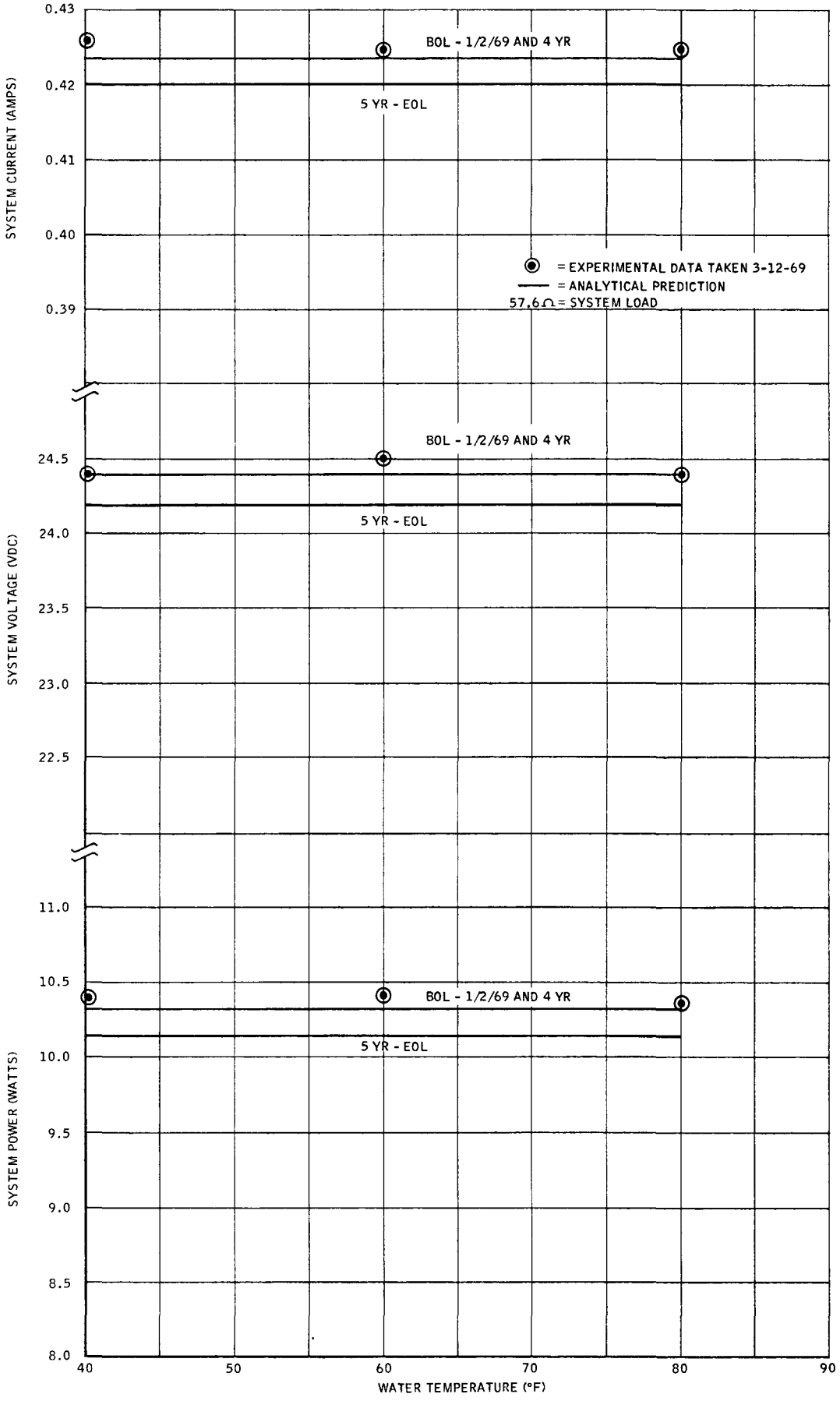

Figure 10. System S10P2 Performance
System Power, Voltage and Current vs. Water Temperature

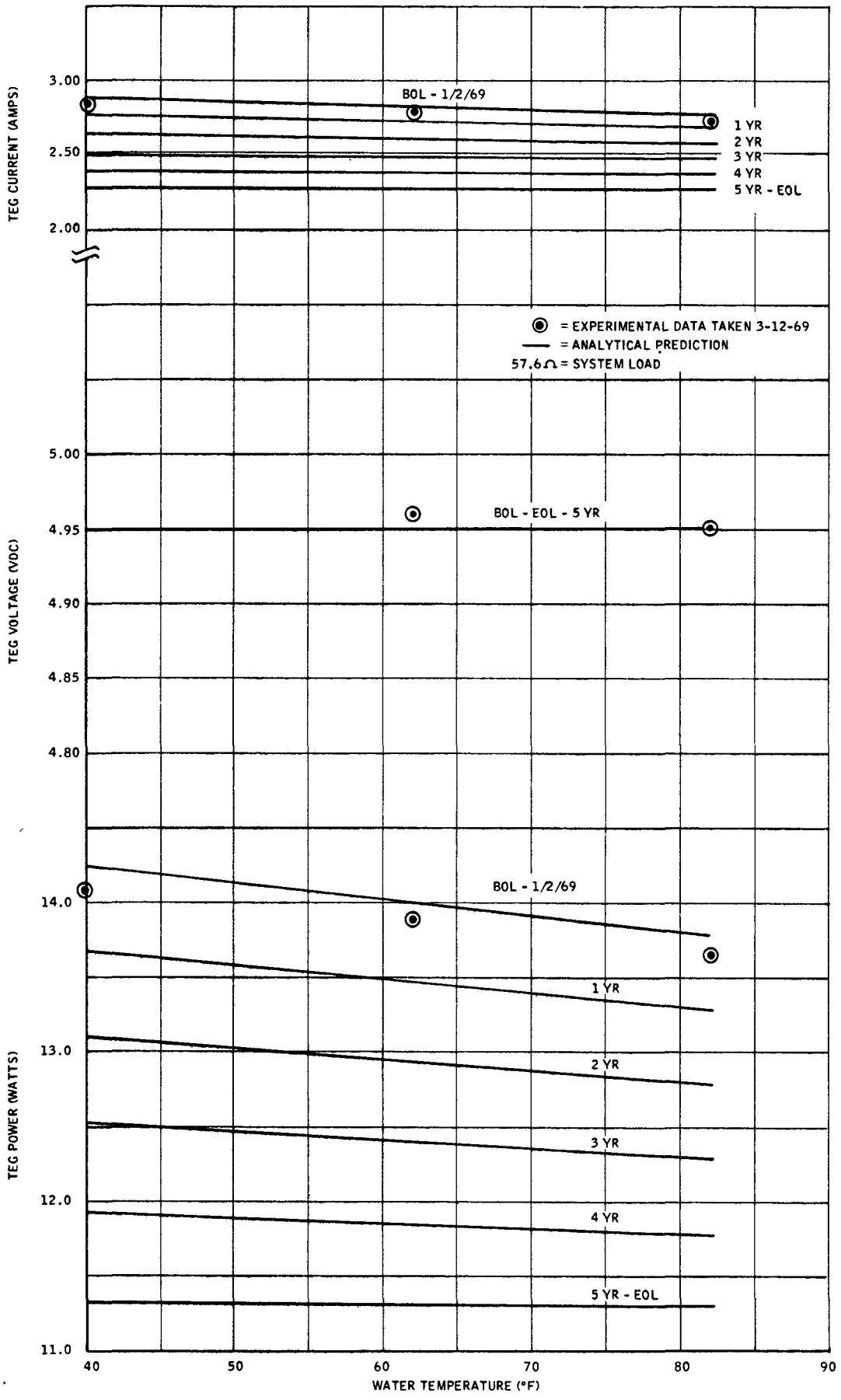

Figure 11. System S10P2 Performance
TEG Power, Voltage and Current vs. Water Temperature

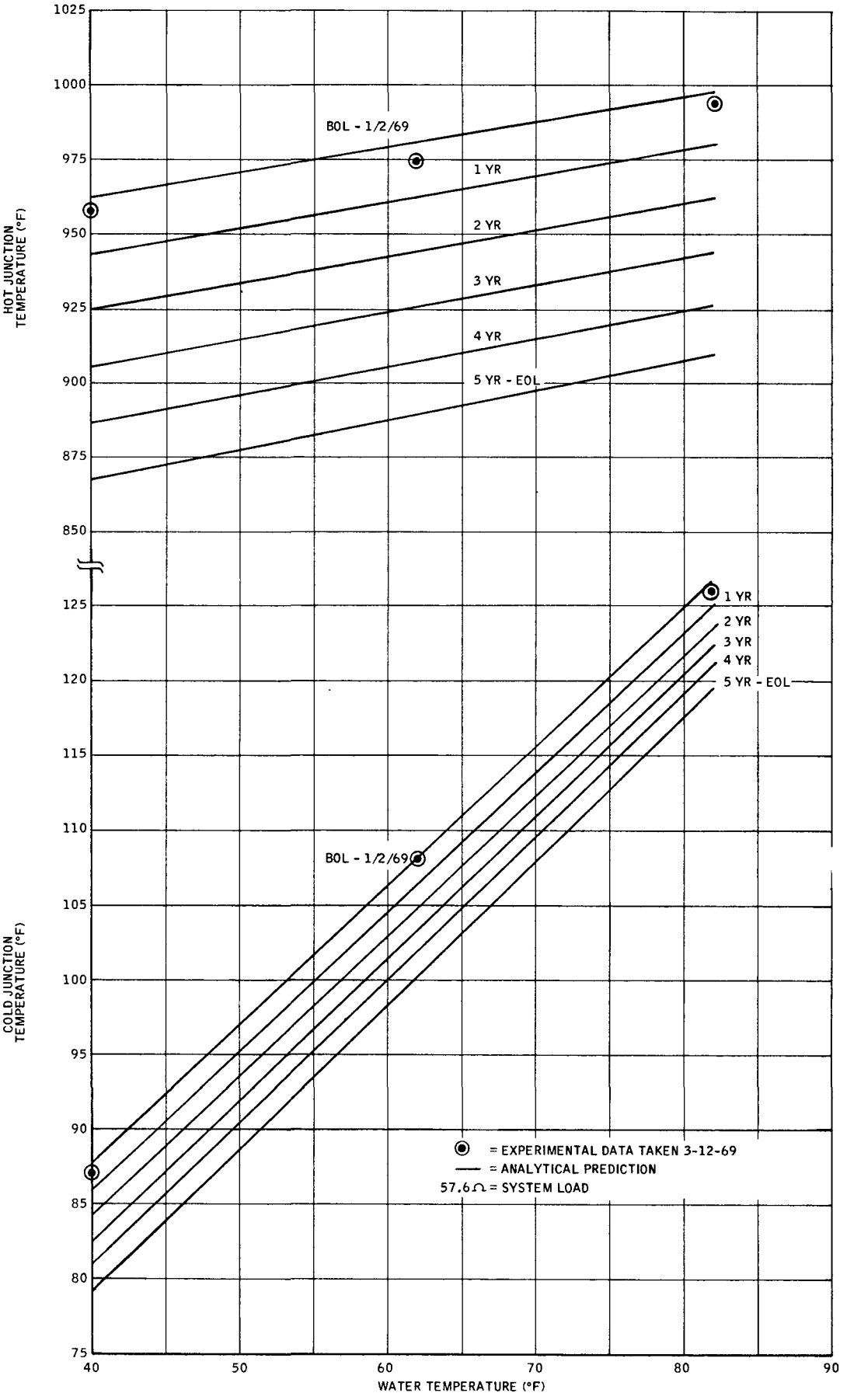

Figure 12. System S10P2 Performance
System Temperatures vs. Water Temperatures

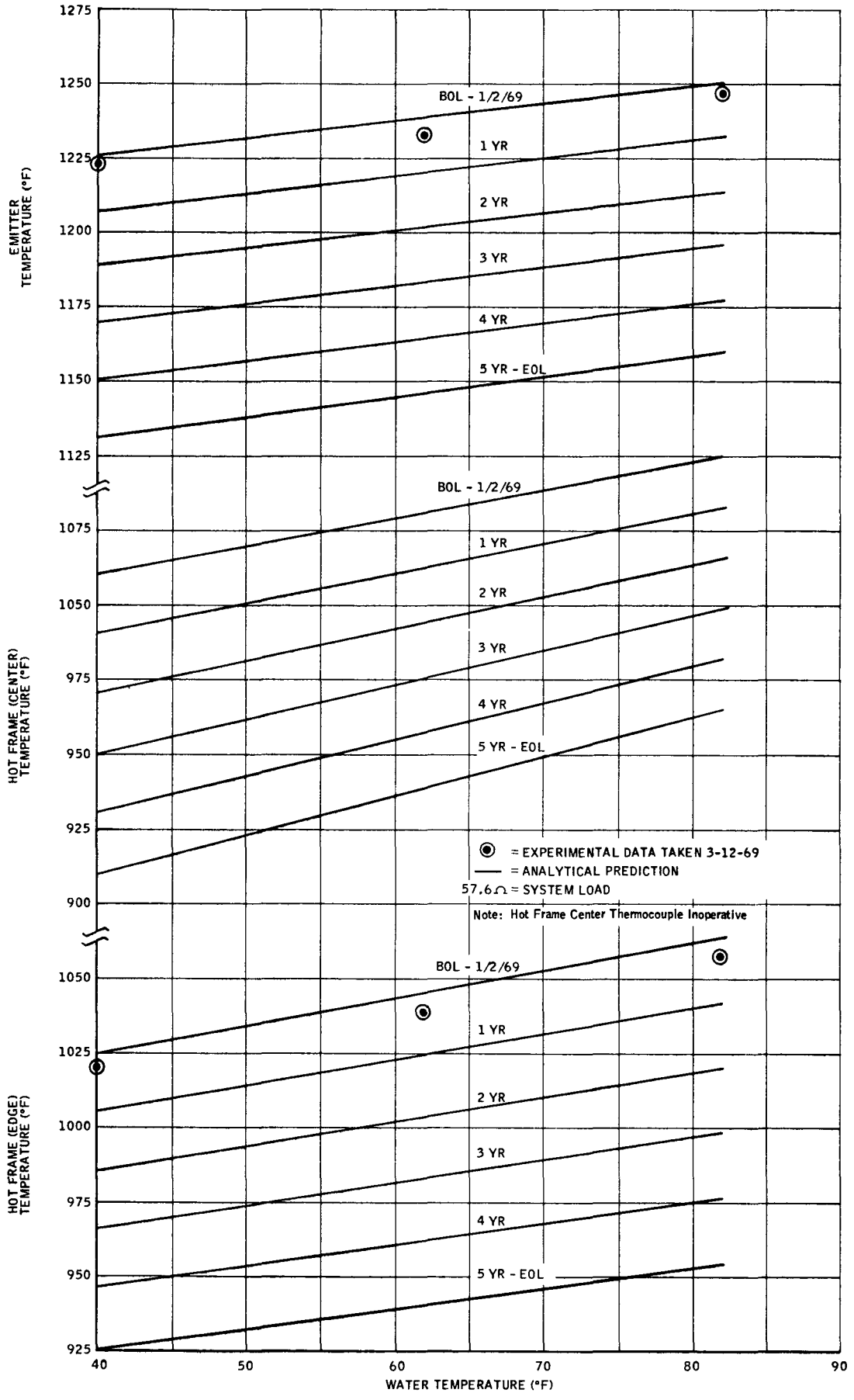

Figure 13. System S10P2 Performance
System Temperatures vs. Water Temperatures

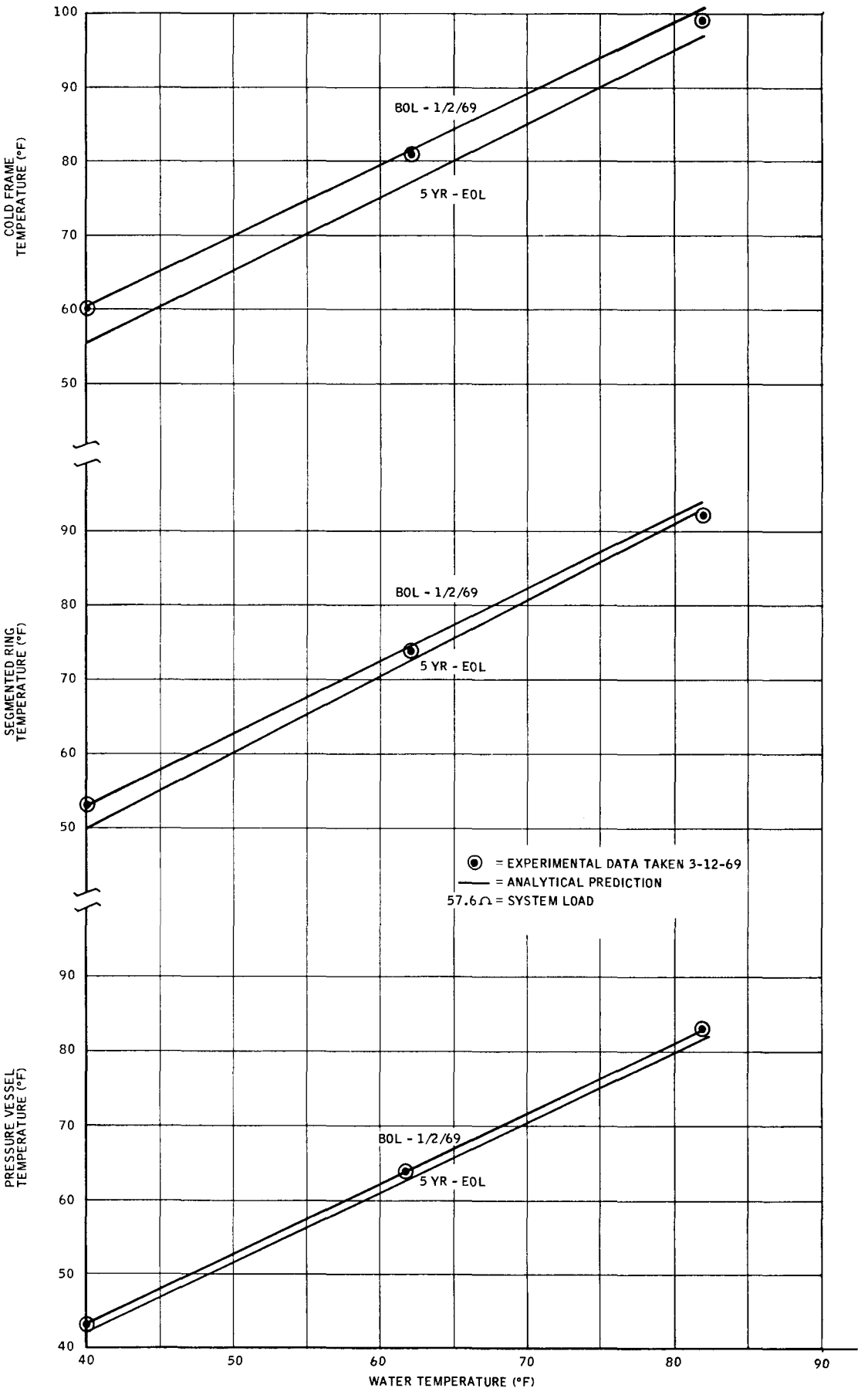

Figure 14. System S10P2 Performance
System Temperatures vs. Water Temperatures

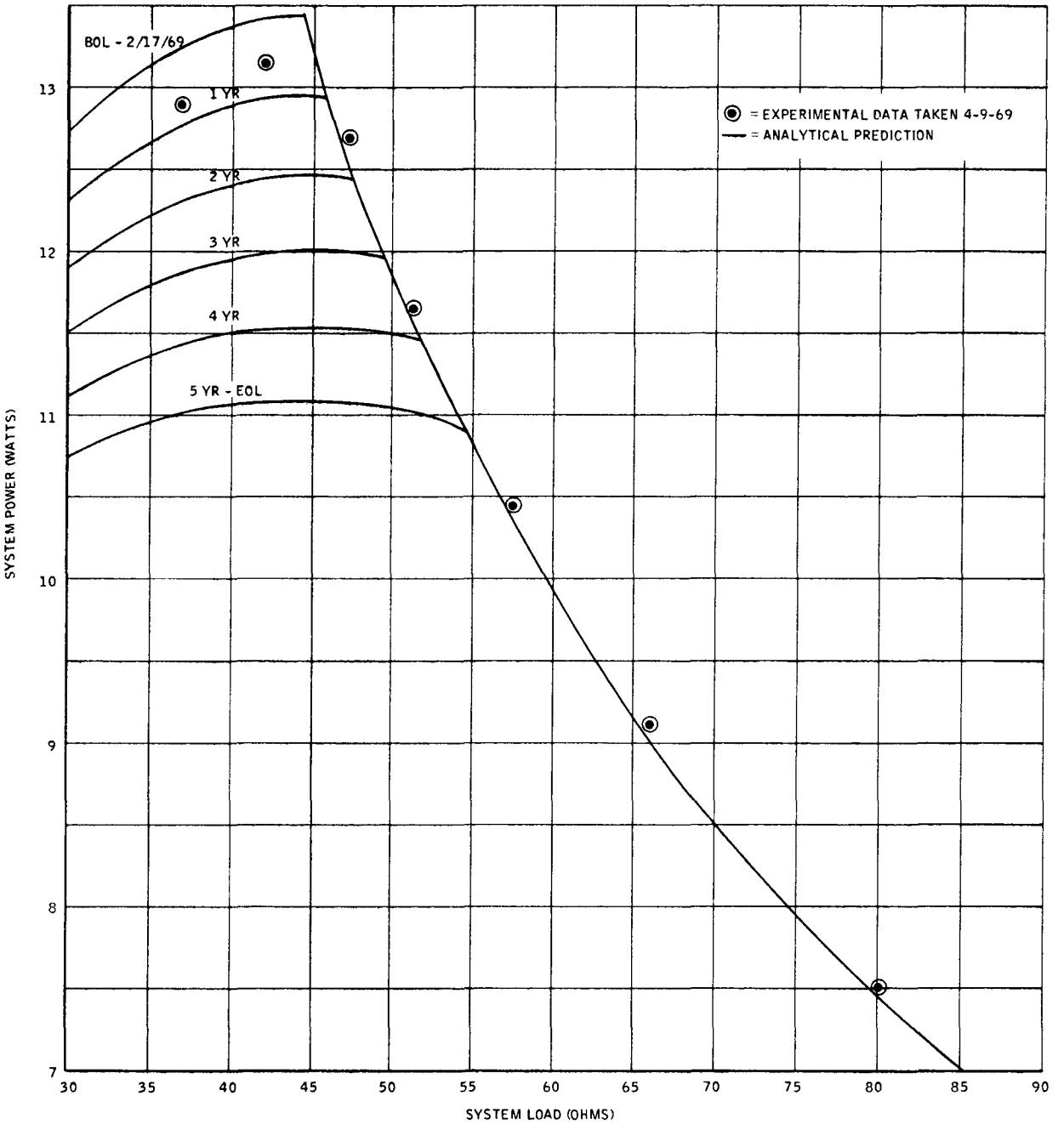

Figure 1. System S10P3 Performance
Power vs. Load Resistance in 40°F Water

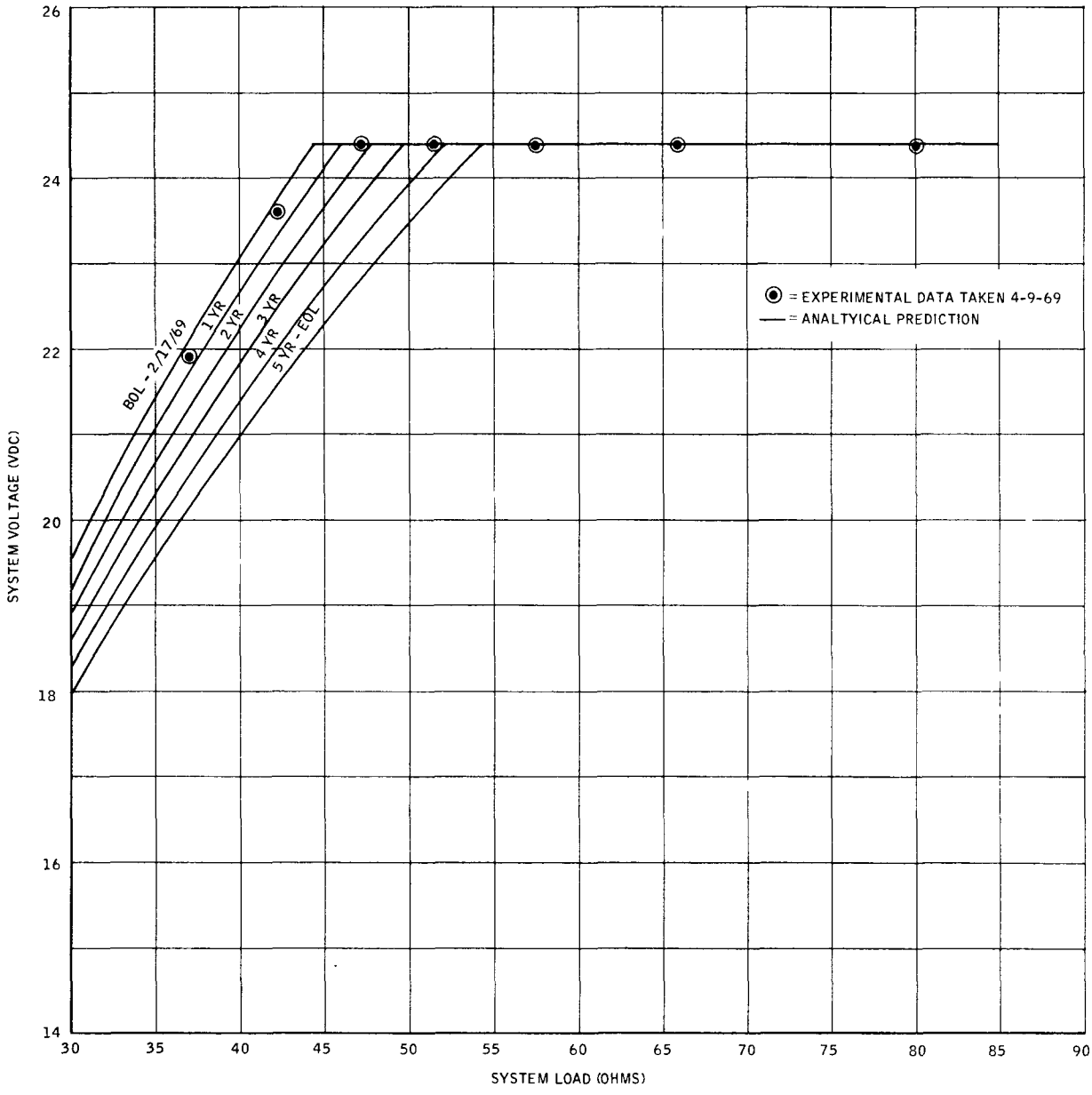

Figure 2. System S10P3 Performance
Voltage vs. Load Resistance in 40°F Water

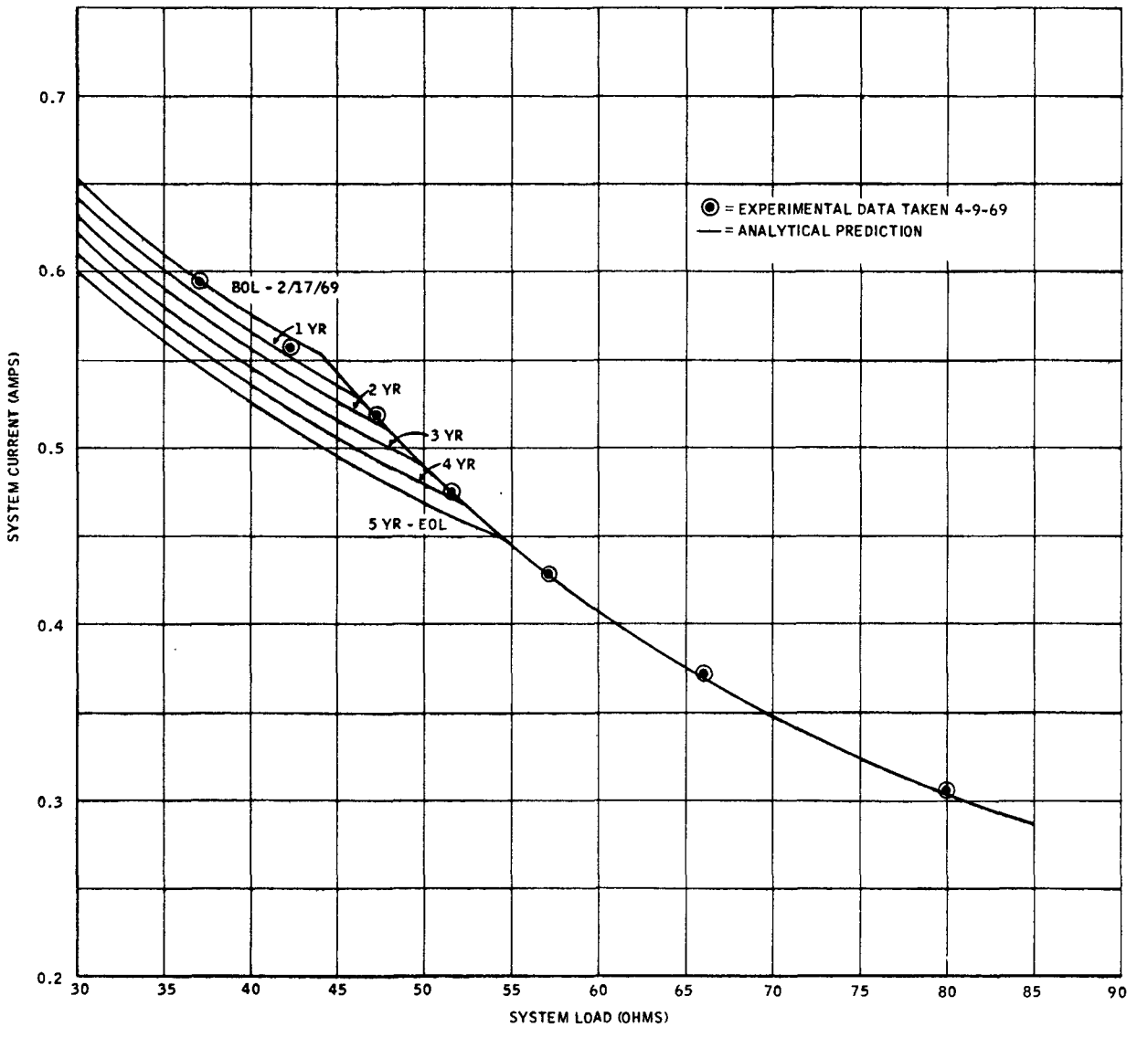

Figure 3. System S10P3 Performance
Current vs. Load Resistance in 40°F Water

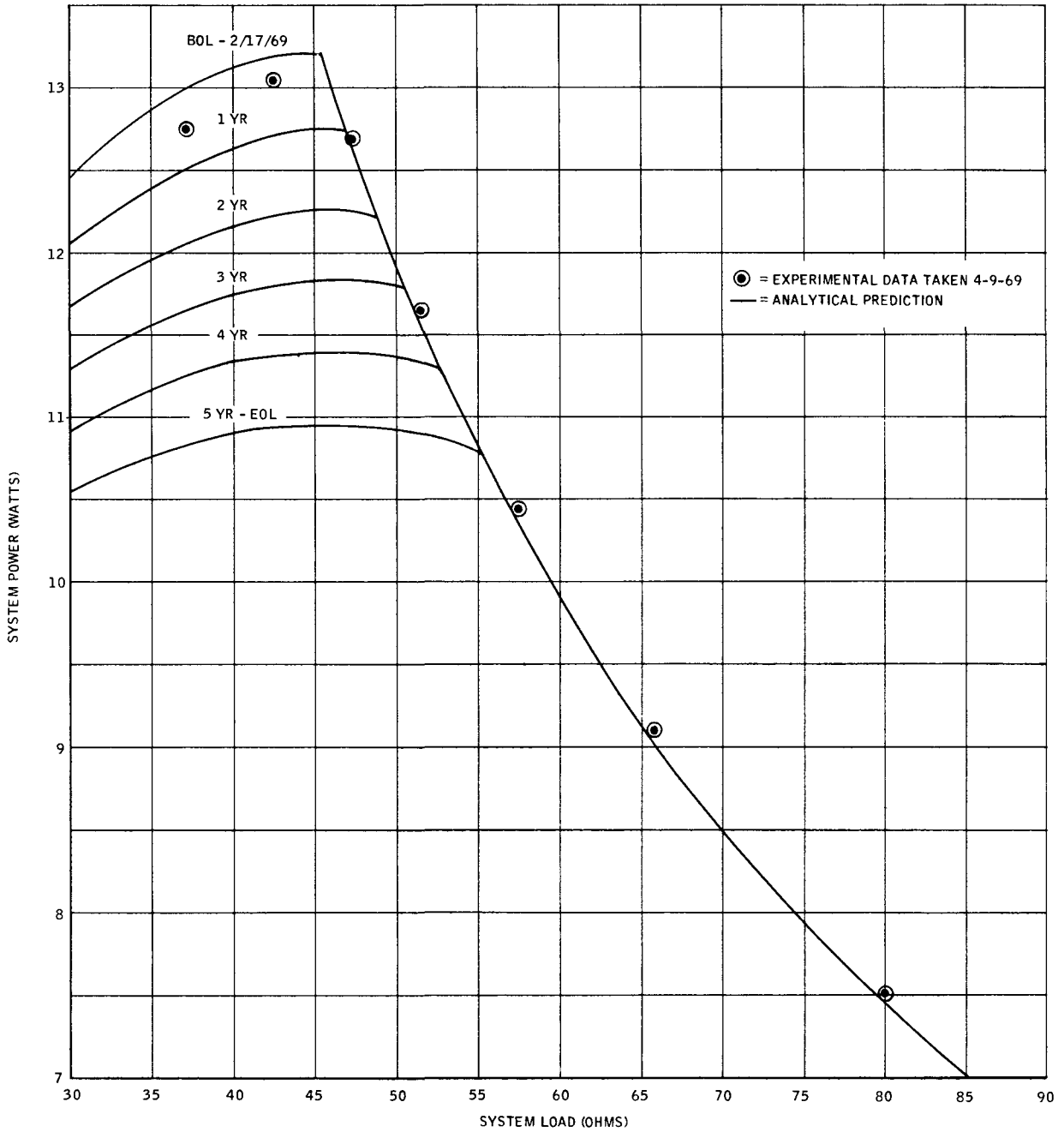

Figure 4. System S10P3 Performance
Power vs. Load Resistance in 60°F Water

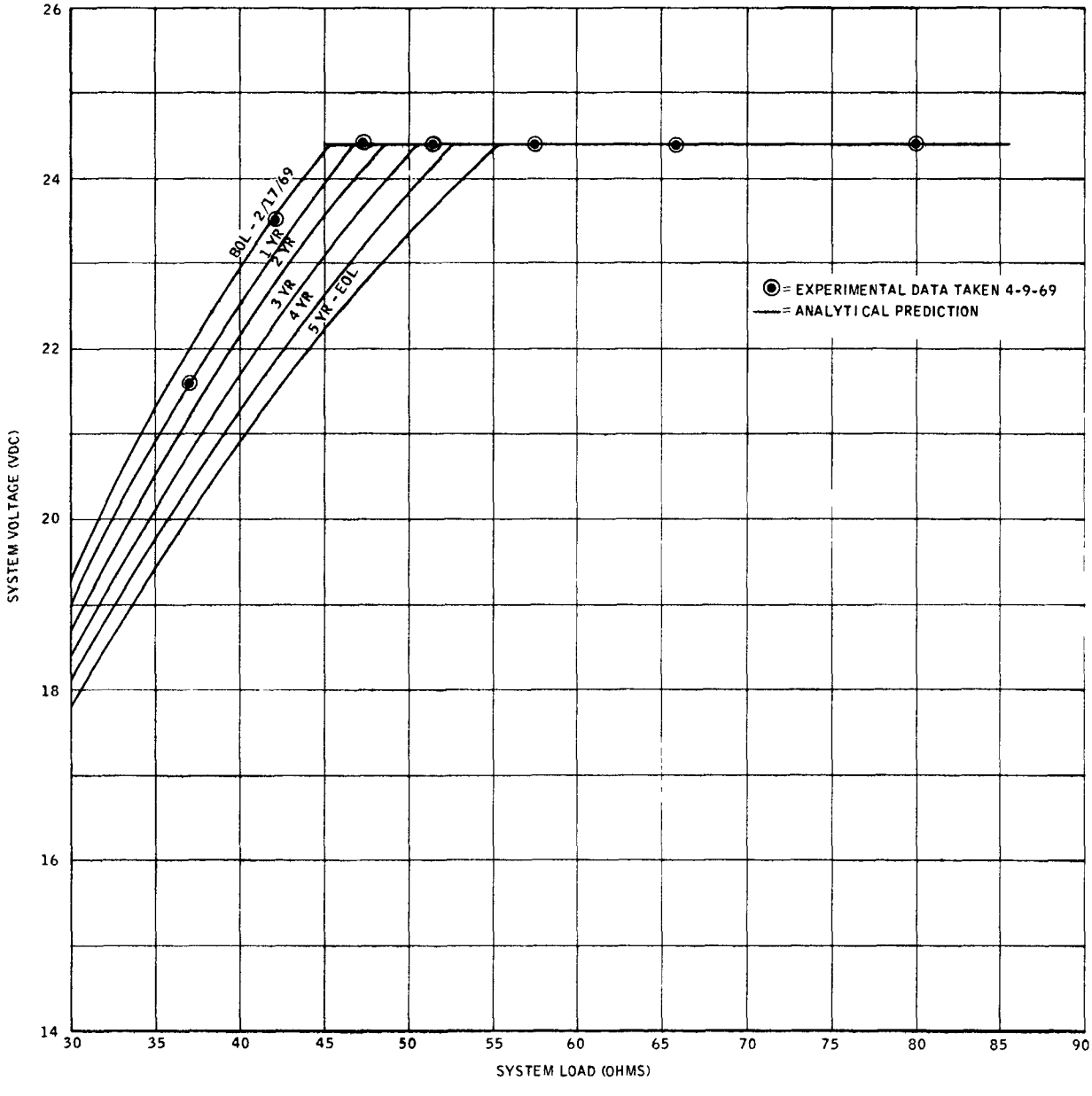

Figure 5. System S10P3 Performance
Voltage vs. Load Resistance in 60°F Water

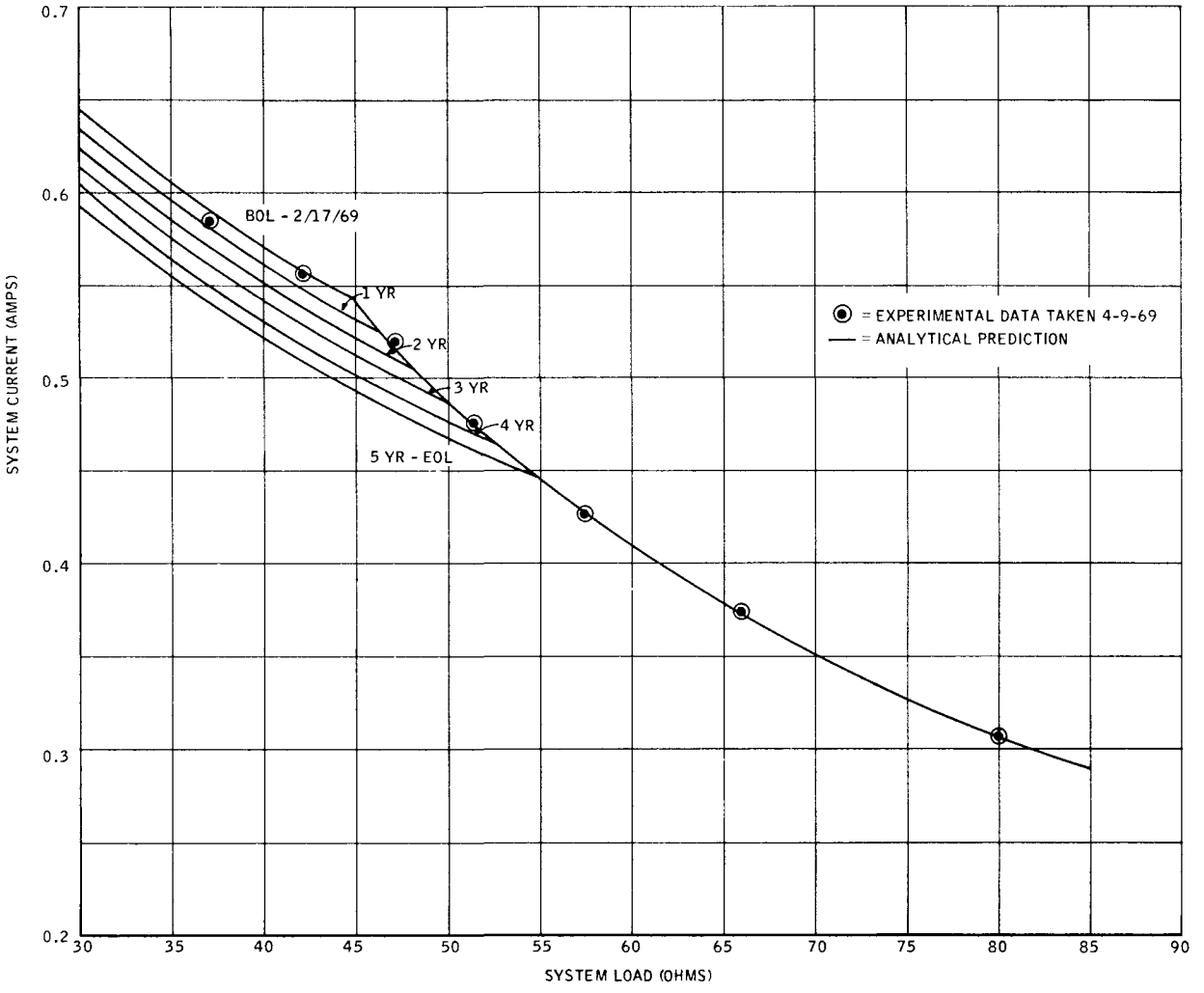

Figure 6. System S10P3 Performance
Current vs. Load Resistance in 60°F Water

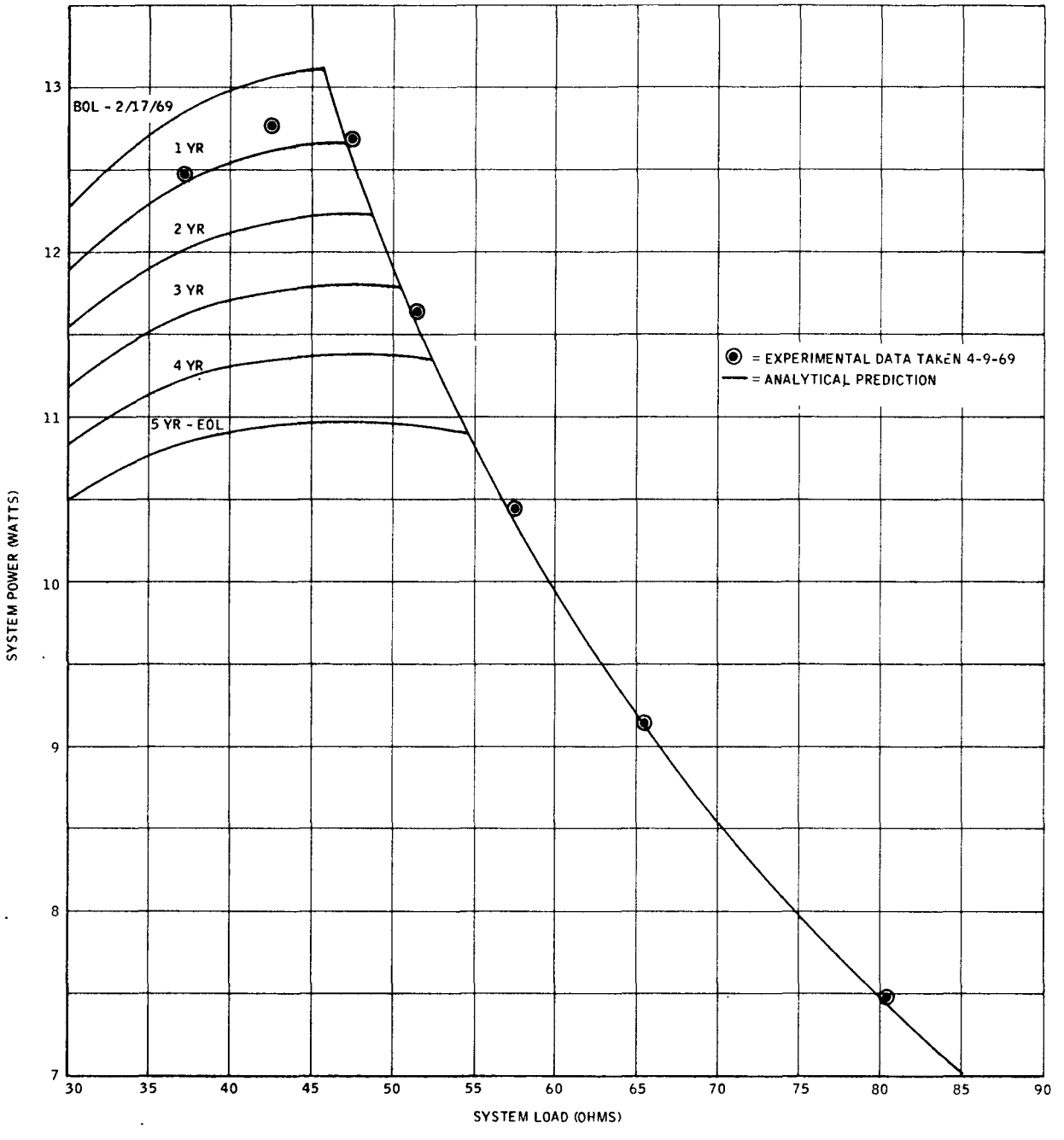

Figure 7. System S10P3 Performance
Power vs. Load Resistance in 80°F Water

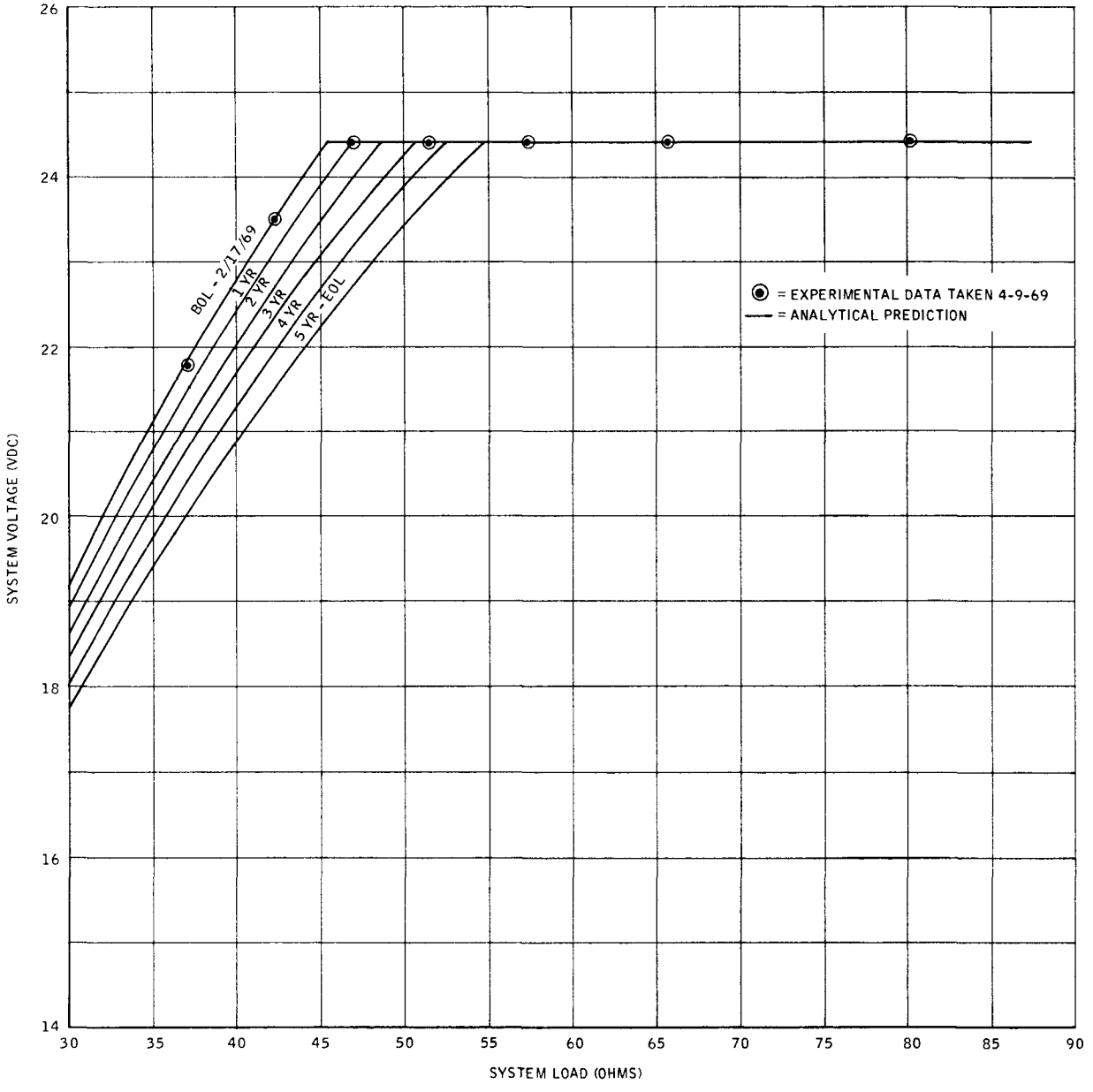

Figure 8. System S10P3 Performance
Voltage vs. Load Resistance in 80°F Water

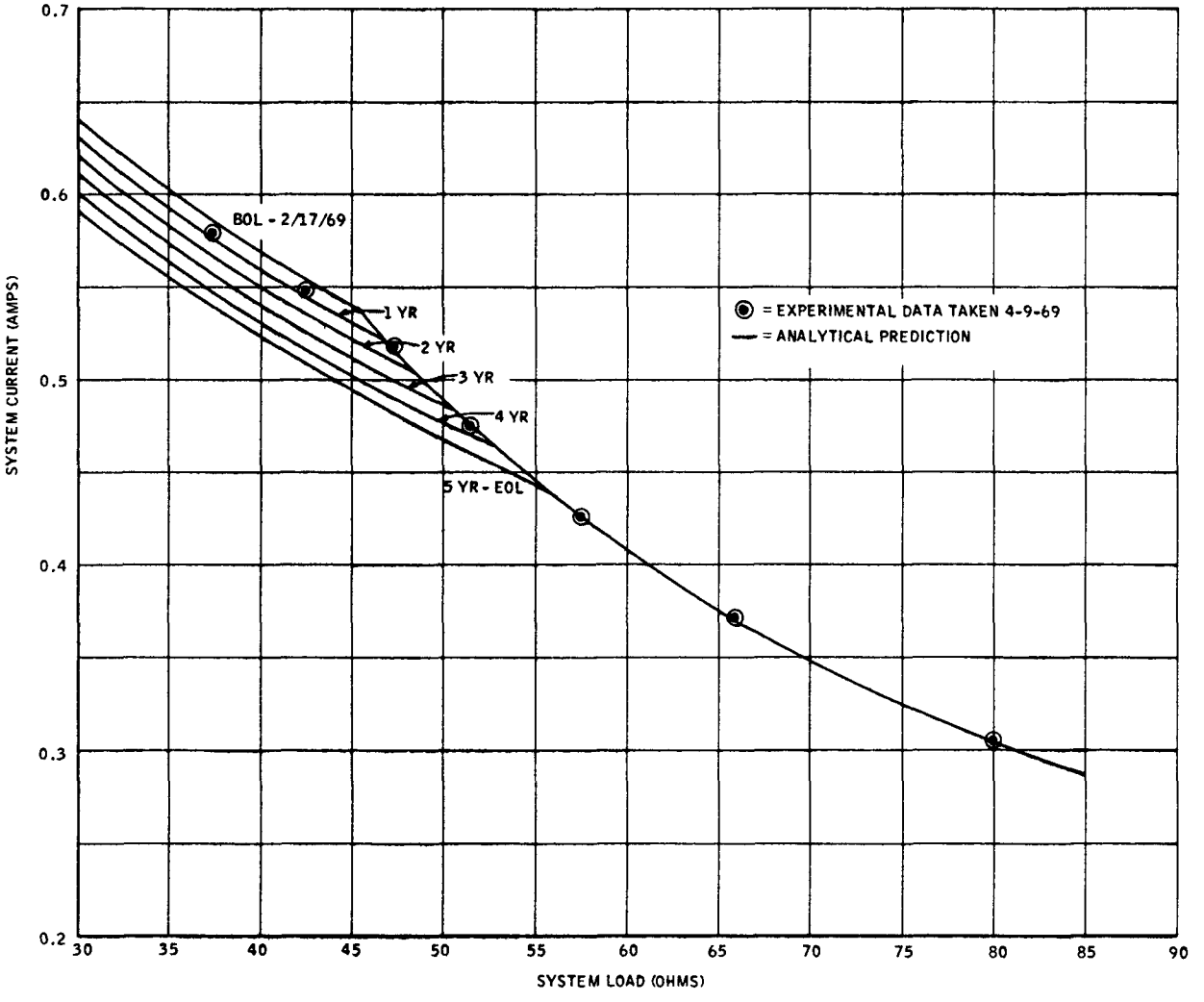

Figure 9. System S10P3 Performance
Current vs. Load Resistance in 80°F Water

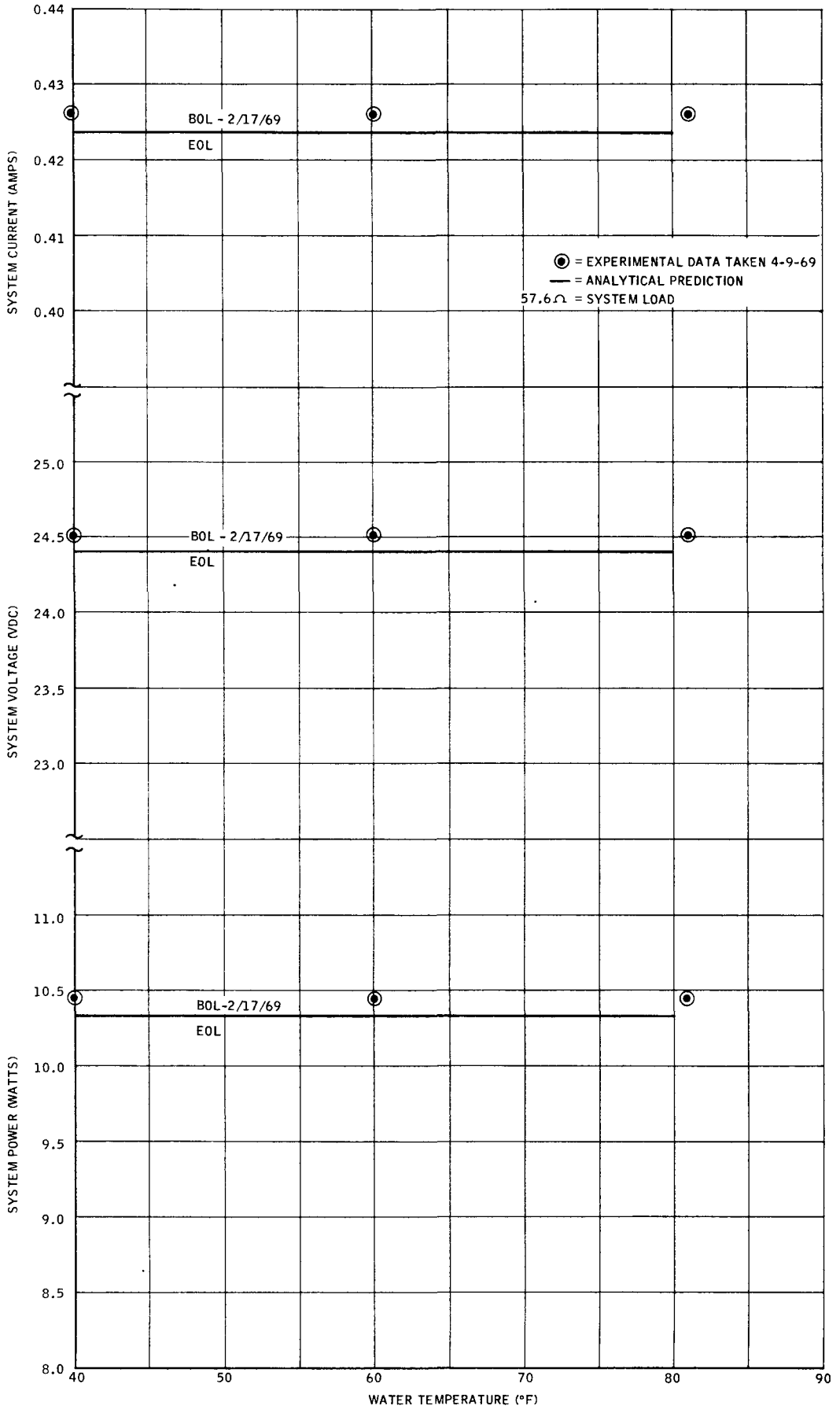

Figure 10. System S10P3 Performance
System Power, Voltage and Current vs. Water Temperature

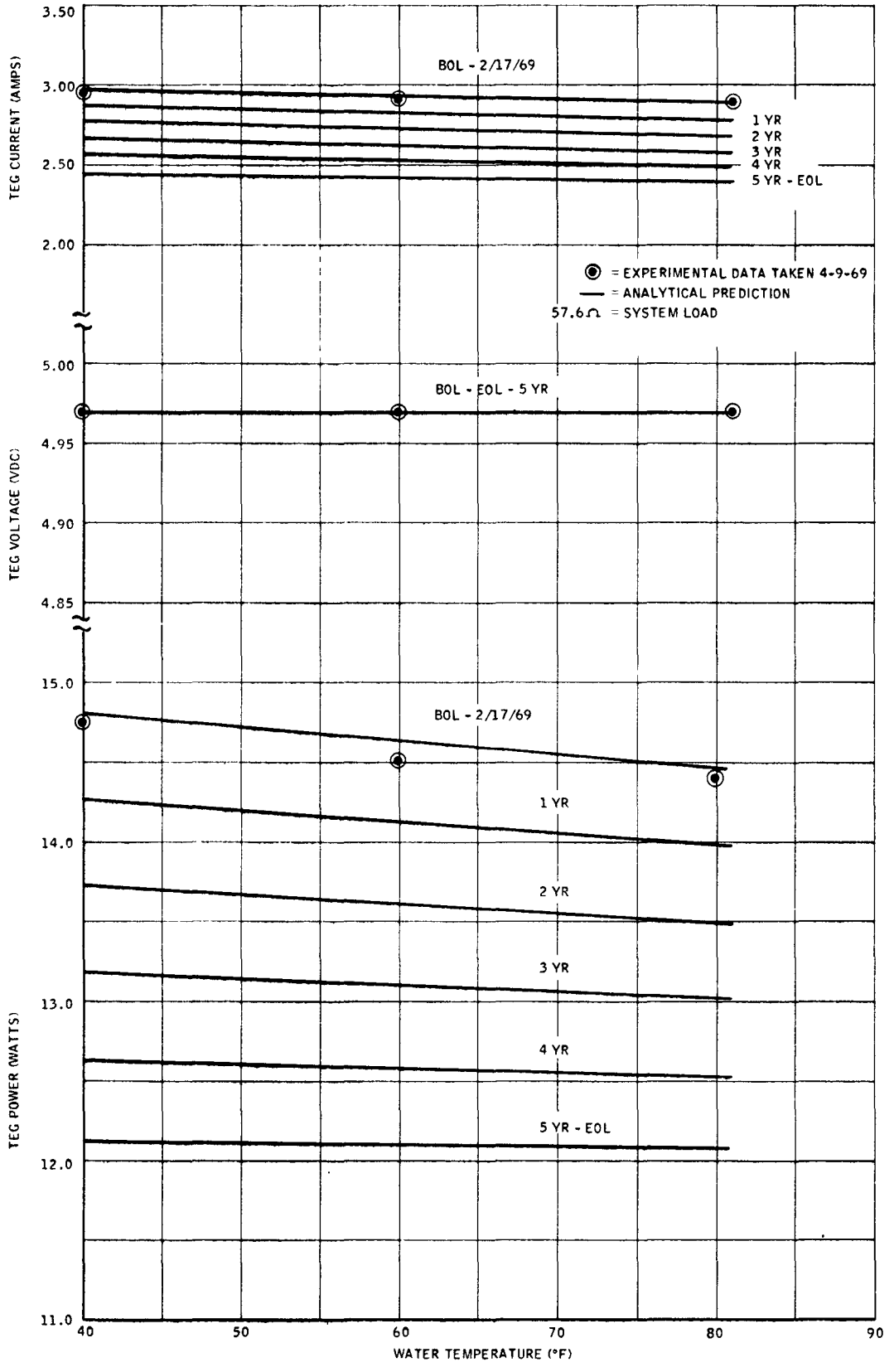

Figure 11. System S10P3 Performance
TEG Power, Voltage and Current vs. Water Temperature

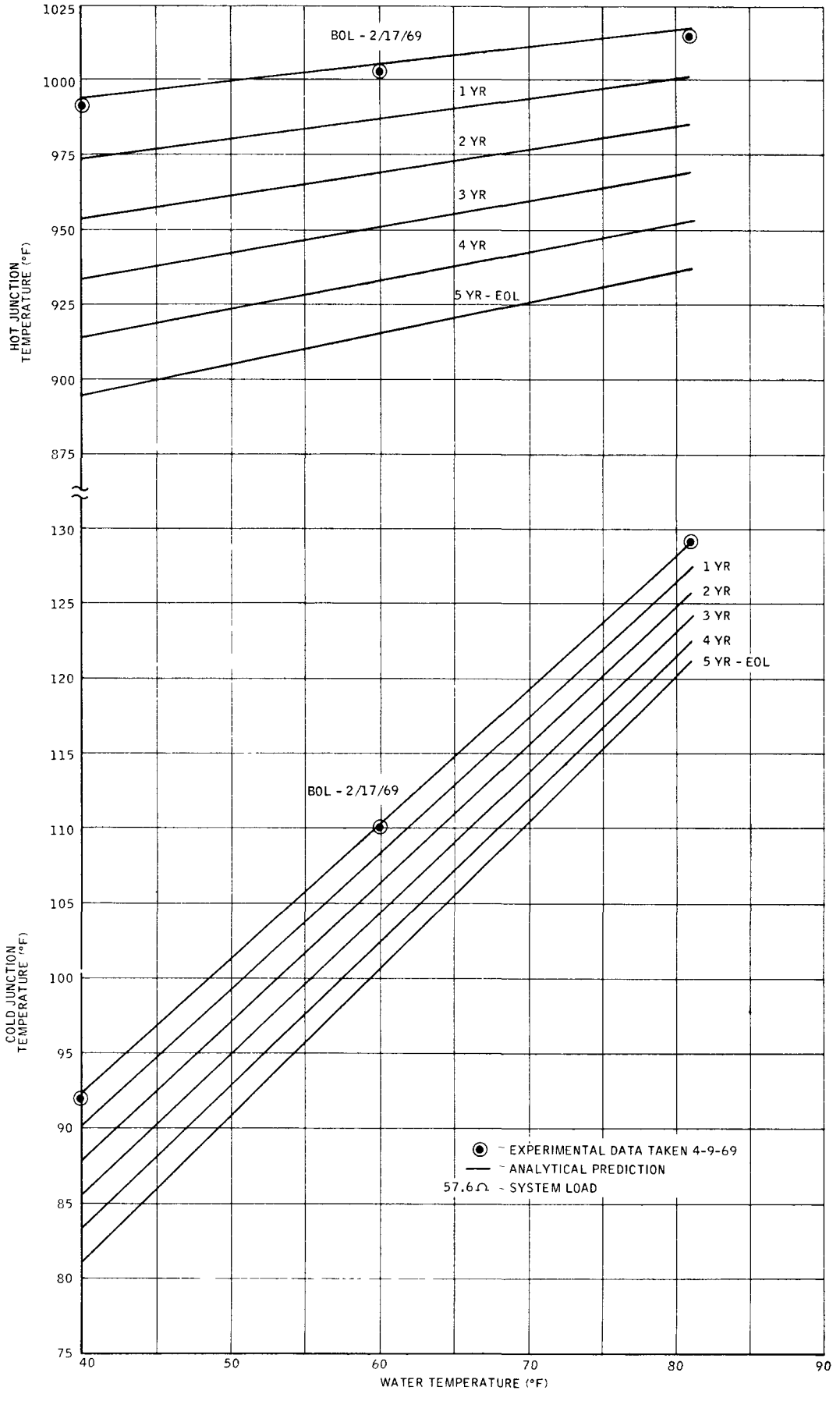

Figure 12. System S10P3 Performance
System Temperatures vs. Water Temperatures

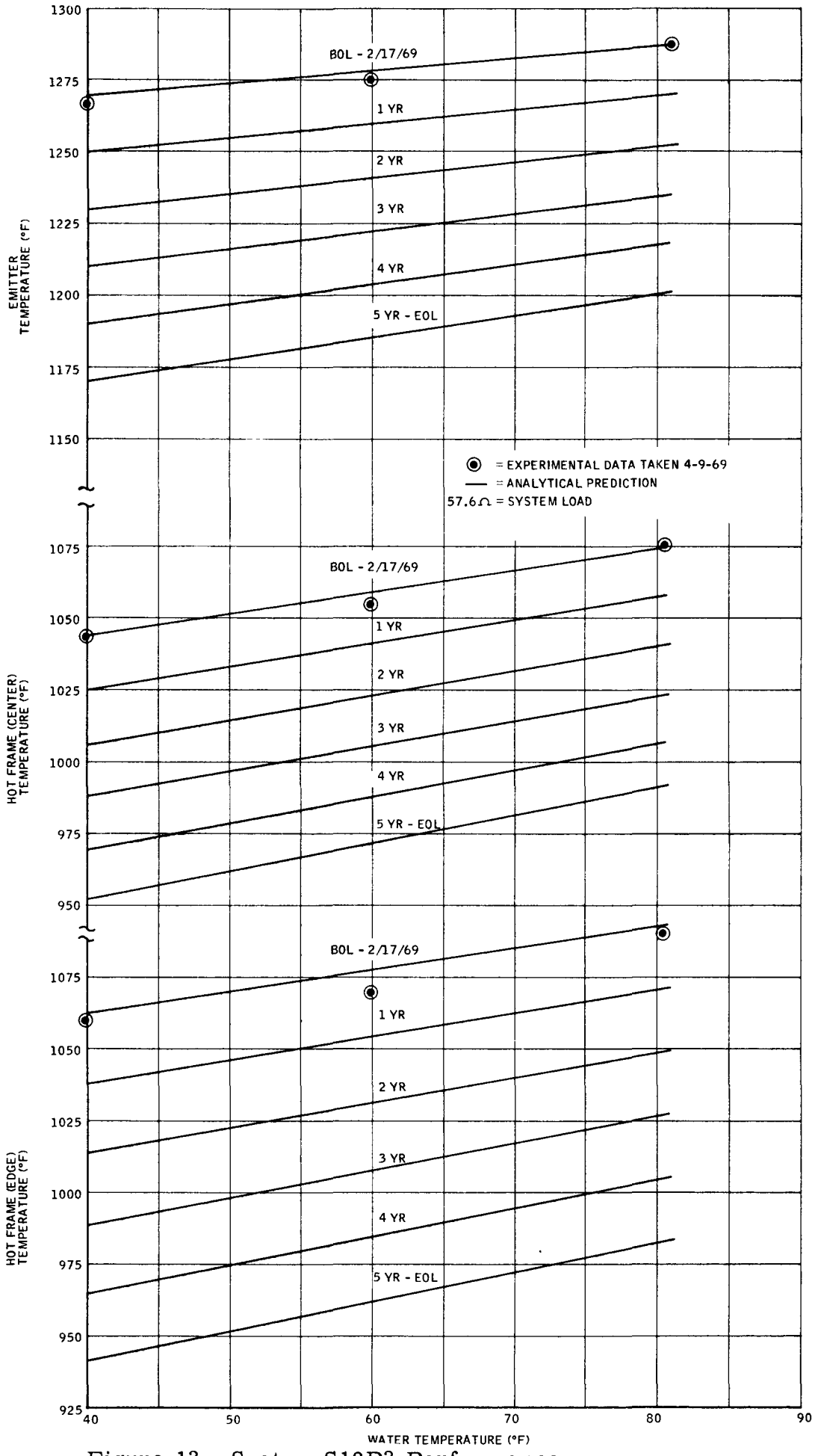

Figure 13. System S10P3 Performance
System Temperatures vs. Water Temperatures

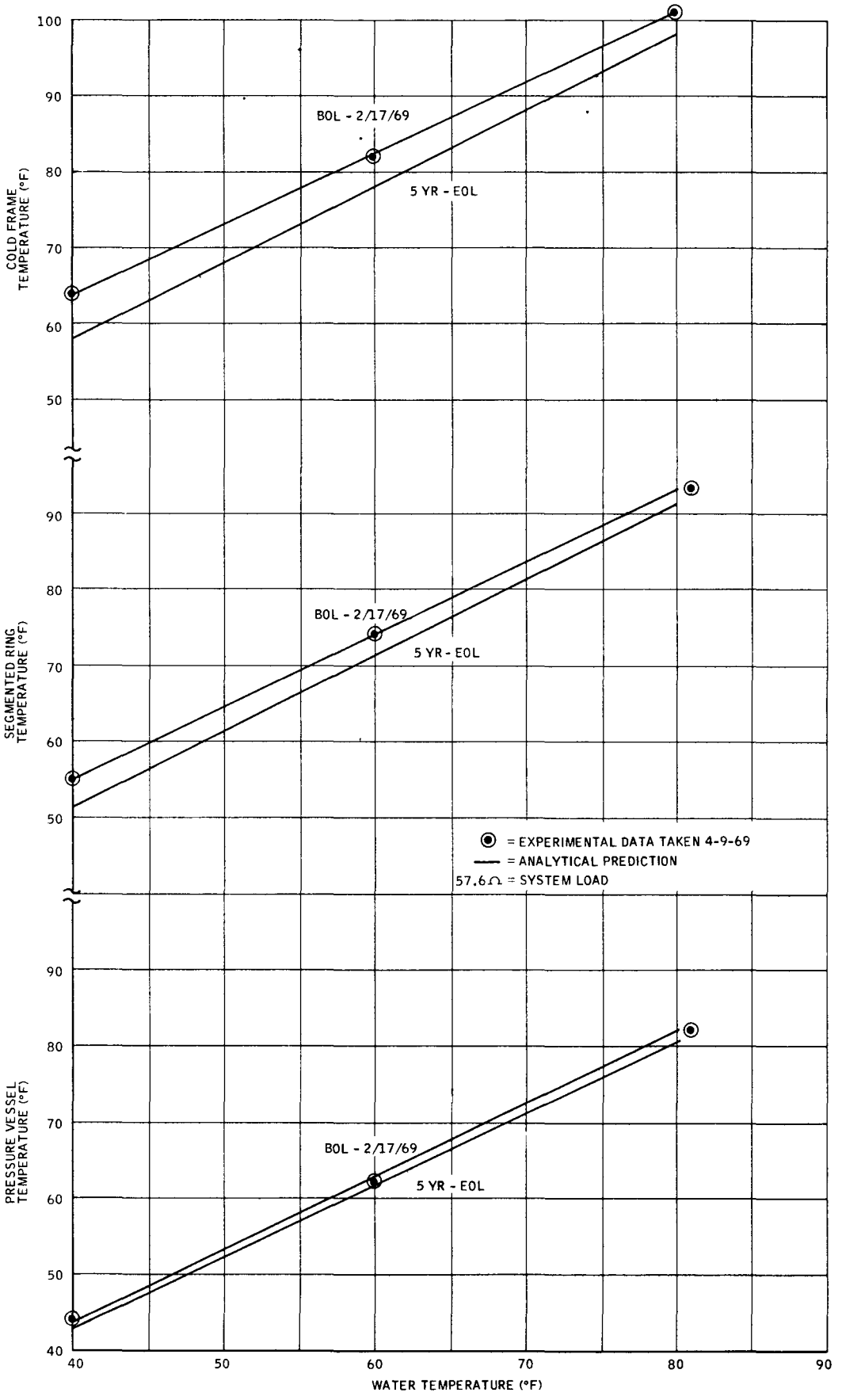

Figure 14. System S10P3 Performance
System Temperatures vs. Water Temperatures

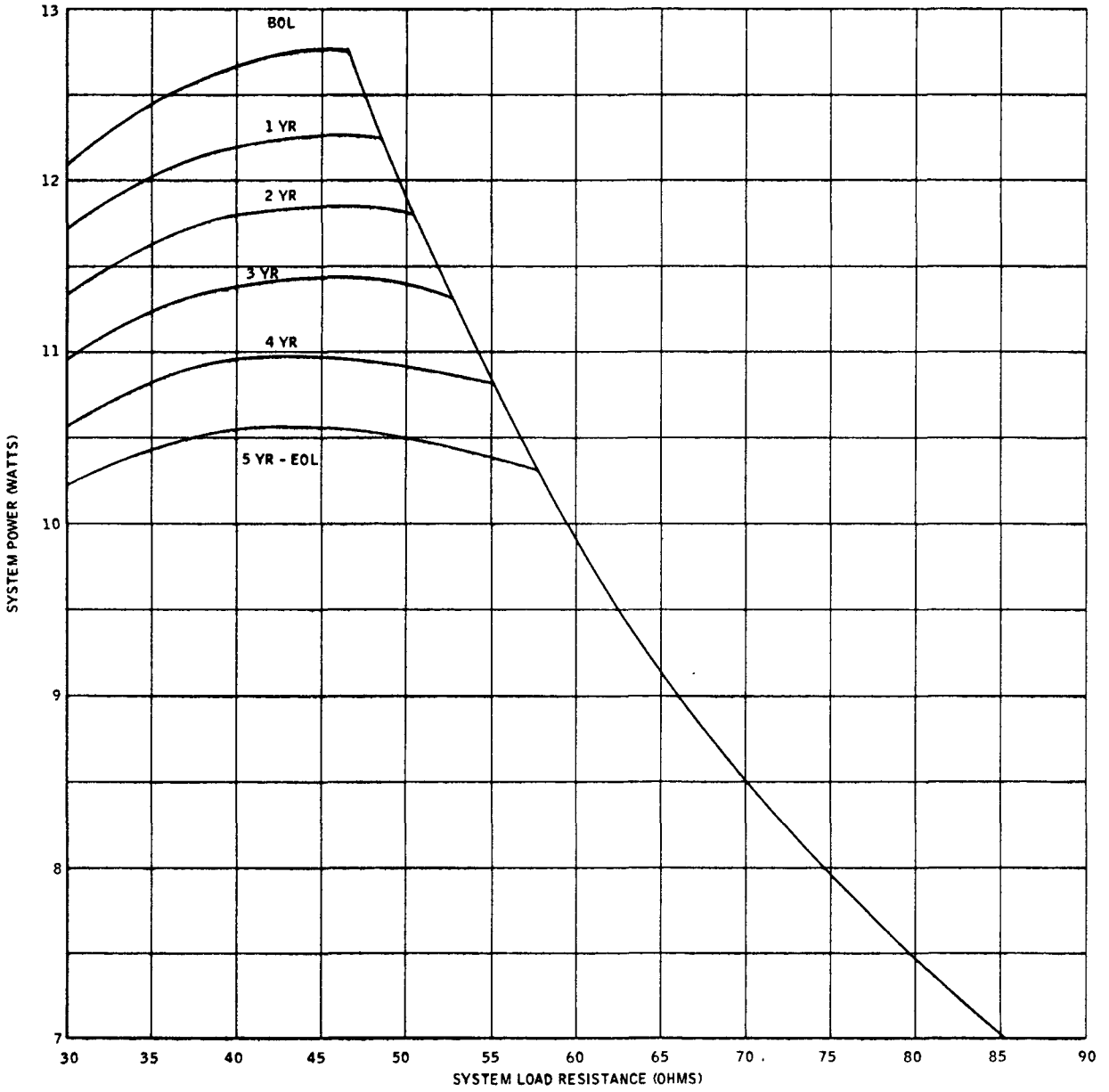

Figure 1. System Performance - 209 Watts
Power vs. Load Resistance in 40°F Water

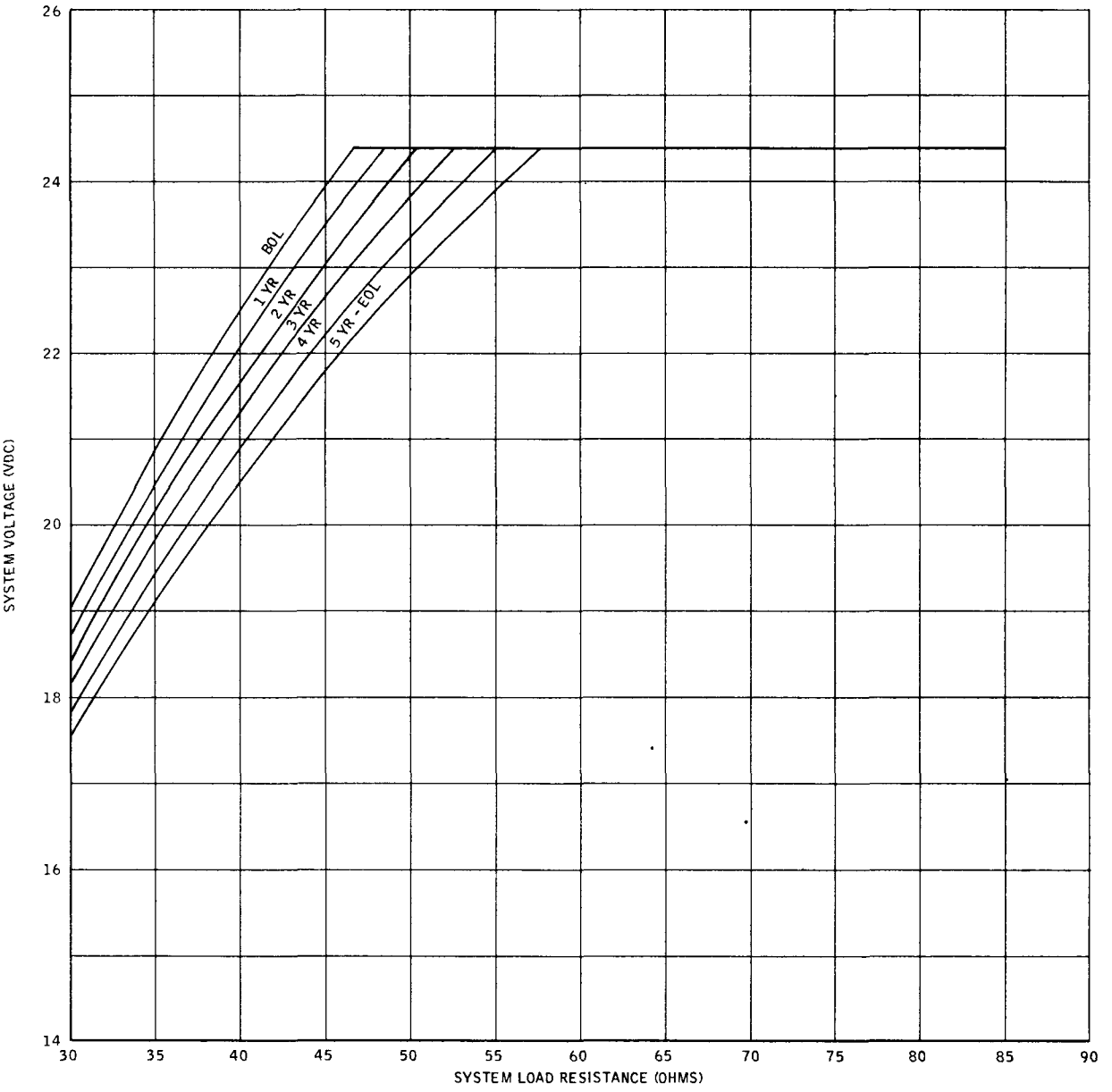

Figure 2. System Performance - 209 Watts
Voltage vs. Load Resistance in 40°F Water

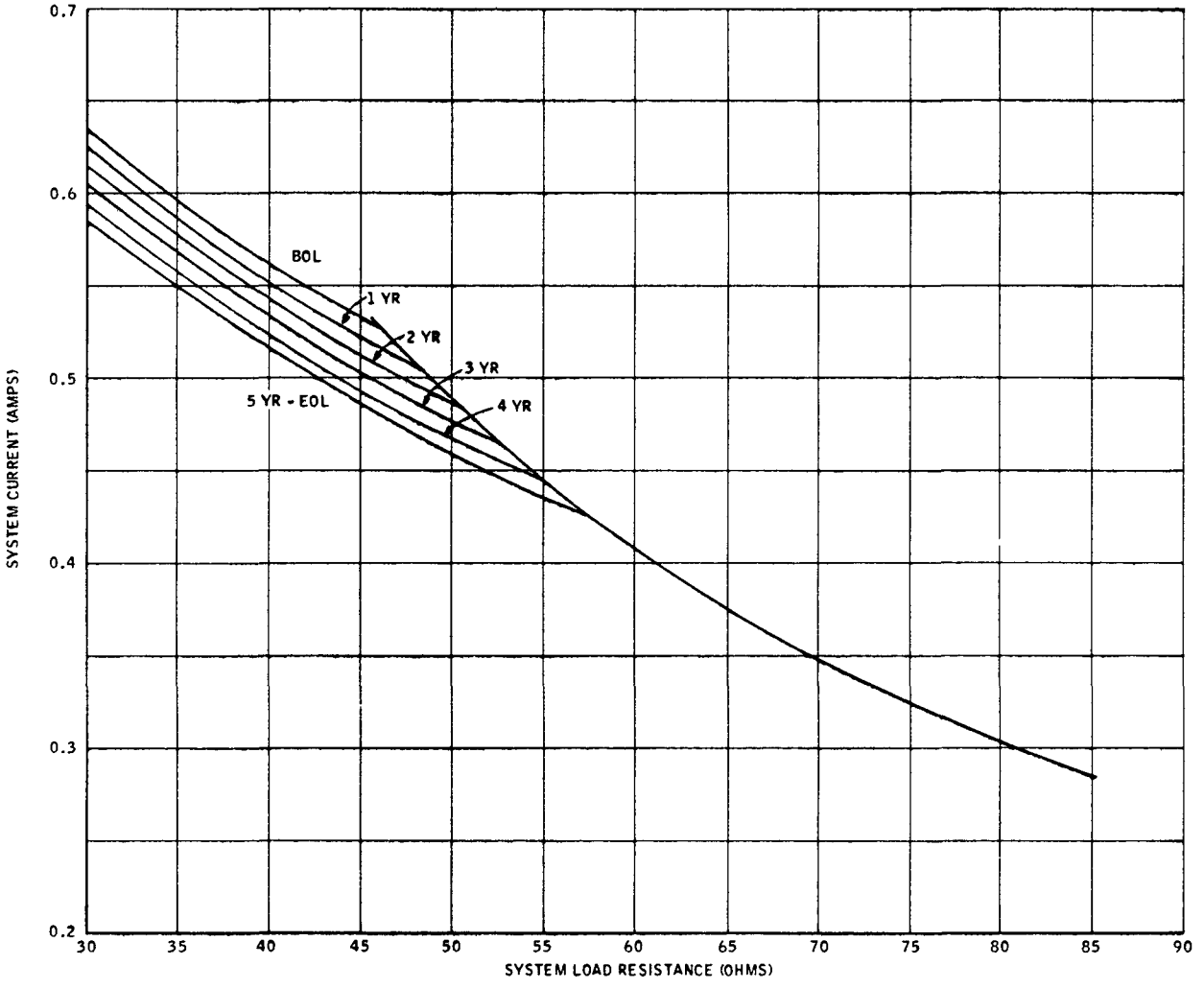

Figure 3. System Performance - 209 Watts
Current vs. Load Resistance in 40°F Water

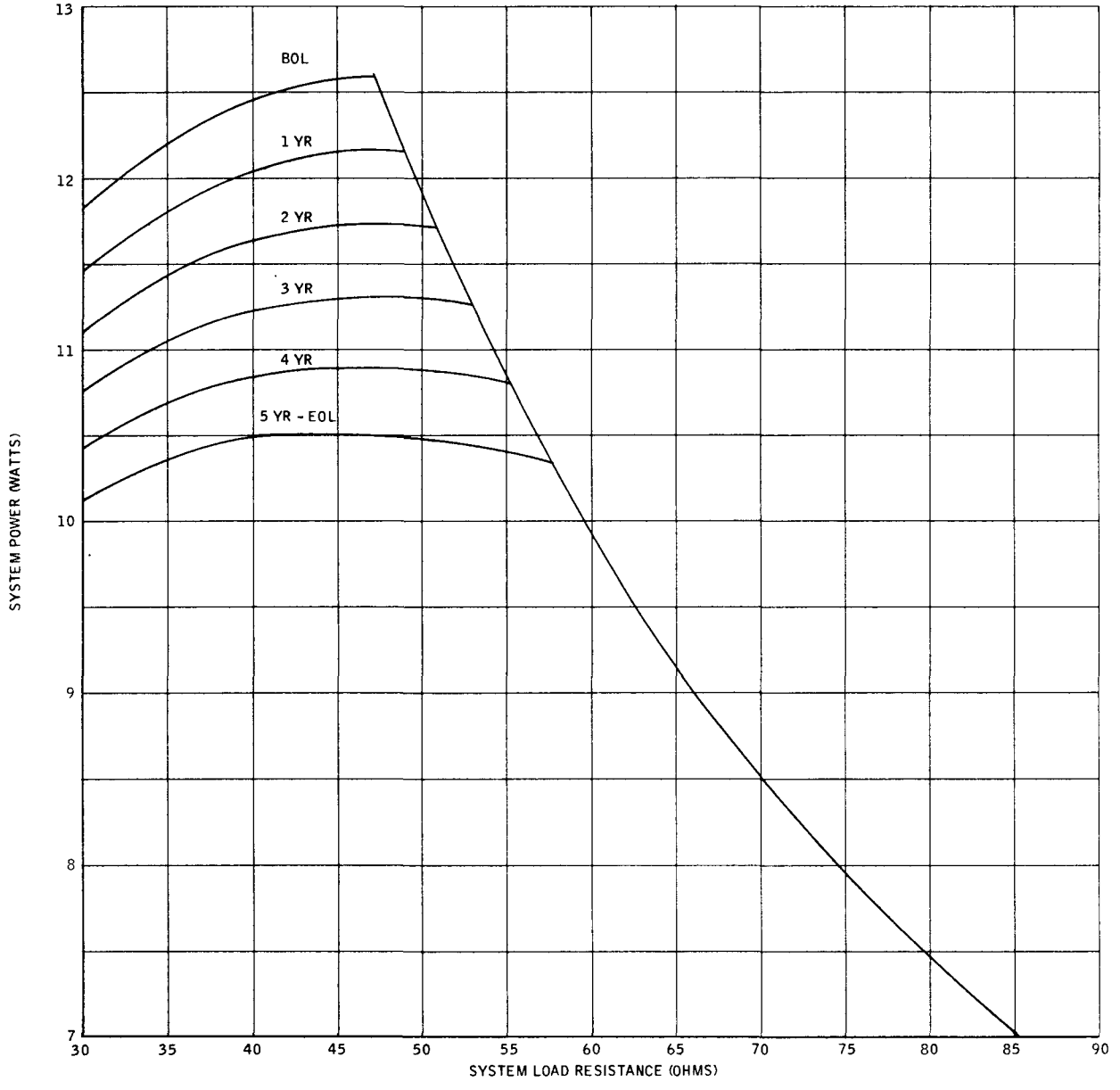

Figure 4. System Performance - 209 Watts
Power vs. Load Resistance in 60°F Water

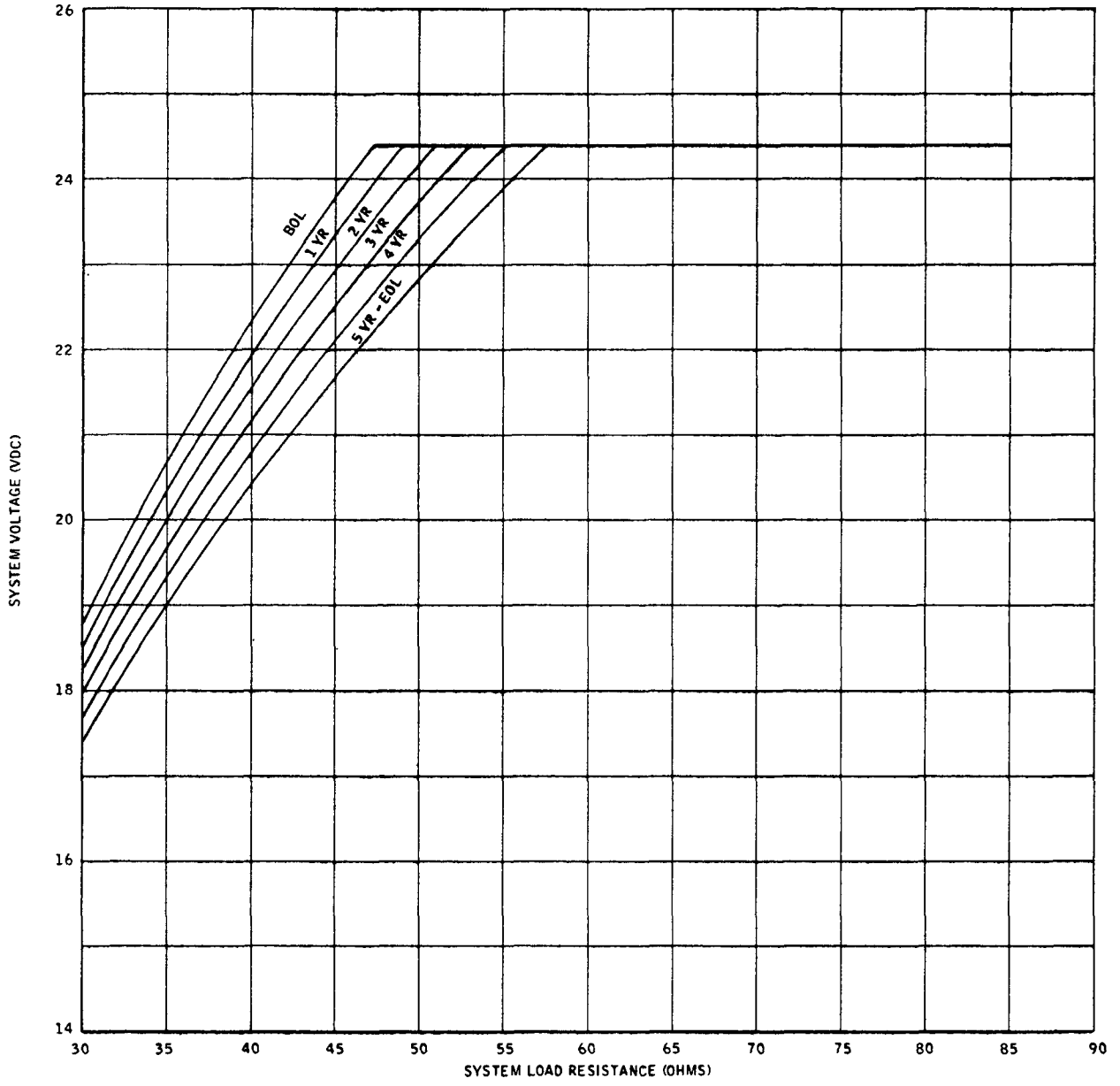

Figure 5. System Performance - 209 Watts
Voltage vs. Load Resistance in 60°F Water

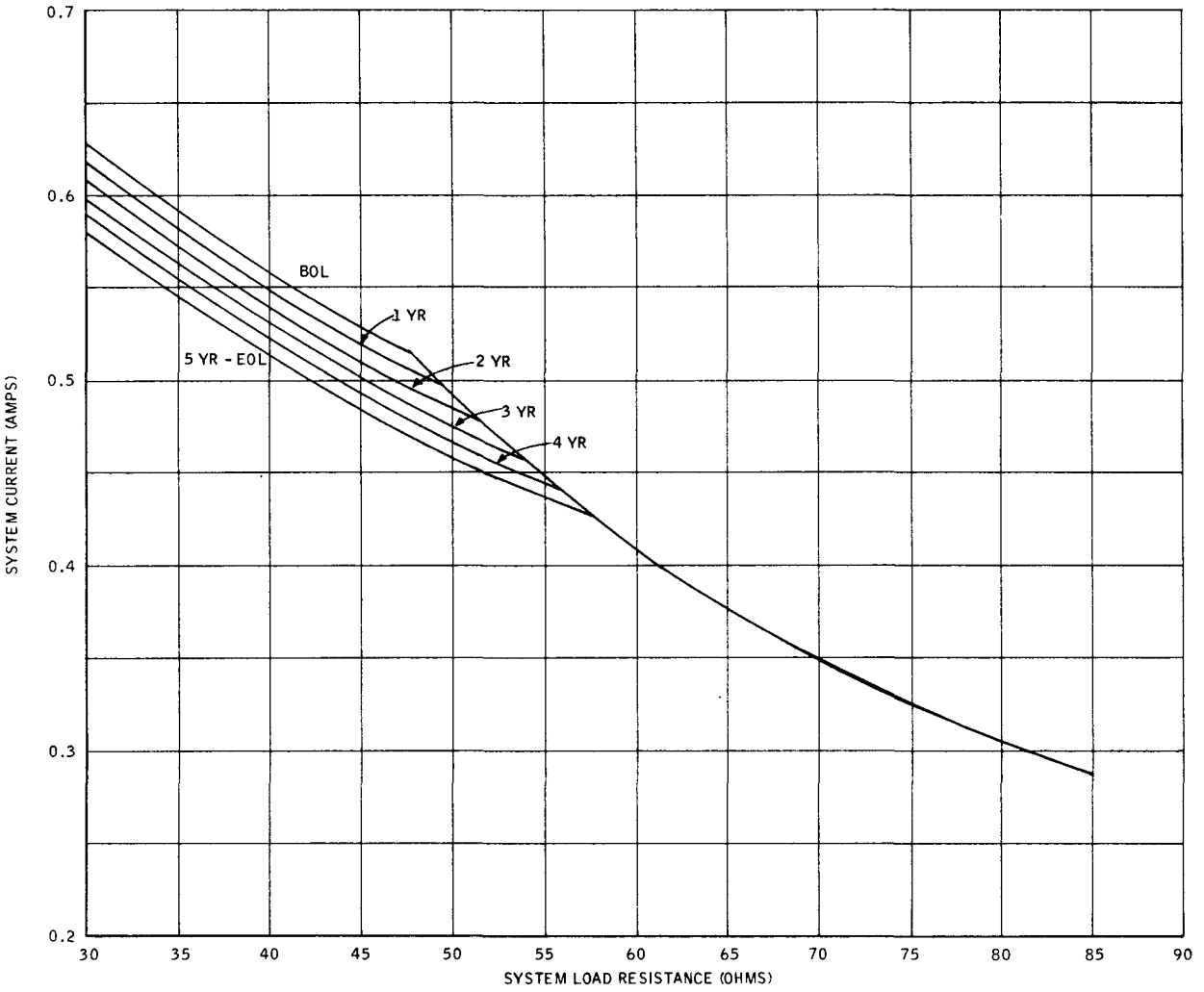

Figure 6. System Performance - 209 Watts
Current vs. Load Resistance in 60°F Water

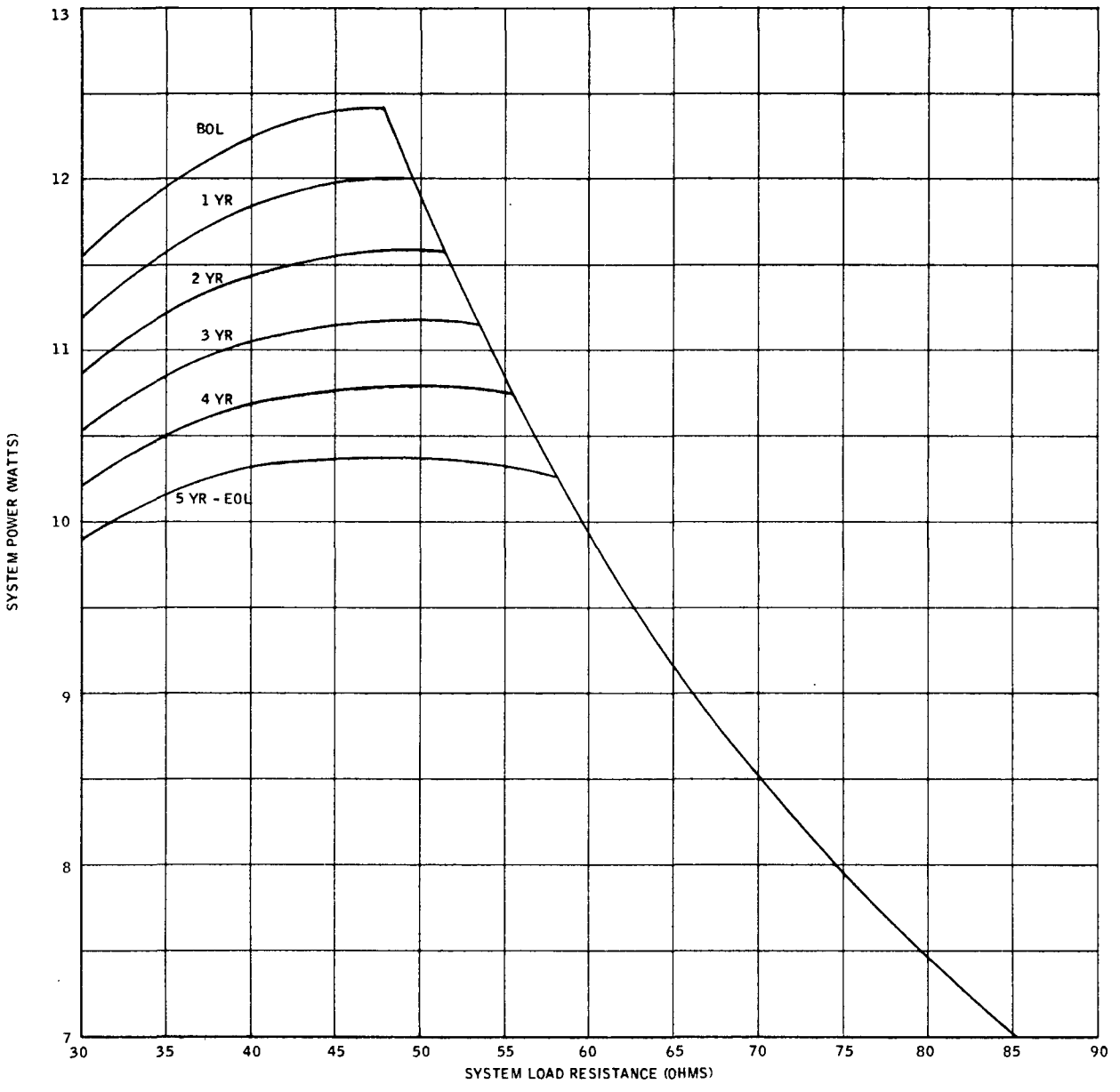

Figure 7. System Performance - 209 Watts
Power vs. Load Resistance in 80°F Water

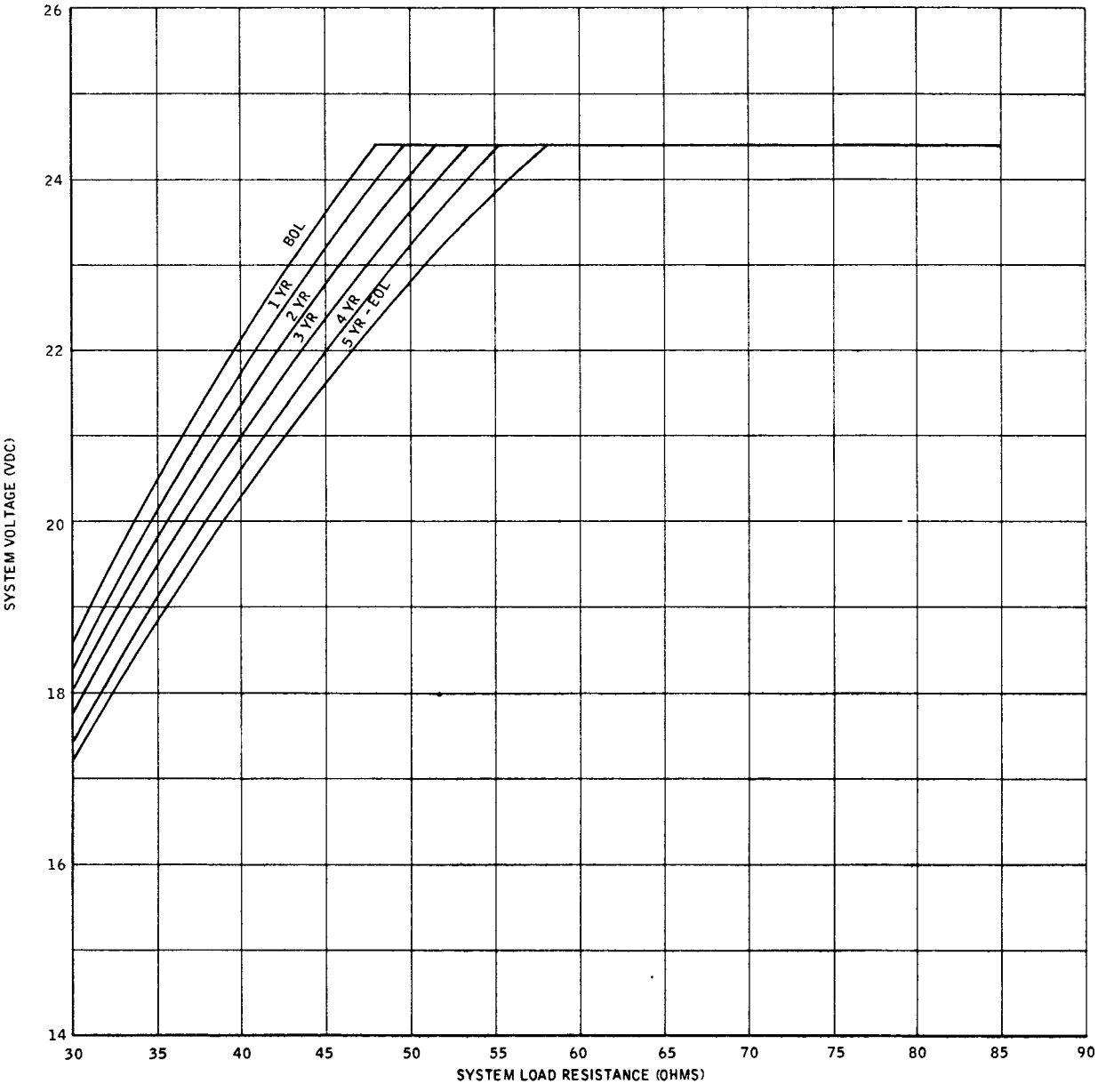

Figure 8. System Performance - 209 Watts
Voltage vs. Load Resistance in 80°F Water

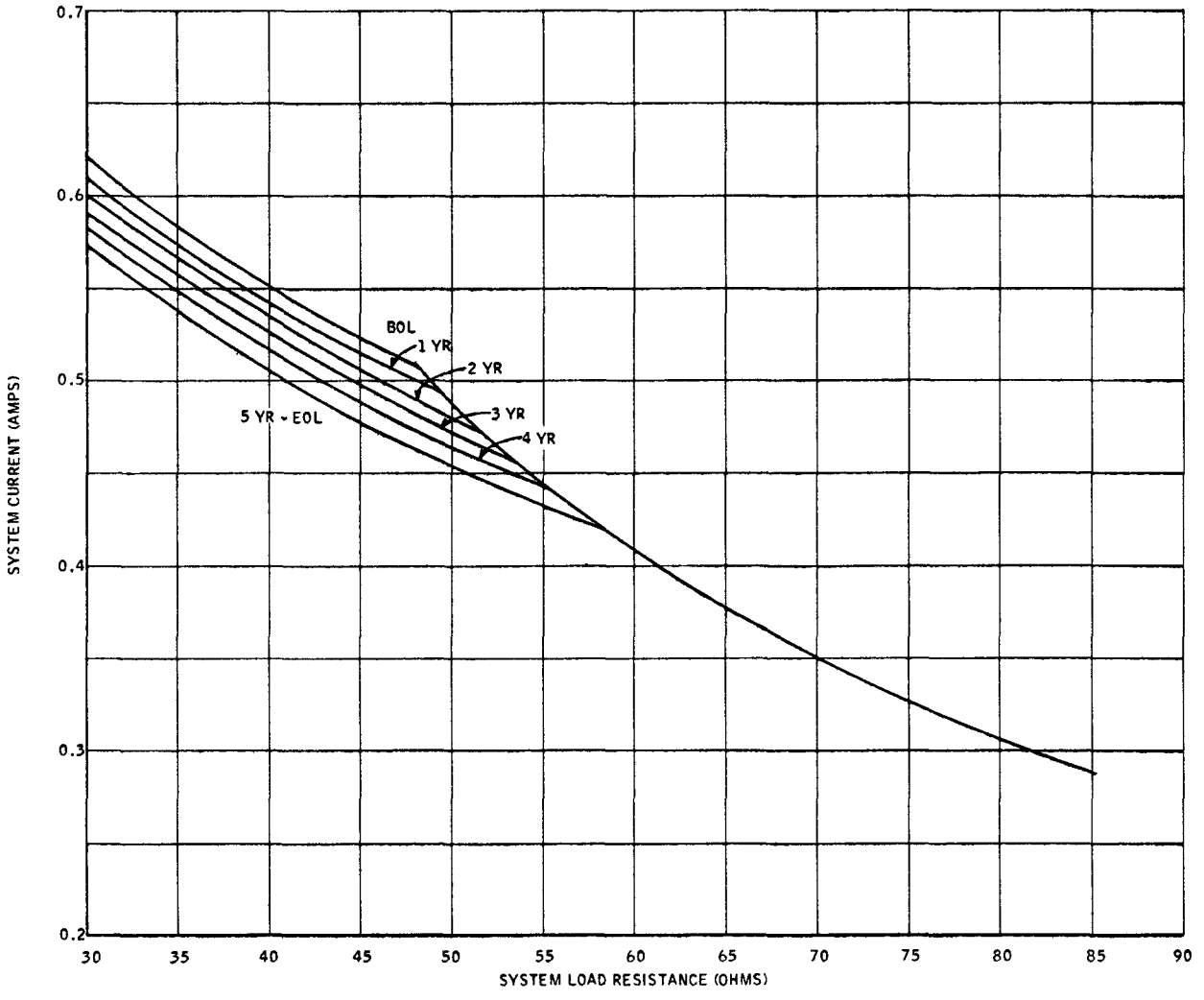

Figure 9. System Performance - 209 Watts
Current vs. Load Resistance in 80°F Water

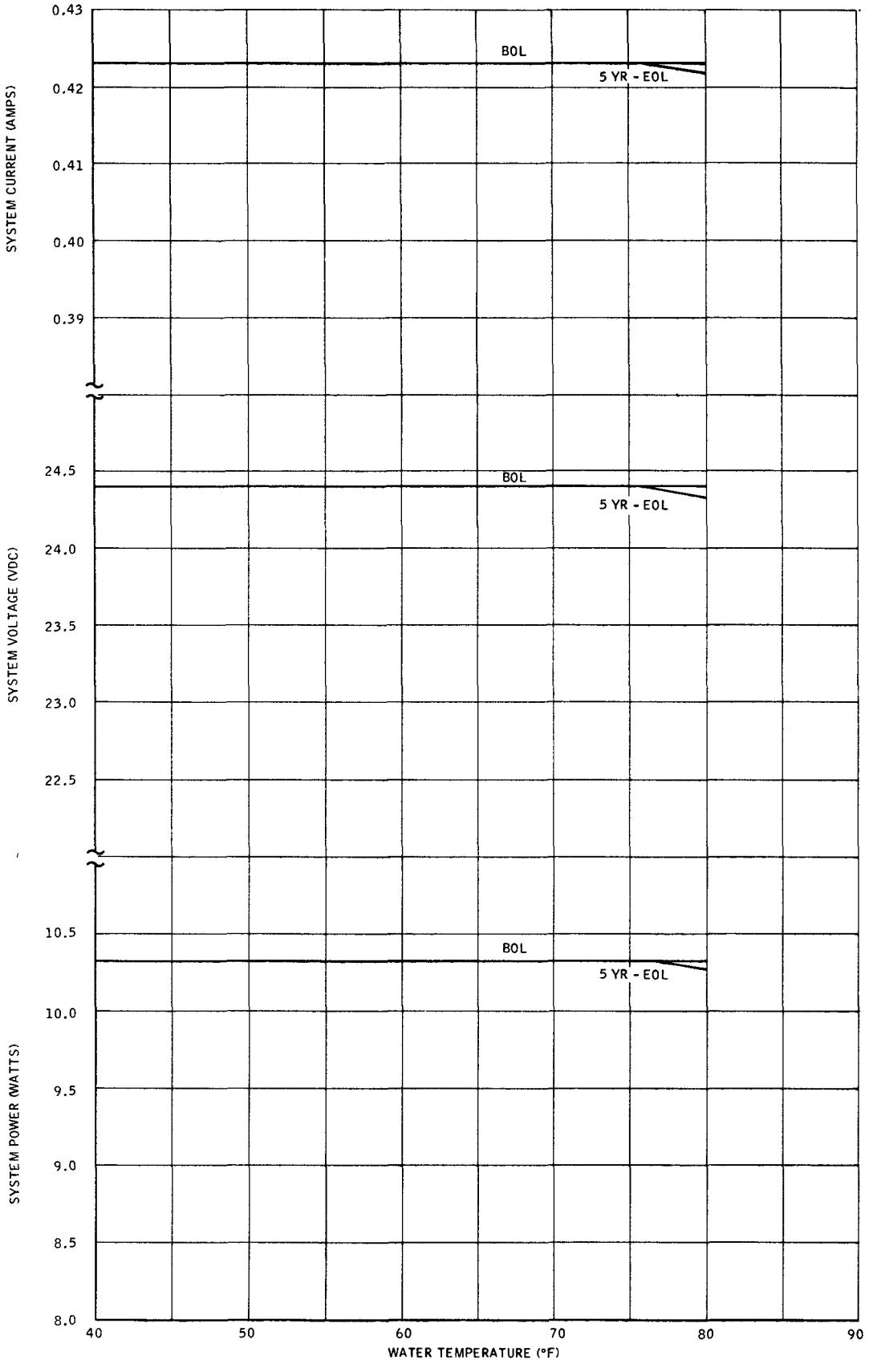

Figure 10. System Performance - 209 Watts
System Power, Voltage and Current vs. Water Temperature

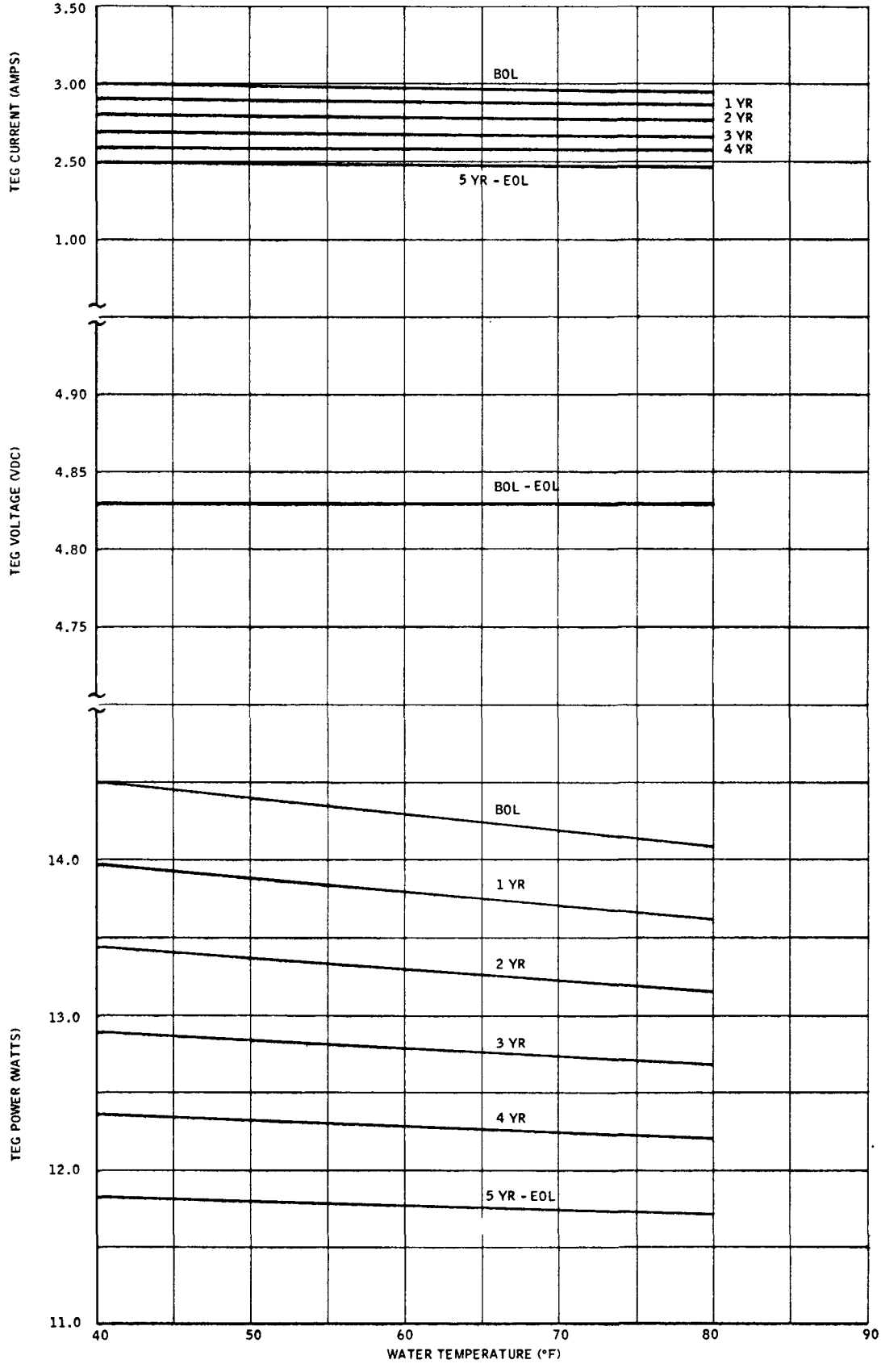

Figure 11. System Performance - 209 Watts
TEG Power, Voltage and Current vs. Water Temperature

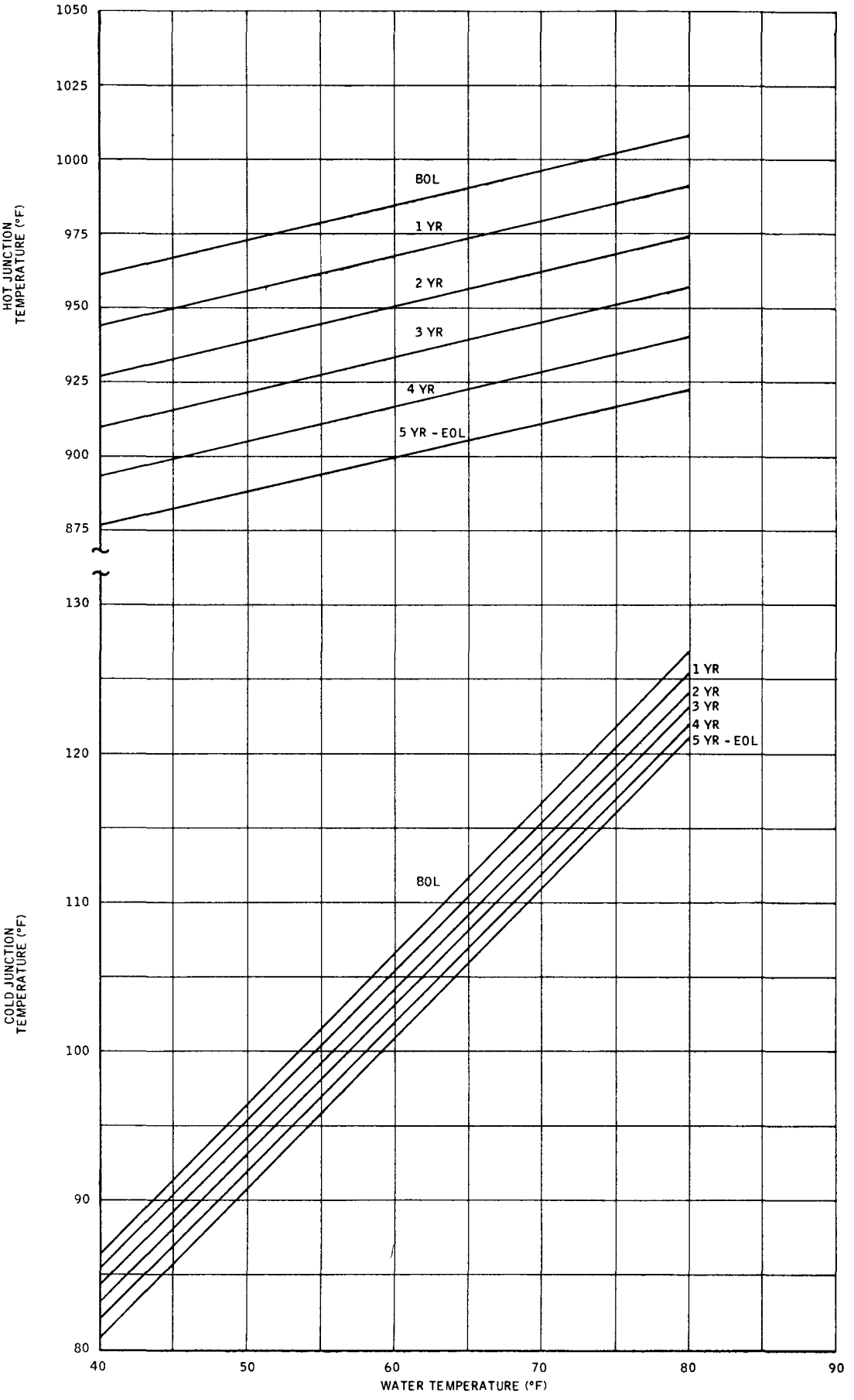

Figure 12. System Performance - 209 Watts
System Temperatures vs. Water Temperatures

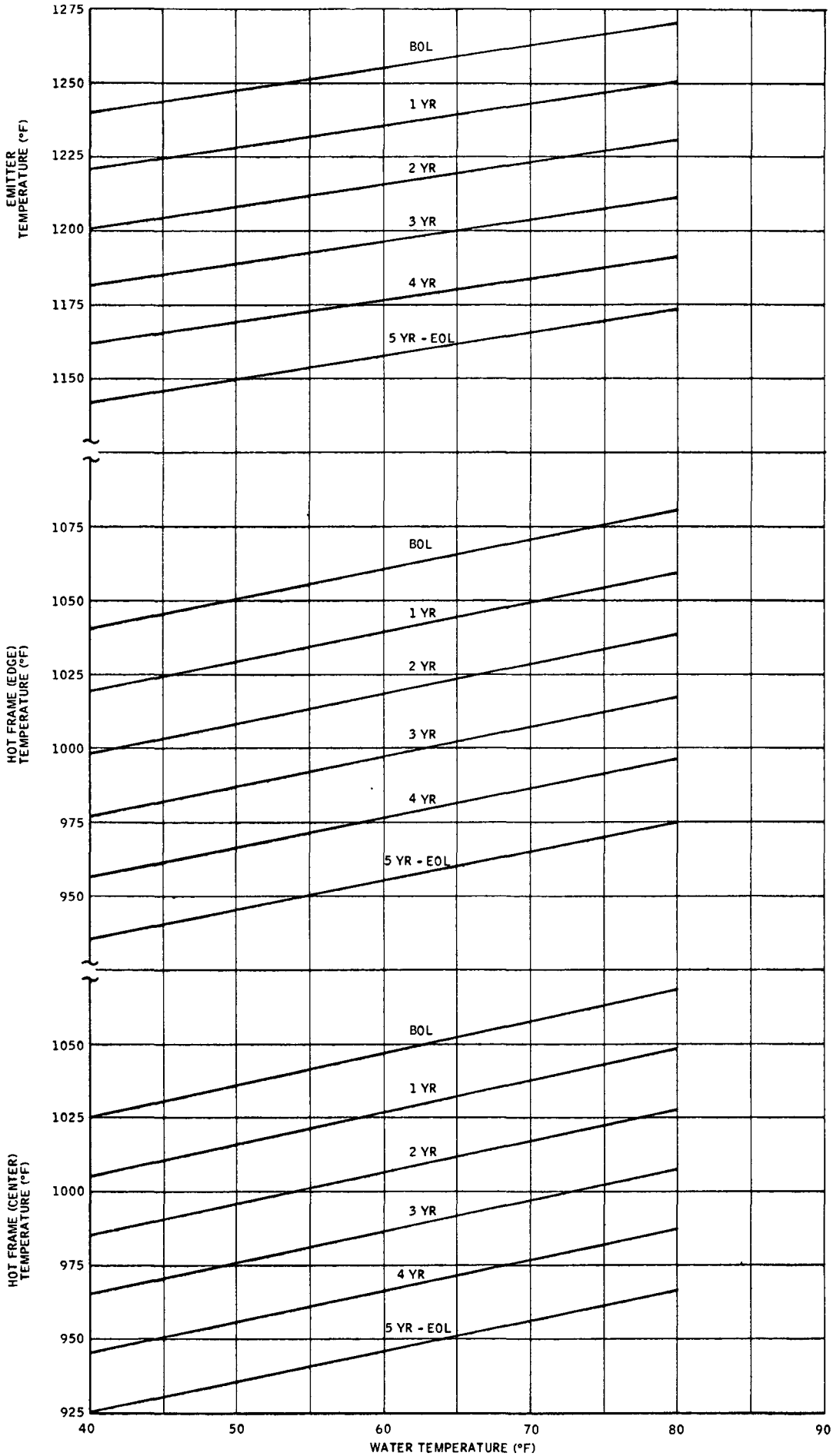

Figure 13. System Performance - 209 Watts
System Temperatures vs. Water Temperatures

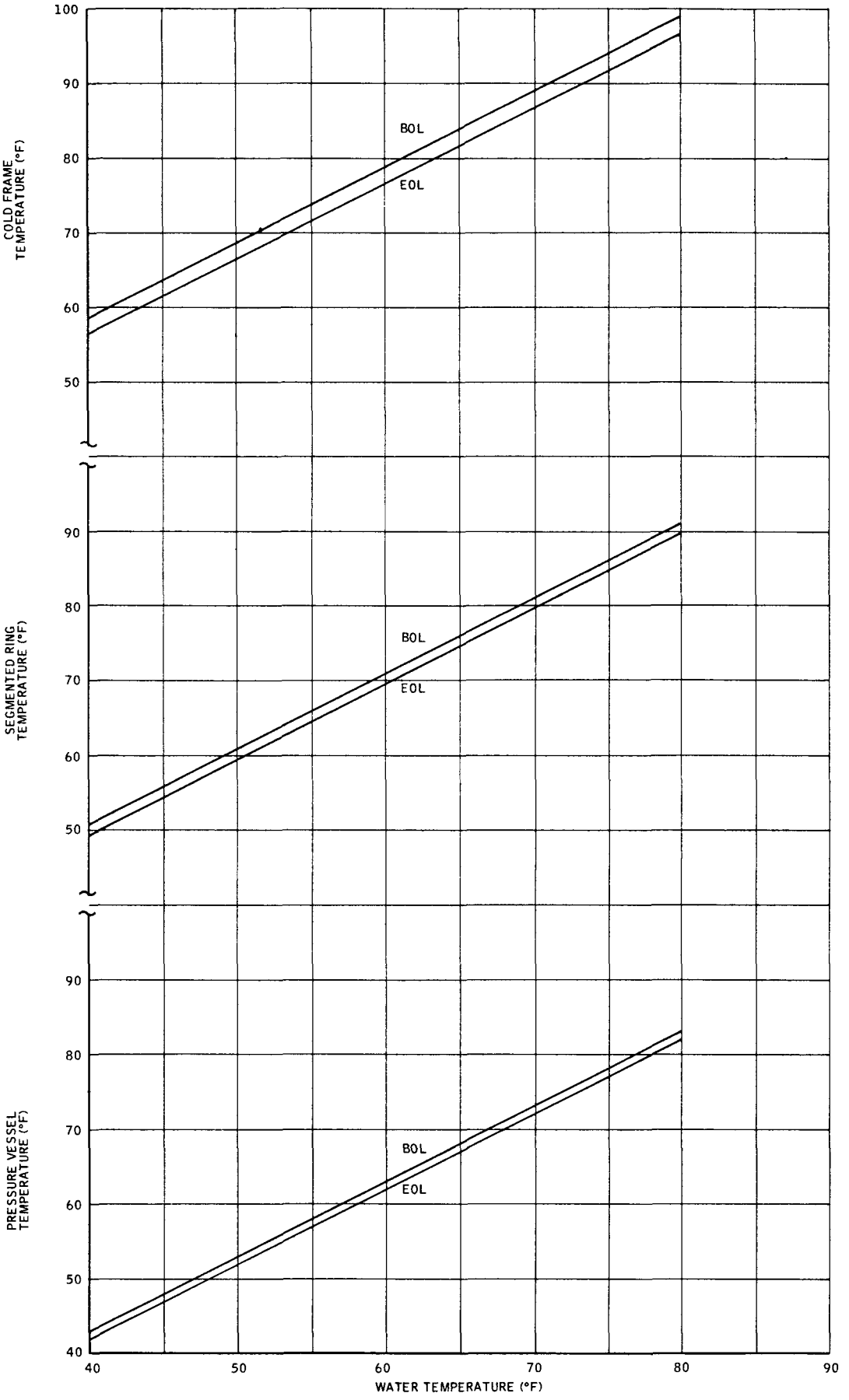

Figure 14. System Performance - 209 Watts
System Temperatures vs. Water Temperatures

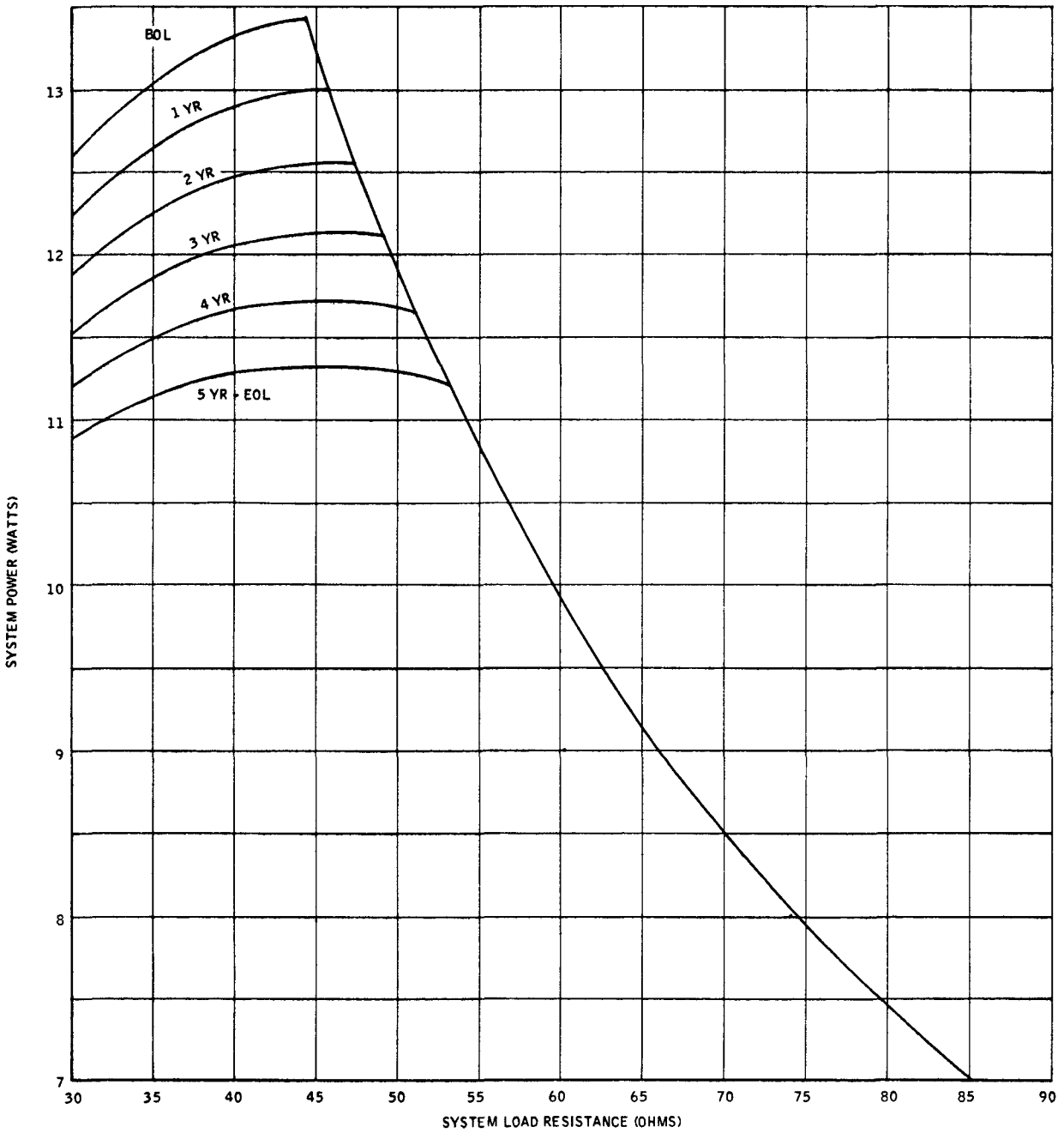

Figure 1. System Performance - 219 Watts
Power vs. Load Resistance in 40°F Water

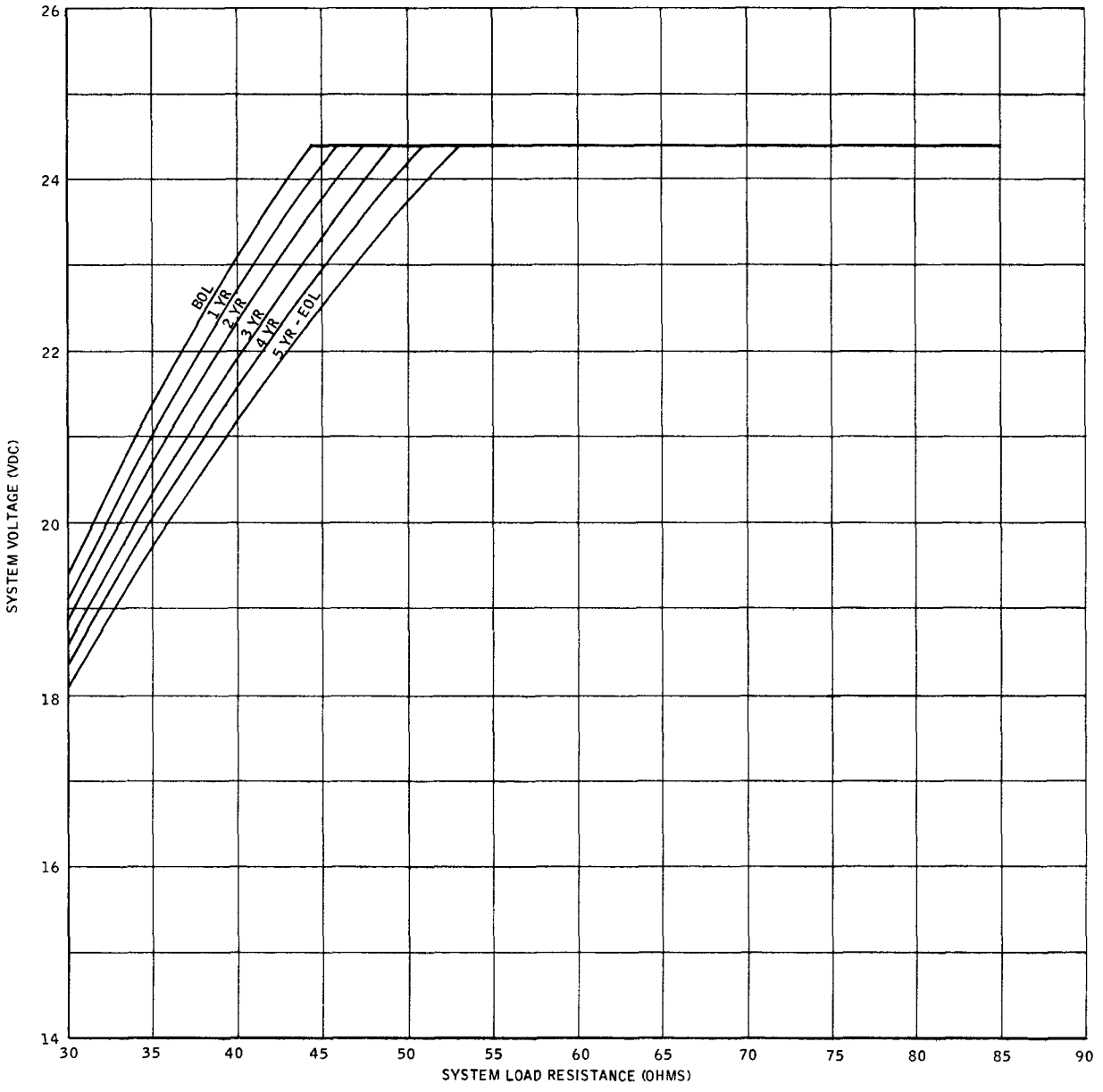

Figure 2. System Performance - 219 Watts
Voltage vs. Load Resistance in 40°F Water

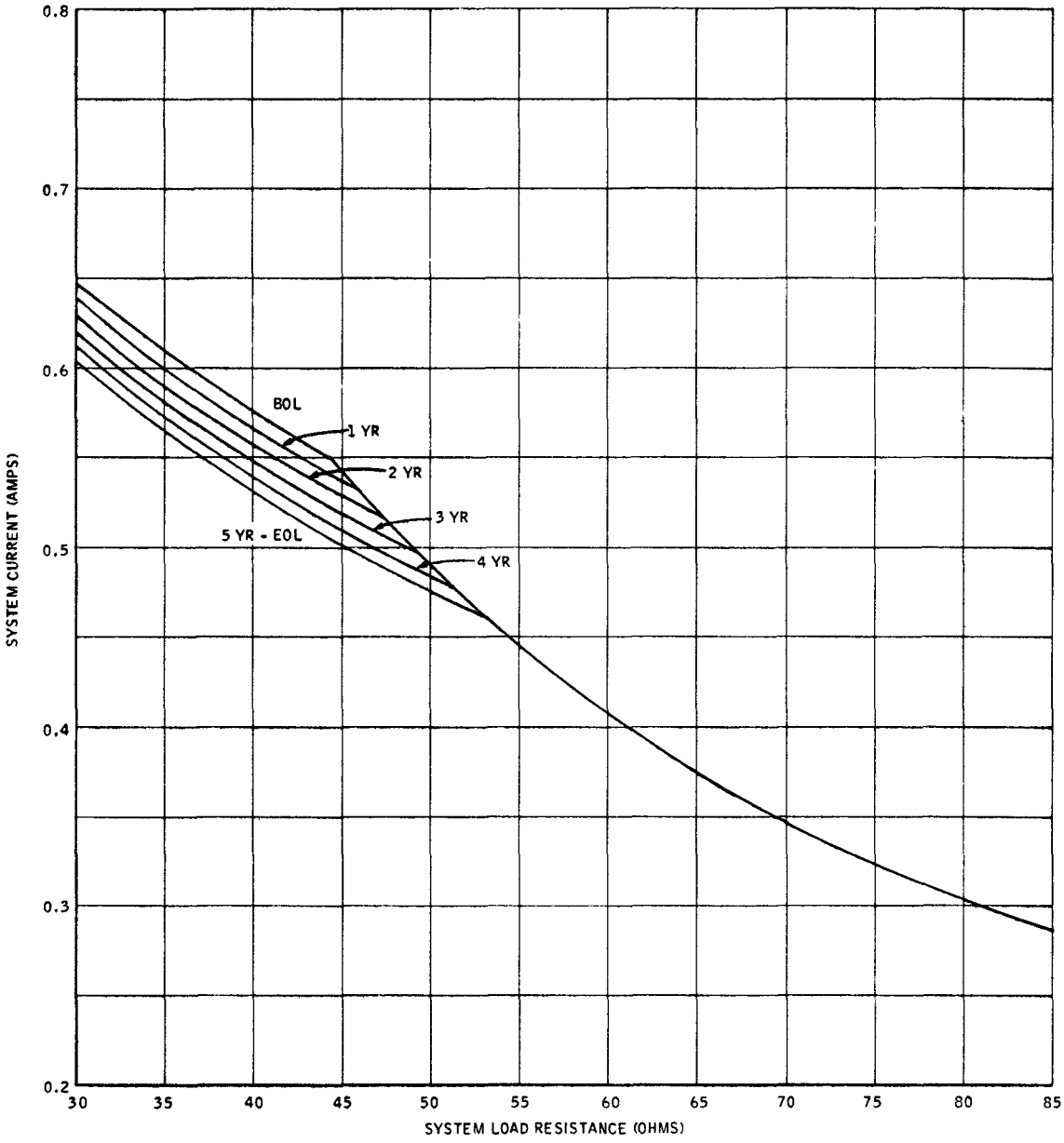

Figure 3. System Performance - 219 Watts
Current vs. Load Resistance in 40°F Water

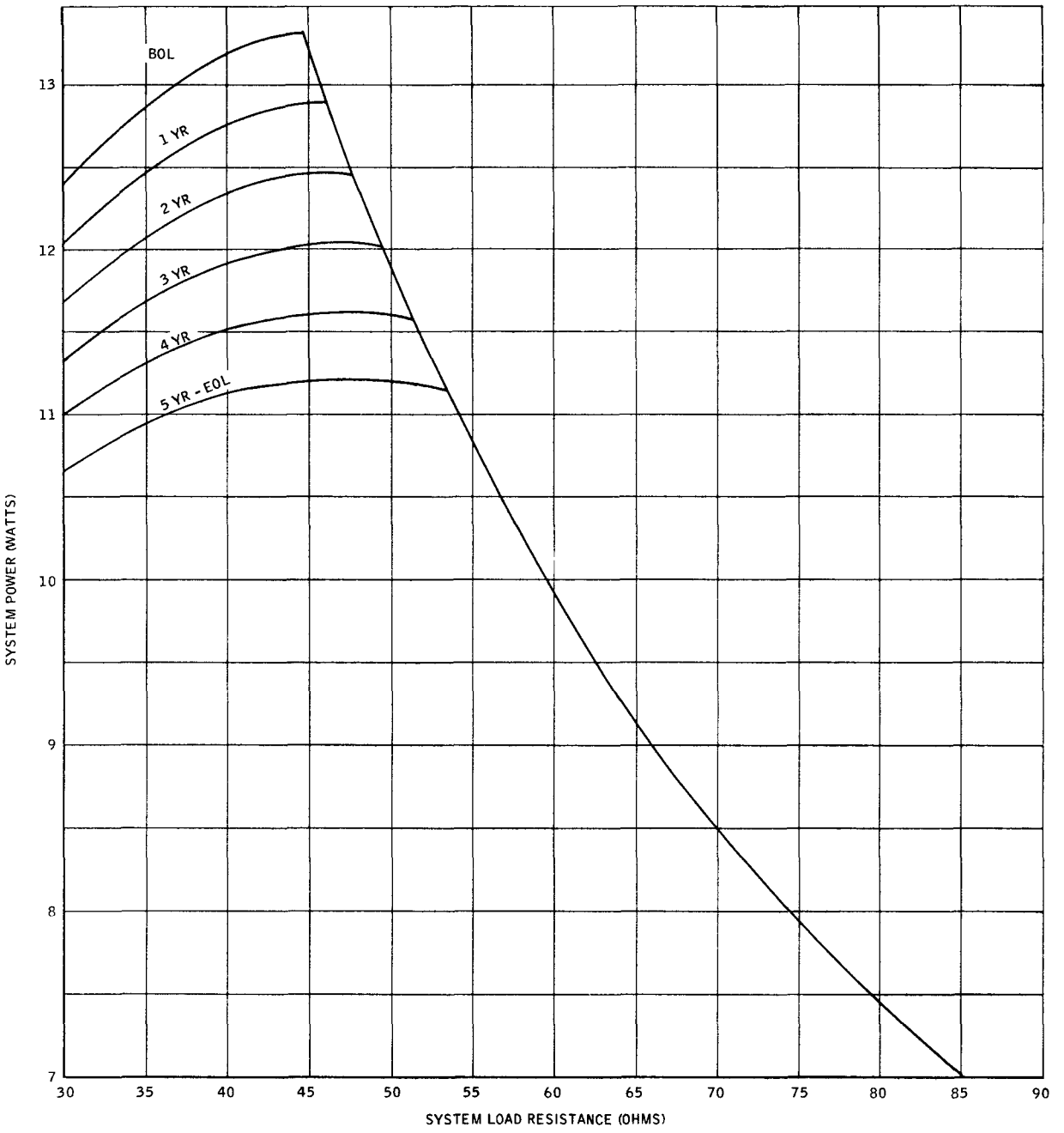

Figure 4. System Performance - 219 Watts
Power vs. Load Resistance in 60°F Water

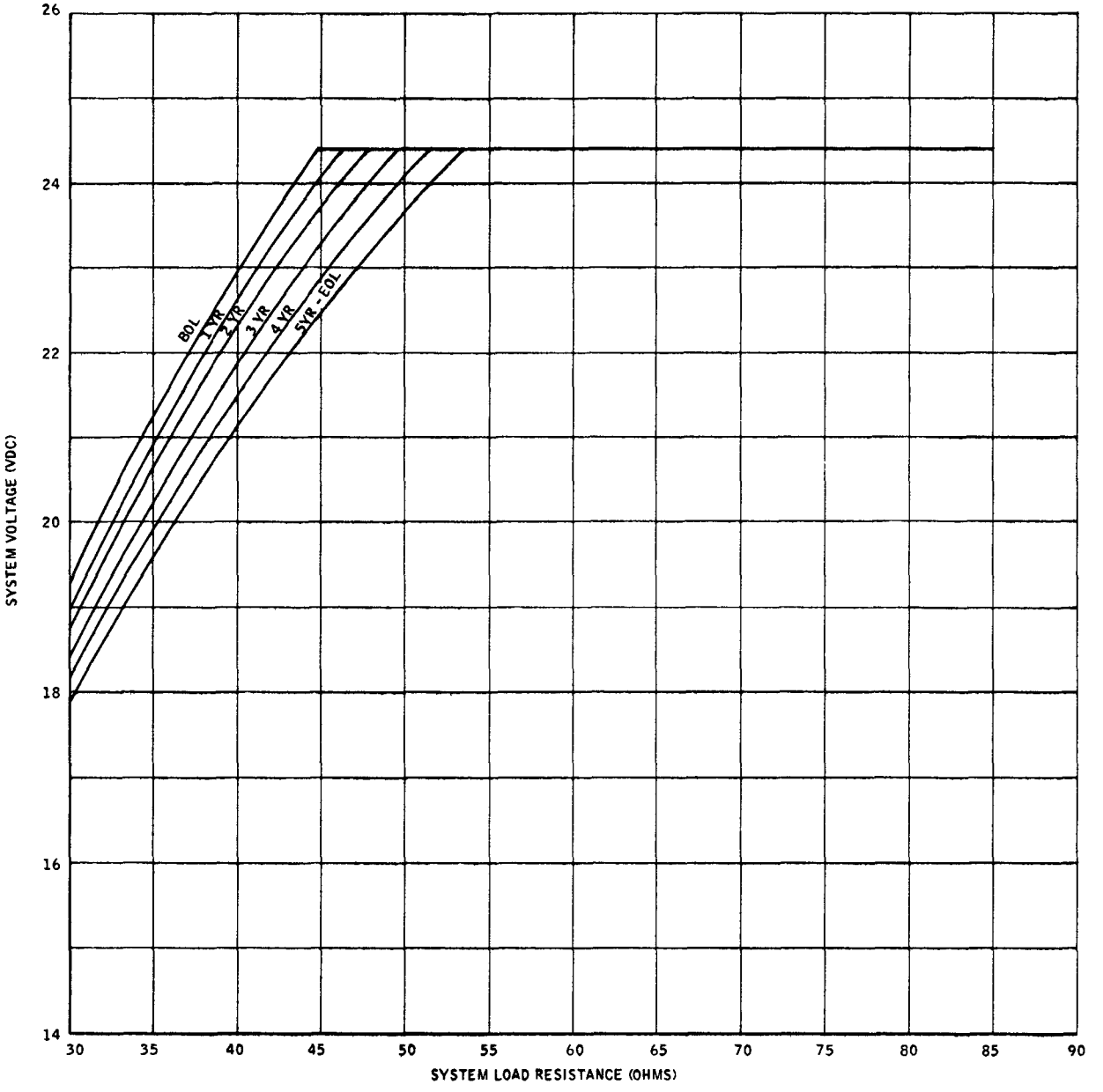

Figure 5. System Performance - 219 Watts
Voltage vs. Load Resistance in 60°F Water

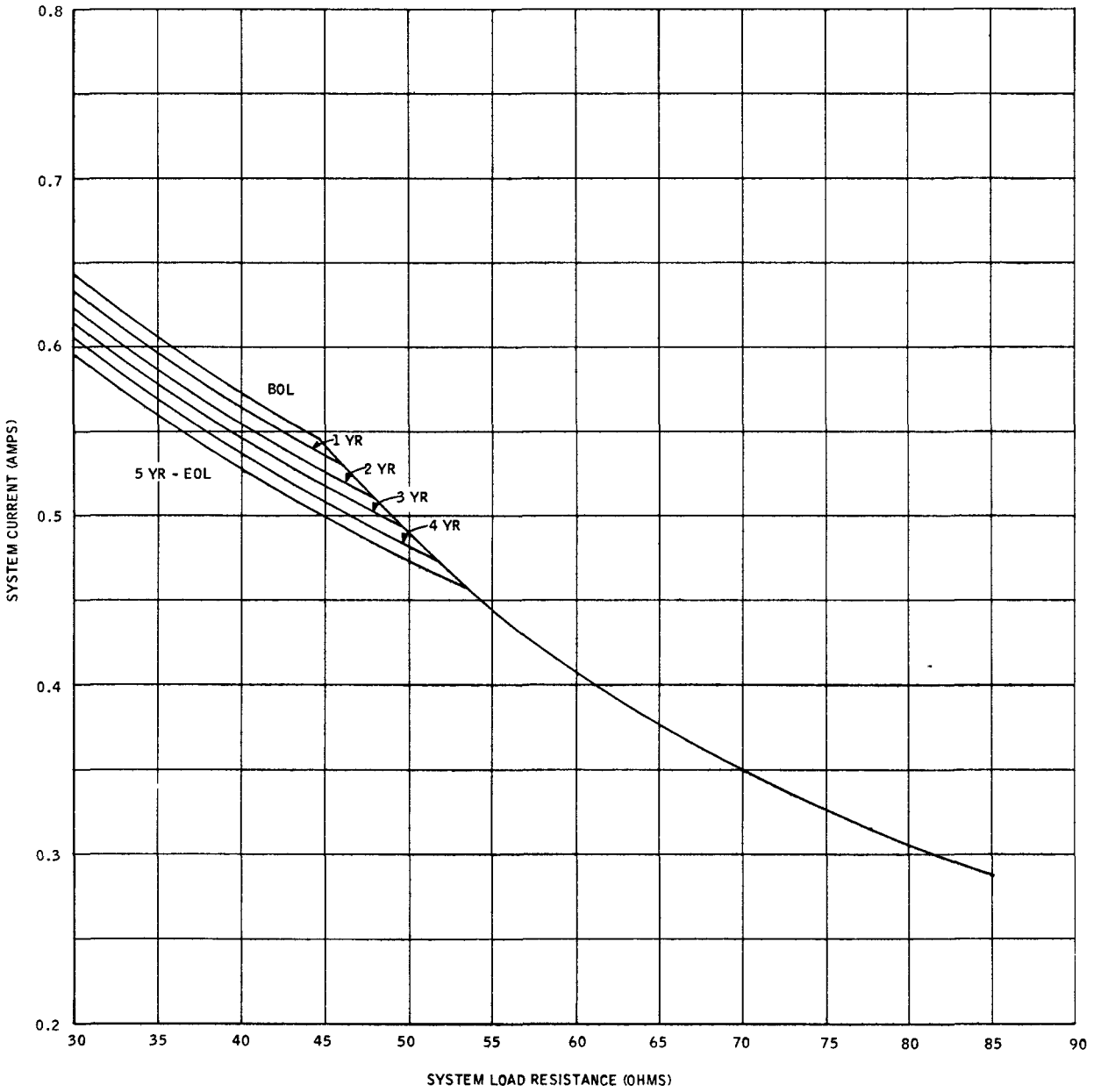

Figure 6. System Performance - 219 Watts
Current vs. Load Resistance in 60°F Water

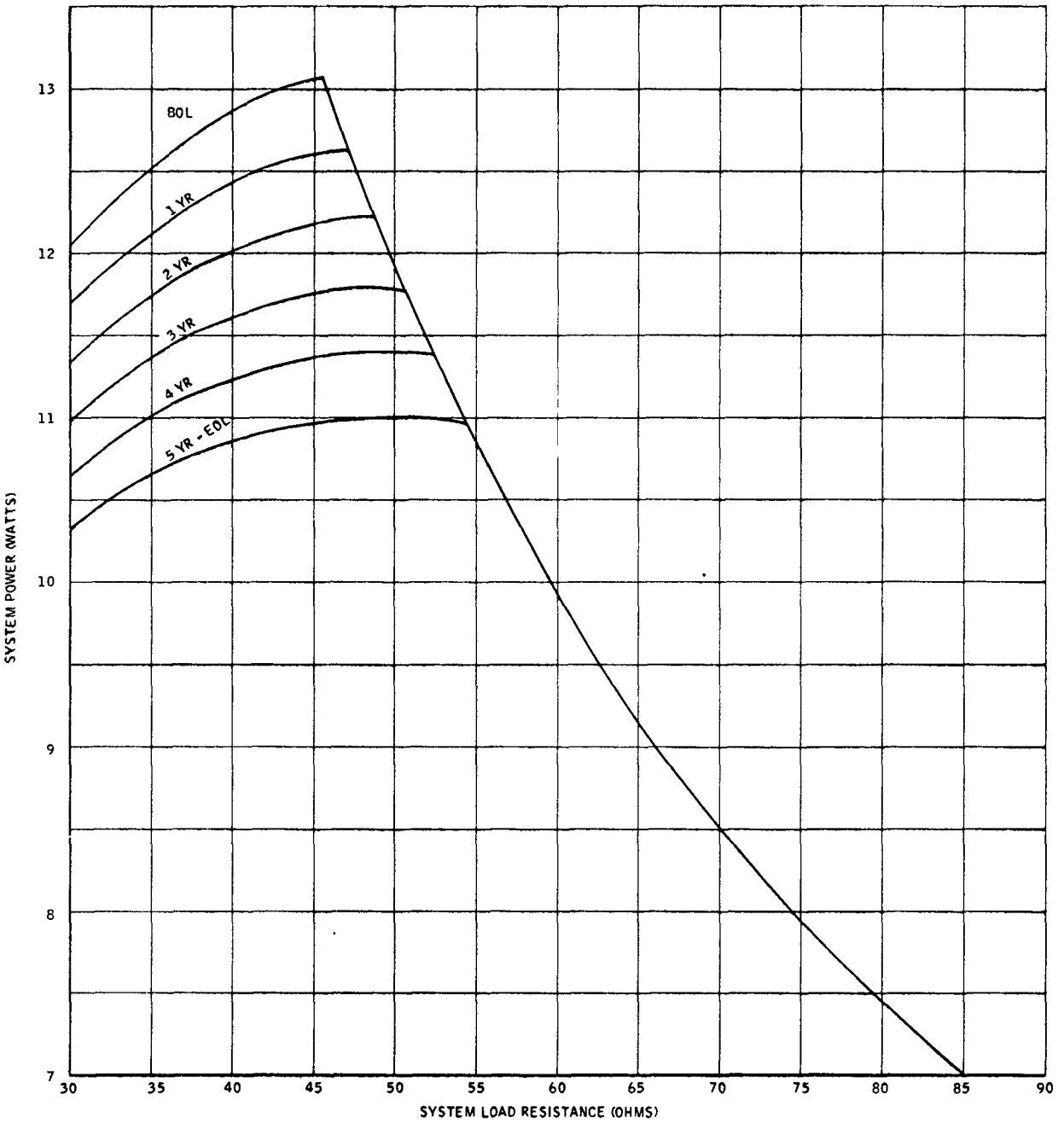

Figure 7. System Performance - 219 Watts
Power vs. Load Resistance in 80°F Water

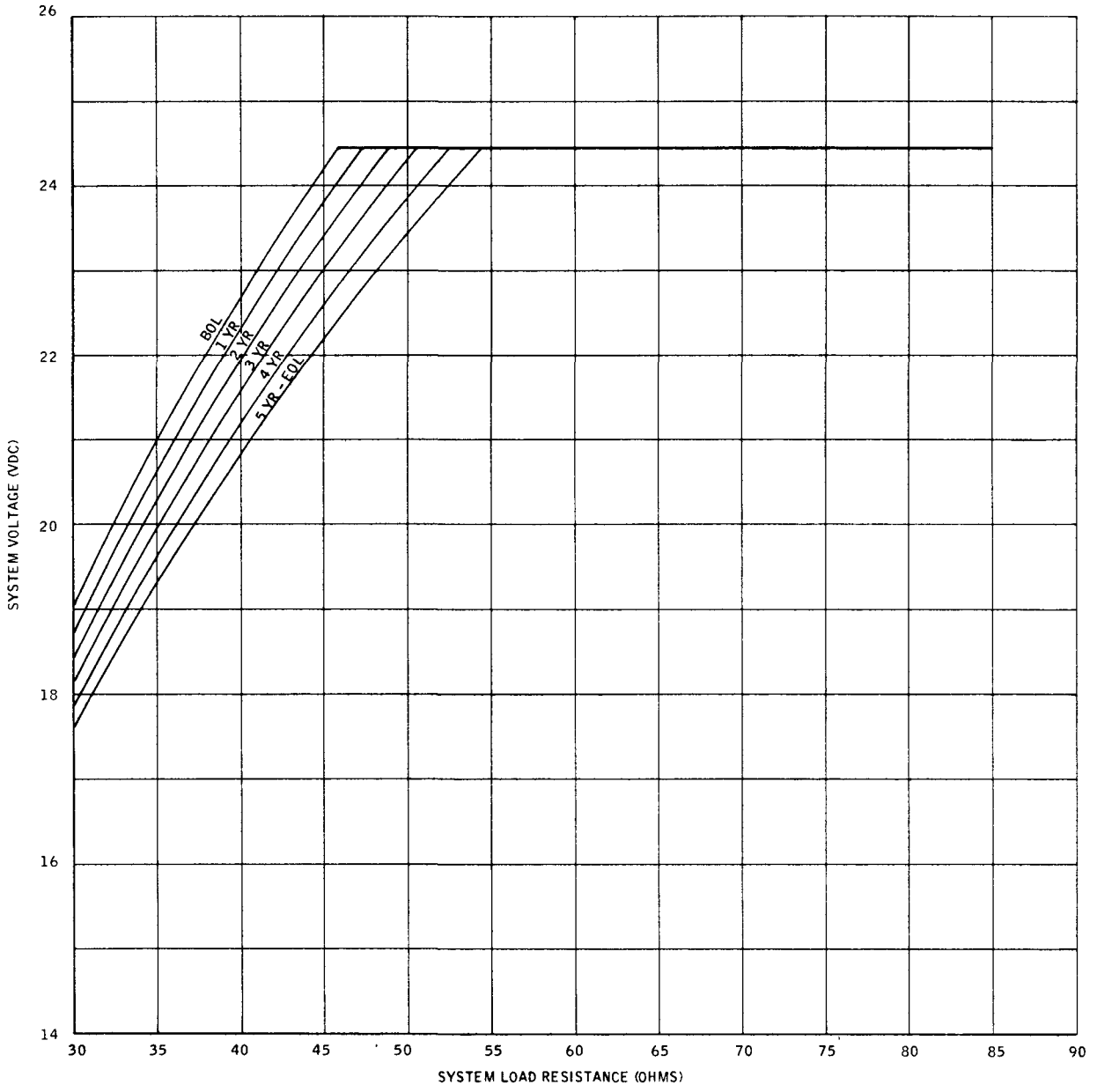

Figure 8. System Performance - 219 Watts
Voltage vs. Load Resistance in 80°F Water

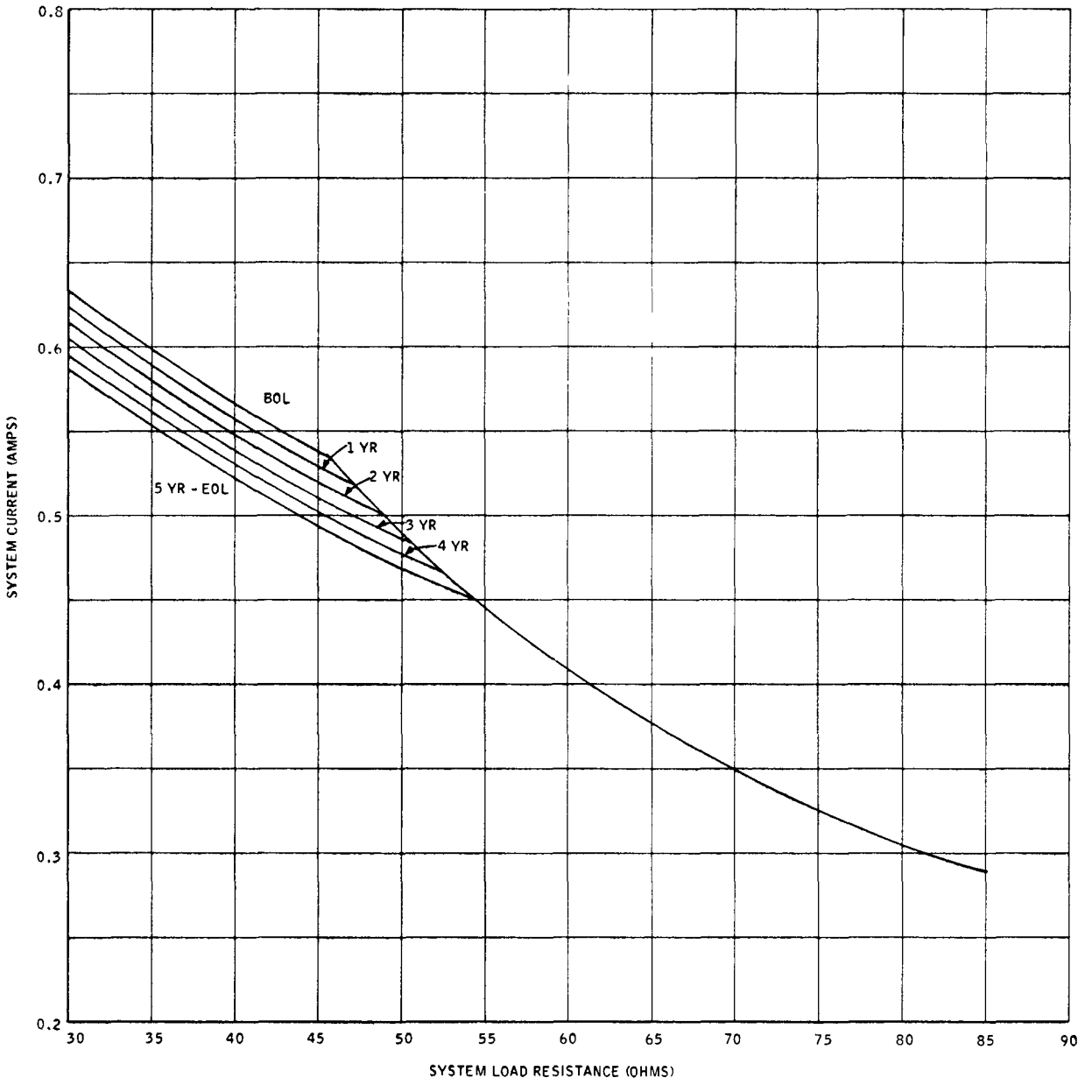

Figure 9. System Performance - 219 Watts
Current vs. Load Resistance in 80°F Water

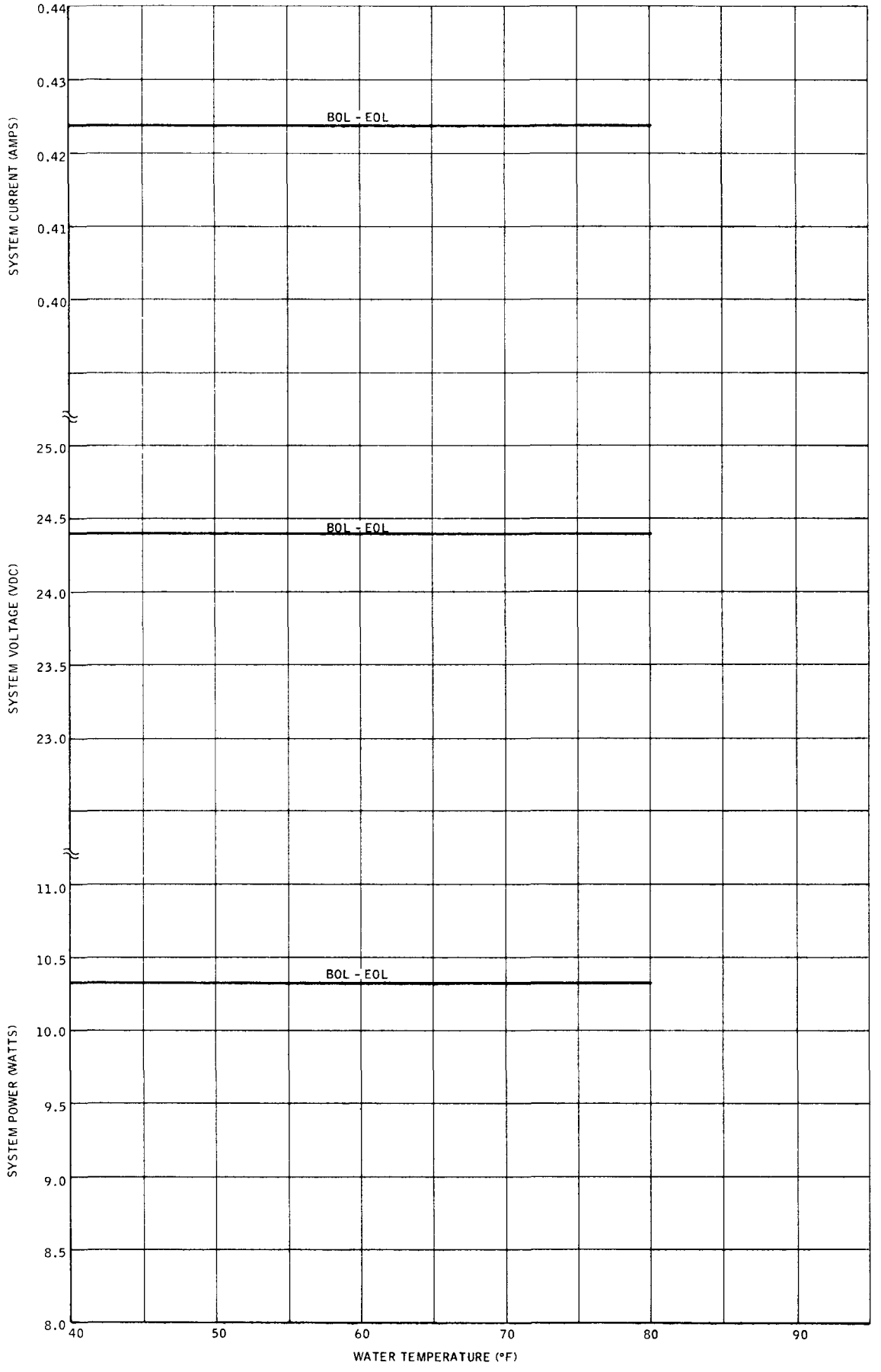

Figure 10. System Performance - 219 Watts
System Power, Voltage and Current vs. Water Temperature

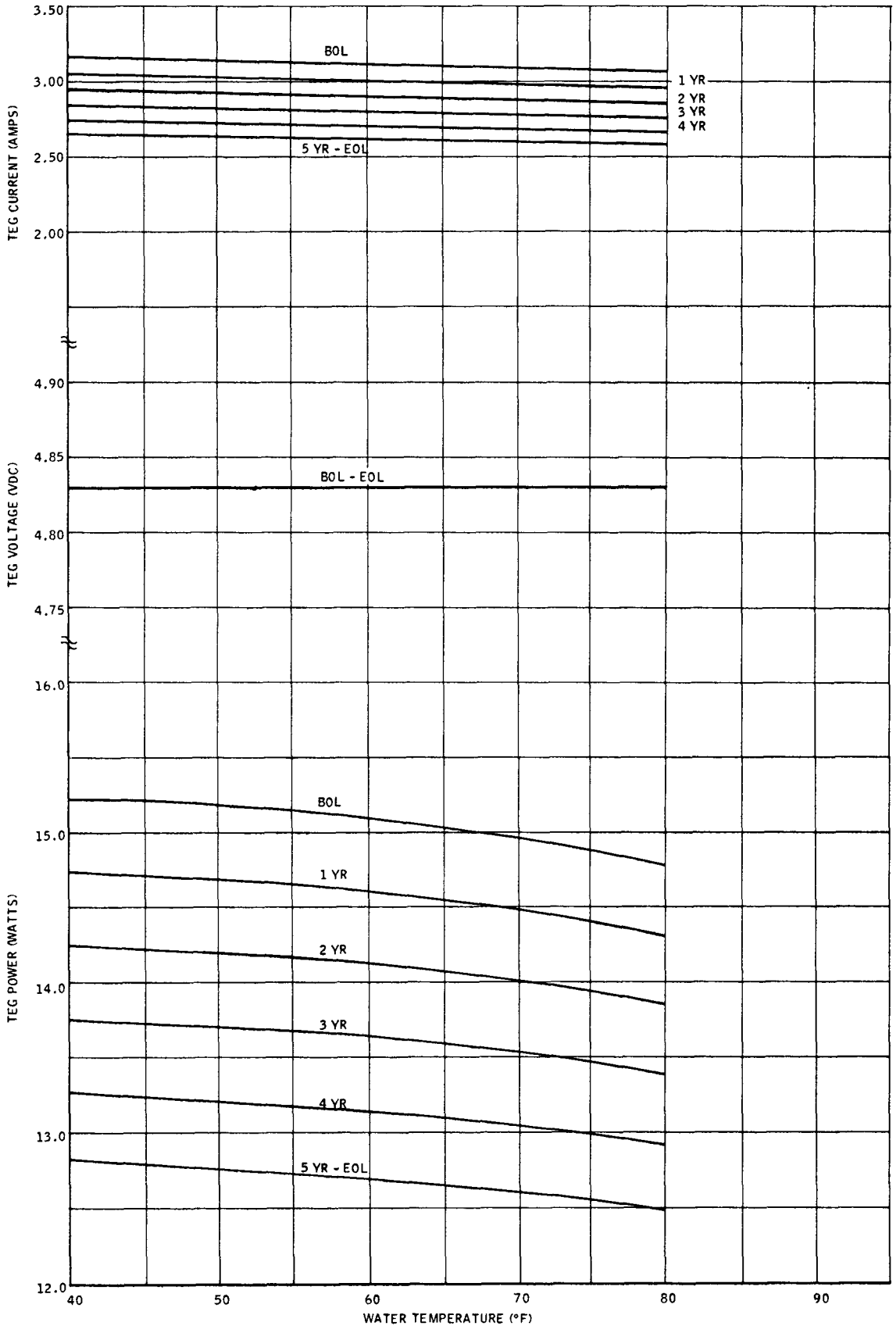

Figure 11. System Performance - 219 Watts
TEG Power, Voltage and Current vs. Water Temperature

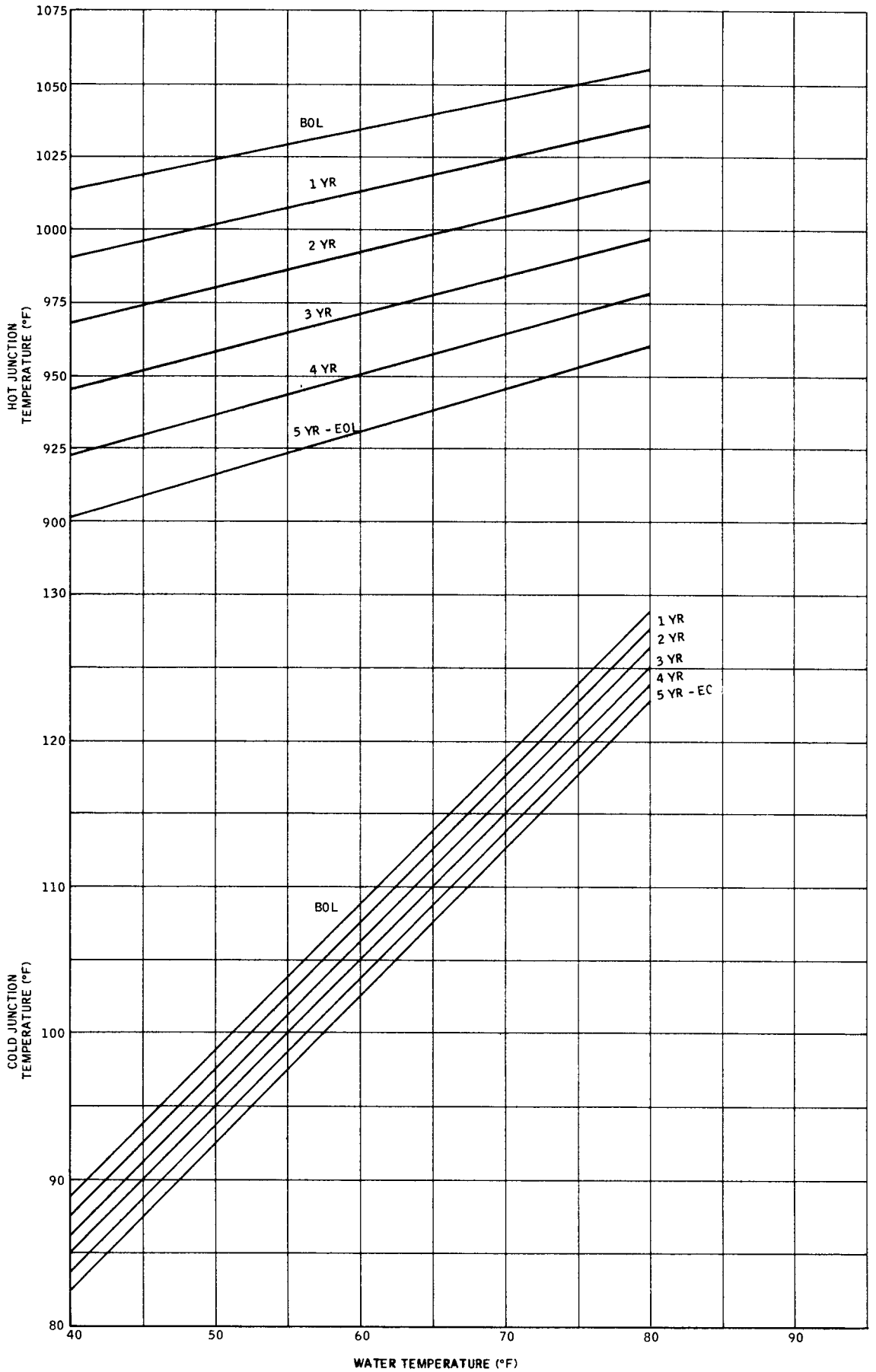

Figure 12. System Performance - 219 Watts
System Temperatures vs. Water Temperatures

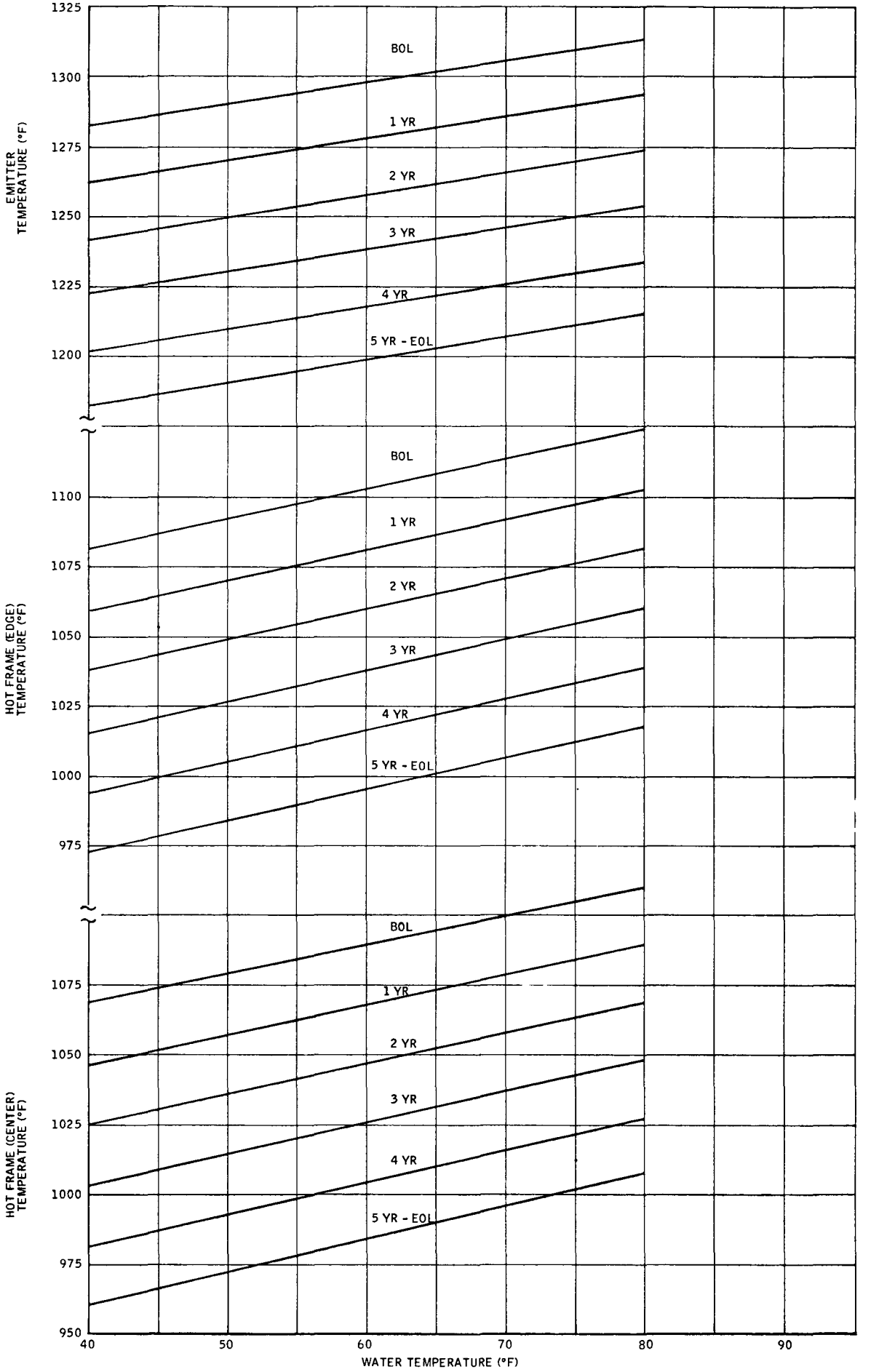

Figure 13. System Performance - 219 Watts
System Temperatures vs. Water Temperatures

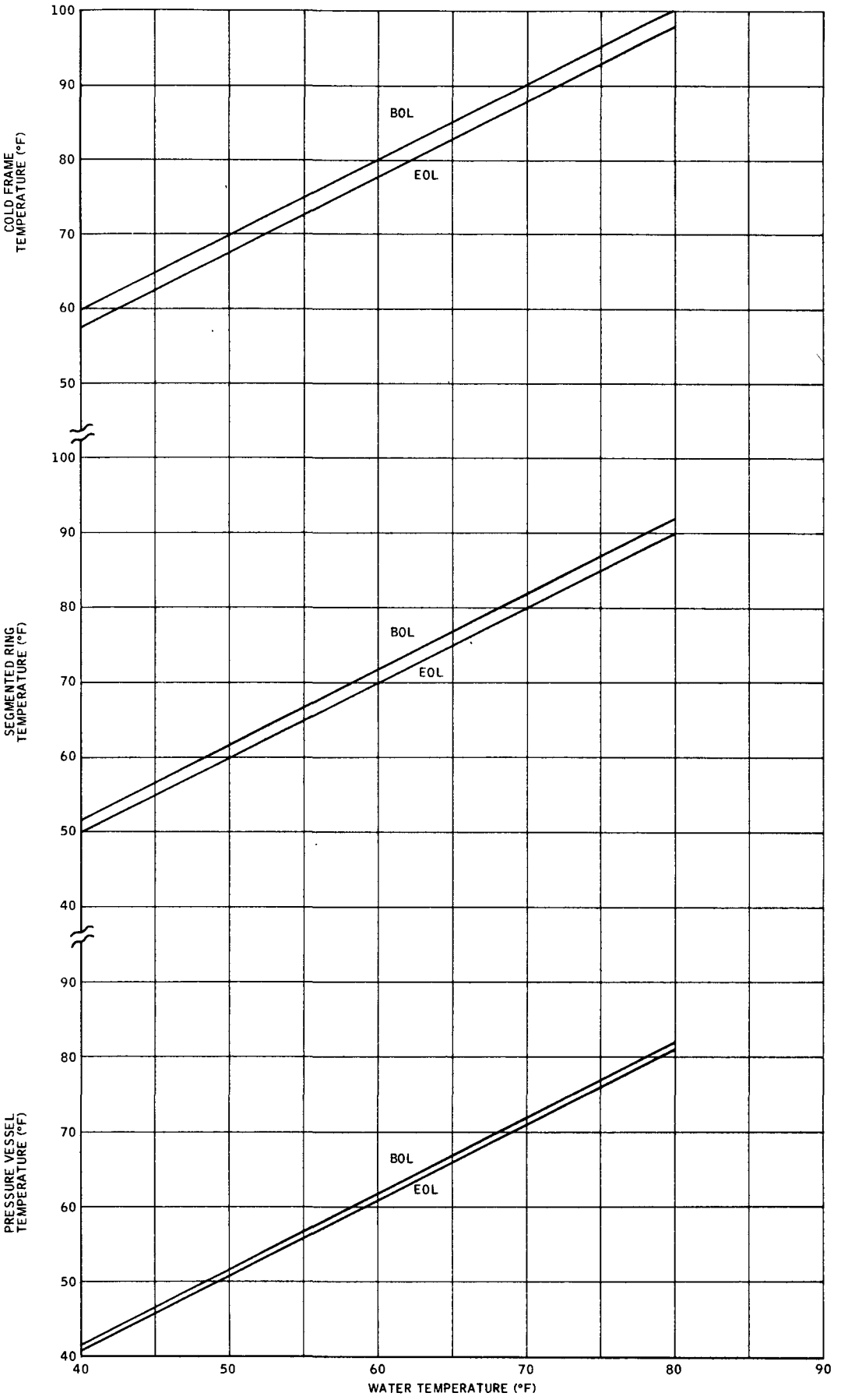

Figure 14. System Performance - 219 Watts
System Temperatures vs. Water Temperatures

APPENDIX B

EXAMPLE OF METHOD USED TO DERIVE A THERMAL MODEL OF A FUELED SNAP-21 SYSTEM

A thermal model for each system was derived using temperature measurements made during system tests in March and April, 1969. The modeling equations were then applied to the three fueled units; S10P1, S10P2, and S10P3. The modeling equations will also be applied to the final fueled system, S10P4, when data is available.

Derivation of the thermal model is based on the following assumptions:

1. Heat flow between points where temperatures are measured is known.
2. Changes in thermal contact conductances and the gap between emitter and hot frame over the range of water temperatures considered are negligible.

The first assumption permits calculation of "lumped" conductances based on assumed known heat flows, Q_{i-j}, and measured temperatures, t_i and t_j, from the equation:

$$K_{i-j} = Q_{i-j}/f\,(t_i,\ t_j)$$

This first assumption is reasonable since there are only two major heat paths from the heat source to the sea water. One is through the insulation system and the other is through the thermoelectric generator. Since the heat loss of the insulation system is carefully measured during its acceptance test, the heat flow through the generator can be obtained by subtracting the insulation system heat loss from the known total heat input of the fuel.

The second assumption is required to permit direct averaging of conductances computed from several sets of temperature data. It is reasonable to assume that very small changes will occur in the conductivities, contact conductances, and gap for

the 40°F to 80°F water temperature range of interest, thus conductances between points were calculated using many data sets for each fueled system. Each value was compared with the average value which permitted rejection of the conductance values if they appeared greatly different from the average value. Only one point in sixteen was rejected in this comparison which helped demonstrate the regularity of the measured temperature data.

The models derived from test temperatures and heat flow data were used to predict temperatures (at one-year intervals) during the five-year mission. The decay in isotope heat production was accounted for in this model and degradation of the thermoelectric materials was included using a degradation analysis technique.

In the degradation model, the time rates of change in generator leg geometry, electrical resistance and thermal conductance can be calculated as functions of the following:

- Hot and cold junction temperatures.
- Hot frame temperature gradient.
- Generator backfill gas pressure.
- Original leg dimensions.
- Activation energy of sublimation.
- Ratio of electrical resistance at the hot junction to the average leg resistance.

The specific factors used in this model are based on test data from the various SNAP programs (SNAP-21, 23, 27). Changes in electrical resistance and thermal conductance predicted for a particular time interval are summed with previous accumulated changes to reflect total changes since BOL.

A schematic indicating the locations of key temperatures in the fueled systems and the corresponding thermal model conductance network used to establish the SNAP-21 thermal model is included (Figure B-1). In the discussion following, the method of calculating each conductance is explained. The values used in predicting system EOL characteristics are tabulated in Appendix C.

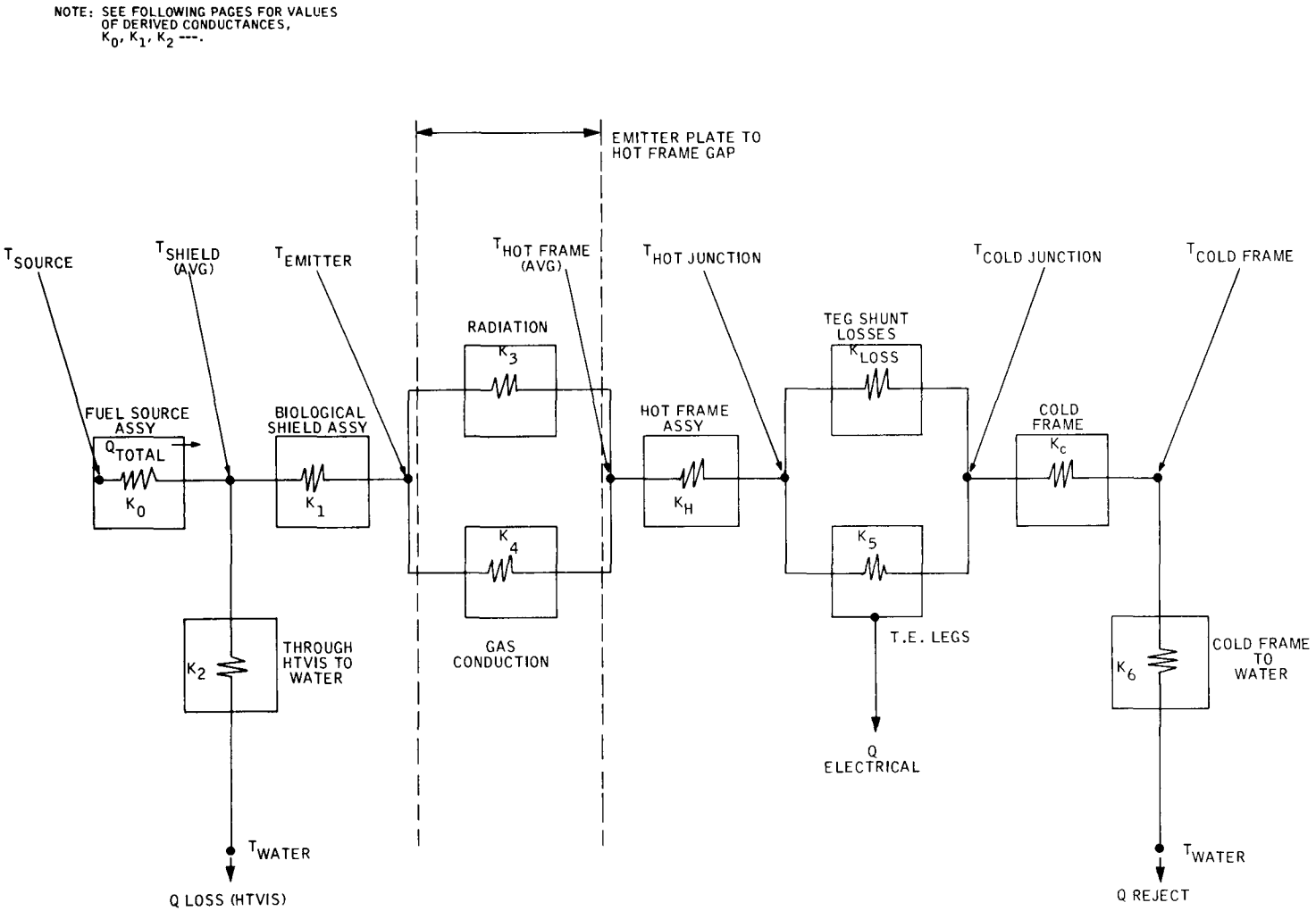

Figure B-1. SNAP-21 10-Watt System Thermal Model Schematic

1. HTVIS (High Temperature Vacuum Insulation System) Thermal Conductance

The calculated HTVIS conductances used in the system models were based on acceptance test measurements of heat loss for each insulation system. These data were used to determine insulation conductance, K_2, for each HTVIS as follows:

$$K_2 = \frac{Q\ (Test)}{(1285 - 100)}$$

This conductance is assumed to be independent of temperature even though the heat loss through the multilayer insulation is predominantly by radiation. This assumption is valid since the portion of heat lost through the multilayer insulation is a small portion of the total HTVIS insulation loss (12 to 14 watts through insulation compared with about 50-watt total). The larger portion of the HTVIS loss occurs by conduction heat transfer along the neck tube and tension tie rods. Over the 40°F to 80°F water temperature range of interest, thermal conductivities of materials used in the HTVIS change less than 1/2%, which is negligible. For the insulation systems used in the three fueled SNAP-21 systems, the values of insulation conductance are:

System Serial Number	HTVIS Serial Number	Acceptance Test Heat Loss, Watts (t)	K_2 (W/°F) HTVIS Conductance
S10P1	B10 DL2	49.1	0.04143
S10P2	B10 DL4	53.9	0.04548
S10P3	B10 DL5	50.8	0.04286

The acceptance test of the HTVIS is conducted by insulating the generator opening inside the neck-tube area and then applying only the amount of heat required to maintain the top of the shield (emitter plate) at the test temperature of 1285°F. Therefore, the heat input is equal to the HTVIS losses plus a small amount of fixed losses through the heater leads and neck-tube insulation. Since the heat flow from the heat source to the emitter plate is very small under these conditions,

the temperature gradient in the shield is negligible. In a fueled system, however, a relatively large amount of heat flows from the heat source to the emitter plate and then through the thermoelectric generator.

This heat flow produces a temperature gradient between the heat source and emitter plate. As a result, for the same emitter plate temperature, the average interior temperature of the shield is higher in a fueled system than during acceptance testing. Tests with electrically heated system S10D2 show approximately 170°F gradient along the shield inner liner for a typical heat flow. In the thermal model, heat flow through the insulation system was assumed to occur as a function of the above computed insulation conductance and a temperature-intermediate between the bottom of the inner liner and the emitter plate. Thus:

$$Q \text{ Insul} = K_2 (t_A - t_W)$$

where t_A is the intermediate temperature and t_W is water temperature.

A comparison of the acceptance test values tabulated above and the calculated insulation heat loss when used in a fueled system in 40°F water is made below.

System	HTVIS	Acceptance Test Heat Loss Watts	Heat Loss Computed with System Thermal Model (BOL) for 40°F Water, Watts		
S10P1	B10 DL2	49.1	52.3	Difference	= 3.2
S10P2	B10 DL4	53.9	56.7	Difference	= 2.8
S10P3	B10 DL5	50.8	55.4	Difference	= 4.6

The higher heat loss of the HTVIS when operating in a system is due to the higher average shield temperature.

2. Conductances Between Heat Source and Emitter

Conductances between the heat source and the emitter plate were based on temperature data from S10D2 (using 169°F temperature difference between the emitter and the bottom of the inner liner). To illustrate the method with S10P1, the following data was recorded during 3M Company performance tests on 12 March 1969 in 40°F water.

Q Source Watts (t)	t Emitter (Ave), °F	External Hot Frame (Ave), °F	External Cold Frame °F	Water °F
209.14	1247	1038	63	40

(Note that the heat input from the radioisotope fuel has been corrected for the amount of thermal decay that occurred between BOL and the test date.)

The average temperature of the fuel capsule surface was assumed to be 169°F higher than the emitter temperature, based on S10D2 tests. Thus, t source = 1247 + 169 = 1416°F. An intermediate temperature of 1316°F was used to calculate the insulation loss.

Thus, the conductance between source and intermediate temperature is:

$$K_0 = Q_{S/(t_S - t_A)} = \frac{209.14}{100} = 2.0914 \text{ W/°F}$$

Conductance between the intermediate temperature and emitter plate must be based on the source power minus the insulation heat loss:

$$K_1 = \frac{Q_S - K_2 (t_A - t_W)}{(t_A - t_E)}$$

For S10P1;

$$K_1 = \frac{209.14 - 0.04143 (1316 - 40)}{(1316 - 1247)} = 2.265 \text{ W/°F}$$

3. Heat Transfer Between Emitter and Hot Frame

The emitter to hot frame heat flow was represented as:

$$Q_{e-h} = \sigma F_{e-h} A_e (T_e^4 - T_h^4) + \frac{k A_e}{b} (t_e - t_h)$$

or: $= K_3 (T_e^4 - T_h^4) + K_4 (t_e - t_h)$

where:

T_e = center emitter plate temperature

t_e =

T_h = average hot frame temperature

t_h =

} capital letters denote °R, lower case denotes °F

σ = 0.173×10^{-8} BTU/Hr Ft^2 $°R^4$

F_{e-h} = radiative interchange coefficient (A function of view factors and emissivities alone)

A_e = hot frame area

k = gas thermal conductivity

b = gap width (at zero external pressure)

For S10P1;

$$K_4 = \frac{0.036 \times 13.79 \text{ in}^2}{0.186 \times 12 \times 3.416} = 0.0651 \text{ W/°F}$$

and:

$$K_3 = \frac{Q_{e-h} - K_4 (t_e - t_h)}{(T_e^4 - T_h^4)} = 4.11003 \times 10^{-11} \text{ W/°R}^4$$

4. Thermoelectric Generator Thermal Conductances

Hot and cold junction temperatures were determined from the curves included in the SNAP-21 Final Development Test Plan (Ref. 3691-9014, Page 22). These curves give hot and cold junction temperatures as functions of the average external hot and cold frame temperatures. The curves were derived from empirical data obtained from generator A10D8 which was completely instrumented. Therefore, the derived hot and cold junction temperatures for S10P1 are:

External Hot Frame (Ave) °F (measured)	Hot Junction (Ave) °F (Derived)	Cold Junction (Ave) °F (Derived)	External Cold Frame °F (measured)	Water
1038	979.2	90.6	63	40

Assuming all heat leaving the emitter plate is transferred to the hot junctions, a conductance between external hot frame and hot junctions can be calculated:

$$K_H = \frac{Q_{SOURCE} - Q_{INSUL}}{(t_{EXTH} - t_{HOT})}$$

For S10P1;

$$K_H = \frac{209.14 - 52.80}{(1038 - 979.2)} = 2.660 \text{ W/°F}$$

The heat flow between hot and cold junctions was represented by an equation which includes direct flow through the thermoelectric legs and a parallel heat loss term which includes all heat flow not passing through legs;

$$Q_{H-C} = K_5 (t_H - t_C) + K_{LOSS} (t_H - t_C) \qquad \text{Eqn 1}$$

The effect of temperature on the conductivity of thermoelectric materials cannot be neglected due to the large temperature gradient and the large percentage of heat flowing through the legs. The apparent thermal conductivity of each leg type (N and P) must be computed by integration of conductivity data over the temperature gradient, generally:

$$\overline{K} = \int_{t_{COLD}}^{t_{HOT}} k(t)\, dt \Big/ (t_{HOT} + t_{COLD})/2$$

The electrical resistivity must be computed in a similar manner since resistivity is also significantly temperature dependent due to the large temperature gradient. Although the hot and cold junction temperatures are known, accurate generator heat flow calculation must include these property temperature dependencies as well as the distribution of Joule, Thomson and Peltier heat effects within the leg. The following schematic (Figure B-2) is included to amplify the detail necessary for an accurate accounting of heat flows within the generator. Computation of generator output characteristics includes all these effects at any time point. For our analysis, the time dependent degradation effects previously mentioned are also included in the computer model.

Returning to the generator heat flow equation (equation 1 above), values of the generator heat flow conductance, K_5, are determined by the computer program and are not included as input model data. The heat loss term, $K_{LOSS}\ (t_H - t_C)$ was preliminarily evaluated from the total generator shunt heat loss curve in 3M Report MMM 3691-34, "SNAP-21, Phase II - Design Description", Page 32. For the hot and cold junction temperatures listed above for S10P1, the curve gives $Q_{LOSS} = 30.4$ watts, the calculated loss conductance therefore is;

$$K_{LOSS} = \frac{30.4}{(979.2 - 90.6)} = 0.0348\ W/°F$$

This value was used in initial calculations using the completed derived model. However, using conductances determined from the referenced curve resulted in heat loss which did not correlate with BOL temperature data. For modeling the generator by the method chosen, a smaller value of the loss conductance must be used to obtain hot and cold junction temperatures comparable to those measured. The difference between conductance required to match temperatures apparently lies either in the interpretation of heat flow between the HTVIS neck tube and the generator outer cylindrical shell or to a slight improvement in the HTVIS due to "clean-up" of the reflective foils by the internal getter.

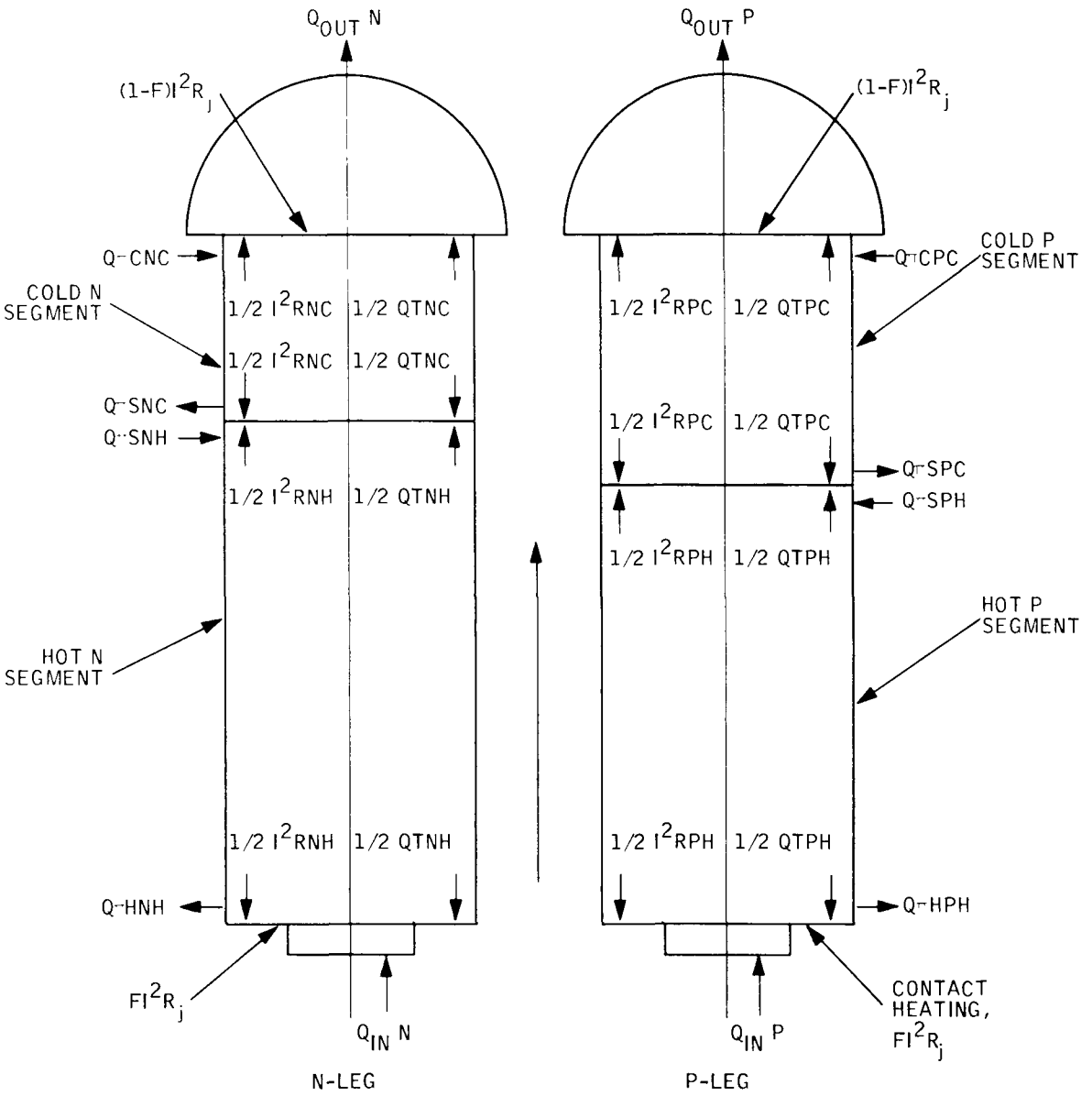

Figure B-2. Thermoelectric Couple Heat Model

The conductance between the cold junction and external cold frame was computed by subtracting the electrical power from the heat entering the generator, i.e.;

$$K_C = \frac{Q_{SOURCE} - Q_{INSUL} - POWER}{(T_{COLD} - T_{EXTC})} = \frac{Q_{REJ}}{(T_{COLD} - T_{EXTC})}$$

or, for S10P1;

$$\frac{209.14 - 52.8 - 14.5}{27.6} = 5.13 \text{ W/°F}$$

The last conductance in the model represents the heat flow between the cold frame and sea water.

For S10P1;

$$K_6 = \frac{Q_{REJ}}{(T_{EXTC} - T_{WATER})} = \frac{141.84}{23} = 6.16 \text{ W/°F}$$

All the conductance values computed as examples above pertain to S10P1 data measured at 40°F water temperature. The calculations were repeated for 60 and 80°F water temperatures, in order to examine any residual temperature dependence of the conductances and to permit rejection of a conductance value if it appeared widely different from the other computed values or from the averages due to possible reading error. A tabulation of computed conductances for all these systems is included in Appendix C.

The modeling equations for each system are based on energy balances. These equations can be written down directly from the thermal model schematic (Figure B-1). Starting with the heat source we obtain:

$$Q_S = K_O (t_S - t_A)$$ Source

$$0 = K_O (t_S - t_A) + K_1 (t_E - t_A) + K_2 (t_W - t_A)$$ Intermediate Point

$$0 = K_1 (t_A - t_E) + K_3 (T_H^4 - T_E^4) + K_4 (t_H - t_E)$$ Emitter Plate

$$0 = K_3 (T_E^4 - T_H^4) + K_4 (T_E - T_H) + K_H (t_{HOT} - t_H)$$ External Hot Frame

$$1/2\ Q_{e1} = K_H (t_H - t_{HOT}) + (K_{LOSS} + K_5) (t_{HOT} - T_{COLD})$$ TEG Hot Junction

$$1/2\ Q_{e1} = K_C (t_{COLD} - t_C) + (K_{LOSS} + K_5) (t_{COLD} - t_{HOT})$$ TEG Cold Junction

$$0 = K_C (t_{COLD} - t_C) + K_6 (t_W - t_C)$$ External Cold Frame

The values of constants used in these equations for S10P1, S10P2 and S10P3 are the average values tabulated in Appendix C.

1. S10P1 MEASURED PERFORMANCE DATA (12 March 1969)

Water Temp, °F	External Cold Frame, °F	External Hot Frame (Average), °F	Emitter Center, °F	TEG Power Output, W	Source Strength Corresponding to Measuring Date
40	63	1038	1247	14.5	209.14 W
60	82	1054.5	1257	14.4	
80	100	1072.5	1270	14.22	

2. CONDUCTANCES DERIVED FROM MEASUREMENTS

Water Temp, °F	K_0 Source to Intermed.	K_1 Intermed. to Emitter	K_2 Through HTVIS to Water	K_3 Emitter to Hot Frame Radiation	K_4 Emitter to Hot Frame Conduction	K_H Hot Frame to Hot Junction	K_C Cold Junction to Cold Frame	K_6 Cold Frame to Water	K_{LOSS} TEG Shunt Loss
40	2.0914	2.265	0.041434	4.1100E-11	0.0651	2.660	5.13	6.16	---
60	2.0914	2.270	0.041434	4.169E-11	0.0651	2.662	5.14	6.48	---
80	2.0914	2.280	0.041434	4.28E-11	0.0651	2.675	5.175	7.15	---
Ave	2.0914	2.270	0.041434	4.17E-11	0.0651	2.66	5.14	6.48	2.54E-4

3. ADDITIONAL TEMPERATURES DERIVED FROM MODEL

Water Temp, °F	Cold Junction, °F	Hot Junction, °F	Intermediate Temp, °F (See Page B-5 of Text)	Source Temp, °F
40	90.6	979.2	1316	1416
60	109.7	995.7	1326	1426
80	127.7	1013.7	1339	1439

*Tabulated number is value required to predict hot and cold junction temperatures (see Page B-9 of text).

1. S10P2 MEASURED PERFORMANCE DATA (12 March 1969)

Water Temp, °F	External Cold Frame, °F	External Hot Frame (Average), °F	Emitter Center, °F	TLG Power Output, W	Source Strength Corresponding to Measuring Date
40	60	1015	1223	14.07	206.58 W
60	79	1032	1231	13.87	
80	98	1051	1246	13.64	

2. CONDUCTANCES DERIVED FROM MEASUREMENTS

Water Temp, °F	K_0 Source to Intermed.	K_1 Intermed. to Emitter	K_2 Through HTVIS to Water	K_3 Emitter to Hot Frame Radiation	K_4 Emitter to Hot Frame Conduction	K_H Hot Frame to Hot Junction	K_C Cold Junction to Cold Frame	K_6 Cold Frame to Water	K_{LOSS} TEG Shunt Loss
40	2.0658	2.237	0.04548	4.1343E-11	0.0651	2.5725	4.9871	6.782	---
60	2.0658	2.243	0.04548	4.2530L-11	0.0651	2.591	5.061	7.192	---
80	2.0658	2.246	0.04548	4.2050L-11	0.0651	2.595	5.069		---
Ave	2.0658	2.242	0.04548	4.1974L-11	0.0651	2.586	5.039	7.192	2.30E-4

3. ADDITIONAL TEMPERATURES DERIVED FROM MODEL

Water Temp, °F	Cold Junction, °F	Hot Junction, °F	Intermediate Temp, °F (See Page B-5 of Text)	Source Temp, °F
40	87.2	956.8	1290	1390
60	106	974	1298	1398
80	125	993	1313	1413

See Page B-9 of text.

Conductance value discarded.

1. S10P3 MEASURED PERFORMANCE DATA (9 April 1969)

Water Temp, °F	External Cold Frame, °F	External Hot Frame (Average), °F	Emitter Center, °F	TEG Power Output, W	Source Strength Corresponding to Measuring Date
40	64	1052	1268	14.75	212.5 W
60	82	1062	1274	14.50	
80	101	1082	1287	14.40	

2. CONDUCTANCES DERIVED FROM MEASUREMENTS

Water Temp, °F	K_0	K_1	K_2	K_3	K_4	K_H	K_C	K_6	K_{LOSS}
				Emitter to Hot Frame					
	Source to Intermed.	Intermed. to Emitter	Through HTVIS to Water	Radiation	Conduction	Hot Frame to Hot Junction	Cold Junction to Cold Frame	Cold Frame to Water	TEG Shunt Loss
40	2.125	2.274	0.04286	3.8468E-11	0.0651	2.655	5.45	5.93	---
60	2.125	2.2827	0.04286	3.8917E-11	0.0651	2.670	5.50	6.51	---
80	2.125	2.2871	0.04286	3.9333E-11	0.0651	2.670	5.51	6.84	---
Ave	2.125	2.2811	0.04286	3.890E-11	0.0651	2.676	5.487	6.426	2.56E-4

3. ADDITIONAL TEMPERATURES DERIVED FROM MODEL

Water Temp, °F	Cold Junction, °F	Hot Junction, °F	Intermediate Temp, °F (See Page B-5 of Text)	Source, Temp, °F
40	90.1	992.9	1337	1437
60	108	1003	1343	1443
80	127	1023	1356	1456

See Page B-9 of text.